EXAMINING THE INFLUENCE OF SKELETAL MUSCLE OXYGEN METABOLISM ON MICROVASCULAR REPERFUSION IN RESPONSE TO ACUTE ISCHEMIA

by

RYAN PHILLIP ROSENBERRY

DISSERTATION

Submitted in partial fulfillment of the requirements
for the degree of Doctor of Philosophy at
The University of Texas at Arlington
December, 2019

Arlington, Texas

Supervising Committee:
Michael D. Nelson, Supervising Professor
Daisha Cipher
Matthew Brothers
Paul J. Fadel
Frank Dinenno (external member)

ABSTRACT

EXAMINING THE INFLUENCE OF SKELETAL MUSCLE OXYGEN METABOLISM ON MICROVASCULAR REPERFUSION IN RESPONSE TO ACUTE ISCHEMIA

Ryan Phillip Rosenberry, Ph.D.

The University of Texas at Arlington, 2019

Supervising Professor: Michael D. Nelson

Cardiovascular disease (CVD) is the single leading cause of morbidity and mortality in the United States (and the world), with a death rate greater than cancer and chronic lower respiratory disease (emphysema, bronchitis, asthma) combined. Therefore, it is critically important to continue developing techniques for assessing cardiovascular disease. Reactive hyperemia (RH), the magnitude of tissue reperfusion following a period of transient ischemia, is a common technique that is conventionally interpreted as an index of microvascular function and has been shown to be a sensitive and powerful predictor of cardiovascular risk factors and future cardiac events. In Chapter 2, we provide historical and clinical context for the measurement of reactive hyperemia, discuss the tools that have been used measure this phenomenon, summarize the mechanisms purportedly driving this response, and discuss emerging analytical approaches. In Chapter 3 we used near-infrared spectroscopy to evaluate the effect of age on reactive hyperemia. In Chapter 4 we further pursued this line of inquiry and incorporated Doppler ultrasound to evaluate the relationship brachial artery reactive hyperemia. In these studies we found that tissue ischemia is an important determinant of the hyperemic response. In Chapter 5 and Appendix A, we manipulated the balance between the ischemic stimulus and microvascular reactivity. In Appendix A, we attempted to acutely impair microvascular by exposing healthy young participants to an

ischemia-reperfusion model, but failed to induce any impairment in reactive hyperemia. In Chapter 5 we employed limb immobilization to induce reductions in skeletal muscle mitochondrial, but again were unable to induce shifts in either mitochondrial function or reactive hyperemia. Overall, these investigations have provided novel insight into the complex, and previously overlooked, relationship between skeletal muscle metabolic rate and reactive hyperemia. However, more work is needed to further explore this complex interrelationship and how it is affected by aging and disease.

TABLE OF CONTENTS

CHAPTER 1

INTRODUCTION

Cardiovascular disease (CVD) is the single leading cause of morbidity and mortality in the United States (and the world), with a death rate greater than cancer and chronic lower respiratory disease (emphysema, bronchitis, asthma) combined (Benjamin et al., 2017). Although other risk factors, such as smoking, obesity, and hypertension increase risk (O'Donnell & Elosua, 2008), age remains the greatest predictor, with nearly 70% of the population over 60 years of age, and 85% of the population over 80 yrs, affected by CVD (Benjamin et al., 2017). Even more troublesome, this burden is only expected to rise, as estimates project 40.5% of the US population to have some form for CVD by the year 2030, costing an estimated $818 billion in direct costs (Benjamin et al., 2017).

In light of this public health threat, it is critically important to continue developing clinical techniques for assessing the progression of cardiovascular disease. One such approach, termed reactive hyperemia (RH), involves measuring the magnitude of tissue reperfusion following a period of transient ischemia, most commonly induced through arterial cuff occlusion. The conventional interpretation has been that the healthier the microvascular system, the greater the microvascular vasodilation in response to the ischemic period, and thus the greater the magnitude of tissue reperfusion upon cuff deflation. Numerous investigations have indeed shown reactive hyperemia to be reduced with age (Dakak et al., 1998; Higashi et al., 2001; Mitchell et al., 2005), and in patients with hypercholesterolemia (Hayoz et al., 1995), renal disease (London et al., 2004), and heart failure (de Berrazueta et al., 2010). Moreover, multiple studies have shown that reactive hyperemia is a sensitive and powerful predictor of cardiovascular risk factors and future cardiac events (Criqui, Coughlin, & Fronek, 1985; Gokce et al., 2003; Huang et al., 2007).

In Chapter 2, we provide historical and clinical context for the measurement of reactive hyperemia and discuss the investigative tools that have been used over the past two decades to measure this phenomenon. We also discuss the proposed mechanisms driving this response, and technical considerations for analysis and reporting of reactive hyperemia.

In Chapter 3, we examine the effect of age on reactive hyperemia using a relatively novel near-infrared spectroscopy (NIRS) approach. This technique has been used to detect impairments in post-occlusive tissue resaturation in patients with peripheral vascular disease (Cheatle et al., 1991; Kooijman, Hopman, Colier, van der Vliet, & Oeseburg, 1997) and sepsis (Creteur et al., 2007). However, this approach had not yet been used to investigate age-dependent differences in microvascular function. To address this gap in the literature, we recruited young and independently living elderly individuals and measured the tissue resaturation rate using NIRS in response to a standardized 5-minute cuff occlusion. Consistent with our hypothesis, we observed an age-dependent reduction in the rate of tissue resaturation. The seminal finding of this investigation however, was that both groups also differed with respect to the desaturation slope (i.e. skeletal muscle metabolic rate), which led to a markedly different magnitude of tissue ischemia (i.e. the stimulus to vasodilate). While the exact mechanism for this finding is beyond the scope of this investigation, it is likely related to age-dependent skeletal muscle atrophy and reductions in oxidative capacity (Conley, Jubrias, & Esselman, 2000; Luhrmann, Bender, Edelmann-Schafer, & Neuhauser-Berthold, 2009; Miljkovic, Lim, Miljkovic, & Frontera, 2015; Volpi, Nazemi, & Fujita, 2004). In light of these findings, we then matched the absolute tissue desaturation in young participants with that of the elderly by reducing the time of cuff occlusion from 5 minutes to 3 minutes. Remarkably, matching the ischemic stimulus between groups completely abrogated group differences in the resaturation rate (i.e. reactive hyperemia).

Recognizing that this study was not without limitation, particularly its reliance on an “indirect” measure of reactive hyperemia (i.e. NIRS), and the lack of dose responsiveness in the elderly group, Chapter 4 describes the results of a follow-up experiment aimed to further explore the relationship between the ischemic stimulus and reactive hyperemia, while paying close attention to the aforementioned limitations. We recruited a new cohort of young and elderly participants and performed simultaneous Doppler ultrasound and NIRS measurements to directly assess reactive hyperemia and the

ischemic stimulus. First, to confirm and extend our initial observations, all participants performed a standardized 5-minute cuff occlusion. Then, to test the dose responsiveness, all participants underwent a 4-, 6-, and 8-minute cuff occlusions in random order. As expected, we observed the same group differences in the post-occlusion hyperemic response between young and elderly following each cuff occlusion (4-, 5-, 6-, 8-min). Moreover, the elderly individuals became far less ischemic during each respective cuff occlusion, regardless of duration. However, after adjusting each respective hyperemic response to its corresponding degree of tissue desaturation, group differences were once again completely abrogated. This is not to suggest that aging is not associated with microvascular dysfunction; rather, our data simply emphasize that reactive hyperemia is highly dependent upon the preceding ischemic stimulus.

In a final attempt to explore the relationship between inter-individual differences in the ischemic stimulus and reactive hyperemia, we performed two intervention trials in an effort to manipulate the balance between the ischemic stimulus and microvascular reactivity. In the first experiment, we attempted to acutely impair microvascular function (independent of changes in the ischemic stimulus) by exposing healthy young participants to an ischemia-reperfusion model. Briefly, subjects were exposed to 20 minutes of arterial cuff inflation, followed by 20 minutes of tissue reperfusion. Indeed, this same model has been shown to impair endothelium-dependent vasodilation (Kharbanda et al., 2002; Kharbanda et al., 2001; Loukogeorgakis et al., 2005; Loukogeorgakis et al., 2007). Unfortunately, in contrast to our hypothesis, and a wealth of previous data used to form the rationale for this investigation, ischemia-reperfusion did not cause any impairment in reactive hyperemia (Appendix A). In light of these disappointing results, we then turned our attention to the other side of the equation; namely, skeletal muscle metabolic rate and the ischemic stimulus. Previous studies have indeed shown that even relatively short periods of limb immobilization produce significant reductions in skeletal muscle mitochondrial function (Homma et al., 2009; Kitahara et al., 2003; Motobe et al., 2004), while others have found

reductions in reactive hyperemia and other measures of endothelium-dependent vasodilation (Birk, Dawson, Timothy Cable, Green, & Thijssen, 2013; de Groot, Bleeker, & Hopman, 2006; Kroese, 1977; Silber & Sinoway, 1990). Based upon these studies we hypothesized that limb immobilization would reduce skeletal muscle metabolic rate, and therefore reduce the ischemic stimulus, and therefore proportionately lower the magnitude of reactive hyperemia. The results are summarized in Chapter 5. Individuals underwent forearm immobilization for an average of 28±2 days, using a wrist brace. Despite thorough compliance with the immobilization protocol, and a large body of supporting evidence for which we based our rationale, we found no measurable change in skeletal muscle metabolic rate or reactive hyperemia following limb immobilization. The most likely explanations for why these two intervention studies were unsuccessful are discussed in their respective sub-sections (i.e. Chapter 5, discussion; and Appendix A).

Overall, these investigations have provided novel insight into the complex, and previously overlooked, relationship between skeletal muscle metabolic rate and reactive hyperemia. The main findings, along with our interpretation of the strengths, limitations, and alternative interpretations to our approach are summarized in Chapter 6. More work is indeed needed to further explore the relationship between skeletal muscle function and microvascular reactivity, with particular attention devoted to challenging the balance between these two interrelated endpoints.

References

Benjamin, E. J., Blaha, M. J., Chiuve, S. E., Cushman, M., Das, S. R., Deo, R., . . . Subcomm, S. S. (2017). Heart Disease and Stroke Statistics-2017 Update A Report From the American Heart Association. *Circulation, 135*(10), E146-E603. doi:10.1161/Cir.0000000000000485

Birk, G. K., Dawson, E. A., Timothy Cable, N., Green, D. J., & Thijssen, D. H. (2013). Effect of unilateral forearm inactivity on endothelium-dependent vasodilator function in humans. *Eur J Appl Physiol, 113*(4), 933-940. doi:10.1007/s00421-012-2505-7

Cheatle, T. R., Potter, L. A., Cope, M., Delpy, D. T., Coleridge Smith, P. D., & Scurr, J. H. (1991). Near-infrared spectroscopy in peripheral vascular disease. *Br J Surg, 78*(4), 405-408. doi:10.1002/bjs.1800780408

Conley, K. E., Jubrias, S. A., & Esselman, P. C. (2000). Oxidative capacity and ageing in human muscle. *J Physiol, 526 Pt 1*, 203-210. doi:10.1111/j.1469-7793.2000.t01-1-00203.x

Creteur, J., Carollo, T., Soldati, G., Buchele, G., De Backer, D., & Vincent, J. L. (2007). The prognostic value of muscle StO2 in septic patients. *Intensive Care Med, 33*(9), 1549-1556. doi:10.1007/s00134-007-0739-3

Criqui, M. H., Coughlin, S. S., & Fronek, A. (1985). Noninvasively diagnosed peripheral arterial disease as a predictor of mortality: results from a prospective study. *Circulation, 72*(4), 768-773.

Dakak, N., Husain, S., Mulcahy, D., Andrews, N. P., Panza, J. A., Waclawiw, M., . . . Quyyumi, A. A. (1998). Contribution of nitric oxide to reactive hyperemia: impact of endothelial dysfunction. *Hypertension, 32*(1), 9-15.

de Berrazueta, J. R., Guerra-Ruiz, A., Garcia-Unzueta, M. T., Toca, G. M., Laso, R. S., de Adana, M. S., . . . Llorca, J. (2010). Endothelial dysfunction, measured by reactive hyperaemia using strain-gauge plethysmography, is an independent predictor of adverse outcome in heart failure. *Eur J Heart Fail, 12*(5), 477-483. doi:10.1093/eurjhf/hfq036

de Groot, P. C., Bleeker, M. W., & Hopman, M. T. (2006). Magnitude and time course of arterial vascular adaptations to inactivity in humans. *Exercise and Sport Sciences Reviews, 34*(2), 65-71.

Gokce, N., Keaney, J. F., Jr., Hunter, L. M., Watkins, M. T., Nedeljkovic, Z. S., Menzoian, J. O., & Vita, J. A. (2003). Predictive value of noninvasively determined endothelial dysfunction for long-term cardiovascular events in patients with peripheral vascular disease. *J Am Coll Cardiol, 41*(10), 1769-1775.

Hayoz, D., Weber, R., Rutschmann, B., Darioli, R., Burnier, M., Waeber, B., & Brunner, H. R. (1995). Postischemic blood flow response in hypercholesterolemic patients. *Hypertension, 26*(3), 497-502. doi:10.1161/01.hyp.26.3.497

Higashi, Y., Sasaki, S., Nakagawa, K., Matsuura, H., Kajiyama, G., & Oshima, T. (2001). A noninvasive measurement of reactive hyperemia that can be used to assess resistance artery endothelial function in humans. *American Journal of Cardiology, 87*(1), 121-+. doi:Doi 10.1016/S0002-9149(00)01288-1

Homma, T., Hamaoka, T., Murase, N., Osada, T., Murakami, M., Kurosawa, Y., . . . Katsumura, T. (2009). Low-volume muscle endurance training prevents decrease in muscle oxidative and endurance function during 21-day forearm immobilization. *Acta Physiol (Oxf), 197*(4), 313-320. doi:10.1111/j.1748-1716.2009.02003.x

Huang, A. L., Silver, A. E., Shvenke, E., Schopfer, D. W., Jahangir, E., Titas, M. A., . . . Vita, J. A. (2007). Predictive value of reactive hyperemia for cardiovascular events in patients with peripheral arterial disease undergoing vascular surgery. *Arterioscler Thromb Vasc Biol, 27*(10), 2113-2119. doi:10.1161/ATVBAHA.107.147322

Kharbanda, R. K., Mortensen, U. M., White, P. A., Kristiansen, S. B., Schmidt, M. R., Hoschtitzky, J. A., . . . MacAllister, R. (2002). Transient limb ischemia induces remote ischemic preconditioning in vivo. *Circulation, 106*(23), 2881-2883.

Kharbanda, R. K., Peters, M., Walton, B., Kattenhorn, M., Mullen, M., Klein, N., . . . MacAllister, R. (2001). Ischemic preconditioning prevents endothelial injury and systemic neutrophil activation during ischemia-reperfusion in humans in vivo. *Circulation, 103*(12), 1624-1630. doi:Doi 10.1161/01.Cir.103.12.1624

Kitahara, A., Hamaoka, T., Murase, N., Homma, T., Kurosawa, Y., Ueda, C., . . . Katsumura, T. (2003). Deterioration of muscle function after 21-day forearm immobilization. *Med Sci Sports Exerc, 35*(10), 1697-1702. doi:10.1249/01.MSS.0000089339.07610.5F

Kooijman, H. M., Hopman, M. T., Colier, W. N., van der Vliet, J. A., & Oeseburg, B. (1997). Near infrared spectroscopy for noninvasive assessment of claudication. *J Surg Res, 72*(1), 1-7. doi:10.1006/jsre.1997.5164

Kroese, A. J. (1977). The effect of inactivity on reactive hyperaemia in the human calf: a study with strain gauge plethysmography. *Scand J Clin Lab Invest, 37*(1), 53-58.

London, G. M., Pannier, B., Agharazii, M., Guerin, A. P., Verbeke, F. H., & Marchais, S. J. (2004). Forearm reactive hyperemia and mortality in end-stage renal disease. *Kidney Int, 65*(2), 700-704. doi:10.1111/j.1523-1755.2004.00434.x

Loukogeorgakis, S. P., Panagiotidou, A. T., Broadhead, M. W., Donald, A., Deanfield, J. E., & MacAllister, R. J. (2005). Remote ischemic preconditioning provides early and late protection against endothelial ischemia-reperfusion injury in humans: role of the autonomic nervous system. *J Am Coll Cardiol, 46*(3), 450-456. doi:10.1016/j.jacc.2005.04.044

Loukogeorgakis, S. P., Williams, R., Panagiotidou, A. T., Kolvekar, S. K., Donald, A., Cole, T. J., . . . MacAllister, R. J. (2007). Transient limb ischemia induces remote preconditioning and remote postconditioning in humans by a K(ATP) channel-dependent mechanism. *Circulation, 116*(12), 1386-1395. doi:10.1161/Circulationaha.106.653782

Luhrmann, P. M., Bender, R., Edelmann-Schafer, B., & Neuhauser-Berthold, M. (2009). Longitudinal changes in energy expenditure in an elderly German population: a 12-year follow-up. *European Journal of Clinical Nutrition, 63*(8), 986-992. doi:10.1038/ejcn.2009.1

Miljkovic, N., Lim, J. Y., Miljkovic, I., & Frontera, W. R. (2015). Aging of skeletal muscle fibers. *Ann Rehabil Med, 39*(2), 155-162. doi:10.5535/arm.2015.39.2.155

Mitchell, G. F., Vita, J. A., Larson, M. G., Parise, H., Keyes, M. J., Warner, E., . . . Benjamin, E. J. (2005). Cross-sectional relations of peripheral microvascular function, cardiovascular disease risk factors, and aortic stiffness: the Framingham Heart Study. *Circulation, 112*(24), 3722-3728. doi:10.1161/CIRCULATIONAHA.105.551168

Motobe, M., Murase, N., Osada, T., Homma, T., Ueda, C., Nagasawa, T., . . . Hamaoka, T. (2004). Noninvasive monitoring of deterioration in skeletal muscle function with forearm cast immobilization and the prevention of deterioration. *Dyn Med, 3*(1), 2. doi:10.1186/1476-5918-3-2

O'Donnell, C. J., & Elosua, R. (2008). [Cardiovascular risk factors. Insights from Framingham Heart Study]. *Rev Esp Cardiol, 61*(3), 299-310.

Silber, D. H., & Sinoway, L. I. (1990). Reversible impairment of forearm vasodilation after forearm casting. *J Appl Physiol (1985), 68*(5), 1945-1949. doi:10.1152/jappl.1990.68.5.1945

Volpi, E., Nazemi, R., & Fujita, S. (2004). Muscle tissue changes with aging. *Curr Opin Clin Nutr Metab Care, 7*(4), 405-410.

CHAPTER 2

REACTIVE HYPEREMIA: A REVIEW OF THE METHODOLOGIES, MECHANISMS, AND DEVLEOPING APPROACHES FOR ASSESSING MICROVASCULAR FUNCTION

Introduction

Reactive hyperemia is a well-established technique for non-invasively assessing peripheral microvascular function, and is a powerful predictor of all-cause and cardiovascular morbidity and mortality (Anderson et al., 2011; Huang et al., 2007; Ishibashi et al., 2006; London et al., 2004; Paine et al., 2016). In its simplest form, reactive hyperemia represents the magnitude of limb reperfusion following a brief period of ischemia induced by arterial occlusion. Over the past two decades, investigators have employed a variety of methods to measure reactive hyperemia, including brachial artery velocity by Doppler ultrasound (Huang et al., 2007), tissue reperfusion by near infrared spectroscopy (NIRS) (Kragelj, Jarm, & Miklavcic, 2000; Mayeur, Campard, Richard, & Teboul, 2011; McLay, Nederveen, Pogliaghi, Paterson, & Murias, 2016), limb distension by venous occlusion plethysmography (Crecelius, Richards, Luckasen, Larson, & Dinenno, 2013; de Berrazueta et al., 2010), and peripheral artery tonometry (Bonetti et al., 2004; Matsuzawa, Kwon, Lennon, Lerman, & Lerman, 2015). Regardless of the tools used to measure reactive hyperemia, the fundamental interpretation common to these studies has been that blunted reactive hyperemia signifies (micro)vascular dysfunction.

With reactive hyperemia becoming increasingly more common, and widely used across multiple disciplines, further consideration is needed regarding several aspects of this approach. For example, does each measurement technique provide the same inherent insight? What is the appropriate time course for measuring reactive hyperemia? What impact does skeletal muscle mass and basal metabolic rate have on between-group and/or inter-individual differences? This review aims to address each of these questions, with the hope of bringing the community closer to a standardized approach for both the measurement and analysis of reactive hyperemia in the peripheral circulation. Emphasis is also placed on the physiological mechanism(s) driving reactive hyperemia.

Measurement Approaches: Past, Present, Future

Venous Occlusion Plethysmography

The majority of early studies measuring reactive hyperemia used venous occlusion plethysmography to measure forearm blood flow (FBF) (**Figure 1**), with continued interest in this approach (Crecelius et al., 2013; Dinenno, Masuki, & Joyner, 2005; Farouque & Meredith, 2003). Using this methodology, reactive hyperemia has primarily been reported in two ways: peak forearm blood flow (Banitt, Smits, Williams, Ganz, & Creager, 1996; Crecelius et al., 2013; Engelke, Halliwill, Proctor, Dietz, & Joyner, 1996; Hayoz et al., 1995; Nugent et al., 1999; Tagawa et al., 1994), measured as the highest forearm blood flow measure detected during the hyperemic response, and total forearm blood flow, measured as the area under the forearm blood flow curve throughout the hyperemic response and recovery towards baseline blood flow (Banitt et al., 1996; Crecelius et al., 2013; Engelke et al., 1996; Farouque & Meredith, 2003; Nugent et al., 1999; Tagawa et al., 1994).

Positive aspects of this methodology include its accuracy and high reproducibility owing to the low technical skill required to place the strain gauge. However, like all techniques, venous occlusion plethysmography suffers from several limitations. Most critically, the inflation/deflation approach required to induce changes in limb volume leads to very low temporal resolution, recording only one measurement ever 5-10 seconds. This is suboptimal as it provides only 1-2 data points during the peak response ($\leq$ 30 sec after cuff deflation, therational for this time frame discussed in more detail in later sections). Second, venous occlusion plethysmography is limited to indirect measurements of limb distension, with hemodynamics inferred. Inter-individual and/or between groups differences in tissue vascularization, vascular stiffness (particularly on the venous side), and perfusion pressure may therefore influence the rate and degree to which limb volume changes during a brief period of reperfusion. While steps can be taken to normalize or control for changes in blood pressure and vascular compliance, these extra measures are not universally practiced.

Doppler Ultrasound

With the development of simultaneous velocity measurement and B-mode imaging, as well as advanced analysis tools, duplex ultrasound has become the clinical standard for measuring reactive hyperemia. Using this technique,

investigators have found reductions in peak hyperemic blood flow in subjects with hypercholesterolemia (Hayoz et al., 1995), mean hyperemic blood flow in subjects with elevated systemic inflammation (Vita 2004), and mean hyperemic velocity in subjects exposed to high levels of air pollution (Wilker et al., 2014). Moreover, Philpott et al and Anderson et al found peak velocity-time integral to be predictive of cardiovascular disease and future cardiac events (Anderson et al., 2011; Philpott et al., 2009), while Huang et al found peak blood velocity to be predictive of future cardiac events and mortality (Huang et al., 2007).

While Doppler ultrasound natively outputs blood velocity, blood flow can be calculated using measurements of arterial diameter. To do this, investigators have relied on two main approaches. First, operators have used on-board calipers to take intermittent measurements of the vessel diameter, allowing for the offline calculation of blood flow using the continuously recorded velocity signal. Emerging more recently, the second approach involves continuous video recording of the B-mode image. The video is then analyzed using complex edge-detection software to acquire continuous measures of brachial artery diameter. Interestingly, peak blood flow appears to be less discriminatory than peak velocity (Huang et al., 2007; Rosenberry, Trojacek, Chung, Cipher, & Nelson, 2019); although this result is not universal (Hayoz et al., 1995; Paine et al., 2016; Wilker et al., 2014). Possible reasons for this discrepancy are discussed in subsequent sections.

As evidenced by the above summary, there is currently no universally agreed upon analytical approach for quantifying reactive hyperemia by Doppler ultrasound (**Figure 2**). Investigators have reported peak velocity (Huang et al., 2007; Philpott et al., 2009; Rosenberry, Trojacek, et al., 2019; Woo et al., 2014), peak blood flow (Amar et al., 2003; Harris, Padilla, Rink, & Wallace, 2006; Rosenberry, Trojacek, et al., 2019; Takase, Akima, Uehata, Ohsuzu, & Kurita, 2004), velocity time integral (Anderson et al., 2011; C. R. Lee et al., 2012; Lee, Martin, Fung, & Anderson, 2012), average hyperemic velocity (Mitchell et al., 2004; Rosenberry, Trojacek, et al., 2019; Wilker et al., 2014), and average hyperemic flow (Rosenberry, Trojacek, et al., 2019; Wilker et al., 2014). For reactive hyperemia to be more widely accepted and adapted for clinical evaluation, this variability will need to be addressed.

Among its greatest many strengths, Doppler ultrasound provides excellent temporal and spatial resolution (conduit vessel imaging), and yields data that may be comprehensively analyzed using a multitude of approaches. Doppler imaging is however highly operator dependent, requiring extensive technical training to acquire and continuously image the conduit artery (most commonly the brachial artery). In addition, this technique is sensitive to motion artifact, and even minor disruptions in the probe position can impair both image and velocity signal quality. Finally, even the most economical ultrasound devices are relatively expensive, with analytic software only adding to this cost.

Near-Infrared Spectroscopy

Recently, near-infrared spectroscopy (NIRS) has emerged as an alternative, non-invasive approach to measuring reactive hyperemia. These devices operate by emitting near-infrared light at wavelengths that are differentially absorbed by oxygenated hemoglobin/myoglobin (HbO_2) and deoxygenated hemoglobin/myoglobin (HHb). By measuring the absorbance of light at each wavelength, near-infrared spectrometers can quantify the concentration of both HbO_2 and HHb present in the tissue (Barstow, 2019), and calculate tissue oxygen saturation.

The rate of tissue oxygen re-saturation (i.e. the reperfusion slope) is most commonly used as an index of tissue reperfusion, sharing a strong relationship with post-occlusive brachial artery blood flow (Bopp, Townsend, Warren, & Barstow, 2014). Indeed, studies examining patients with peripheral vascular disease show blunted rates of tissue reperfusion (Cheatle et al., 1991; Cheng et al., 2004; Kooijman, Hopman, Colier, van der Vliet, & Oeseburg, 1997) and prolonged time to achieve maximum tissue saturation (StO_2) (Kooijman et al., 1997). In patients with sepsis, Creteur et al found that reperfusion rate was significantly blunted compared to controls, and that a lack of improvements in reperfusion rate over a 48 hour period were predictive of mortality (Creteur et al., 2007). Although these investigations provide evidence for the utility of NIRS in a clinical/diagnostic role, this approach has not yet been employed in large clinical trials, and thus the utility of NIRS as a predictive of prognostic tool for cardiovascular events or mortality has yet to be determined.

As illustrated in **Figure 3**, there are multiple analytical endpoints that have been reported from NIRS-derived reactive hyperemia. Among these common endpoints are: the reperfusion rate (Cheatle et al., 1991; Cheng et al., 2004; Creteur et al., 2007; Hammer et al., 2019; Kooijman et al., 1997; Lacroix et al., 2012; Mayeur et al., 2011; McLay, Fontana, et al., 2016; McLay, Nederveen, et al., 2016; Rosenberry et al., 2018), maximum tissue saturations (Cheng et al., 2004; Chung et al., 2018; Creteur et al., 2007; Hammer et al., 2019; Kragelj, Jarm, Erjavec, Presern-Strukelj, & Miklavcic, 2001; McLay, Fontana, et al., 2016; McLay, Nederveen, et al., 2016; Rosenberry et al., 2018), and the area under the curve during recovery (Lacroix et al., 2012; Mayeur et al., 2011; Rosenberry et al., 2018; Siafaka et al., 2007). While these studies have established reperfusion rate as the most common investigative endpoint, no such consensus appears to have been reached regarding the other analytical endpoints. Further studies are needed to determine whether maximal tissue saturation and/or the hyperemic recovery area provide additional clinical or predictive value.

From a more technical stand-point, there are multiple forms of near-infrared spectrometers— time domain, continuous wave, and frequency domain— each of which functions differently and provides different assessments of tissue oxygenation (Barstow, 2019). Recent work comparing continuous wave and frequency domain devices has shown that continuous wave devices significantly overestimate important NIRS-derived parameters, including reperfusion slopes (Hammer et al., 2019). This error arises from their assumption of constant tissue optical properties. Conversely, frequency domain devices are capable of measuring tissue absorbance and scatter in real time and thus are not vulnerable to this overestimation (Hammer et al., 2019). This is a critical point of consideration because the rate of tissue reperfusion is arguably the most commonly reported endpoint and appears to provide the most clinical insight. In light of these limitations, caution is warranted when directly comparing results from continuous wave versus frequency domain NIRS devices as differences may be attributable to this overestimation.

This approach holds multiple advantages over the previously described venous occlusion plethysmography and Doppler ultrasound. In addition to measuring reactive hyperemia at the level of the microvasculature, NIRS also

provides insight into skeletal muscle oxygen metabolism in the tissue, a factor we recently identified as a critical determinant of the hyperemic response (Rosenberry, Trojacek, et al., 2019); described in detail in subsequent sections. Although some training is necessary in order to reliably place the NIRS probe and operate the device, studies have shown that it is possible to achieve low inter-operator variability (Lacroix et al., 2012), making this a potentially powerful tool for deployment in large clinical trials or multicenter investigations. Despite these positive attributes, NIRS suffers from several limitations. In order to quantify HbO_2 and HHb, the light must pass through the skin, underlying adipose tissue, and muscle. Consequently, excessive adipose tissue thickness prevents adequate light penetration of the muscle and causes light to scatter prior to reaching the muscle. This poses a confounding limitation when undertaking to study patient populations in whom obesity is common, such as Type 2 diabetes and heart failure.

Peripheral Artery Tonometry

Much like NIRS, peripheral artery tonometry has gained widespread popularity given its ease of use and portability, coupled with the simplicity of the analysis. Unlike the aforementioned techniques, this method assesses reactive hyperemia, not as a velocity or volume, but through changes in the amplitude of pulsations in finger pressure. The primary outcome measure, termed the reactive hyperemia index (RHI) (**Figure 4**) (Bonetti et al., 2004; Celermajer, 2008; Hamburg & Benjamin, 2009), has been employed in numerous investigations and has proven useful for predicting endothelial dysfunction (Kuvin et al., 2003), coronary atherosclerosis (Bonetti et al., 2004), coronary artery disease (Matsue et al., 2014), microvascular dysfunction secondary to sepsis (Darcy et al., 2011), and coronary plaque formation (Schoenenberger et al., 2012). Blunted reactive hyperemia index has been shown to be correlated with risk factors for developing cardiovascular disease (Hamburg et al., 2008), as well increased risk of future adverse cardiac events (Rubinshtein et al., 2010).

It should be noted that RH-PAT is often described as a measure of endothelial function, which naturally breeds comparison with flow-mediated dilation, by far the most ubiquitous clinical tool used to measure endothelium

dependent, shear-mediated dilation of conduit arteries. This comparison is understandable, considering that these two measures offer similar clinical insights and have been shown to be correlated (Matsuzawa et al., 2015; Woo et al., 2014). However, it is likely that RH-PAT is driven by both endothelium dependent and endothelium independent mechanisms. Moreover, RH-PAT does not directly measure vasodilation, but rather augmentations in finger pressure, which are thought to be reflective of microvascular dilation (Darcy et al., 2011; Davis et al., 2009; Dhindsa et al., 2008; Lian & Keaney, 2010; Matsuzawa et al., 2010; Rubinshtein et al., 2010; Woo et al., 2014). In this way, dilation of the microvasculature decreases resistance downstream allowing for the hyperemic surge of blood to reperfuse the limb— greater magnitudes of reperfusion are assumed to arise from more extensively dilated microvessels. Indeed, RH-PAT is correlated with conduit artery hyperemic flow (Dhindsa et al., 2008).

As mentioned, one of the benefits of this technique is that instrumentation and operation are relatively simple; these devices are portable and require minimal operator training in order to operate them effectively. This allows many users to be trained and deployed rapidly, facilitating the use of RH-PAT large clinical settings while ensuring robust inter-operator reproducibility. In addition to being simple to operate, the results are often processed automatically and the reactive hyperemia index supplied to the technician without any further analysis. This may be viewed as a benefit, as it minimizes training and skill requirements for data analysis. However, it also forces users of this device to rely on the “black box” of proprietary software and data analysis methods. In the case of aberrant physiological responses or other artifacts that would necessitate critical analysis of the data, users may find themselves limited by the closed system nature of the device.

Other Techniques

Thus far we have highlighted the most common techniques used for measuring reactive hyperemia, however this is by no means an exhaustive list. For example, reactive hyperemia has also been measured invasively, using

Doppler flow wires inserted into a conduit artery (Dakak et al., 1998; Olivecrona, Gotberg, Harnek, Van der Pals, & Erlinge, 2007). While this approach indeed provides direct, quantitative, assessment of reactive hyperemia, it is not scalable to the clinic or large clinical trials due to its invasiveness and limited accessibility. Arterial spin labeling— a magnetic resonance based approach— has also been used to measure reactive hyperemia, frequently in the lower limb (Englund et al., 2013; Lopez et al., 2015; Raynaud et al., 2001). While this approach avoids many of the limitations associated with invasive Doppler guidewire, does not require contrast injections, does not expose participants to ionizing radiation, and directly measures tissue perfusion (both regionally, as well as across the entire muscle cross-section), it is of course limited in temporal resolution (typically ~4 s), and accessibility; with much higher operating costs than the aforementioned techniques.

Proposed Mechanisms of Reactive Hyperemia

By way of the experimental approach used to study reactive hyperemia (i.e. cuff occlusion of a limb), the fundamental stimulus driving reactive hyperemia is tissue hypoxia; a potent stimulus for vasodilation, with numerous mechanisms proposed (**Figure 5**).

Nitric Oxide

The potent vasoactive effects of nitric oxide (NO) have been studied for decades. Thus it is not surprising that it is among the earliest substances investigated for its role in mediating RH. Central to our discussion is one form of nitric oxide synthesizing enzyme, endothelial nitric oxide synthase (eNOS). When activated, this enzyme oxidizes L-arginine, producing NO and L-citrulline (Stuehr, 2004). Nitric oxide is a highly reactive gas, and diffuses rapidly from the endothelial cell to the underlying vascular smooth muscle where it activates soluble guanylate cyclase. The subsequent production of cyclic guanosine monophosphate and activation of protein kinase G induces vasorelaxation by reducing intracellular calcium concentration. This is achieved through its inhibition of calcium influx through voltage gated calcium channels and through enhanced uptake of calcium by the sarcoplasmic reticulum (Jackson, 2000; Sandoo, van Zanten, Metsios, Carroll, & Kitas, 2010; Zhao, Vanhoutte, & Leung, 2015). Reduced intracellular calcium causes inactivation of myosin light chain kinase and activation of myosin light chain

phosphatase, which reduces actin-myosin cross-bridge formation and vasorelaxation. Protein kinase G also activates potassium channels, hyperpolarizing the myocyte and further contributing to vasorelaxation (Jackson, 2000; Zhao et al., 2015).

Although NO has been well-established as the driving metabolite behind flow-mediated dilation of larger arteries, its role in reactive hyperemia is less clear. One approach that investigators have taken is to measure RH before and after infusion of L-N-monomethyl arginine (L-NMMA), which inhibits the synthesis of nitric oxide. Their hypothesis has been that if RH is significantly reduced following infusion, then NO must be a significant contributor driving the phenomenon. While testing this hypothesis, separate studies by Tagawa et al and Bank et al found that L-NMMA infusion did not reduce peak FBF, but did result in blunted FBF during the minutes following cuff release, as measured using venous occlusion plethysmography (Bank, Sih, Mullen, Osayamwen, & Lee, 2000; Tagawa et al., 1994). Also employing strain gauge plethysmography and L-NMMA, independent studies by Engelke et al and Nugent et al found that neither peak nor total FBF measured in the minutes following cuff deflation were affected by L-NMMA infusion (Engelke et al., 1996; Nugent et al., 1999). Given that NO is a primary driver of flow-mediated dilation (Green, Dawson, Groenewoud, Jones, & Thijssen, 2014; Thijssen et al., 2011), which peaks within approximately 45-90 seconds after cuff deflation (Black, Cable, Thijssen, & Green, 2008; Corretti et al., 2002; Evanoff, Kelly, Steinberger, & Dengel, 2016; Thijssen et al., 2011), it is likely that the role of NO in the sustained hyperemic response is dependent upon shear-stimulated activation of eNOS following cuff deflation, and *not* synthesis of NO during the ischemic period.

Prostaglandins

Unlike NO, which is a highly soluble and rapidly degraded gaseous messenger, prostaglandins are lipid hormones that elicit a range of effects, including vasodilation. Of specific interest is one form of prostaglandin, prostacyclin (PGI_2). Under hypoxic conditions, intracellular calcium concentration rises, leading to the stimulation of phospholipase A, which catalyzes the production of arachidonic acid, the substrate for PGI_2 synthesis by cyclooxygenase (COX) (**Figure 5**) (Michiels, Arnould, Knott, Dieu, & Remacle, 1993). Once produced, PGI_2 can then

bind to receptors on the luminal surface of the endothelium, stimulating the production of cyclic adenosine monophosphate, and subsequent activation of protein kinase A. This enzyme then activates potassium channels, inducing hyperpolarization and smooth muscle relaxation (**Figure 5**) (Edwards, Feletou, & Weston, 2010; Quayle, Nelson, & Standen, 1997).

As with NO, investigators have taken a similar approach to determine the role of prostaglandins in mediating reactive hyperemia, first measuring RH at baseline and then administering a cyclooxygenase inhibitor to quantify the drug-induced decrement. In a study by Engelke et al, RH was measured with strain gauge plethysmography before and after inhibition of COX by orally administered ibuprofen. In this study, the authors found that COX blockade significantly reduced peak FBF, but had no effect on total FBF in the subsequent minutes (Engelke et al., 1996). Conversely, studies by Addor et al, who used lysine acetylsalicylate to block COX, and Kilbom et al, who utilized indomethacin, found that both peak and total FBF were blunted following inhibition of prostaglandin synthesis (Addor et al., 2008; Kilbom & Wennmalm, 1976). These disparate findings may be attributable to differences in both the tools used to measure FBF as well as differences in the drugs used to inhibit COX. To measure FBF, Kilbom et al employed an air-filled rubber cuff which measured pressure changes associated with fluctuations in limb volume. The bladder was calibrated by using known volumes of air and measuring the associated changes in pressure. However, Addor et al. used mercury strain gauge venous occlusion plethysmography, similar to Engelke et al. Another potential explanation for these disparate responses is that each group utilized different drugs, which may lead to variances in COX inhibition. Overall, without further studies employing more uniform methods and achieving more unanimous results, it is not possible to definitively identify prostaglandins as the primary mediator of reactive hyperemia.

Adenosine

Similar to prostaglandins, adenosine elicits its vasoactive effects by binding to membrane-bound receptors, activating an internal G-protein-mediated cascade (**Figure 5**). Binding of adenosine activates adenyl cyclase, stimulating the production of cyclic adenosine monophosphate. This second messenger then activates protein

kinase A, opening potassium channels, resulting in hyperpolarization of the smooth muscle myocyte (Quayle et al., 1997).

In order to assess whether adenosine mediates RH, Carlsson et al (Carlsson, Sollevi, & Wennmalm, 1987) measured FBF during reactive hyperemia using venous occlusion plethysmography. After establishing baseline responses, they assessed RH after administration of theophylline, an adenosine receptor blocker, and dipyridamole which inhibits the re-uptake of adenosine, thus prolonging and enhancing its effects. They found that blocking adenosine blunted the total FBF response, but had no effect on peak forearm blood flow. After administration of dipyridamole, they found that total FBF was elevated, but again there was no augmentation of peak blood flow. These findings suggest that adenosine does not mediate the peak response, but does play a role in the prolonged flow response following ischemia. These findings are at odds with those of Meijer et al (Meijer et al., 2008) who found that dipyridamole significantly enhanced peak hyperemia. Thus, while adenosine would seem to be the ideal mediator of RH, given its direct relationship with tissue ischemia (ATP → ADP → AMP → adenosine) the exact role of adenosine in RH therefore remains equivocal.

Potassium (K^+)

In contrast to adenosine, prostaglandins, and NO, which are all metabolic vasodilators that function by activating an enzymatic signaling cascade, K^+ contributes to the regulation of vascular tone through alterations in the polarization state of both endothelial and vascular smooth muscle cells. In endothelial cells, ATP-sensitive K^+ channels are inhibited by even very low concentrations of ATP (Ko, Han, Jung, & Park, 2008). However, under conditions that lower ATP concentration, such as hypoxia, these channels begin to open (Jackson, 2000, 2017; Nilius & Droogmans, 2001; Quayle et al., 1997; Shimoda & Polak, 2011). The subsequent efflux of K^+ hyperpolarizes the endothelial cell and raises the driving force for Ca^{2+} to enter the cell, leading to the activation of endothelial nitric oxide synthase and phospholipase A, and the subsequent production of NO and PGI_2 respectively (**Figure 5**) (Edwards et al., 2010; Feletou, 2009). These channels can also be opened by protein kinase

A, which is activated following adenosine and prostacyclin binding their respective receptors (Feletou, 2009; Jackson, 2000, 2017; Quayle et al., 1997).

ATP-sensitive K^+ channels are also located on vascular smooth muscle cells and function in the same manner as described above to induce hyperpolarization during hypoxia. Similar to protein kinase A, K^+ channels are also opened by protein kinase G, which is activated as part of the NO signaling cascade (Jackson, 2017) (Jackson 2017). In addition to these mechanisms, studies have shown that Ca^{2+} sensitive K^+ channels are opened in response to low partial pressures of oxygen (Gebremedhin et al., 1994; Shimoda & Polak, 2011). The sum of these activities is increased K^+ efflux, leading to myocyte hyperpolarization and closure of voltage gated Ca^{2+} channels. This results in decreased intracellular calcium concentration, leading to vasorelaxation (**Figure 5**) (Feletou, 2009; Jackson, 2000, 2017; Quayle et al., 1997).

Despite the well-established role of K^+ channels in regulating vascular tone, as we have seen in studies centered on NO and prostaglandins, there are conflicting results surrounding its role in mediating reactive hyperemia. Farouque et al (Farouque & Meredith, 2003) employed venous occlusion plethysmography, and infused glibenclamide to inhibit ATP-sensitive K^+ channels. In this investigation they found that glibenclamide had no effect on the peak FBF response, nor did it attenuate the sustained hyperemia throughout the recovery period. Banitt et al also employed strain gauge venous occlusion plethysmography to measure FBF before and after administering tolbutamide, another ATP-sensitive K^+ channel blocker (Banitt et al., 1996). Similarly, they observed no effect on the peak response following arterial cuff occlusion, but did note that tolbutamide reduced the total hyperemic blood flow during the minutes following deflation of the occlusive cuff. In a third investigation, Crecelius et al infused barium chloride ($BaCl_2$), another K^+ channel blocker. Unlike either of the previously mentioned investigations, there was a significant attenuation in both the peak and total FBF following $BaCl_2$ infusion (Crecelius et al., 2013).

These findings provide interesting points of discussion, as they each observed different contributions of K^+ channels to reactive hyperemia. Despite each using the same technique (i.e. arterial cuff occlusion), and analytical

approaches, these three studies yielded three conflicting interpretations. One potential, if not probable, explanation for these conflicting results is the different pharmacological agent used in each of the studies. Glibenclamide and tolbutamide are members of the sulfonylurea class of drugs, which specifically inhibits ATP-sensitive K^+ channels. Conversely, $BaCl_2$ inhibits inwardly rectifying K^+ channels, but has also been shown to inhibit ATP-sensitive K^+ channels (Tykocki, Boerman, & Jackson, 2017) albeit at much higher concentrations than those utilized by Creclius et al (Crecelius et al., 2013). Nevertheless, it is possible that differences in specificity, potency, and dosage between these agents may underlie the disparity in these findings.

Methodological Considerations

Temporal Considerations

Reactive hyperemia is the rapid and exaggerated reperfusion following a period of ischemia. Vasodilation in response to ischemia markedly reduces resistance in the microvasculature, allowing the hyperemic surge to reperfuse the oxygen-starved tissue, thus correcting the ischemic error signal before recovering to a basal state. Under this assumption, the rate or magnitude of reperfusion is proportional to the microvasculature's ability to dilate during ischemia.

When measurements are taken immediately following the release of the occlusive cuff ($\leq$ 30 sec), they provide insight into the truly *reactive* phase of reperfusion, i.e. the blood flow response arising entirely from the ischemic stimulus and the resulting microvascular dilation. As measurements are continued beyond this initial phase, the hyperemic response, and associated shear along the blood vessels in the experimental limb, confound the assessment by stimulating vessel dilation and increasing overall flow (Evanoff et al., 2016; Pyke & Tschakovsky, 2005).

Strictly speaking, reactive hyperemia is meant to reflect the *microvasculature's* ability to dilate in response to a period of acute ischemia. Therefore, one may draw the distinction between "reactive" hyperemia, and "responsive" hyperemia, which we view as being mediated or sustained by factors arising *after* or *because* of the initial hyperemic surge of blood. Reactive hyperemia is inherently a negative feedback loop, the purpose of which

is to correct the ischemic error signal and restore the tissue to a homeostatic state. Therefore, it is also important to consider potential differences in skeletal muscle oxidative ability. Individuals who exhibit impaired diffusive oxygen conductance and/or mitochondrial dysfunction may require a prolonged period of sustained hyperemia before returning to homeostasis. Correction of the "error signal" is therefore equally confounding to the interpretation of blood flow beyond the initial *reactive period*.

Taken together, careful consideration is warranted when interpreting data collected beyond the reactive period, which we estimate to be < 30 seconds after tissue reperfusion.

Ischemic Stimulus

As previously discussed, reactive hyperemia is a well-established clinical tool and has a demonstrated record of predictive and prognostic power. Under the conventional view, reactive hyperemia predicts cardiovascular events and mortality because of its ability to detect impaired vasodilatory function. This interpretation assumes that the stimulus to dilate (e.g. standardized 5 minute arterial cuff occlusion) is either effectively equal across all subjects or that it is not an important contributor to the hyperemic response, and thus any reductions in the magnitude of reperfusion reflect impairments in microvascular dilatory function. Given that inter-individual differences exist in basal skeletal metabolic rate (Conley, Jubrias, & Esselman, 2000; Luhrmann, Bender, Edelmann-Schafer, & Neuhauser-Berthold, 2009), it is reasonable to assume that the degree of ischemia, to the same period of arterial cuff occlusion, is not equal across individuals or groups of individuals (e.g. patients vs. controls).

In a recent publication from our laboratory, we sought to investigate age-dependent differences in reactive hyperemia following a 5-minute cuff occlusion using NIRS. We hypothesized that the reperfusion rate, defined as the tissue saturation slope immediately following deflation of the occlusive cuff, would be blunted; evidence of microvascular dysfunction (Rosenberry et al., 2018). While we observed a marked reduction in the reperfusion slope between groups, in response to the same 5 minute arterial cuff occlusion, we also noted significant differences in the rate at which tissue saturation declined (**Figure 6C**), leading to significant differences in the minimum tissue saturation achieved during the fixed occlusive period (**Figure 6D**). This led us to hypothesize that

perhaps the group differences in minimum tissue saturation contributed significantly to the difference in reperfusion rate. To test this hypothesis, we also performed a 3-minute cuff occlusion in a group of young individuals. Because the young individuals desaturated at a greater rate relative to the elderly individuals, they were able to achieve the same minimum tissue saturation in 3 minutes as the elderly individuals achieved in 5 minutes. After standardizing the minimum tissue saturation between groups by altering the occlusion time, group differences in tissue reperfusion rate were eliminated (**Figure 6G**). We have since extended these findings by integrating Doppler-derived measures of brachial artery blood velocity with measures of tissue saturation to characterize the relationship between the ischemic stimulus and reactive hyperemia (Rosenberry, Trojacek, et al., 2019) (**Figure 7**).

Although future studies are necessary to further probe this relationship, these data demonstrate the utility of ischemic stimulus quantification in characterizing the balance between microvascular and skeletal muscle oxidative function as determinants of the hyperemic response. This approach may assist investigators and clinicians in identifying underlying phenotypic differences within patient populations, e.g. impaired vascular function versus impaired skeletal muscle oxidative function. By differentiating these phenotypes, one can then provide more individualized treatment by targeting the vascular or metabolic deficit specifically.

Emerging Future Direction

More recently, our lab has explored the utility of near-infrared diffuse correlation spectroscopy (Rosenberry, Tucker, et al., 2019; Tucker et al., 2019), a validated optical imaging approach regarded as a direct measure of skeletal muscle microvascular perfusion. This approach has indeed been validated against laser Doppler (Shang, Chen, Toborek, & Yu, 2011), Xenon-CT (Kim et al., 2010), microsphere flow measurements (Zhou et al., 2009), arterial spin labeling (Yu et al., 2007), and Doppler ultrasound (Bangalore-Yogananda et al., 2018), and has been used most recently for measuring skeletal muscle (Baker et al., 2017; Carp, Farzam, Redes, Hueber, & Franceschini, 2017; Gurley, Shang, & Yu, 2012; Hammer et al., 2018; Henry et al., 2015) and cerebral perfusion (Shang, Li, & Yu, 2017).

Here we show a representative record collected in our laboratory from a young healthy individual (**Figure 8**). Doppler ultrasound blood velocity is overlaid on the same time scale as DCS-derived blood flow index, showing a remarkably different temporal pattern. Indeed, peak brachial artery reactive hyperemia is evident immediately following deflation of the cuff, peaking within ≈15 seconds before returning towards baseline. Conversely, DCS-derived blood flow index exhibits a more gradual rise before plateauing and then recovering towards baseline. While we find these data intriguing, before this novel approach can be incorporated into the "main stream", several important questions will need to first be addressed. For example, which analytical end-point best reflects "microvascular function": peak BFI, time to peak BFI, or area under the curve? How do we explain the apparent dissociation between the conduit velocity and microvascular perfusion? Do these measures simply reflect differing transit times, or are they measuring actual differences along the arterial-to-capillary cascade?

Summary

In summary, there are a variety of techniques that have been employed to measure reactive hyperemia. The ideal technique with which to measure reactive hyperemia is one that is reproducible, reasonably accessible, has excellent temporal resolution, and provides comprehensive data output enabling investigators to analyze and report all relevant endpoints (**Table 1**). Consensus is needed regarding several fundamental aspects, including the time course for which measurements can/should be made. Moreover, investigators need to consider the role of skeletal muscle metabolic rate on the ischemic stimulus, and move towards controlling for this important variable in future investigations. With many recent methodological advancements, more comprehensive reporting of outcome measures, and improved assessment of the ischemic stimulus, reactive hyperemia has the potential to provide even greater clinical utility for investigating microvascular function across the health span.

Figures and Tables

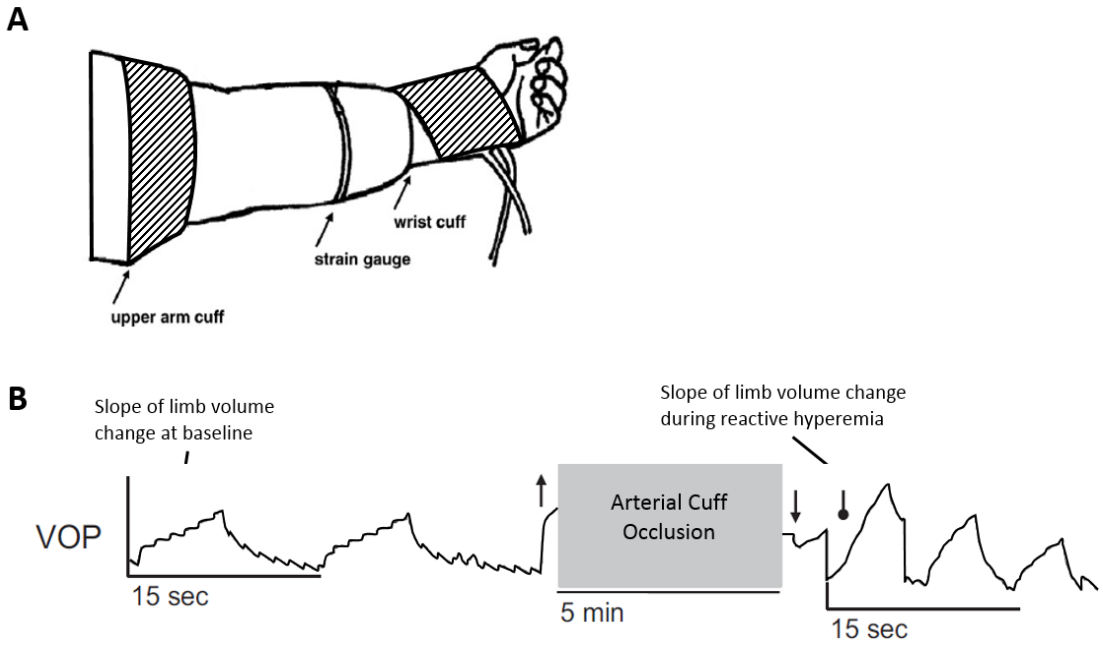

Figure 1. Measuring Reactive Hyperemia with Venous Occlusion Plethysmography
A) A cuff placed around the upper arm is inflated to induce ischemia, and subsequently, reactive hyperemia. The strain gauge is placed around the largest part of the forearm to detect changes in limb volume. Just prior to the end of the ischemic period, a cuff placed around the wrist is inflated to suprasystolic pressures, preventing blood from flowing into the hand and confounding measures of forearm blood flow. B) At the prescribed time, the upper arm cuff is deflated and then quickly re-inflated at a lower pressure sufficient to arrest the venous circulation while allowing the higher-pressure arterial circulation to perfuse the forearm. This low-pressure cuff is then rapidly inflated and deflated at short, regular intervals over the following minutes. During each low-pressure inflation, arterial blood floods into the limb while venous blood is prevented from exiting. The engorged vasculature causes the limb to swell sufficiently to increase limb volume. By measuring the rate of change in forearm volume, arterial blood flow can be inferred. *Panel A adapted from Riksen et al 2008; Panel B adapted from Crecelius et al 2013*

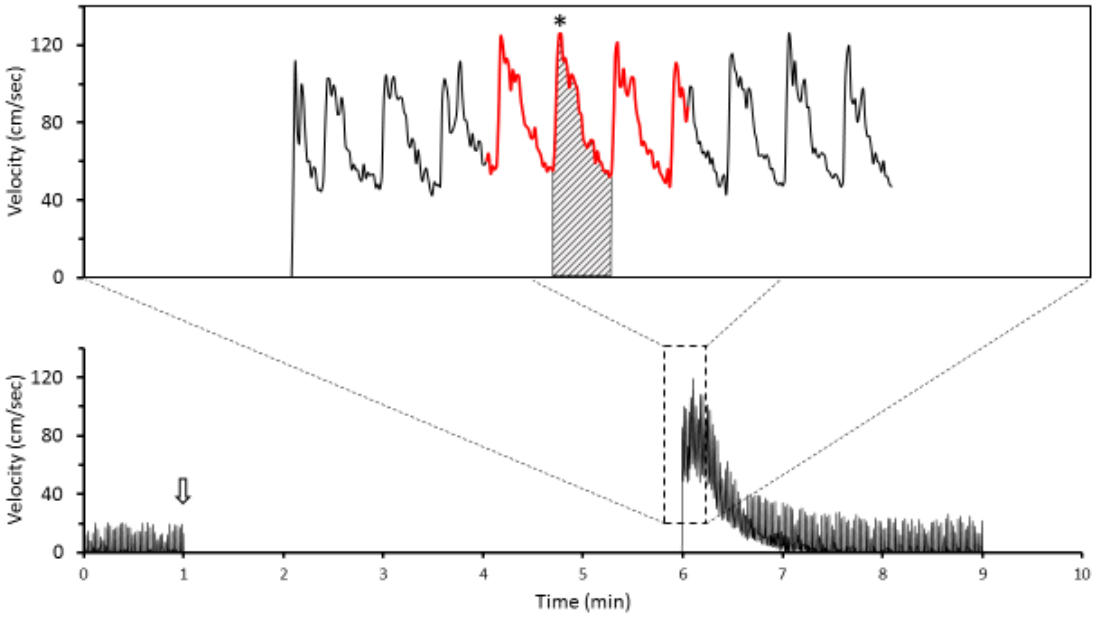

Figure 2. Measurement of Reactive Hyperemia by Doppler Ultrasound
XX year old, healthy male; Bottom: Following establishment of a stable, baseline brachial artery velocity, the occlusive cuff is inflated (arrow), preventing blood from flowing through the brachial artery. The cuff remains inflated for 5 minutes causing the tissue distal to the cuff to become ischemic. After the 5 minutes of arterial occlusion have elapsed, the cuff is rapidly deflated (minute 6) whereupon reactive hyperemia occurs. Top: The initial 15 seconds of the hyperemic response have been expanded to highlight common analytical endpoints. The asterisk indicates peak brachial artery velocity from a single cardiac cycle; the red trace represents a 5-second selection of the peak response. 5-second average hyperemic velocity and hyperemic flow may be calculated from this selection; the shaded region represents the area under curve (velocity time integral) of the highest velocity cardiac cycle.

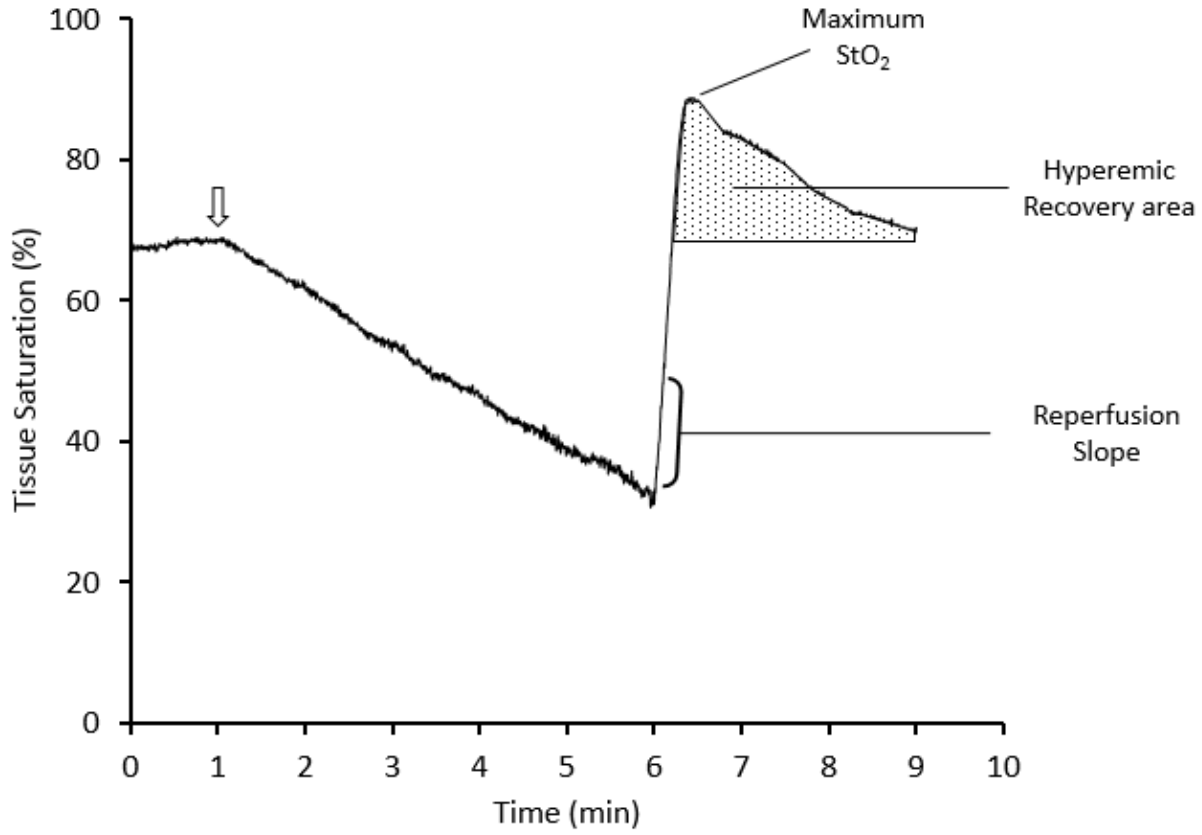

Figure 3. Near-infrared-derived tissue saturation profile during and after a 5-minute cuff occlusion
Tissue saturation profile from a healthy, 20 year old male. Beginning from a stable tissue saturation, the occlusive cuff is inflated on the arm (arrow). During the following 5-minutes, continued oxygen consumption in the absence of arterial oxygen delivery causes the muscle to desaturate. After 5 minutes of occlusion, the cuff is released and the tissue is rapidly reperfused. The reperfusion slope, maximum StO_2, and hyperemic recovery area have been previously evaluated as representative measures of tissue reactive hyperemia.

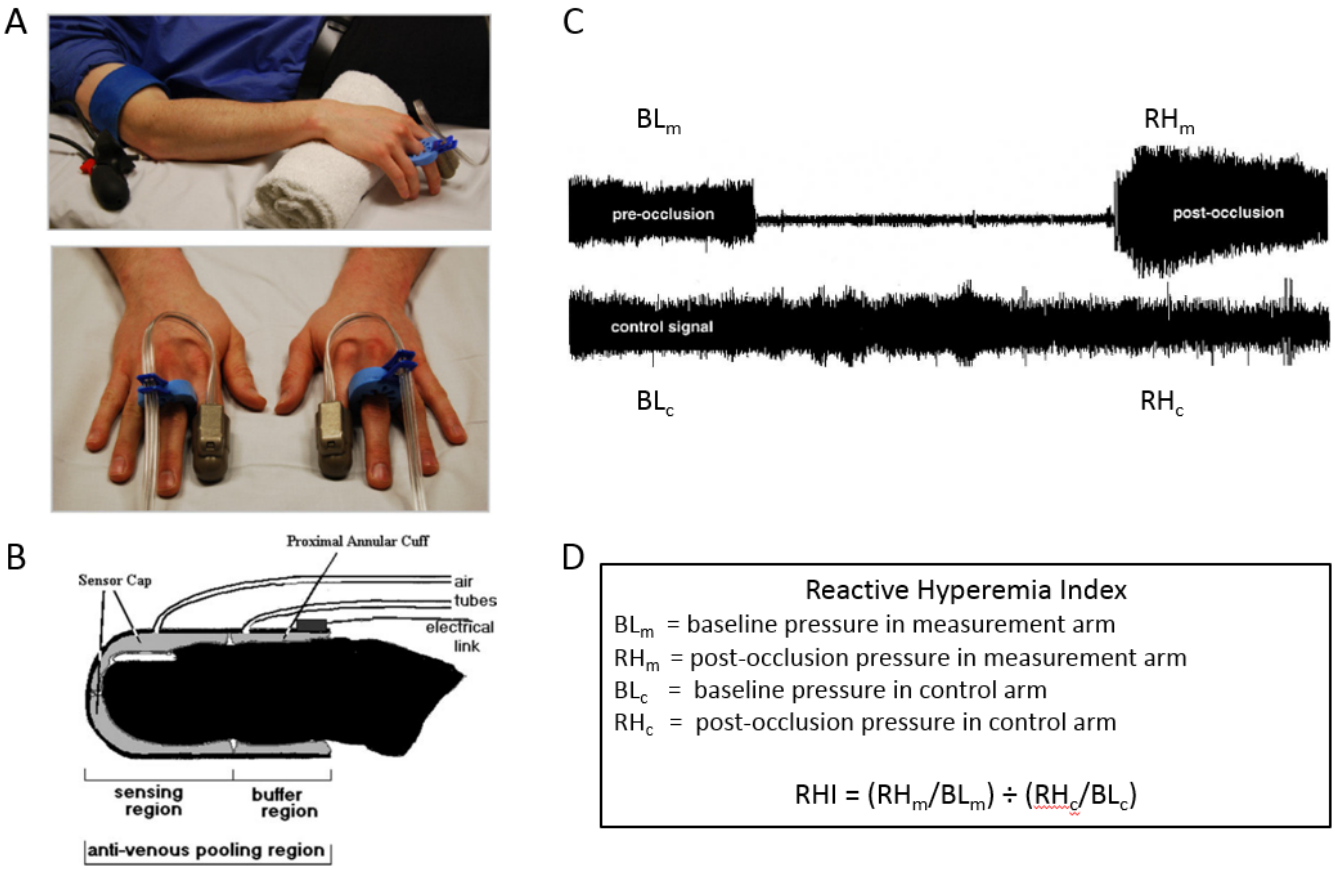

Figure 4. Measuring Reactive Hyperemia with Pulse Wave Tonometry

A) An occlusive cuff is placed around one of the subject's upper arms. Their arms are rested in a slightly elevated position to facilitate venous draining of the finger. B) Pressure-sensitive, thimble-like cuffs are placed on the middle finger of each hand. C) After establishing a stable baseline, the cuff is inflated on the measurement arm for a predetermined period of time eliminating the pressure pulsations in the finger. After the occlusive period has elapsed, the arm cuff is deflated. The hyperemic surge of blood causes the amplitude of finger blood pressure to increase in the measurement limb. D) Reactive hyperemia index (RHI) is determined by calculating the ratio between the hyperemic pressure (RH_m) and baseline pressure (BL_m) in the measurement and control arms (RH_c, BL_c respectively). The ratio between these two quotients is then calculated yielding the RHI. Further transformations or adjustment factors may be applied to this ratio to account for baseline fluctuations or non-linearity of the response. *Adapted from Hamburg et al 2009 (A), Celermajer et al 2008 (B), and Bonetti et al 2004 (C)*

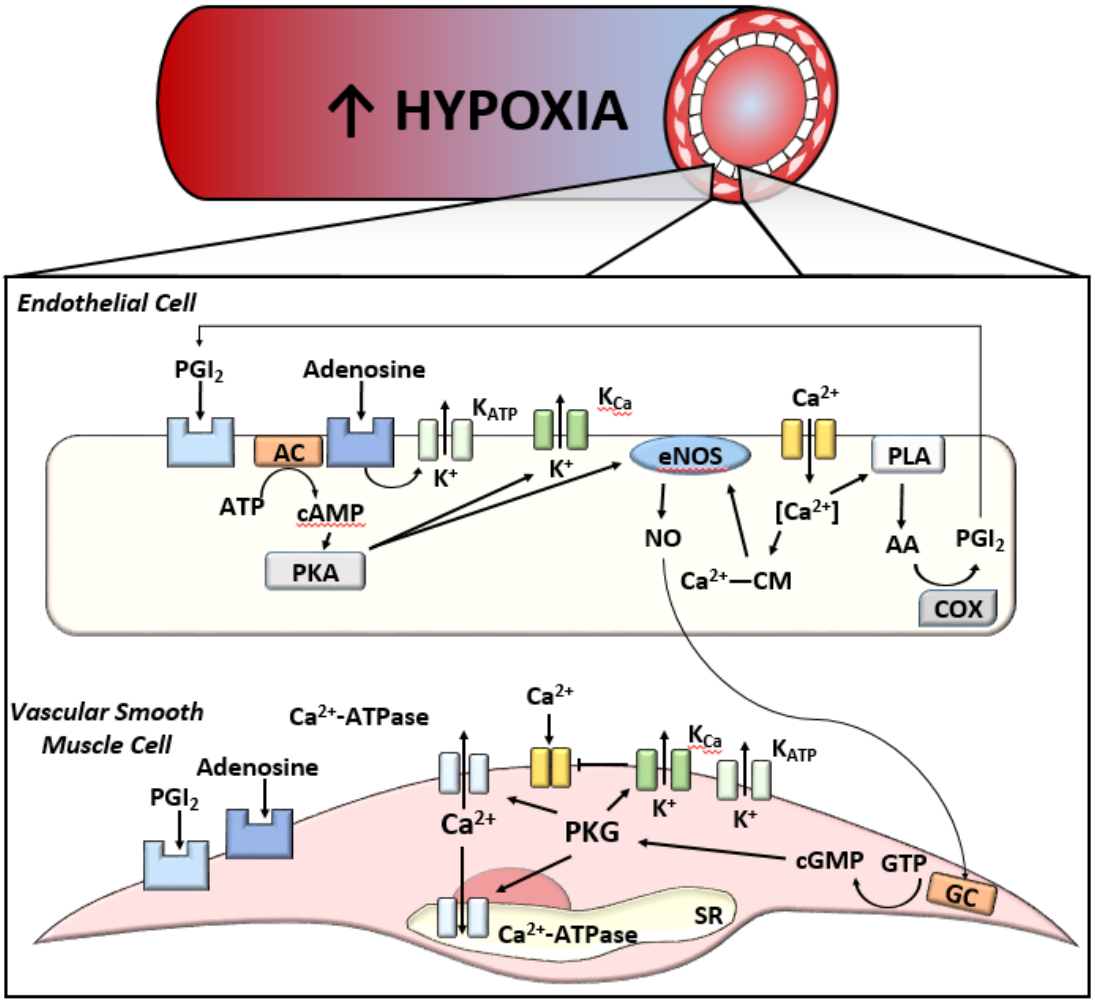

Figure 5. Mechanisms of Vasorelaxation Mediating Reactive Hyperemia

Hypoxia stimulates vasodilation through redundant mechanisms involving prostacyclin (PGI_2), adenosine, nitric oxide (NO), and K^+-channel mediated hyperpolarization. Adenosine and PGI_2 binding their receptors leads to the activation of adneyl cyclase (AC). This enzyme catalyzes the production of cyclic adenosine monophosphate (cAMP) from adenosine triphosphate (ATP). This second messenger then activates protein kinase A (PKA), which goes on to directly activate endothelial nitric oxide synthase (eNOS), increasing the production of nitric oxide (NO). Adenosine receptor binding also activates ATP-sensitive potassium channels (K_{ATP}), while PKA activates calcium sensitive potassium channels (K_{Ca}). K^+-channel activation causes the efflux of K^+ from the cell, resulting in hyperpolarization. Endothelial cell hyperpolarization raises the driving force for Ca^{2+} to enter the cell. Increased intracellular calcium concentration promotes Ca^{2+} binding to calmodulin, which also activates eNOS, and increases NO production. Increased intracellular Ca^{2+} also activates phospholipase A (PLA) which catalyzes the production of arachidonic acid (AA), which is converted by cyclooxygenase (COX) into PGI_2. When released by the endothelial cell, PGI_2 can bind in an autocrine or paracrine fashion to further stimulate this cascade. Once produced, NO rapidly diffuses out of the endothelial cell and into the underlying vascular smooth muscle where it activates guanylyl cyclase (GC). This enzyme converts guanosine triphosphate (GTP) into cyclic guanosine monophosphate (cGMP). This messenger then activates protein kinase G (PKG). PKG mediates vasorelaxation by activating potassium channels (K_{Ca}), causing them to efflux K^+. The resulting hyperpolarization causes voltage sensitive Ca^{2+} channels to close, preventing Ca^{2+}influx. PKG also activates Ca^{2+}-ATPase pumps, increasing expulsion of Ca^{2+} from the myocyte and sequestration of Ca^{2+} into the sarcoplasmic reticulum (SR). The net result of these actions is decreased intracellular Ca^{2+} concentration, shifting the balance in activity between myosin light chain kinase (MLCK) and myosin light chain phosphatase (MLCP) to favor phosphatase activity. This decreases the phosphorylation of myosin, thus reducing smooth muscle contraction.

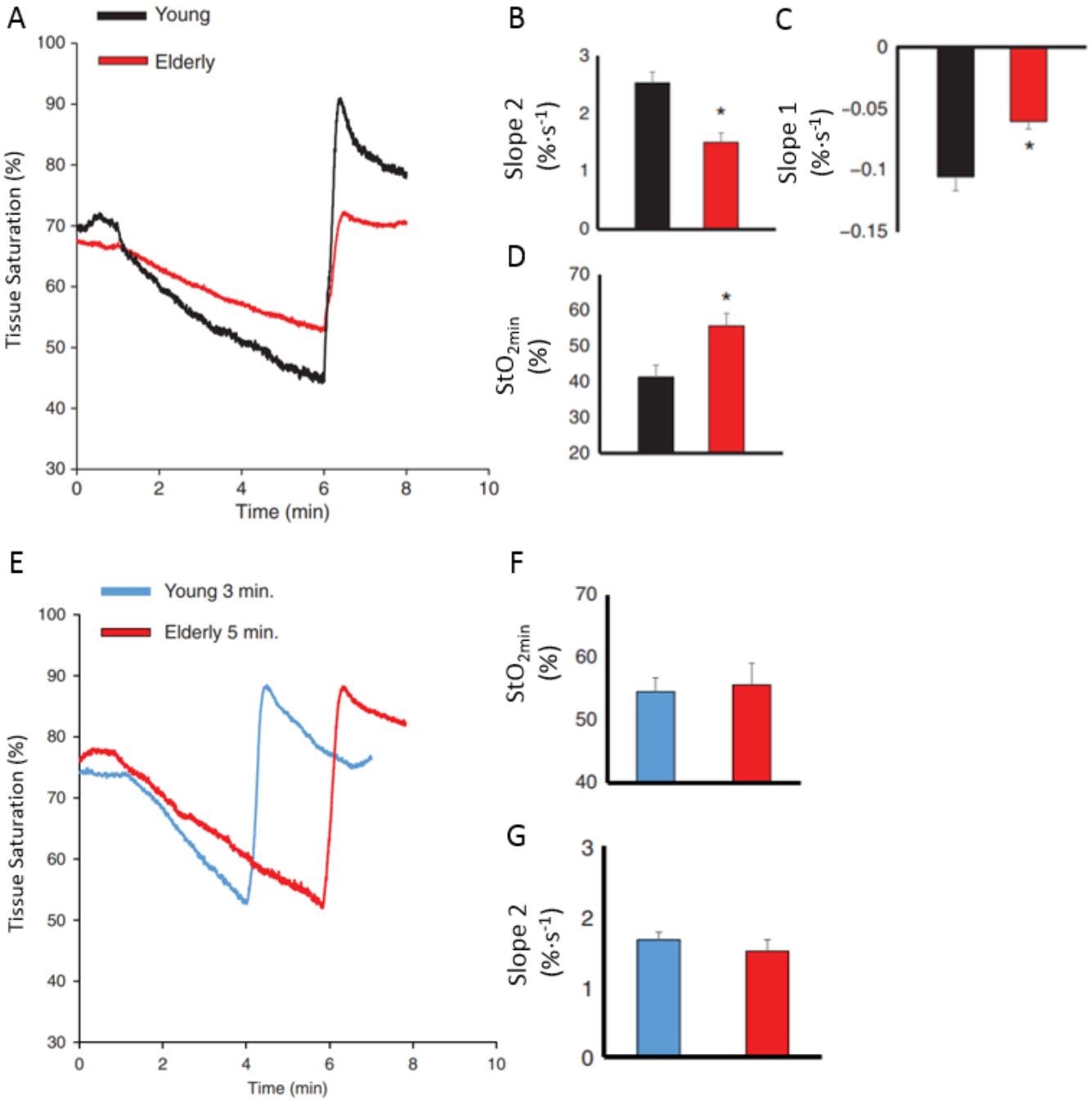

Figure 6. Age-dependent differences in tissue saturation profiles during and after a 5-minute cuff occlusion
A) Representative tissue saturation tracings from one young (black) and one elderly individual (red) during a 5-minute arterial cuff occlusion. B) Reperfusion rates following release of the occlusive cuff. C) Desaturation rates during the 5-minute arterial occlusion. D) Minimum tissue saturations measured in the final moments before deflating the cuff.
E) Representative tissue saturation tracings from one young individual during 3-minutes of occlusion (blue) and one elderly individual during a 5-minute arterial cuff occlusion (red). F) Minimum tissue saturations, controlled for by adjusting the duration of cuff occlusion. G) Reperfusion rates after controlling for occlusion time are not different between young and elderly individuals. (Adapted from Rosenberry et al 2018)

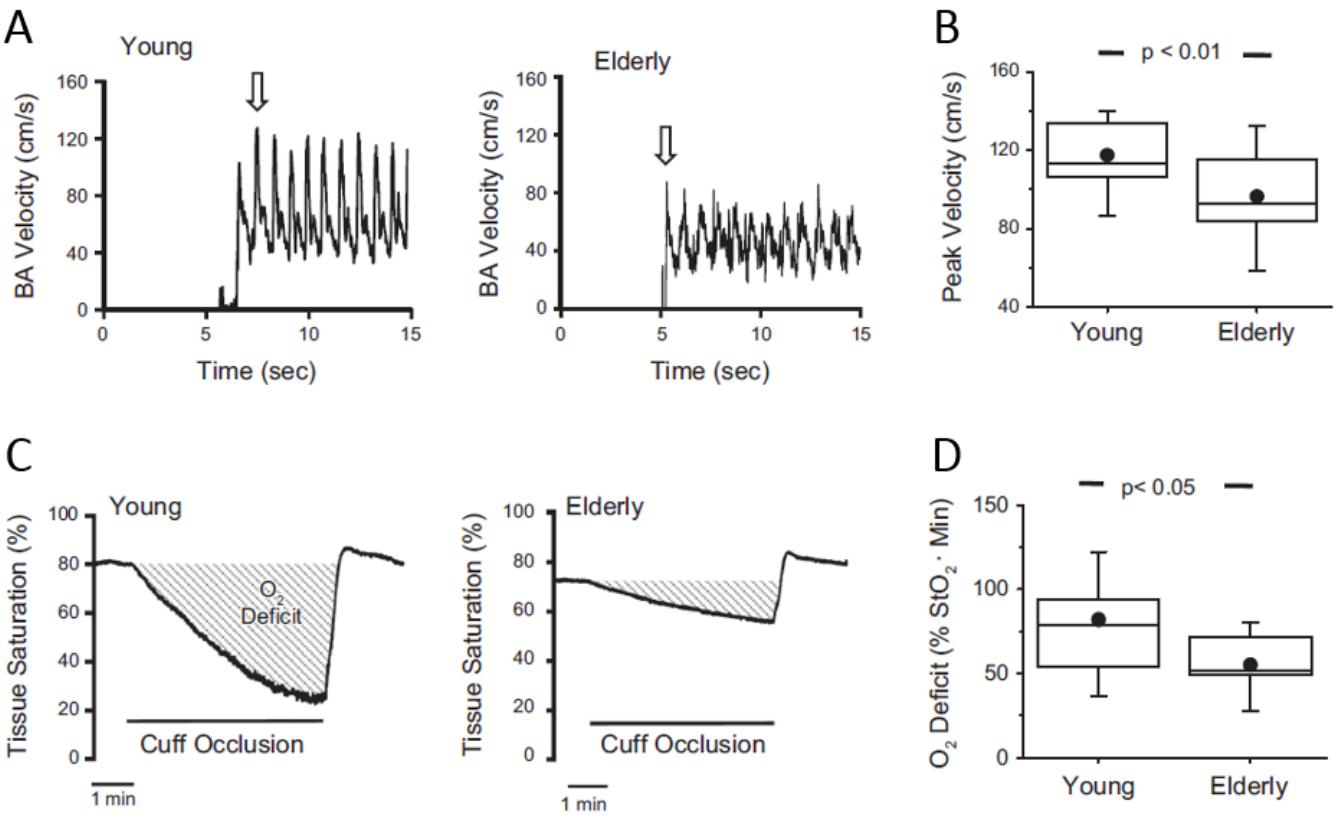

Figure 7. Age-dependent differences in brachial artery velocity and tissue saturation during and after 5-minutes of arterial occlusion

A) Representative brachial artery velocity tracings from one young (left) and one elderly (right) individual following 5 minutes of occlusion. Arrow indicates peak velocity. B) Group data from 12 young and 11 elderly individuals showing significant differences in peak brachial artery velocity. C) Tissue saturation tracings from the same young and elderly individuals shown in A. The shaded region represents the oxygen deficit incurred during arterial occlusion, referred to as the ischemic stimulus. D) Group data from 12 young and 11 elderly individuals showing significantly lower oxygen deficit in the elderly group. (*Adapted from Rosenberry et al, Am J Physiol Regul Integr Comp Physiol 2019*)

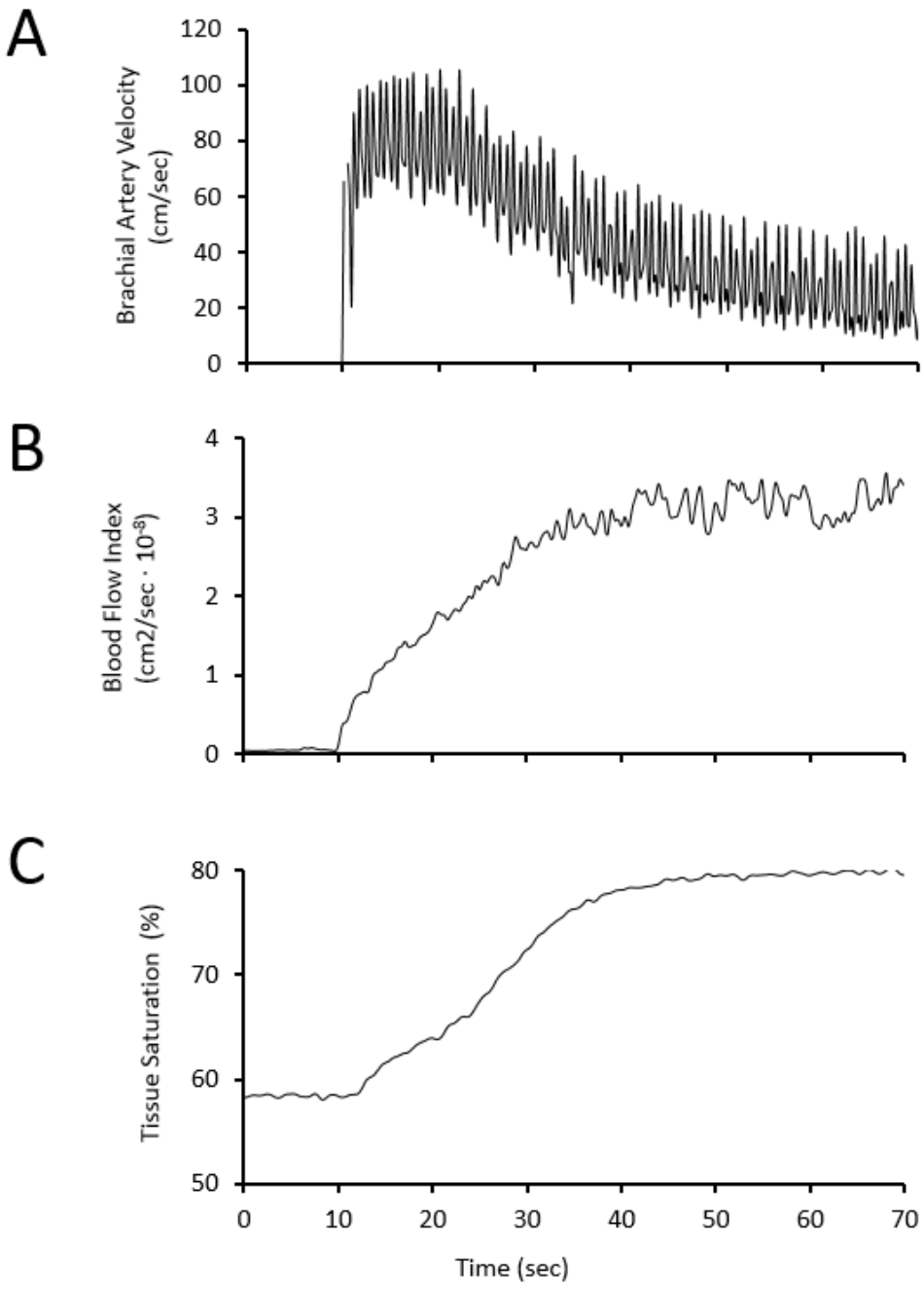

Figure 8. Brachial artery velocity, blood flow index, and tissue saturation during reactive hyperemia
Representative tracings from a young, healthy male individual. Data displays the final 10-seconds of a 5-minute cuff occlusion and the first 60 seconds following release of the occlusive cuff. Visual inspection of A) Doppler-derived brachial artery velocity B) DCS-derived blood flow index and C) NIRS-derived tissue saturation reveal dissociated hyperemic kinetics.

Table 1. Benefits and Limitations of Reactive Hyperemia Techniques

	Benefits	Limitations
Venous Occlusion Plethysmography	*Low requirement for technical training, simple operation and analysis*	*Poor temporal resolution, only indirectly measures blood flow by tracking changes in limb volume*
Doppler Ultrasound	*High temporal resolution, comprehensive evaluation of hyperemic response, direct measure of conduit artery hemodynamics*	*High degree of technical training required and cost-prohibitive unit price may prevent deployment in large, multi-center studies*
RH-PAT	*High temporal resolution, low technical training, simple instrumentation, easily graspable, indexed data output*	*Limited exportation of raw data precluding more critical, in-depth analysis*
NIRS	*High temporal resolution, measures reactive hyperemia at the level of the tissue, provides important quantification of the ischemic stimulus*	*Less accessible, requires moderate degree of technical training to operate*

References

Addor, G., Delachaux, A., Dischl, B., Hayoz, D., Liaudet, L., Waeber, B., & Feihl, F. (2008). A comparative study of reactive hyperemia in human forearm skin and muscle. *Physiol Res, 57*(5), 685-692.

Amar, S., Gokce, N., Morgan, S., Loukideli, M., Van Dyke, T. E., & Vita, J. A. (2003). Periodontal disease is associated with brachial artery endothelial dysfunction and systemic inflammation. *Arterioscler Thromb Vasc Biol, 23*(7), 1245-1249. doi:10.1161/01.ATV.0000078603.90302.4A

Anderson, T. J., Charbonneau, F., Title, L. M., Buithieu, J., Rose, M. S., Conradson, H., . . . Lonn, E. M. (2011). Microvascular function predicts cardiovascular events in primary prevention: long-term results from the Firefighters and Their Endothelium (FATE) study. *Circulation, 123*(2), 163-169. doi:10.1161/CIRCULATIONAHA.110.953653

Baker, W. B., Li, Z., Schenkel, S. S., Chandra, M., Busch, D. R., Englund, E. K., . . . Mohler, E. R., 3rd. (2017). Effects of exercise training on calf muscle oxygen extraction and blood flow in patients with peripheral artery disease. *J Appl Physiol (1985), 123*(6), 1599-1609. doi:10.1152/japplphysiol.00585.2017

Bangalore-Yogananda, C. G., Rosenberry, R., Soni, S., Liu, H., Nelson, M. D., & Tian, F. (2018). Concurrent measurement of skeletal muscle blood flow during exercise with diffuse correlation spectroscopy and Doppler ultrasound. *Biomed Opt Express, 9*(1), 131-141. doi:10.1364/boe.9.000131

Banitt, P. F., Smits, P., Williams, S. B., Ganz, P., & Creager, M. A. (1996). Activation of ATP-sensitive potassium channels contributes to reactive hyperemia in humans. *Am J Physiol, 271*(4 Pt 2), H1594-1598. doi:10.1152/ajpheart.1996.271.4.H1594

Bank, A. J., Sih, R., Mullen, K., Osayamwen, M., & Lee, P. C. (2000). Vascular ATP-dependent potassium channels, nitric oxide, and human forearm reactive hyperemia. *Cardiovasc Drugs Ther, 14*(1), 23-29.

Barstow, T. J. (2019). Understanding near infrared spectroscopy and its application to skeletal muscle research. *J Appl Physiol (1985), 126*(5), 1360-1376. doi:10.1152/japplphysiol.00166.2018

Black, M. A., Cable, N. T., Thijssen, D. H., & Green, D. J. (2008). Importance of measuring the time course of flow-mediated dilatation in humans. *Hypertension, 51*(2), 203-210. doi:10.1161/HYPERTENSIONAHA.107.101014

Bonetti, P. O., Pumper, G. M., Higano, S. T., Holmes, D. R., Jr., Kuvin, J. T., & Lerman, A. (2004). Noninvasive identification of patients with early coronary atherosclerosis by assessment of digital reactive hyperemia. *J Am Coll Cardiol, 44*(11), 2137-2141. doi:10.1016/j.jacc.2004.08.062

Bopp, C. M., Townsend, D. K., Warren, S., & Barstow, T. J. (2014). Relationship between brachial artery blood flow and total [hemoglobin+myoglobin] during post-occlusive reactive hyperemia. *Microvasc Res, 91*, 37-43. doi:10.1016/j.mvr.2013.10.004

Carlsson, I., Sollevi, A., & Wennmalm, A. (1987). The role of myogenic relaxation, adenosine and prostaglandins in human forearm reactive hyperaemia. *J Physiol, 389*, 147-161.

Carp, S. A., Farzam, P., Redes, N., Hueber, D. M., & Franceschini, M. A. (2017). Combined multi-distance frequency domain and diffuse correlation spectroscopy system with simultaneous data acquisition and real-time analysis. *Biomed Opt Express, 8*(9), 3993-4006. doi:10.1364/BOE.8.003993

Celermajer, D. S. (2008). Reliable endothelial function testing: at our fingertips? *Circulation, 117*(19), 2428-2430. doi:10.1161/CIRCULATIONAHA.108.775155

Cheatle, T. R., Potter, L. A., Cope, M., Delpy, D. T., Coleridge Smith, P. D., & Scurr, J. H. (1991). Near-infrared spectroscopy in peripheral vascular disease. *Br J Surg, 78*(4), 405-408. doi:10.1002/bjs.1800780408

Cheng, X., Mao, J. M., Xu, X., Elmandjra, M., Bush, R., Christenson, L., . . . Bry, J. (2004). Post-occlusive reactive hyperemia in patients with peripheral vascular disease. *Clin Hemorheol Microcirc, 31*(1), 11-21.

Chung, S., Rosenberry, R., Ryan, T. E., Munson, M., Dombrowsky, T., Park, S., . . . Nelson, M. D. (2018). Near-infrared spectroscopy detects age-related differences in skeletal muscle oxidative function: promising implications for geroscience. *Physiol Rep, 6*(3). doi:10.14814/phy2.13588

Conley, K. E., Jubrias, S. A., & Esselman, P. C. (2000). Oxidative capacity and ageing in human muscle. *J Physiol, 526 Pt 1*, 203-210. doi:10.1111/j.1469-7793.2000.t01-1-00203.x

Corretti, M. C., Anderson, T. J., Benjamin, E. J., Celermajer, D., Charbonneau, F., Creager, M. A., . . . International Brachial Artery Reactivity Task, F. (2002). Guidelines for the ultrasound assessment of endothelial-dependent flow-mediated vasodilation of the brachial artery: a report of the International Brachial Artery Reactivity Task Force. *J Am Coll Cardiol, 39*(2), 257-265.

Crecelius, A. R., Richards, J. C., Luckasen, G. J., Larson, D. G., & Dinenno, F. A. (2013). Reactive hyperemia occurs via activation of inwardly rectifying potassium channels and Na+/K+-ATPase in humans. *Circ Res, 113*(8), 1023-1032. doi:10.1161/CIRCRESAHA.113.301675

Creteur, J., Carollo, T., Soldati, G., Buchele, G., De Backer, D., & Vincent, J. L. (2007). The prognostic value of muscle StO2 in septic patients. *Intensive Care Med, 33*(9), 1549-1556. doi:10.1007/s00134-007-0739-3

Dakak, N., Husain, S., Mulcahy, D., Andrews, N. P., Panza, J. A., Waclawiw, M., . . . Quyyumi, A. A. (1998). Contribution of nitric oxide to reactive hyperemia: impact of endothelial dysfunction. *Hypertension, 32*(1), 9-15.

Darcy, C. J., Davis, J. S., Woodberry, T., McNeil, Y. R., Stephens, D. P., Yeo, T. W., & Anstey, N. M. (2011). An observational cohort study of the kynurenine to tryptophan ratio in sepsis: association with impaired immune and microvascular function. *PLoS One, 6*(6), e21185. doi:10.1371/journal.pone.0021185

Davis, J. S., Yeo, T. W., Thomas, J. H., McMillan, M., Darcy, C. J., McNeil, Y. R., . . . Anstey, N. M. (2009). Sepsis-associated microvascular dysfunction measured by peripheral arterial tonometry: an observational study. *Crit Care, 13*(5), R155. doi:10.1186/cc8055

de Berrazueta, J. R., Guerra-Ruiz, A., Garcia-Unzueta, M. T., Toca, G. M., Laso, R. S., de Adana, M. S., . . . Llorca, J. (2010). Endothelial dysfunction, measured by reactive hyperaemia using strain-gauge plethysmography, is an independent predictor of adverse outcome in heart failure. *Eur J Heart Fail, 12*(5), 477-483. doi:10.1093/eurjhf/hfq036

Dhindsa, M., Sommerlad, S. M., DeVan, A. E., Barnes, J. N., Sugawara, J., Ley, O., & Tanaka, H. (2008). Interrelationships among noninvasive measures of postischemic macro- and microvascular reactivity. *J Appl Physiol (1985), 105*(2), 427-432. doi:10.1152/japplphysiol.90431.2008

Dinenno, F. A., Masuki, S., & Joyner, M. J. (2005). Impaired modulation of sympathetic alpha-adrenergic vasoconstriction in contracting forearm muscle of ageing men. *Journal of Physiology-London, 567*(1), 311-321. doi:10.1113/jphysiol.2005.087668

Edwards, G., Feletou, M., & Weston, A. H. (2010). Endothelium-derived hyperpolarising factors and associated pathways: a synopsis. *Pflugers Arch, 459*(6), 863-879. doi:10.1007/s00424-010-0817-1

Engelke, K. A., Halliwill, J. R., Proctor, D. N., Dietz, N. M., & Joyner, M. J. (1996). Contribution of nitric oxide and prostaglandins to reactive hyperemia in human forearm. *J Appl Physiol (1985), 81*(4), 1807-1814. doi:10.1152/jappl.1996.81.4.1807

Englund, E. K., Langham, M. C., Li, C., Rodgers, Z. B., Floyd, T. F., Mohler, E. R., & Wehrli, F. W. (2013). Combined measurement of perfusion, venous oxygen saturation, and skeletal muscle T2* during reactive hyperemia in the leg. *J Cardiovasc Magn Reson, 15*, 70. doi:10.1186/1532-429X-15-70

Evanoff, N. G., Kelly, A. S., Steinberger, J., & Dengel, D. R. (2016). Peak shear and peak flow mediated dilation: a time-course relationship. *J Clin Ultrasound, 44*(3), 182-187. doi:10.1002/jcu.22324

Farouque, H. M., & Meredith, I. T. (2003). Inhibition of vascular ATP-sensitive K+ channels does not affect reactive hyperemia in human forearm. *Am J Physiol Heart Circ Physiol, 284*(2), H711-718. doi:10.1152/ajpheart.00315.2002

Feletou, M. (2009). Calcium-activated potassium channels and endothelial dysfunction: therapeutic options? *Br J Pharmacol, 156*(4), 545-562. doi:10.1111/j.1476-5381.2009.00052.x

Gebremedhin, D., Bonnet, P., Greene, A. S., England, S. K., Rusch, N. J., Lombard, J. H., & Harder, D. R. (1994). Hypoxia increases the activity of Ca(2+)-sensitive K+ channels in cat cerebral arterial muscle cell membranes. *Pflugers Arch, 428*(5-6), 621-630. doi:10.1007/bf00374586

Green, D. J., Dawson, E. A., Groenewoud, H. M., Jones, H., & Thijssen, D. H. (2014). Is flow-mediated dilation nitric oxide mediated?: A meta-analysis. *Hypertension, 63*(2), 376-382. doi:10.1161/HYPERTENSIONAHA.113.02044

Gurley, K., Shang, Y., & Yu, G. (2012). Noninvasive optical quantification of absolute blood flow, blood oxygenation, and oxygen consumption rate in exercising skeletal muscle. *J Biomed Opt, 17*(7), 075010. doi:10.1117/1.jbo.17.7.075010

Hamburg, N. M., & Benjamin, E. J. (2009). Assessment of endothelial function using digital pulse amplitude tonometry. *Trends Cardiovasc Med, 19*(1), 6-11. doi:10.1016/j.tcm.2009.03.001

Hamburg, N. M., Keyes, M. J., Larson, M. G., Vasan, R. S., Schnabel, R., Pryde, M. M., . . . Benjamin, E. J. (2008). Cross-sectional relations of digital vascular function to cardiovascular risk factors in the Framingham Heart Study. *Circulation, 117*(19), 2467-2474. doi:10.1161/CIRCULATIONAHA.107.748574

Hammer, S. M., Alexander, A. M., Didier, K. D., Smith, J. R., Caldwell, J. T., Sutterfield, S. L., . . . Barstow, T. J. (2018). The noninvasive simultaneous measurement of tissue oxygenation and microvascular hemodynamics during incremental handgrip exercise. *Journal of Applied Physiology, 124*(3), 604-614. doi:10.1152/japplphysiol.00815.2017

Hammer, S. M., Hueber, D. M., Townsend, D. K., Huckaby, L. M., Alexander, A. M., Didier, K. D., & Barstow, T. J. (2019). Effect of assuming constant tissue scattering on measured tissue oxygenation values during tissue ischemia and vascular reperfusion. *J Appl Physiol (1985)*. doi:10.1152/japplphysiol.01138.2018

Harris, R. A., Padilla, J., Rink, L. D., & Wallace, J. P. (2006). Variability of flow-mediated dilation measurements with repetitive reactive hyperemia. *Vasc Med, 11*(1), 1-6. doi:10.1191/1358863x06vm641oa

Hayoz, D., Weber, R., Rutschmann, B., Darioli, R., Burnier, M., Waeber, B., & Brunner, H. R. (1995). Postischemic blood flow response in hypercholesterolemic patients. *Hypertension, 26*(3), 497-502. doi:10.1161/01.hyp.26.3.497

Henry, B., Zhao, M., Shang, Y., Uhl, T., Thomas, D. T., Xenos, E. S., . . . Yu, G. (2015). Hybrid diffuse optical techniques for continuous hemodynamic measurement in gastrocnemius during plantar flexion exercise. *J Biomed Opt, 20*(12), 125006. doi:10.1117/1.JBO.20.12.125006

Huang, A. L., Silver, A. E., Shvenke, E., Schopfer, D. W., Jahangir, E., Titas, M. A., . . . Vita, J. A. (2007). Predictive value of reactive hyperemia for cardiovascular events in patients with peripheral arterial disease undergoing vascular surgery. *Arterioscler Thromb Vasc Biol, 27*(10), 2113-2119. doi:10.1161/ATVBAHA.107.147322

Ishibashi, Y., Takahashi, N., Shimada, T., Sugamori, T., Sakane, T., Umeno, T., . . . Murakami, Y. (2006). Short duration of reactive hyperemia in the forearm of subjects with multiple cardiovascular risk factors. *Circ J, 70*(1), 115-123.

Jackson, W. F. (2000). Ion channels and vascular tone. *Hypertension, 35*(1 Pt 2), 173-178. doi:10.1161/01.hyp.35.1.173

Jackson, W. F. (2017). Potassium Channels in Regulation of Vascular Smooth Muscle Contraction and Growth. *Adv Pharmacol, 78*, 89-144. doi:10.1016/bs.apha.2016.07.001

Kilbom, A., & Wennmalm, A. (1976). Endogenous prostaglandins as local regulators of blood flow in man: effect of indomethacin on reactive and functional hyperaemia. *J Physiol, 257*(1), 109-121.

Kim, M. N., Durduran, T., Frangos, S., Edlow, B. L., Buckley, E. M., Moss, H. E., . . . Kofke, W. A. (2010). Noninvasive measurement of cerebral blood flow and blood oxygenation using near-infrared and diffuse correlation spectroscopies in critically brain-injured adults. *Neurocrit Care, 12*(2), 173-180. doi:10.1007/s12028-009-9305-x

Ko, E. A., Han, J., Jung, I. D., & Park, W. S. (2008). Physiological roles of K+ channels in vascular smooth muscle cells. *J Smooth Muscle Res, 44*(2), 65-81. doi:10.1540/jsmr.44.65

Kooijman, H. M., Hopman, M. T., Colier, W. N., van der Vliet, J. A., & Oeseburg, B. (1997). Near infrared spectroscopy for noninvasive assessment of claudication. *J Surg Res, 72*(1), 1-7. doi:10.1006/jsre.1997.5164

Kragelj, R., Jarm, T., Erjavec, T., Presern-Strukelj, M., & Miklavcic, D. (2001). Parameters of postocclusive reactive hyperemia measured by near infrared spectroscopy in patients with peripheral vascular disease and in healthy volunteers. *Annals of Biomedical Engineering, 29*(4), 311-320. doi:Doi 10.1114/1.1359451

Kragelj, R., Jarm, T., & Miklavcic, D. (2000). Reproducibility of parameters of postocclusive reactive hyperemia measured by near infrared spectroscopy and transcutaneous oximetry. *Ann Biomed Eng, 28*(2), 168-173.

Kuvin, J. T., Patel, A. R., Sliney, K. A., Pandian, N. G., Sheffy, J., Schnall, R. P., . . . Udelson, J. E. (2003). Assessment of peripheral vascular endothelial function with finger arterial pulse wave amplitude. *Am Heart J, 146*(1), 168-174. doi:10.1016/S0002-8703(03)00094-2

Lacroix, S., Gayda, M., Gremeaux, V., Juneau, M., Tardif, J. C., & Nigam, A. (2012). Reproducibility of near-infrared spectroscopy parameters measured during brachial artery occlusion and reactive hyperemia in healthy men. *J Biomed Opt, 17*(7), 077010. doi:10.1117/1.JBO.17.7.077010

Lee, C. R., Bass, A., Ellis, K., Tran, B., Steele, S., Caughey, M., . . . Hinderliter, A. L. (2012). Relation between digital peripheral arterial tonometry and brachial artery ultrasound measures of vascular function in patients with coronary artery disease and in healthy volunteers. *Am J Cardiol, 109*(5), 651-657. doi:10.1016/j.amjcard.2011.10.023

Lee, V., Martin, B. J., Fung, M., & Anderson, T. J. (2012). The optimal measure of microvascular function with velocity time integral for cardiovascular risk prediction. *Vasc Med, 17*(5), 287-293. doi:10.1177/1358863X12451337

Lian, B. Q., & Keaney, J. F., Jr. (2010). Predicting ischemic heart disease in women: the value of endothelial function. *J Am Coll Cardiol, 55*(16), 1697-1699. doi:10.1016/j.jacc.2009.10.074

London, G. M., Pannier, B., Agharazii, M., Guerin, A. P., Verbeke, F. H., & Marchais, S. J. (2004). Forearm reactive hyperemia and mortality in end-stage renal disease. *Kidney Int, 65*(2), 700-704. doi:10.1111/j.1523-1755.2004.00434.x

Lopez, D., Pollak, A. W., Meyer, C. H., Epstein, F. H., Zhao, L., Pesch, A. J., . . . Kramer, C. M. (2015). Arterial spin labeling perfusion cardiovascular magnetic resonance of the calf in peripheral arterial disease: cuff occlusion hyperemia vs exercise. *J Cardiovasc Magn Reson, 17*, 23. doi:10.1186/s12968-015-0128-y

Luhrmann, P. M., Bender, R., Edelmann-Schafer, B., & Neuhauser-Berthold, M. (2009). Longitudinal changes in energy expenditure in an elderly German population: a 12-year follow-up. *European Journal of Clinical Nutrition, 63*(8), 986-992. doi:10.1038/ejcn.2009.1

Matsue, Y., Yoshida, K., Nagahori, W., Ohno, M., Suzuki, M., Matsumura, A., . . . Yoshida, M. (2014). Peripheral microvascular dysfunction predicts residual risk in coronary artery disease patients on statin therapy. *Atherosclerosis, 232*(1), 186-190. doi:10.1016/j.atherosclerosis.2013.11.038

Matsuzawa, Y., Kwon, T. G., Lennon, R. J., Lerman, L. O., & Lerman, A. (2015). Prognostic Value of Flow-Mediated Vasodilation in Brachial Artery and Fingertip Artery for Cardiovascular Events: A Systematic Review and Meta-Analysis. *J Am Heart Assoc, 4*(11). doi:10.1161/jaha.115.002270

Matsuzawa, Y., Sugiyama, S., Sugamura, K., Nozaki, T., Ohba, K., Konishi, M., . . . Ogawa, H. (2010). Digital assessment of endothelial function and ischemic heart disease in women. *J Am Coll Cardiol, 55*(16), 1688-1696. doi:10.1016/j.jacc.2009.10.073

Mayeur, C., Campard, S., Richard, C., & Teboul, J. L. (2011). Comparison of four different vascular occlusion tests for assessing reactive hyperemia using near-infrared spectroscopy. *Critical Care Medicine, 39*(4), 695-701. doi:10.1097/CCM.0b013e318206d256

McLay, K. M., Fontana, F. Y., Nederveen, J. P., Guida, F. F., Paterson, D. H., Pogliaghi, S., & Murias, J. M. (2016). Vascular responsiveness determined by near-infrared spectroscopy measures of oxygen saturation. *Experimental Physiology, 101*(1), 34-40. doi:10.1113/EP085406

McLay, K. M., Nederveen, J. P., Pogliaghi, S., Paterson, D. H., & Murias, J. M. (2016). Repeatability of vascular responsiveness measures derived from near-infrared spectroscopy. *Physiol Rep, 4*(9). doi:10.14814/phy2.12772

Meijer, P., Wouters, C. W., van den Broek, P. H., Scheffer, G. J., Riksen, N. P., Smits, P., & Rongen, G. A. (2008). Dipyridamole enhances ischaemia-induced reactive hyperaemia by increased adenosine receptor stimulation. *Br J Pharmacol, 153*(6), 1169-1176. doi:10.1038/bjp.2008.10

Michiels, C., Arnould, T., Knott, I., Dieu, M., & Remacle, J. (1993). Stimulation of prostaglandin synthesis by human endothelial cells exposed to hypoxia. *Am J Physiol, 264*(4 Pt 1), C866-874. doi:10.1152/ajpcell.1993.264.4.C866

Mitchell, G. F., Parise, H., Vita, J. A., Larson, M. G., Warner, E., Keaney, J. F., Jr., . . . Benjamin, E. J. (2004). Local shear stress and brachial artery flow-mediated dilation: the Framingham Heart Study. *Hypertension, 44*(2), 134-139. doi:10.1161/01.HYP.0000137305.77635.68

Nilius, B., & Droogmans, G. (2001). Ion channels and their functional role in vascular endothelium. *Physiol Rev, 81*(4), 1415-1459. doi:10.1152/physrev.2001.81.4.1415

Nugent, A. G., McGurk, C., McAuley, D., Maguire, S., Silke, B., & Johnston, G. D. (1999). Forearm reactive hyperaemia is not mediated by nitric oxide in healthy volunteers. *Br J Clin Pharmacol, 48*(3), 457-459.

Olivecrona, G. K., Gotberg, M., Harnek, J., Van der Pals, J., & Erlinge, D. (2007). Mild hypothermia reduces cardiac post-ischemic reactive hyperemia. *BMC Cardiovasc Disord, 7*, 5. doi:10.1186/1471-2261-7-5

Paine, N. J., Hinderliter, A. L., Blumenthal, J. A., Adams, K. F., Jr., Sueta, C. A., Chang, P. P., . . . Sherwood, A. (2016). Reactive hyperemia is associated with adverse clinical outcomes in heart failure. *Am Heart J, 178*, 108-114. doi:10.1016/j.ahj.2016.05.008

Philpott, A. C., Lonn, E., Title, L. M., Verma, S., Buithieu, J., Charbonneau, F., & Anderson, T. J. (2009). Comparison of new measures of vascular function to flow mediated dilatation as a measure of cardiovascular risk factors. *Am J Cardiol, 103*(11), 1610-1615. doi:10.1016/j.amjcard.2009.01.376

Pyke, K. E., & Tschakovsky, M. E. (2005). The relationship between shear stress and flow-mediated dilatation: implications for the assessment of endothelial function. *J Physiol, 568*(Pt 2), 357-369. doi:10.1113/jphysiol.2005.089755

Quayle, J. M., Nelson, M. T., & Standen, N. B. (1997). ATP-sensitive and inwardly rectifying potassium channels in smooth muscle. *Physiol Rev, 77*(4), 1165-1232. doi:10.1152/physrev.1997.77.4.1165

Raynaud, J. S., Duteil, S., Vaughan, J. T., Hennel, F., Wary, C., Leroy-Willig, A., & Carlier, P. G. (2001). Determination of skeletal muscle perfusion using arterial spin labeling NMRI: validation by comparison with venous occlusion plethysmography. *Magn Reson Med, 46*(2), 305-311. doi:10.1002/mrm.1192

Rosenberry, R., Munson, M., Chung, S., Samuel, T. J., Patik, J., Tucker, W. J., . . . Nelson, M. D. (2018). Age-related microvascular dysfunction: novel insight from near-infrared spectroscopy. *Exp Physiol, 103*(2), 190-200. doi:10.1113/EP086639

Rosenberry, R., Trojacek, D., Chung, S., Cipher, D. J., & Nelson, M. D. (2019). Inter-individual differences in the ischemic stimulus and other technical considerations when assessing reactive hyperemia. *Am J Physiol Regul Integr Comp Physiol*. doi:10.1152/ajpregu.00157.2019

Rosenberry, R., Tucker, W. J., Haykowsky, M. J., Trojacek, D., Chamseddine, H. H., Arena-Marshall, C. A., . . . Nelson, M. D. (2019). Determinants of skeletal muscle oxygen consumption assessed by near-infrared diffuse correlation spectroscopy during incremental handgrip exercise. *J Appl Physiol (1985)*. doi:10.1152/japplphysiol.00273.2019

Rubinshtein, R., Kuvin, J. T., Soffler, M., Lennon, R. J., Lavi, S., Nelson, R. E., . . . Lerman, A. (2010). Assessment of endothelial function by non-invasive peripheral arterial tonometry predicts late cardiovascular adverse events. *Eur Heart J, 31*(9), 1142-1148. doi:10.1093/eurheartj/ehq010

Sandoo, A., van Zanten, J. J., Metsios, G. S., Carroll, D., & Kitas, G. D. (2010). The endothelium and its role in regulating vascular tone. *Open Cardiovasc Med J, 4*, 302-312. doi:10.2174/1874192401004010302

Schoenenberger, A. W., Urbanek, N., Bergner, M., Toggweiler, S., Resink, T. J., & Erne, P. (2012). Associations of reactive hyperemia index and intravascular ultrasound-assessed coronary plaque morphology in patients with coronary artery disease. *Am J Cardiol, 109*(12), 1711-1716. doi:10.1016/j.amjcard.2012.02.011

Shang, Y., Chen, L., Toborek, M., & Yu, G. (2011). Diffuse optical monitoring of repeated cerebral ischemia in mice. *Opt Express, 19*(21), 20301-20315. doi:10.1364/OE.19.020301

Shang, Y., Li, T., & Yu, G. (2017). Clinical applications of near-infrared diffuse correlation spectroscopy and tomography for tissue blood flow monitoring and imaging. *Physiol Meas, 38*(4), R1-R26. doi:10.1088/1361-6579/aa60b7

Shimoda, L. A., & Polak, J. (2011). Hypoxia. 4. Hypoxia and ion channel function. *Am J Physiol Cell Physiol, 300*(5), C951-967. doi:10.1152/ajpcell.00512.2010

Siafaka, A., Angelopoulos, E., Kritikos, K., Poriazi, M., Basios, N., Gerovasili, V., . . . Nanas, S. (2007). Acute effects of smoking on skeletal muscle microcirculation monitored by near-infrared spectroscopy. *Chest, 131*(5), 1479-1485. doi:10.1378/chest.06-2017

Stuehr, D. J. (2004). Enzymes of the L-arginine to nitric oxide pathway. *J Nutr, 134*(10 Suppl), 2748S-2751S; discussion 2765S-2767S. doi:10.1093/jn/134.10.2748S

Tagawa, T., Imaizumi, T., Endo, T., Shiramoto, M., Harasawa, Y., & Takeshita, A. (1994). Role of nitric oxide in reactive hyperemia in human forearm vessels. *Circulation, 90*(5), 2285-2290.

Takase, B., Akima, T., Uehata, A., Ohsuzu, F., & Kurita, A. (2004). Effect of chronic stress and sleep deprivation on both flow-mediated dilation in the brachial artery and the intracellular magnesium level in humans. *Clin Cardiol, 27*(4), 223-227. doi:10.1002/clc.4960270411

Thijssen, D. H., Black, M. A., Pyke, K. E., Padilla, J., Atkinson, G., Harris, R. A., . . . Green, D. J. (2011). Assessment of flow-mediated dilation in humans: a methodological and physiological guideline. *Am J Physiol Heart Circ Physiol, 300*(1), H2-12. doi:10.1152/ajpheart.00471.2010

Tucker, W. J., Rosenberry, R., Trojacek, D., Chamseddine, H. H., Arena-Marshall, C. A., Zhu, Y., . . . Nelson, M. D. (2019). Studies into the determinants of skeletal muscle oxygen consumption: novel insight from near-infrared diffuse correlation spectroscopy. *J Physiol, 597*(11), 2887-2901. doi:10.1113/JP277580

Tykocki, N. R., Boerman, E. M., & Jackson, W. F. (2017). Smooth Muscle Ion Channels and Regulation of Vascular Tone in Resistance Arteries and Arterioles. *Compr Physiol, 7*(2), 485-581. doi:10.1002/cphy.c160011

Wilker, E. H., Ljungman, P. L., Rice, M. B., Kloog, I., Schwartz, J., Gold, D. R., . . . Mittleman, M. A. (2014). Relation of long-term exposure to air pollution to brachial artery flow-mediated dilation and reactive hyperemia. *Am J Cardiol, 113*(12), 2057-2063. doi:10.1016/j.amjcard.2014.03.048

Woo, J. S., Jang, W. S., Kim, H. S., Lee, J. H., Choi, E. Y., Kim, J. B., . . . Kim, W. (2014). Comparison of peripheral arterial tonometry and flow-mediated vasodilation for assessment of the severity and complexity of coronary artery disease. *Coron Artery Dis, 25*(5), 421-426. doi:10.1097/MCA.0000000000000094

Yu, G., Floyd, T. F., Durduran, T., Zhou, C., Wang, J., Detre, J. A., & Yodh, A. G. (2007). Validation of diffuse correlation spectroscopy for muscle blood flow with concurrent arterial spin labeled perfusion MRI. *Opt Express, 15*(3), 1064-1075. doi:10.1364/oe.15.001064

Zhao, Y., Vanhoutte, P. M., & Leung, S. W. (2015). Vascular nitric oxide: Beyond eNOS. *J Pharmacol Sci, 129*(2), 83-94. doi:10.1016/j.jphs.2015.09.002

Zhou, C., Eucker, S. A., Durduran, T., Yu, G., Ralston, J., Friess, S. H., . . . Yodh, A. G. (2009). Diffuse optical monitoring of hemodynamic changes in piglet brain with closed head injury. *J Biomed Opt, 14*(3), 034015. doi:10.1117/1.3146814

CHAPTER 3

AGE-RELATED MICROVASCULAR DYSFUNCTION: NOVEL INSIGHT FROM NEAR-INFRARED SPECTROSCOPY*

Ryan Rosenberry, Madison Munson, Susie Chung, Thomas Jake Samuel, Jordan Patik, Wesley J. Tucker, Mark J. Haykowsky, Michael D. Nelson. (2018), Age-related microvascular dysfunction: novel insight from near-infrared spectroscopy. Exp Physiol, 103: 190-200. doi:10.1113/EP086639

*Used with permission of the publisher

Introduction

Advancing age is the single most powerful predictor of cardiovascular disease which has been attributed—at least in part— to vascular dysfunction (Castelli, 1984; Jousilahti, Vartiainen, Tuomilehto, & Puska, 1999). Indeed, aging is associated with reduced bioavailability of endothelial-derived nitric oxide (NO) secondary to increased vascular oxidative stress (van der Loo et al., 2000). Aging is also associated with increased bioactivity of the potent endothelial-derived constricting factor endothelin-1 (ET-1) (Donato et al., 2009), reduced endothelial production of dilatory prostaglandins (Singh, Prasad, Singer, & MacAllister, 2002), development of vascular inflammation (Tousoulis, Charakida, & Stefanadis, 2006), and formation of advanced glycation end-products (Asif et al., 2000; Bruel & Oxlund, 1996; Tousoulis et al., 2006).

Post-occlusive reactive hyperemia is a well-established technique used to evaluate both macro- and microvascular function in a variety of clinical populations (Inoue et al., 2008; Korkmaz & Onalan, 2008; Matsuzawa, Kwon, Lennon, Lerman, & Lerman, 2015; Poredos & Jezovnik, 2013; Tomiyama & Yamashina, 2010), including aging (Creager et al., 1990). During occlusion of a conduit artery, downstream arterioles dilate in an effort to offset the ischemic insult. Upon release of the cuff, the decreased vascular resistance results in hyperemia and, in turn, shear stress along the conduit artery. Together, this coordinated response results in flow mediated dilation (FMD), which is currently one of the most widely used methods for non-invasive assessment of vascular endothelial function (i.e. macrovascular function). With the advent of duplex ultrasound and our increased understanding of the basic mechanisms governing post-occlusive reactive hyperemia, investigators also routinely measure the peak hyperemic blood flow response. As described above, the peak hyperemic blood flow response is dictated by one's ability to dilate the downstream microvasculature, and is thus is an indirect measure of microvascular function. Both FMD and reactive hyperemia are impaired with aging (Celermajer et al., 1994; Creager et al., 1990); however, each of these measures remains highly operator dependent— requiring extensive skill and

training—and requires sophisticated, high-cost, data acquisition hardware and post-processing software. Moreover, these ultrasound approaches focus entirely on upstream conduit vessel flow/dilation, which may reduce overall specificity. While direct measures of microvascular perfusion by contrast-enhanced ultrasound (Krix et al., 2005; Wei et al., 1998), Xenon clearance (Grimby, Haggendal, & Saltin, 1967), arterial spin labelled MRI (Raynaud et al., 2001; Yu et al., 2007), and positron emission tomography (Heinonen et al., 2011) are indeed possible, application of these approaches also remains limited due to the overall sophistication, expense, invasiveness and exposure to radiation (Xenon imaging and PET) involved in these techniques.

Near-infrared spectroscopy (NIRS) is a well-established method for measuring oxygen saturation and oxidative capacity in skeletal muscle and cerebral tissue (Khan et al., 2010; Ryan, Southern, Reynolds, & McCully, 2013; Southern, Ryan, Reynolds, & McCully, 2014; Tian et al., 2010). Compared to Doppler ultrasound, NIRS is relatively low cost and easy to use. Moreover, it can be used to directly interrogate specific regions of interest (i.e. skeletal muscle), increasing its overall specificity. To-date, several studies have evaluated tissue oxygen saturation (StO_2) kinetics following circulatory occlusion in healthy young subjects (Christopher M. Bopp, Dana K. Townsend, & Thomas J. Barstow, 2011; Bopp, Townsend, Warren, & Barstow, 2014; Fellahi et al., 2014), patients with peripheral artery disease (Kragelj, Jarm, Erjavec, Presern-Strukelj, & Miklavcic, 2001), tobacco-users (Zamparini et al., 2015), and patients with sepsis (Kevin C. Doerschug, Angela S. Delsing, Gregory A. Schmidt, & William G. Haynes, 2007; Mayeur, Campard, Richard, & Teboul, 2011). The results suggest that NIRS-derived post-occlusion tissue oxygen saturation kinetics is a robust and easy to use approach to evaluate vascular function *in vivo*. Whether NIRS can be used to assess age-related impairments in microvascular function has not been tested. Addressing this fundamental question is critical to advance current clinical assessment practices and/or the design of large clinical trials focused on age-related diseases (for which current techniques may not be suitable).

The purpose of this study was therefore to compare NIRS-derived post-occlusion tissue oxygen saturation recovery kinetics between two distinct age groups (<35 vs. >65 years) using the aforementioned NIRS approach. We hypothesized that aging would prolong the recovery rate of muscle oxygen saturation, compared to young individuals, demonstrating the clinical utility of this novel approach.

Methods

Ethical Approval

The study was approved by the Institutional Review Board for research involving Human Subjects at the University of Texas at Arlington (PRO2016-0586), and conformed to the Declaration of Helsinki. All subjects gave written informed consent. The study was not registered in a database.

Participants

A total of twenty-four healthy young and ten elderly adults volunteered to participate in the study. All subjects were recruited from the local community. Participants were divided into two groups based on age (young >18 and < 35 yrs; aging >65 and < 80 yrs). Exclusion criteria included: morbid obesity (BMI > 35 kg/m^2); heart failure and/or history of myocardial infarction, uncontrolled hypertension, history of stroke or neurological disease, and diabetes.

Activity level was self-reported. Subjects were asked if they performed regular exercise, as well as frequency, duration and type. Activity level was then quantified by multiplying the frequency by duration and reported as minutes per week. Walking was defined as mild-to-moderate, whereas cycling or running was defined as moderate-to-vigorous.

Experimental Protocol

All tests were performed in a quiet, temperature-controlled room (21-23ºC). Participants were studied in a fasted state, having abstained from alcohol and vigorous exercise for at least 24 hr and caffeine for 12 hr.

Prior to placement of the NIRS probe, each subject's maximum voluntary contraction was measured. With the arm resting on a bedside table in a supinated and slightly adducted position, the subject was instructed to squeeze a hand grip dynamometer as forcefully as possible using only their hand and forearm muscles. After a brief recovery period, the subject was asked to repeat their maximum effort two more times. The highest value achieved was recorded as maximal voluntary contraction (MVC).

Skeletal muscle oxygenation was monitored continuously using a Dual-channel OxiplexTS (ISS, Inc., Champaign, IL, USA) near-infrared spectroscopy device. The NIRS device was calibrated at the beginning of each session, after the instrument warmed up for at least 30 minutes. The calibration was performed with the probe placed on a calibration block with known absorption and scattering coefficients. A lightweight plastic NIRS probe consisted of two parallel rows of light-emitting fibers and one detector fiber bundle. The probe was placed over the flexor digitorum profundus, secured in place with an elastic strap tightened to prevent movement, and covered with an optically dense black vinyl sheet to minimize intrusion of extraneous light. By measuring changes in light absorption at different wavelengths, changes in oxygenated hemoglobin (HbO_2) and deoxygenated hemoglobin (Hb) can be measured, and tissue oxygen saturation (StO_2) can be calculated ($[HbO_2]/([HbO_2]+[Hb])$. Data were stored online, and also captured using an auxiliary output system which integrated directly into our data acquisition system (PowerLab, ADInstruments, Colorado Springs, CO).

The NIRS parameters calculated are depicted in **Figure 1**. Baseline StO_2 was calculated as the average StO_2 prior to the onset of arterial cuff occlusion. The desaturation rate during cuff occlusion was defined as slope 1. Because oxygen rich blood is prevented from flowing into the forearm during arterial cuff occlusion, any reduction in forearm tissue oxygenation is directly related to oxygen consumption.

Thus, slope 1 can be considered an indirect measure of skeletal muscle metabolic rate (K. C. Doerschug, A. S. Delsing, G. A. Schmidt, & W. G. Haynes, 2007). The lowest StO_2 value obtained during ischemia (StO_{2min}) was taken as a measure of the magnitude of ischemic insult (the stimulus to vasodilate). The StO_2 reperfusion rate was quantified as the average upslope following cuff release and defined as slope 2. Maximum StO_2 was calculated as the highest StO_2 value reached after cuff release (denoted as StO_{2max}), and the reactive hyperemia area under the curve was calculated from the time of cuff release to 1-, 2- and 3-min post cuff-occlusion (AUC 1-min, AUC 2-min, and AUC 3-min, respectively). Lastly, hyperemic reserve was calculated as the change in StO_2 above baseline and reported as a percent change.

Protocol 1 – Effect of age on post cuff occlusion recovery kinetics. To assess the effects of age on NIRS-derived post-occlusion tissue oxygen saturation kinetics, we compared two distinct age groups: young (*n* = 14, age = 25 ± 3 years) vs. elderly (*n* = 10, age = 73 ± 5 years). NIRS measurements were collected continuously for at least 3 minutes at baseline, during 5 min of brachial artery occlusion, and for at least three minutes of reactive hyperemia.

To assess reproducibility, a subset of participants (9 young and 5 elderly) underwent repeat measurements within 30-90 min of the original cuff occlusion protocol.

Protocol 2 – Effect of oxygen desaturation level of reactive hyperemia. To assess the influence of absolute desaturation level (i.e. vasodilatory stimulus) on NIRS-derived post-occlusion tissue oxygen saturation recovery kinetics, we recruited an additional 12 young volunteers. All 12 subjects repeated the above cuff occlusion protocol with 3, 4, and 5 min occlusions separated by 20 min.

Statistics

All data are expressed as mean $\pm$ SEM (unless otherwise specified) and significance was set *a priori* at $P < 0.05$. All data were evaluated for normality with Shapiro-Wilk test. If distribution was not normal, variables were log-transformed and Shapiro-Wilk repeated to ensure normality prior to analysis. Data from protocol 1 were analyzed using an unpaired t-test, comparing young vs. elderly participants. To

compare the effect of cuff occlusion time (3-, 4-, 5 min cuff occlusion) on NIRS parameters in *protocol 2*, a one-way repeated measures ANOVA was used. When a significant time difference was present, pairwise comparisons were made using the Tukey post-hoc method. To determine the impact of matching tissue ischemia with NIRS-derived post-occlusion recovery kinetics, an unpaired t-test was then used to compare the 3 minute cuff occlusion data in the young participants with the 5 minute cuff occlusion data in the elderly participants. Test-retest reproducibility was assessed using both paired sample t-tests and reported as a coefficient of variation (expressed both as a percentage and in absolute terms). Power calculations were performed using G*Power (3.1.9.2) to assess the practical significance of the data reported.

Results

There were no adverse events or contraindications to testing.

Protocol 1

Individual characteristics for both groups (young vs. elderly) are shown in **Table 1**. By design, the elderly participants were significantly older, had more cardiovascular risk factors, and were taking more medications than young participants.

In accordance with our hypothesis, NIRS-derived indices of microvascular function, were impaired in the elderly compared to young participants using a conventional 5 min cuff-occlusion protocol (**Figure 2**). Both groups shared similar baseline tissue saturation (74.1 $\pm$ 1.0% vs 75.3 $\pm$ 3.6%, young vs. elderly, respectively, P = 0.874). After 5 minutes of arterial cuff occlusion however, the rate of StO_2 recovery (Slope 2) was much slower, and StO_{2max}, the reactive hyperemia time integral (AUC), and the hyperemic reserve were all significantly lower in the elderly compared to the young participants (**Figure 2**). Cohen's effect size values for each of our primary outcome variables ranged between 0.93 and 1.84, suggesting a high level of practical significance.

Figure 2 also clearly illustrates the markedly different skeletal muscle metabolic rate between the two groups (slower in the elderly), which resulted in significantly higher StO_{2min} in the elderly compared to the young participants, and a markedly different vasodilatory stimulus between the two groups.

Protocol 2

To evaluate the dependency of absolute hemoglobin desaturation level on NIRS-derived post-occlusion oxygen saturation recovery kinetics, twelve young participants (7 male/5 female, age: 25 ± 3 yrs; BMI 22.3 ± 2.3 kg/m^2) repeated the cuff occlusion protocol described in Protocol 1, with varying occlusion times (3-, 4-, and 5 min cuff occlusion, respectively). As illustrated in **Figure 3**, baseline tissue saturation remained constant across all three occlusion protocols. Moreover, the metabolic rate (Slope 1) did not differ across all three occlusion protocols, and as a result, the level of desaturation was time dependent. Importantly, we found that the oxygen recovery kinetics (Slope 2), StO_{2max}, the reactive hyperemia time integral at 1-, 2-, and 3-min post recovery, and the hyperemic reserve, were all significantly dependent on the level of desaturation achieved (**Figure 3**).

In light of these new observations, we then compared the 3 minute cuff occlusion data in the young group with the 5 minute cuff occlusion data in the elderly (**Figure 4**). The baseline saturation level remained similar between the two groups, as was the minimal saturation level achieved (by design). Remarkably, when we controlled for the vasodilatory stimulus (i.e. the level of desaturation), we observed no major differences in the oxygen recovery kinetics (Slope 2), the maximal saturation achieved, the reactive hyperemia time integral (AUC) at 1-, 2-, or 3-min post recovery, or the hyperemic reserve (**Figure 4**).

Reproducibility of Measures

The reproducibility of measurements was studied by repeating the same 5 minute protocol in 14 participants, at least 30 minutes apart. Repeated measurements showed no significant difference among

trials, indicating that the measurements were reproducible. The mean values of the coefficient of variation varied between 3.9% and 15.4% (**Table 2**).

Discussion

The main goal of this study was to determine whether NIRS-derived post-occlusion tissue oxygen saturation recovery kinetics could detect age-related impairments in microvascular function. The major novel findings of this investigation were two-fold: First, using a previously established 5-minute cuff occlusion protocol, we found that NIRS-derived indices of microvascular function were markedly reduced in elderly compared to young participants. In contrast, when we controlled for the absolute level of vasodilatory stimulus, and matched the tissue desaturation level between groups, we found similar responses in young and elderly participants. Taken together, we believe that NIRS-derived post-occlusive tissue oxygen saturation kinetics holds great promise in clinical vascular biology, given its low-cost, reproducibility, and operator independence. Moreover, the additive information regarding vasodilatory stimulus this approach gives over other more traditional measures, shines new light on an old problem and opens new possibilities for cardiovascular research across the health continuum.

NIRS-derived post-occlusion tissue oxygen saturation recovery kinetics has previously been used to assess peripheral microvascular function across the disease continuum, including healthy young subjects (Christopher M. Bopp et al., 2011; Bopp et al., 2014; Fellahi et al., 2014), patients with peripheral artery disease (Kragelj et al., 2001), tobacco-users (Zamparini et al., 2015), and patients with sepsis (Kevin C. Doerschug et al., 2007; Mayeur et al., 2011). To our knowledge, this is the first study to use this approach to assess age-related microvascular dysfunction. Using the same conventional 5 minute cuff occlusion protocol utilized in the above referenced studies, we found marked age-related impairments in microvascular function. This result is consistent with a growing body of work using ultrasound, showing age-related impairments in both reactive hyperemia (Celermajer, Sorensen, Spiegelhalter, Georgakopoulos, & Deanfield, 1993) and flow mediated dilation (i.e. endothelial function) (Yeboah,

Crouse, Hsu, Burke, & Herrington, 2007). Unlike these prior investigations however, the data herein were obtained without the need for a skilled sonographer, or sophisticated, high-cost, data acquisition hardware and post-processing software. In addition, NIRS-derived post-occlusion tissue oxygen saturation kinetics has previously been shown to be highly reproducible (Gomez et al., 2008; Lacroix et al., 2012; McLay, Nederveen, Pogliaghi, Paterson, & Murias, 2016), and valid compared to Doppler ultrasound derived reactive hyperemia (Bopp et al., 2014) and flow mediated dilation (McLay, Fontana, et al., 2016), further highlighting the clinical utility of this robust and easy to use technique. Indeed, our own results support the reproducibility of this technique, showing low test-retest variability (average CV 9.2 ± 4.3 %).

That NIRS provides information about tissue saturation throughout the entire cuff occlusion protocol, is a major advantage over other more traditional approaches (e.g. Doppler ultrasound or venous occlusion plethysmography). With NIRS we are able to observe both metabolic activity (i.e. Slope 1, the oxygen extraction rate), the extent of tissue ischemia (i.e. StO_{2min}) and thus the vasodilatory stimulus, and the reactive hyperemia (i.e. Slope 2, StO_{2max} and the post-cuff occlusion StO_2 time integral). With this added information, we found marked differences in the metabolic rate (slope 1) and vasodilatory stimulus (StO_{2min}) between our elderly and young participants when the cuff occlusion protocol was standardized to 5 minutes. We believe this is an important observation, as it greatly influences the interpretation of our aging results. Indeed, when we standardized the level of tissue ischemia across our two age groups (*protocol 2*), the differences in reactive hyperemia previously observed were now entirely abrogated. In light of these new findings, we believe controlling for the level of tissue ischemia is critically important, and that NIRS provides a convenient platform to address this.

We recognize that 5 minutes of arterial cuff occlusion is not only the conventional approach most commonly used for this type of experiment, but that it is also predictive of hard cardiovascular endpoints (Anderson et al., 2011; Gokce et al., 2003; Huang et al., 2007; Suryapranata et al., 1994); which in many

ways contradicts the above findings. However, if we accept that metabolic rate will invariably change across patients and disease cohorts, and if we accept that the level of tissue ischemia is proportional to the time of cuff occlusion and the metabolic rate of a particular individual, than it is interesting to speculate that the predictive power of these prior observations has less to do with microvascular function and more to do with muscle oxidative capacity. That is, someone with normal muscle metabolic rate will produce more vasodilatory substances during a fixed ischemic time period compared to someone with poor muscle function and a lower metabolic rate. This rationale is further supported by the fact that grip strength remains one of the strongest predictors of cardiovascular morbidity and mortality (Rantanen et al., 2003; Sasaki, Kasagi, Yamada, & Fujita, 2007), independent of vascular reactivity. We therefore believe that caution is warranted when interpreting reactive hyperemia results which do not standardize the level of tissue ischemia; especially given the potential for between group differences in metabolic rate. Indeed, normalizing tissue ischemia with post-occlusion hyperemia is the basis for controlling for shear rate when measuring FMD (Thijssen et al., 2011). Moreover, the conventional 5 minute cuff occlusion protocol emerged from early observations showing no additional change in vasodilation of an upstream conduit vessel beyond 5 minutes, using data analysis methods (i.e. calipers) which have since evolved (Corretti et al., 2002; Uehata et al., 1997).

While the present study did not directly compare NIRS-derived post-occlusion tissue saturation recovery kinetics with either Doppler-derived reactive hyperemia or endothelial function measurements, these comparisons have previously been made with good agreement (C. M. Bopp, D. K. Townsend, & T. J. Barstow, 2011; McLay, Fontana, et al., 2016). Our reproducibility measures and the repeat cuff occlusion experiments in *protocol 2* were all performed on the same day to avoid day-to-day vascular function variability and allow consistent placement of the NIRS optodes. It is therefore possible that repeat episodes of ischemia-induced hyperemia may have influenced our results; however, serial ischemia-reperfusion trials do not appear to affect subsequent vascular reactivity (Harris, Padilla, Rink, & Wallace,

2006). The consistency of our probe placement, and resultant low test-retest variability, also highlights the need for standardizing procedures, especially if this technique is used to assess disease progression or intervention effectiveness. It is also important to acknowledge that NIRS is inherently limited by adipose tissue thickness (Ferrari, Mottola, & Quaresima, 2004). While we did not specifically screen participants by adipose tissue thickness, all of the participants included in this study were relatively lean. This will need to be accounted for if this methodology is going to be widely adopted, especially in clinical populations. Though we did not specifically control for menstrual cycle in our young female participants— which can affect vascular reactivity (Webb, Rusch, & Vanhoutte, 1981)— we do not believe this effected our interpretation of the present results given the fact that all age-related differences disappeared when we controlled for tissue ischemia. Finally, our elderly group consisted of only ten relatively healthy seniors in the seventh decade of life. Our findings are therefore, in no way, representative of the entire aging population. Instead, this cross-sectional study represents a unique opportunity to explore a relatively novel imaging approach to assess microvascular reactivity in an at-risk population and sheds new light on an old problem.

In conclusion, we believe NIRS-derived post-occlusive tissue oxygen saturation kinetics can serve an important role in clinical vascular biology and assessment. The data herein highlight the need for assessing tissue ischemia during cuff occlusion protocols, particularly in group comparisons where skeletal muscle metabolic rate is expected to differ.

Figures and Tables

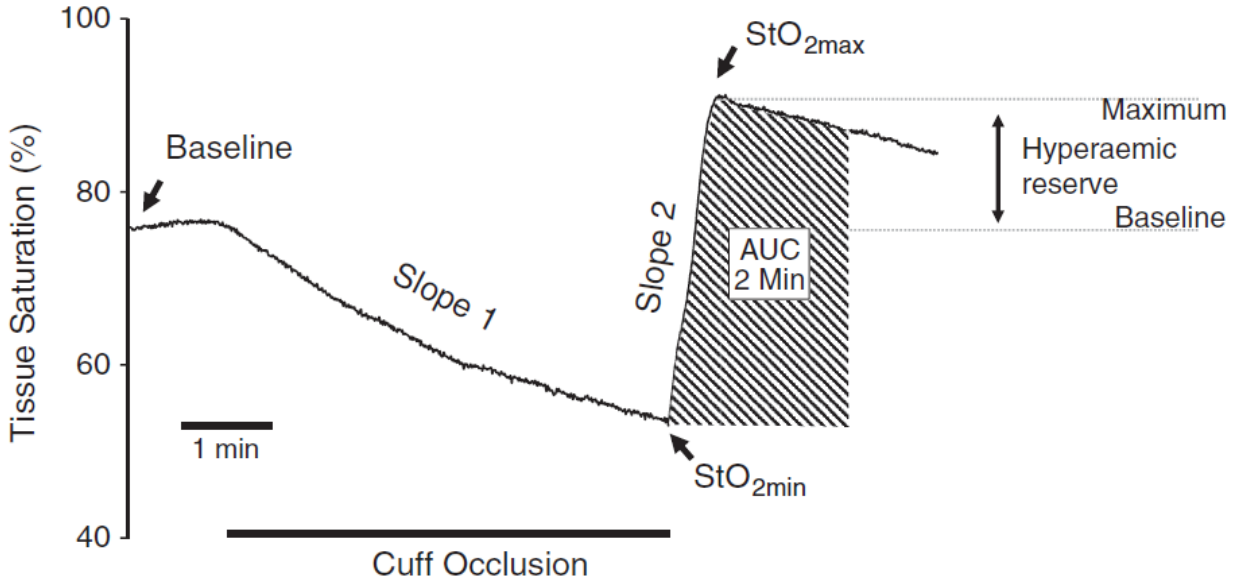

Figure 1. Representative near-infrared spectroscopy profile of percentage tissue oxygen saturation (StO2), during a typical arterial cuff occlusion test. Baseline defines the period of time before arterial cuff occlusion.

Slope 1 defines the desaturation rate during cuff occlusion and is regarded as a measure of skeletal muscle metabolic rate. The lowest StO2 value obtained during ischaemia is defined as StO2 min and is regarded as a measure of the ischaemic stimulus to vasodilate. The tissue saturation reperfusion rate is denoted as slope 2 and is an index of reactive hyperaemia; as are StO2 max and the reactive hyperaemia area under the curve (AUC). To gain insight into the hyperaemic reserve, the StO2 maxis expressed as a percentage change from baseline.

Table 1. Subject characteristics for protocol 1

Characteristics	Young	Elderly	P Value
n	14	10	—
Male/Female	6-Aug	8-Feb	—
Age (years)	25 ± 3	73 ± 5	<0.001
Height (cm)	171.8 ± 7.9	164.9 ± 7.4	0.04
Weight (kg)	72.6 ± 11.7	71.2 ± 10.3	0.76
BMI ($kg \cdot m^{-2}$)	24.5 ± 3.1	26.2 ± 3.4	0.24
MVC (kg)	39.6 ± 13.3	20.9 ± 5.3	<0.001
Arterial blood pressure (mmHg)			
Systolic blood pressure	114 ± 9	126 ± 12	0.01
Diastolic blood pressure	72 ± 5	74 ± 4	0.23
Physical activity level [min $week^{-1}$] (n)			
Mild to moderate	120 ± 60 (2)	194 ± 71 (8)	—
Moderate to vigorous	168 ± 1403 (9)	—	—
Cadiovascular risk factors (n)			
Hypertension	—	5	—
Hypercholesterolemia	—	4	—
Smoking history	—	3	—
Medications (n)			
Beta blockers	—	0	—
ACE inhibitors	—	1	—
ARB	—	1	—
Thyroid Hormones	—	1	—
Statins	—	1	—
NSAIDs/blood thinners	—	2	—
Immunosuppressants	—	1	—
a2-Agonists	—	0	—
Biguanides	—	1	—

Data are reported as means ± SD. Abbreviations: ACE, angiotensin-converting enzyme; ARB, angiotensin receptor blocker; BMI, body mass index; MVC, maximal voluntary handgrip contraction; and NSAID, non-steroidal anti-inflammatory.

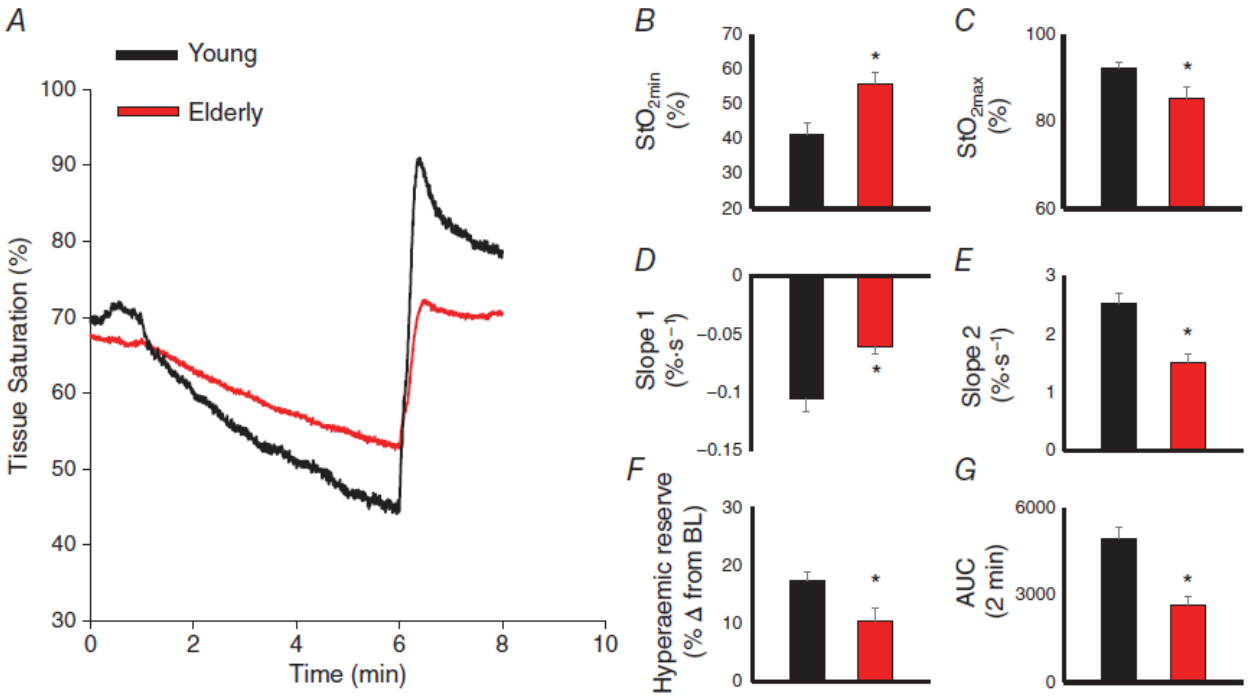

Figure 2. Effect of age on reactive hyperemia following a standardized 5 minute cuff occlusion.
A, near-infrared spectroscopy profile of percentage tissue oxygen saturation (StO2) for two representative subjects (young versus elderly) during a typical arterial cuff occlusion test. Summary data (young n = 14; elderly n = 10) are also displayed, showing group differences in the minimal tissue oxygen saturation (StO2 min; B), maximal tissue oxygen saturation (StO2 max; C), slope 1 (D), slope 2 (E), hyperaemic reserve (F) and the hyperaemic area under the curve (AUC; G). ∗Significant ($P < 0.05$) difference between groups.

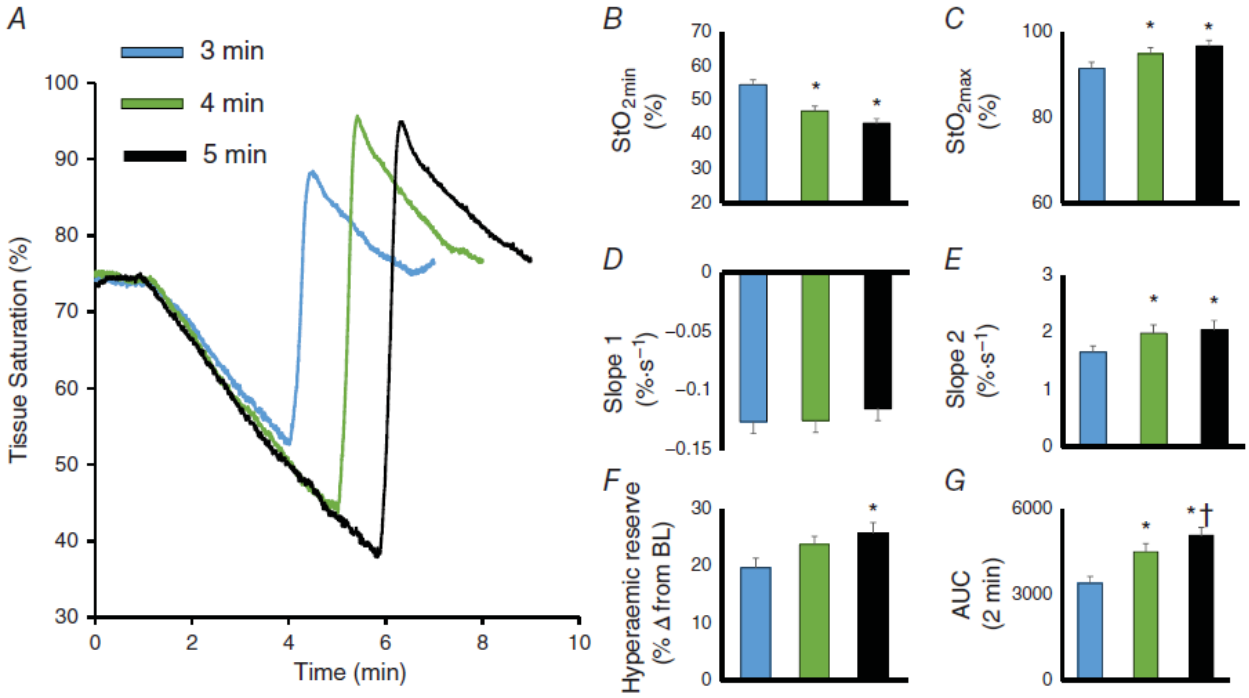

Figure 3. Effect of cuff occlusion duration on reactive hyperemia.
A, near-infrared spectroscopy profile of percentage tissue oxygen saturation (*S*tO2) for a representative young subject during repeat arterial cuff occlusion tests for 3, 4 and 5 min. Summary data (young, $n = 12$) show a significant effect of cuff occlusion time on the minimal tissue oxygen saturation (*S*tO2 min; *B*), maximal tissue oxygen saturation (*S*tO2 max; *C*), reactive hyperaemia (slope 2; *E*), hyperaemic reserve (*F*) and the hyperaemic area under the curve (AUC; *G*). The only parameter that did not change with time was slope 1 (the skeletal metabolic rate; *D*). ∗Significant ($P < 0.05$) difference from 3 min. †Significant ($P < 0.05$) difference from 4 min.

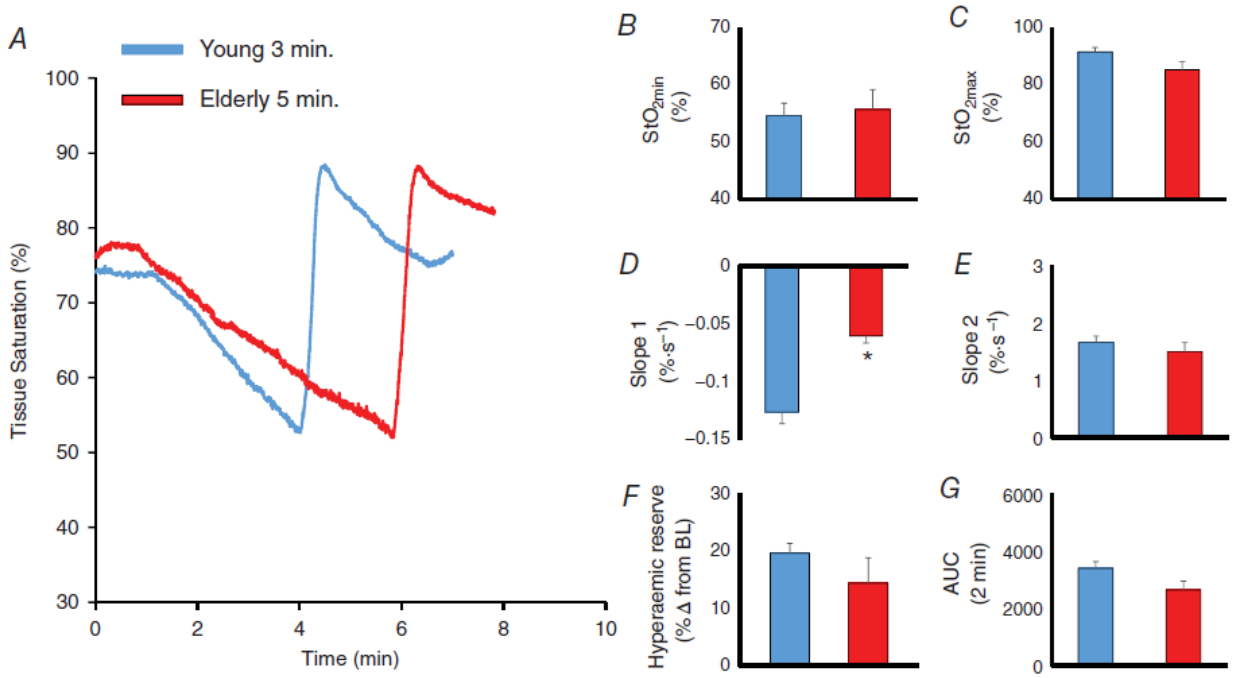

Figure 4. Controlling for tissue desaturation abrogates age-dependent differences in reactive hyperemia
A, near-infrared spectroscopy profile of percentage tissue oxygen saturation (*St*O2) for a representative young subject during a 3 min cuff occlusion test and a representative elderly subject during a 5 min cuff occlusion test. Summary data (young, $n = 12$; elderly, $n = 10$) show that when the level of tissue ischaemia is matched between groups (*St*O2 min; *B*), the differences in maximal tissue oxygen saturation (*St*O2 max; *C*), reactive hyperaemia (slope 2; *E*), hyperaemic reserve (*F*) and the hyperaemic area under the curve (AUC; *G*) are completely abrogated. As expected, the rate of tissue desaturation remained different between groups (the skeletal metabolic rate; *D*). ∗Significant ($P < 0.05$) difference between groups.

Table 2. Repeatability of measures

	Test 1	Test 2	CV (%)	CV (abs)	P Value
Tissue Saturation (%)					
Baseline	75.7	76	4.9	3.7	0.94
StO_{2max}	91.3	91.6	3.9	3.5	0.91
StO_{2min}	48.7	47.4	11	5.3	0.75
Slope 1	-0.088	-0.089	15.4	0.01	0.91
Slope 2	2.34	2.33	13.2	0.3	0.97
2 min AUC	3724.4	3882.0	8.5	322.6	0.80

Abbreviations: CV, coefficient of variation; CV (abs), variability expressed in absolute terms; StO2 max, highest tissue saturation achieved post-cuff occlusion; and StO2 min, lowest tissue saturation achieved during cuff occlusion.

References

Anderson, T. J., Charbonneau, F., Title, L. M., Buithieu, J., Rose, M. S., Conradson, H., . . . Lonn, E. M. (2011). Microvascular function predicts cardiovascular events in primary prevention: long-term results from the Firefighters and Their Endothelium (FATE) study. *Circulation, 123*(2), 163-169. doi:10.1161/CIRCULATIONAHA.110.953653

Asif, M., Egan, J., Vasan, S., Jyothirmayi, G. N., Masurekar, M. R., Lopez, S., . . . Regan, T. J. (2000). An advanced glycation endproduct cross-link breaker can reverse age-related increases in myocardial stiffness. *Proceedings of the National Academy of Sciences of the United States of America, 97*(6), 2809-2813. doi:DOI 10.1073/pnas.040558497

Bopp, C. M., Townsend, D. K., & Barstow, T. J. (2011). Characterizing near-infrared spectroscopy responses to forearm post-occlusive reactive hyperemia in healthy subjects. *European Journal of Applied Physiology, 111*(11), 2753. doi:10.1007/s00421-011-1898-z

Bopp, C. M., Townsend, D. K., & Barstow, T. J. (2011). Characterizing near-infrared spectroscopy responses to forearm post-occlusive reactive hyperemia in healthy subjects. *Eur J Appl Physiol, 111*(11), 2753-2761. doi:10.1007/s00421-011-1898-z

Bopp, C. M., Townsend, D. K., Warren, S., & Barstow, T. J. (2014). Relationship between brachial artery blood flow and total [hemoglobin+myoglobin] during post-occlusive reactive hyperemia. *Microvasc Res, 91*, 37-43. doi:10.1016/j.mvr.2013.10.004

Bruel, A., & Oxlund, H. (1996). Changes in biomechanical properties, composition of collagen and elastin, and advanced glycation endproducts of the rat aorta in relation to age. *Atherosclerosis, 127*(2), 155-165. doi:Doi 10.1016/S0021-9150(96)05947-3

Castelli, W. P. (1984). Epidemiology of coronary heart disease: the Framingham study. *American Journal of Medicine, 76*(2A), 4-12.

Celermajer, D. S., Sorensen, K. E., Spiegelhalter, D. J., Georgakopoulos, D., & Deanfield, J. E. (1993). Aging Is Associated with Endothelial Dysfunction in Healthy-Men Years before the Age-Related Decline in Women. *Circulation, 88*(4), 78-78.

Celermajer, D. S., Sorensen, K. E., Spiegelhalter, D. J., Georgakopoulos, D., Robinson, J., & Deanfield, J. E. (1994). Aging Is Associated with Endothelial Dysfunction in Healthy-Men Years before the Age-Related Decline in Women. *Journal of the American College of Cardiology, 24*(2), 471-476.

Corretti, M. C., Anderson, T. J., Benjamin, E. J., Celermajer, D., Charbonneau, F., Creager, M. A., . . . International Brachial Artery Reactivity Task, F. (2002). Guidelines for the ultrasound assessment of endothelial-dependent flow-mediated vasodilation of the brachial artery: a report of the International Brachial Artery Reactivity Task Force. *J Am Coll Cardiol, 39*(2), 257-265.

Creager, M. A., Cooke, J. P., Mendelsohn, M. E., Gallagher, S. J., Coleman, S. M., Loscalzo, J., & Dzau, V. J. (1990). Impaired vasodilation of forearm resistance vessels in hypercholesterolemic humans. *J Clin Invest, 86*(1), 228-234. doi:10.1172/JCI114688

Doerschug, K. C., Delsing, A. S., Schmidt, G. A., & Haynes, W. G. (2007). Impairments in microvascular reactivity are related to organ failure in human sepsis. *American Journal of Physiology - Heart and Circulatory Physiology, 293*(2), H1065-H1071. doi:10.1152/ajpheart.01237.2006

Doerschug, K. C., Delsing, A. S., Schmidt, G. A., & Haynes, W. G. (2007). Impairments in microvascular reactivity are related to organ failure in human sepsis. *American Journal of Physiology-Heart and Circulatory Physiology, 293*(2), H1065-H1071. doi:10.1152/ajpheart.01237.2006

Donato, A. J., Gano, L. B., Eskurza, I., Silver, A. E., Gates, P. E., Jablonski, K., & Seals, D. R. (2009). Vascular endothelial dysfunction with aging: endothelin-1 and endothelial nitric oxide synthase. *Am J Physiol Heart Circ Physiol, 297*(1), H425-432. doi:10.1152/ajpheart.00689.2008

Fellahi, J. L., Butin, G., Zamparini, G., Fischer, M. O., Gérard, J. L., & Hanouz, J. L. (2014). Lower limb peripheral NIRS parameters during a vascular occlusion test: An experimental study in healthy

volunteers. *Annales Françaises d'Anesthésie et de Réanimation, 33*(1), e9-e14. doi:http://dx.doi.org/10.1016/j.annfar.2013.11.014

Ferrari, M., Mottola, L., & Quaresima, V. (2004). Principles, Techniques, and Limitations of Near Infrared Spectroscopy. *Canadian Journal of Applied Physiology, 29*(4), 463-487. doi:10.1139/h04-031

Gokce, N., Keaney, J. F., Jr., Hunter, L. M., Watkins, M. T., Nedeljkovic, Z. S., Menzoian, J. O., & Vita, J. A. (2003). Predictive value of noninvasively determined endothelial dysfunction for long-term cardiovascular events in patients with peripheral vascular disease. *J Am Coll Cardiol, 41*(10), 1769-1775.

Gomez, H., Torres, A., Polanco, P., Kim, H. K., Zenker, S., Puyana, J. C., & Pinsky, M. R. (2008). Use of non-invasive NIRS during a vascular occlusion test to assess dynamic tissue O-2 saturation response. *Intensive Care Medicine, 34*(9), 1600-1607. doi:10.1007/s00134-008-1145-1

Grimby, G., Haggendal, E., & Saltin, B. (1967). Local xenon 133 clearance from the quadriceps muscle during exercise in man. *Journal of Applied Physiology, 22*(2), 305-310.

Harris, R. A., Padilla, J., Rink, L. D., & Wallace, J. P. (2006). Variability of flow-mediated dilation measurements with repetitive reactive hyperemia. *Vascular Medicine, 11*(1), 1-6. doi:10.1191/1358863x06vm641oa

Heinonen, I., Brothers, R. M., Kemppainen, J., Knuuti, J., Kalliokoski, K. K., & Crandall, C. G. (2011). Local heating, but not indirect whole body heating, increases human skeletal muscle blood flow. *Journal of Applied Physiology, 111*(3), 818-824. doi:10.1152/japplphysiol.00269.2011

Huang, A. L., Silver, A. E., Shvenke, E., Schopfer, D. W., Jahangir, E., Titas, M. A., . . . Vita, J. A. (2007). Predictive value of reactive hyperemia for cardiovascular events in patients with peripheral arterial disease undergoing vascular surgery. *Arterioscler Thromb Vasc Biol, 27*(10), 2113-2119. doi:10.1161/ATVBAHA.107.147322

Inoue, T., Matsuoka, H., Higashi, Y., Ueda, S., Sata, M., Shimada, K. E., . . . Node, K. (2008). Flow-mediated vasodilation as a diagnostic modality for vascular failure. *Hypertens Res, 31*(12), 2105-2113. doi:10.1291/hypres.31.2105

Jousilahti, P., Vartiainen, E., Tuomilehto, J., & Puska, P. (1999). Sex, age, cardiovascular risk factors, and coronary heart disease: a prospective follow-up study of 14 786 middle-aged men and women in Finland. *Circulation, 99*(9), 1165-1172.

Khan, B., Tian, F., Behbehani, K., Romero, M. I., Delgado, M. R., Clegg, N. J., . . . Alexandrakis, G. (2010). Identification of abnormal motor cortex activation patterns in children with cerebral palsy by functional near-infrared spectroscopy. *J Biomed Opt, 15*(3), 036008. doi:10.1117/1.3432746

Korkmaz, H., & Onalan, O. (2008). Evaluation of endothelial dysfunction: flow-mediated dilation. *Endothelium, 15*(4), 157-163. doi:10.1080/10623320802228872

Kragelj, R., Jarm, T., Erjavec, T., Presern-Strukelj, M., & Miklavcic, D. (2001). Parameters of postocclusive reactive hyperemia measured by near infrared spectroscopy in patients with peripheral vascular disease and in healthy volunteers. *Ann Biomed Eng, 29*(4), 311-320.

Krix, M., Weber, M. A., Krakowski-Roosen, H., Huttner, H. B., Delorme, S., Kauczor, H. U., & Hildebrandt, W. (2005). Assessment of skeletal muscle perfusion using contrast-enhanced ultrasonography. *J Ultrasound Med, 24*(4), 431-441.

Lacroix, S., Gayda, M., Gremeaux, V., Juneau, M., Tardif, J. C., & Nigam, A. (2012). Reproducibility of near-infrared spectroscopy parameters measured during brachial artery occlusion and reactive hyperemia in healthy men. *J Biomed Opt, 17*(7), 077010. doi:10.1117/1.JBO.17.7.077010

Matsuzawa, Y., Kwon, T. G., Lennon, R. J., Lerman, L. O., & Lerman, A. (2015). Prognostic Value of Flow-Mediated Vasodilation in Brachial Artery and Fingertip Artery for Cardiovascular Events: A Systematic Review and Meta-Analysis. *J Am Heart Assoc, 4*(11). doi:10.1161/JAHA.115.002270

Mayeur, C., Campard, S., Richard, C., & Teboul, J. L. (2011). Comparison of four different vascular occlusion tests for assessing reactive hyperemia using near-infrared spectroscopy. *Crit Care Med, 39*(4), 695-701. doi:10.1097/CCM.0b013e318206d256

McLay, K. M., Fontana, F. Y., Nederveen, J. P., Guida, F. F., Paterson, D. H., Pogliaghi, S., & Murias, J. M. (2016). Vascular responsiveness determined by near-infrared spectroscopy measures of oxygen saturation. *Experimental Physiology, 101*(1), 34-40. doi:10.1113/EP085406

McLay, K. M., Nederveen, J. P., Pogliaghi, S., Paterson, D. H., & Murias, J. M. (2016). Repeatability of vascular responsiveness measures derived from near-infrared spectroscopy. *Physiol Rep, 4*(9). doi:10.14814/phy2.12772

Poredos, P., & Jezovnik, M. K. (2013). Testing endothelial function and its clinical relevance. *J Atheroscler Thromb, 20*(1), 1-8.

Rantanen, T., Volpato, S., Ferrucci, L., Heikkinen, E., Fried, L. P., & Guralnik, J. M. (2003). Handgrip strength and cause-specific and total mortality in older disabled women: exploring the mechanism. *J Am Geriatr Soc, 51*(5), 636-641.

Raynaud, J. S., Duteil, S., Vaughan, J. T., Hennel, F., Wary, C., Leroy-Willig, A., & Carlier, P. G. (2001). Determination of skeletal muscle perfusion using arterial spin labeling NMRI: validation by comparison with venous occlusion plethysmography. *Magn Reson Med, 46*(2), 305-311.

Ryan, T. E., Southern, W. M., Reynolds, M. A., & McCully, K. K. (2013). A cross-validation of near-infrared spectroscopy measurements of skeletal muscle oxidative capacity with phosphorus magnetic resonance spectroscopy. *J Appl Physiol (1985), 115*(12), 1757-1766. doi:10.1152/japplphysiol.00835.2013

Sasaki, H., Kasagi, F., Yamada, M., & Fujita, S. (2007). Grip strength predicts cause-specific mortality in middle-aged and elderly persons. *American Journal of Medicine, 120*(4), 337-342. doi:10.1016/j.amjmed.2006.04.018

Singh, N., Prasad, S., Singer, D. R. J., & MacAllister, R. J. (2002). Ageing is associated with oxide and prostanoid impairment of nitric dilator pathways in the human forearm. *Clinical Science, 102*(5), 595-600. doi:Doi 10.1042/Cs20010262

Southern, W. M., Ryan, T. E., Reynolds, M. A., & McCully, K. (2014). Reproducibility of near-infrared spectroscopy measurements of oxidative function and postexercise recovery kinetics in the medial gastrocnemius muscle. *Appl Physiol Nutr Metab, 39*(5), 521-529. doi:10.1139/apnm-2013-0347

Suryapranata, H., Zijlstra, F., MacLeod, D. C., van den Brand, M., de Feyter, P. J., & Serruys, P. W. (1994). Predictive value of reactive hyperemic response on reperfusion on recovery of regional myocardial function after coronary angioplasty in acute myocardial infarction. *Circulation, 89*(3), 1109-1117.

Thijssen, D. H., Black, M. A., Pyke, K. E., Padilla, J., Atkinson, G., Harris, R. A., . . . Green, D. J. (2011). Assessment of flow-mediated dilation in humans: a methodological and physiological guideline. *Am J Physiol Heart Circ Physiol, 300*(1), H2-12. doi:10.1152/ajpheart.00471.2010

Tian, F., Delgado, M. R., Dhamne, S. C., Khan, B., Alexandrakis, G., Romero, M. I., . . . Liu, H. (2010). Quantification of functional near infrared spectroscopy to assess cortical reorganization in children with cerebral palsy. *Opt Express, 18*(25), 25973-25986. doi:10.1364/OE.18.025973

Tomiyama, H., & Yamashina, A. (2010). Non-invasive vascular function tests: their pathophysiological background and clinical application. *Circ J, 74*(1), 24-33.

Tousoulis, D., Charakida, M., & Stefanadis, C. (2006). Endothelial function and inflammation in coronary artery disease. *Heart, 92*(4), 441-444. doi:10.1136/hrt.2005.066936

Uehata, A., Lieberman, E. H., Gerhard, M. D., Anderson, T. J., Ganz, P., Polak, J. F., . . . Yeung, A. C. (1997). Noninvasive assessment of endothelium-dependent flow-mediated dilation of the brachial artery. *Vasc Med, 2*(2), 87-92. doi:10.1177/1358863X9700200203

van der Loo, B., Labugger, R., Skepper, J. N., Bachschmid, M., Kilo, J., Powell, J. M., . . . Luscher, T. F. (2000). Enhanced peroxynitrite formation is associated with vascular aging. *Journal of Experimental Medicine, 192*(12), 1731-1743. doi:DOI 10.1084/jem.192.12.1731

Webb, R. C., Rusch, N. J., & Vanhoutte, P. M. (1981). Influence of sex difference and oral contraceptives on forearm reactive hyperemia. *Blood Vessels, 18*(4-5), 161-170.

Wei, K., Jayaweera, A. R., Firoozan, S., Linka, A., Skyba, D. M., & Kaul, S. (1998). Quantification of myocardial blood flow with ultrasound-induced destruction of microbubbles administered as a constant venous infusion. *Circulation, 97*(5), 473-483.

Yeboah, J., Crouse, J. R., Hsu, F. C., Burke, G. L., & Herrington, D. M. (2007). Brachial flow-mediated dilation predicts incident cardiovascular events in older adults: the Cardiovascular Health Study. *Circulation, 115*(18), 2390-2397. doi:10.1161/CIRCULATIONAHA.106.678276

Yu, G. Q., Floyd, T. F., Durduran, T., Zhou, C., Wang, J. J., Detre, J. A., & Yodh, A. G. (2007). Validation of diffuse correlation spectroscopy for muscle blood flow with concurrent arterial spin labeled perfusion MRI. *Optics Express, 15*(3), 1064-1075. doi:Doi 10.1364/Oe.15.001064

Zamparini, G., Butin, G., Fischer, M.-O., Gérard, J.-L., Hanouz, J.-L., & Fellahi, J.-L. (2015). Noninvasive assessment of peripheral microcirculation by near-infrared spectroscopy: a comparative study in healthy smoking and nonsmoking volunteers. *Journal of Clinical Monitoring and Computing, 29*(5), 555-559. doi:10.1007/s10877-014-9631-1

CHAPTER 4

INTER-INDIVIDUAL DIFFERENCES IN THE ISCHEMIC STIMULUS AND OTHER TECHNICAL CONSIDERATIONS WHEN ASSESSING REACTIVE HYPEREMIA*

Ryan Rosenberry, Darian Trojacek, Daisha Cipher, Michael D. Nelson. (2019). Inter-individual differences in the ischemic stimulus and other technical considerations when assessing reactive hyperemia. *Am J Physiol Regul Integr Comp Physiol*.

Introduction

Reactive hyperemia is an established, non-invasive technique to assess peripheral microvascular function, and is a powerful predictor of all-cause and cardiovascular morbidity and mortality (Anderson et al., 2011; Huang et al., 2007; Ishibashi et al., 2006; London et al., 2004; Paine et al., 2016). In its most simplistic form, reactive hyperemia represents the magnitude of limb reperfusion in response to a period of arterial occlusion. Many different approaches have been adopted over the past decade to assess reactive hyperemia, including brachial artery velocity by Doppler ultrasound (Huang et al., 2007), tissue reperfusion by near infrared spectroscopy (NIRS) (Kragelj, Jarm, & Miklavcic, 2000; Mayeur, Campard, Richard, & Teboul, 2011; McLay, Nederveen, Pogliaghi, Paterson, & Murias, 2016), limb distension by venous occlusion plethysmography (Crecelius, Richards, Luckasen, Larson, & Dinenno, 2013; de Berrazueta et al., 2010), and peripheral artery tonometry (Bonetti et al., 2004; Matsuzawa, Kwon, Lennon, Lerman, & Lerman, 2015). Regardless of measurement technique, the fundamental interpretation across these studies has been that impaired reactive hyperemia signifies (micro)vascular dysfunction. Emerging data from our laboratory, however, challenge this interpretation.

In our hands, reactive hyperemia is closely linked to the metabolic rate of the ischemic limb (Rosenberry et al., 2018). Indeed, we have shown marked differences in skeletal muscle tissue desaturation (i.e. the stimulus to vasodilate), both within and between groups, in response to the same 5-minute arterial cuff occlusion; a response likely related to the quantity/quality of skeletal muscle (Rosenberry et al., 2018). Moreover, we have shown that when the magnitude of tissue desaturation is controlled for — by varying the duration of arterial cuff occlusion between groups — differences in tissue reperfusion disappear (Rosenberry et al., 2018). We believe this is an important area for future research, given the prognostic significance, and popularity, of this measure.

Accordingly, in the present study, we sought to more comprehensively evaluate the relationship between the magnitude of tissue ischemia and the level of reactive hyperemia, by combining gold-

standard Doppler ultrasound with near infrared spectroscopy in a group of young, healthy individuals, and a group of independently living, seniors (a group believed to have impairments in microvascular function). Based on our previous work in this area, as well as similar prior investigations examining the role of cuff occlusion time on flow mediated dilation (Leeson et al., 1997), we hypothesized that the degree of tissue desaturation would be closely associated with the magnitude of reactive hyperemia (measured as the peak velocity immediately post arterial occlusion). In addition to this primary objective, we also sought to explore the impact of measuring a five-second post-occlusion average velocity, versus the more conventional single-beat peak velocity approach, with the hypothesis that the five-second velocity would be less variable, and therefore more representative, than the single-beat approach. Along this same rationale, we also sought to evaluate the within group, and possible between group, influence of vessel diameter on measures of reactive hyperemia. Indeed, velocity is inversely related to radius squared. We therefore reasoned that body habitus, independent of microvascular function, could significantly impact measures of reactive hyperemia. To accomplish this later objective, post-occlusion brachial artery flow was also calculated using the five-second average velocity taken immediately post cuff occlusion.

Methods

Ethical Approval and Subjects

This study was approved by the Institutional Review Board for research involving Human Subjects at the University of Texas at Arlington. All subjects gave written informed consent.

Twelve young and elven elderly individuals participated in this investigation. Subjects with overt cardiovascular or metabolic diseases (e.g. heart failure, diabetes) were excluded to minimize the magnitude of confounding variables that may affect responses to arterial cuff occlusion. Premenopausal women were asked to participate during the early follicular phase of their menstrual cycle (Days 1-7) to reduce potential variability in vascular responsiveness. Individuals with significant peripheral adiposity were also excluded to ensure optimal near infrared spectroscopy signal quality. Subjects arrived to the

laboratory fasted and having abstained from alcohol, caffeine, and vigorous exercise for at least 24 hours prior to the visit. Subjects on medication were not asked to deviate from their typical regimen. All tests were performed in a temperature (≈22°C) and ambient light controlled laboratory.

Instrumentation

Upon arriving to the laboratory, subject height and weight were measured with dual-function weight scale and stadiometer (Professional 500KL, Health-O-Meter, McCook, IL, USA). To ensure adequate near-infrared light penetration of the muscle, forearm adipose tissue thickness was measured over the flexor digitorum profundus using skinfold calipers. Subjects were then asked to lie supine on a bed with their non-dominant arm resting on a bedside table at heart level in an extended and slightly abducted position.

Brachial artery blood pressure was measured intermittently in the dominant arm using an automated blood pressure cuff (Connex Spot Monitor, Model 71WX-B, Welch Allyn, Skaneateles Falls, NY, USA). Continuous finger blood pressure, measured via finger plethysmography in the dominant hand, was calibrated from the brachial artery pressures (Finometer PRO, Finapres Medical Systems, Arnhem, The Netherlands). Heart rate was measured via three-lead electrocardiography (ECG) using CM_5 configuration (MLA 0313; ADInstruments Inc., Colorado Springs, CO, USA). The aforementioned signals were captured by the ADInstruments Powerlab, physiologic data acquisition system (Powerlab 16/35, ADInstruments Inc, Colorado Springs, CO, USA).

A cuff was placed on the upper arm of the non-dominant limb and attached to a rapid cuff inflation device (Hokanson SC5, D. E. Hokanson Inc, Bellevue, WA). After careful palpation, a near-infrared probe (OxiplexTS, ISS Inc., Champaign, IL) was placed over the belly of the flexor digitorum profundus of the non-dominant arm and secured with a Velcro elastic strap. To prevent ambient light interference, the probe and forearm were draped with an optically dense, black vinyl cloth.

Brachial artery velocity and diameter were measured using duplex ultrasound (Vivid-i, GE Healthcare, Little Chalfont, United Kingdom) on the medial aspect of the upper arm distal to the occlusive cuff. Brachial artery diameters were measured by a single experienced technician using ultrasound calipers. Images were acquired in the final 30 seconds of the resting period, and immediately after cuff deflation. A 12 Mhz linear array probe was used with a 60 degree angle of insonation. The Doppler audio signal was transmitted to the data acquisition system via a Doppler Audio Translator (Herr et al., 2010), which transformed the audio signal into a velocity waveform which could be recorded via PowerLab.

Experimental Protocol

Protocol A, Conventional Protocol

To evaluate the contribution of tissue ischemia on reactive hyperemia, subjects rested quietly for at least 5 minutes before baseline measurements were obtained. After baseline data acquisition, the arterial cuff was inflated to 220 mmHg and remained inflated for 5 minutes. Post-occlusion recovery was monitored for at least three minutes.

Protocol B, Multiple Cuff Occlusions of Varying Duration

To evaluate the relationship between the magnitude of tissue ischemia and the level of reactive hyperemia, each subject completed a series of three arterial cuff occlusions (4, 6, and 8 minutes), randomized to avoid an ordering effect. Each vascular occlusion test was separated by a minimum of 20 minutes of recovery to prevent carry-over effects from the preceding occlusion test (Crecelius et al., 2013; Dakak et al., 1998).

Data and Statistical Analysis

By convention, reactive hyperemia was first assessed as the highest brachial artery velocity observed immediately after arterial cuff deflation, defined as “peak velocity” and measured using ADInstruments labchart peak analysis function. Reactive hyperemia was also assessed as the 5-second

average velocity immediately post cuff occlusion, defined as the "5-sec hyperemic velocity", and measured using the ADInstruments Labchart mean signal-averaging tool. To account for differences in brachial artery diameter, and its associated influence on velocity, reactive hyperemia was also reported as the peak hyperemic flow, calculated using the 5-sec average velocity immediately following cuff occlusion, multiplied by $\pi \cdot r^2 \cdot 60$; where r is the radius of the diameter immediately post cuff occlusion. Finally, reactive hyperemia was also expressed as the slope of tissue reperfusion during the first 10 seconds after cuff deflation, as previously reported (McLay, Fontana, et al., 2016; McLay, Nederveen, et al., 2016).

The ischemic stimulus was quantified using the near-infrared tissue saturation profile during arterial cuff occlusion. In order to account for individual differences in both the rate of tissue desaturation, and the time spent at "maximal" tissue desaturation, we measured the total oxygen deficit; calculated as the area enclosed within the tissue desaturation signal, using commercially available software (OriginPro, OriginLab Corporation, Northhampton, MA). This area was selected from the moment of cuff inflation to the moment of cuff deflation; the lower border was formed by the tissue saturation profile, while the upper bound was defined as a horizontal line equal to the average of the baseline tissue saturation. Pearson correlations were computed to evaluate the relationship between the ischemic stimulus (i.e. oxygen deficit), and the level of reactive hyperemia (defined as peak brachial artery velocity, 5-sec hyperemic velocity, and peak hyperemic flow). In addition, to assess an ischemia normalized, or "stimulus-adjusted", assessment of reactive hyperemia, we divided each of our three reactive hyperemia metrics (peak velocity, 5-sec hyperemic velocity, and peak hyperemic flow) by the area enclosed within the above described region, referred to as oxygen deficit.

Data are expressed as mean ± standard error unless otherwise stated. Group differences in reactive hyperemia (peak velocity, 5-sec average post-occlusion velocity, hyperemic flow, and tissue reperfusion rate) and tissue saturation during the 5-minute cuff occlusion protocol were compared using

independent samples t-tests. To compare the results from the cuff occlusion series (4-, 6-, and 8-minute protocols), we performed a mixed factorial MANOVA. Duration of cuff occlusion was the within subjects factor, and age (young or elderly) was the between subjects factor. The dependent variables were peak brachial artery velocity, the ischemic stimulus, and the stimulus-adjusted peak velocity. The study alpha was set to 0.05 and statistical analyses were performed with SPSS 25 for Windows.

Results

Subject demographics are shown in Table 1. By design, the elderly group was older, and as expected, had greater history of cardiovascular risk factors and medication use. We observed no significant group differences in resting heart rate or systolic blood pressure; however, diastolic blood pressure was higher in the elderly group, which contributed to a higher mean arterial pressure.

Protocol A – Conventional 5-minute cuff occlusion

Baseline brachial artery velocity and tissue saturation, prior to the 5-minute cuff occlusion, were not significantly different between groups (9.2 $\pm$ 1.4 cm/s vs. 6.1 $\pm$ 0.9 cm/s; 73.6 $\pm$ 1.1 vs. 69.8 $\pm$ 1.5 %, young vs. old, respectively $p = 0.085$ and $p = 0.053$, respectively). As illustrated in **Figure 1**, peak brachial artery velocity, immediately after the conventional 5-minute arterial cuff occlusion, was significantly higher in the young group compared to the elderly group ($p < 0.01$). Likewise, 5-second average hyperemic velocity was also significantly higher in the young group compared to the elderly group ($p < 0.001$). In contrast, tissue reperfusion rate (young vs. elderly: 1.63 ± 0.15 vs. 1.38 ± 0.13, respectively; $p = 0.24$) and peak hyperemic flow (**Figure 1**, $p = 0.18$) were not significantly different between groups. The latter finding is likely explained by large inter-individual differences in brachial artery diameter, leading to the absence of statistically meaningful differences in brachial artery diameter between groups (0.38 ± 0.02 cm vs. 0.40 ± 0.02 cm, young vs. old, $p = 0.35$).

To evaluate our primary hypothesis, we then assessed the near-infrared spectroscopy derived tissue saturation profiles in the young and elderly subjects throughout the 5-min cuff occlusion protocol (**Figure 1E).** Consistent with our prior observations, tissue desaturation was much more pronounced in young individuals compared to the elderly (**Figure 1F**, $p < 0.05$). In an effort to account for this group difference, we adjusted each of our reactive hyperemia measures for oxygen deficit (i.e. the ischemic vasodilatory stimulus). Remarkably, once adjusted, group differences in both peak velocity and 5-sec hyperemic velocity disappeared (**Table 2**).

Protocol B – Multiple cuff occlusions of varying durations

To further explore the determinants of reactive hyperemia, and the influence of age and ischemic stimulus, we assessed reactive hyperemia in the young and elderly individuals following a series of cuff occlusions of varying durations (i.e. 4, 6, and 8 minutes). As illustrated in **Figure 2**, peak brachial artery velocity ($p = 0.066$), 5-sec hyperemic velocity ($p < 0.001$), hyperemic flow ($p < 0.01$), and tissue reperfusion rate (Young 4-min 1.71 ± 0.15, 6-min 1.90 ± 0.2,1 8-min 1.89 ± 0.19; Elderly 4-min 1.25 ± 0.18, 6-min 1.49 ± 0.23, 8-min 1.49 ± 0.18; $p < 0.01$) increased in a cuff duration-dependent manner in both groups. However, as in Protocol A, only peak velocity and 5-sec hyperemic velocity were higher in the young group compared to the elderly (both $p < 0.01$), while tissue reperfusion rate and hyperemic flow showed no difference between groups. We observed no between-group differences in brachial artery diameter at baseline ($p = 0.278$) or peak ($p = 0.094$), nor were there any within group differences between baseline and peak.

Mean arterial pressure was different between groups at baseline (Young 4-min 85 ± 2, 6-min 86 ± 2, 8-min 86 ± 3; Elderly 4-min 94 ± 2, 6-min 94 ± 2, 8-min 96 ± 3; $p < 0.01$) and during peak reactive hyperemia (Young 4-min 85 ± 2, 6-min 86 ± 2, 8-min 87 ± 2; Elderly 4-min 94 ± 1, 6-min 95 ± 2, 8-min 95 ±

3; $p < 0.01$). However, mean arterial pressure did not change from baseline to reactive hyperemia within either group.

Consistent with Protocol A, skeletal muscle tissue desaturation was significantly more pronounced in the young group compared to the elderly group, across all three cuff occlusion times (**Figure 2C and 2D,** $p < 0.01$). To account for this group difference, we once again adjusted reactive hyperemia for oxygen deficit (**Table 2**), confirming our above observations that when reactive hyperemia was adjusted for the ischemic vasodilatory stimulus, group differences in reactive hyperemia were abrogated. To extend this observation, and take advantage of the repeat cuff occlusion protocol employed herein, we also evaluated the intra-individual relationship between reactive hyperemia (peak velocity, 5-sec hyperemic velocity, and flow) and the NIRS-derived oxygen deficit (**Table 3**), revealing three important findings: First, we observed strong intra-individual relationships between the ischemic stimulus and reactive hyperemia in many of the subjects (regardless of age or sex), but not all. Second, in some individuals, reporting the 5-sec average hyperemic velocity and/or hyperemic flow helped to strengthen the relationship with the ischemic stimulus, when a relationship with conventional peak velocity was weak or absent. Third, we identify two groups of "non-responders": (1) individuals who do not respond to increasing levels of tissue ischemia because they seemingly respond "maximally" to low levels of ischemia, and (2) individuals who do not respond to increasing levels of tissue ischemia because they fail to respond appropriately to even the highest levels of tissue ischemia.

Discussion

The major new findings of this study are two-fold: First, we show that the ischemic vasodilatory stimulus varies across individuals, and that the magnitude of reactive hyperemia is often related to the magnitude of tissue desaturation. Second, we highlight important differences between hyperemic velocity and flow, which greatly influence the interpretation and subsequent conclusions made when

assessing within group and between group differences in reactive hyperemia. Together, these data are hypothesis generating and raise several important questions regarding a decades-old approach of assessing “microvascular function”, which indeed warrants further investigation.

Reactive hyperemia is a complex, homeostatic response to replenish the oxygen deficit that occurs after a period of tissue ischemia. The response depends on the local production of multiple vasodilating factors, including adenosine (Carlsson, Sollevi, & Wennmalm, 1987; Meijer et al., 2008), nitric oxide (Dakak et al., 1998; Nugent et al., 1999; Tagawa et al., 1994), prostaglandins (Addor et al., 2008; Kilbom & Wennmalm, 1976), potassium (acting through inwardly rectifying channels and Na^+/K^+ ATPase) (Banitt, Smits, Williams, Ganz, & Creager, 1996; Bank, Sih, Mullen, Osayamwen, & Lee, 2000; Crecelius et al., 2013), pH, and hydrogen peroxide (Sparks & Belloni, 1978; Wolin, Rodenburg, Messina, & Kaley, 1990). Importantly, production of these vasodilatory factors is directly dependent on the level of tissue ischemia. The conventional standard employed across the community for several decades, has been to occlude the distal limb for 5 minutes, regardless of age, sex or disease phenotype, and assess the reactive hyperemia in response to this standardized occlusion period. However, our near-infrared spectroscopy data raise important questions about this approach, and shows marked differences in the magnitude of tissue desaturation both within a group of individuals of similar age, and between age groups. Indeed, when we adjusted peak velocity and 5-sec hyperemic velocity by the level of tissue desaturation (i.e. the ischemic stimulus), group differences were completely abrogated. Likewise, we observed moderate to high intra-individual relationships between reactive hyperemia (defined here as peak velocity or 5-sec hyperemic velocity) and oxygen deficit, in many of our subjects. Together, we believe these data support the hypothesis that inter-individual differences in tissue ischemia play an important role in determining the level of reactive hyperemia.

In no way are we disputing that reactive hyperemia — as measured previously by conventional approaches — is predictive of cardiovascular risk (Anderson et al., 2011; Huang et al., 2007), nor are we

suggesting that microvascular function is not impaired with age, or with cardiovascular disease. Our data, however, raise two important questions. First, to what extent is *microvascular dysfunction* the primary mechanism driving cardiovascular risk in patients with impaired reactive hyperemia? In light of the present results, it would appear that impaired skeletal muscle function, in addition to microvascular dysfunction, plays an important role in "reducing" overall reactive hyperemia. This is not completely inconceivable, given that grip strength is a powerful independent predictor of cardiovascular risk and all-cause mortality (Gale, Martyn, Cooper, & Sayer, 2007; Metter, Talbot, Schrager, & Conwit, 2002; Wu, Wang, Liu, & Zhang, 2017). Indeed, low grip strength would reflect reduced muscle quality/quantity, which would negatively influence tissue desaturation rate during a vascular occlusion test. Aging is indeed associated with sarcopenia and impaired skeletal muscle oxidative capacity, two phenomenon that are reciprocally linked to oxygen metabolism(Johnson, Robinson, & Nair, 2013). Thus, while it was not directly measured in this investigation, we reason that reduced skeletal muscle oxidative function and lower muscle mass likely contributed to the attenuated tissue desaturation in the elderly group studied herein.

The second major question raised is, what do we do with this new information? If the normalized reactive hyperemia is found to be preserved, what treatment/intervention can be implemented to avoid future cardiovascular events? While the answer to this later question is beyond the scope of the present proof-of-concept study, our data point to improving skeletal muscle metabolism, rather than treating the microvasculature per se. To that end, an attenuated rate of tissue desaturation is likely caused by either mitochondrial dysfunction, and/or limitation in diffusive oxygen conductance. Therapies or interventions aimed at improving these endpoints would therefore seem far more warranted than treatments targeting the micro-vessels.

We acknowledge that reactive hyperemia was not always related to the ischemic stimulus. We find this particularly interesting, as it raises important fundamental questions. While we cannot be sure, based on this single investigation, we speculate that the non-responders fall into two potential categories,

and may be providing important pathophysiologic insight. For example, subjects 13, 21 and 18 show very little hyperemic reserve; however, they also exhibit velocities on par with or even exceeding the group means. We reason that this may actually reflect “good microvascular function” (i.e. maximal vasodilation for the smallest stimulus). In contrast, subjects 14 and 20 also have limited hyperemic reserve, but have some of the lowest hyperemic velocities and flow values (below the mean for each respective group), possibly indicating “microvascular dysfunction”? We believe this is an important observation that warrants further investigation.

In addition to the above considerations regarding the ischemic stimulus, our data also raise important questions about the end-point measure of reactive hyperemia itself. Indeed, vessel diameter varies considerably between individuals, the result of which can have a profound independent effect on velocity. With all things being equal, an individual with a large diameter will have a lower absolute velocity— independent of microvascular function— while someone with a small brachial artery diameter will have a high velocity. We therefore explored the value of reporting hyperemic flow, because (a) the mathematical derivation of flow intrinsically accounts for differences in vessel diameter; and (b) the mean velocity included in the calculation of flow was sampled over a five-second period, thus accounting for some of the variability associated with single peak velocity analysis. To our surprise, differences between the young and elderly groups were eliminated when reactive hyperemia was assessed as hyperemic flow, which we interpret to reflect the inter-individual variability of vessel diameter in our cohorts. This is consistent with at least one prior observation (Huang et al., 2007), which found the predictive value of reactive hyperemia to be eliminated when expressed as flow compared to velocity. It interesting however, that hyperemic flow did share a similar relationship with oxygen deficit as peak velocity, once again reinforcing the potential importance of this key determinant. Moreover, we observed several cases (subjects 13, 23, and 18) where evaluating velocity alone, failed to provide a clear understanding of the microvascular responsiveness to a given ischemic stimulus. In these three cases, velocity was greatly

influenced by changes in brachial artery diameter; which, when accounted for, showed a strong relationship between reactive hyperemia and the ischemic stimulus. Finally, flow measurements were restricted to the first 10 seconds after cuff deflation, to avoid potential influence from shear-mediated vasodilation, and metabolic stimulus. Indeed, shear-mediated dilation of the brachial artery introduces a new confounding factor, i.e. macrovascular endothelial function. Likewise, it remains unclear what role skeletal muscle metabolism plays beyond the initial reactive hyperemia period. One could imagine, in the setting of impaired diffusive oxygen conductance, that a prolonged error signal (i.e. delayed ischemia recovery) could influence post-occlusion hyperemia independent of microvascular function per se. This is therefore an important area, which requires further consideration.

In addition to considering measures of velocity and flow, it may be equally important to consider the potential influence of blood pressure on reactive hyperemia . In the present investigation, mean arterial pressure was consistent across all measurements, both within and between groups. As a result,peak vascular conductance was no more informative than flow. However, this may prove more important for other investigations, depending on the patient/study population, and thus should be considered moving forward. That mean arterial pressure was higher in the elderly group however, suggests that we may have underestimated the group differences, making the normalization data even more interesting.

Experimental Considerations

While we believe our findings hold great promise, this was admittedly a proof-of-concept study conducted in a relatively small group of individuals. By design, these subjects were chosen because they represent an average elderly individual living independently in the community. Although free from severe cardiovascular disease, many of our patients had a history of cardiovascular risk factors, and many were taking concomitant cardiovascular medications. It is therefore possible that both the risk factors

themselves, and/or the medications taken to treat them, may have influenced the present results.. Thus, further investigations involving much larger cohorts and clinical populations with known co-morbidities and underlying cardiovascular dysfunction are therefore needed to fully test the implications of this relationship. Likewise, studies designed to evaluate the influence of common cardiovascular medications on resting metabolic rate and reactive hyperemia are warranted. Only then can the "true" contribution of microvascular dysfunction to cardiovascular risk be predicted.

Moreover, we chose to evaluate reactive hyperemia using Doppler ultrasound given its widespread use in the seminal papers in this area of research. However, other modalities, including peripheral artery tonometry and strain gauge plethysmography, have also been used. Indeed, given its simplicity, peripheral artery tonometry has arguably become the preferred choice for vascular occlusion tests. Accordingly, future studies are also needed to test the relationship between tissue desaturation against these other measures of reactive hyperemia.

Figures and Tables

Table 1. Subject Characteristics

		Young	Elderly
n		12	11
Male/Female		6/6	6/5
Age (years)		23 ± 3	74 ± 6*
Height (m)		1.7 ± 0.12	1.7 ± 0.10
Weight (kg)		70.4 ± 11.5	83.7 ± 20.7
BMI (kg/m^2)		24.2 ± 1.8	29.5 ± 5.6*
Baseline Hemodynamics			
Systolic Blood Pressure (mmHg)		117 ± 13	124 ± 10
Diastolic Blood Pressure (mmHg)		66 ± 9	75 ± 6*
Mean Arterial Pressure (mmHg)		83 ± 9	91 ± 6*
Heart Rate (bpm)		61 ± 5	67 ± 10
Health History		n	n
	Cardiac Arrhythmia	0	3
	Hypertension	0	4
	Hypercholesterolemia	0	6
	Thyroid Disorder	0	2
	Arthritis	0	7
	Cancer	0	3
Cardiovascular Medications		n	n
	Beta Blocker	0	2
	Angiotensin Receptor Blocker	0	2
	Diuretic	0	1
	Statin	0	4
	Calcium Channel Blocker	0	2
	Diuretic	0	1
	NSAIDs/blood thinners	0	4

* $P < 0.05$

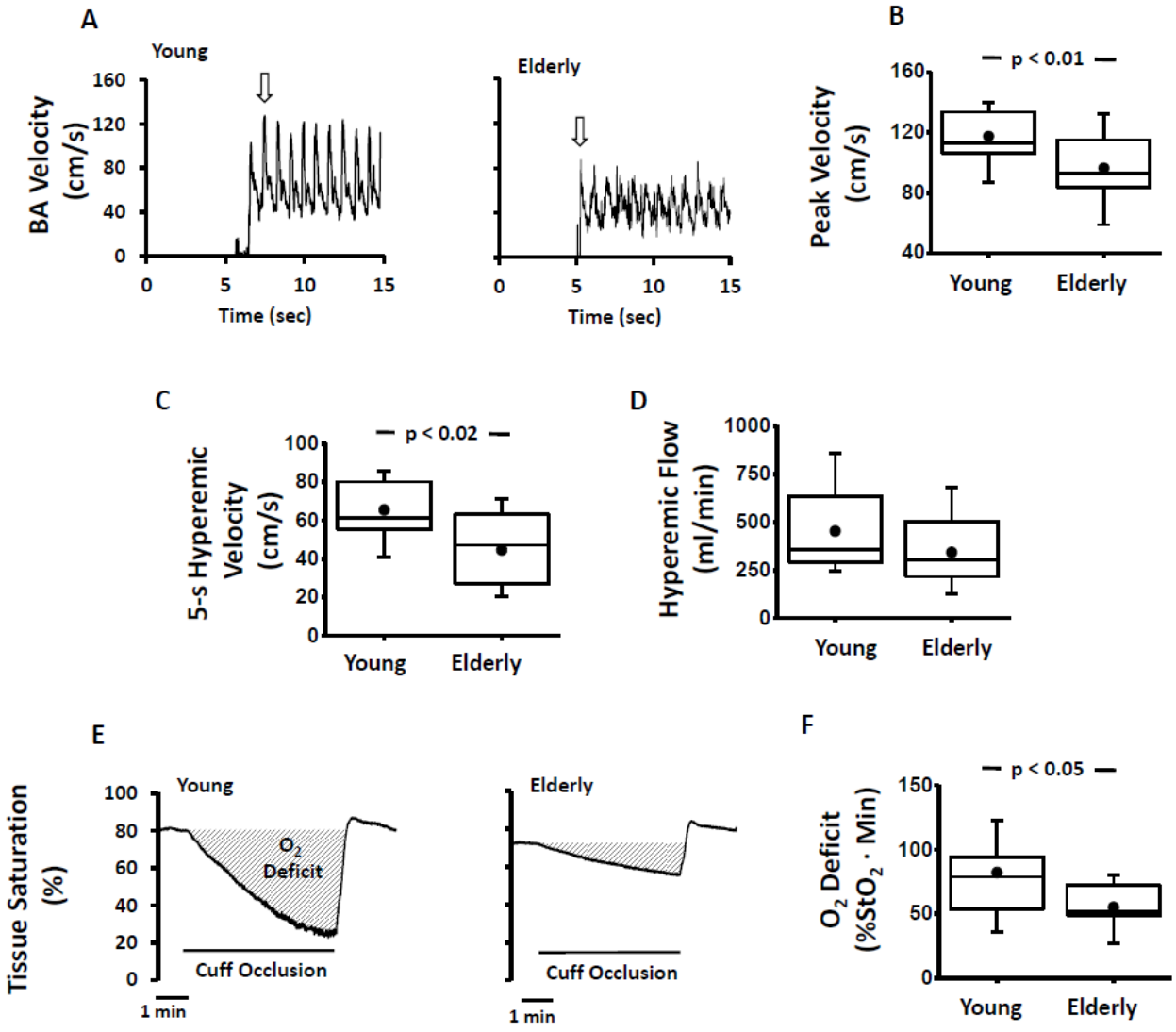

Figure 1. Influence of age on reactive hyperemia, and its determinants, following a standardized 5-min vascular occlusion. (**A**) Representative brachial artery velocity from a young (left) and elderly (right) subject, immediately following cuff deflation. Arrow signifies the peak velocity. Summary group data showing the average peak brachial artery velocity (**B**), average 5 second hyperemic velocity (**C**), and average hyperemic flow (**D**) following a 5-minute arterial cuff occlusion in twelve young subjects (6 male/6 female) and eleven elderly subjects (6 male/5 female). (**E**) Representative tissue saturation profile, measured by near-infrared spectroscopy, during a 5-minute vascular occlusion test from the same young (left) and elderly (right) individuals illustrated in panel A. Shaded area represents the oxygen deficit (i.e. the ischemic stimulus to vasodilate). (**F**) Summary data showing the average change in tissue desaturation, expressed as the area enclosed within the desaturation curve, during the 5 minutes of arterial occlusion in the twelve young and eleven elderly subjects. Data analyzed using independent samples t-tests.

Table 2. Stimulus-Adjusted Measures of Reactive Hyperemia

	Group	Peak Velocity	5-s Hyperemic Velocity	Hyperemic Flow
Protocol A				
5-Min	Elderly	1.97 ± 0.32	0.93 ± 0.20	7.25 ± 1.89
	Young	1.70 ± 0.23	0.94 ± 0.12	5.78 ± 0.53
Protocol B				
4-Min	Elderly	3.72 ± 0.81	1.66 ± 0.39	12.76 ± 3.13
	Young	2.72 ± 0.34	1.69 ± 0.22	10.84 ± 1.42
6-Min	Elderly	1.60 ± 0.22	0.79 ± 0.12	6.03 ± 0.81
	Young	1.34 ± 0.18	0.81 ± 0.11	6.00 ± 1.20
8-Min	Elderly	0.96 ± 0.15	0.49 ± 0.08	4.15 ± 0.62
	Young	0.91 ± 0.10	0.54 ± 0.07	3.59 ± 0.39

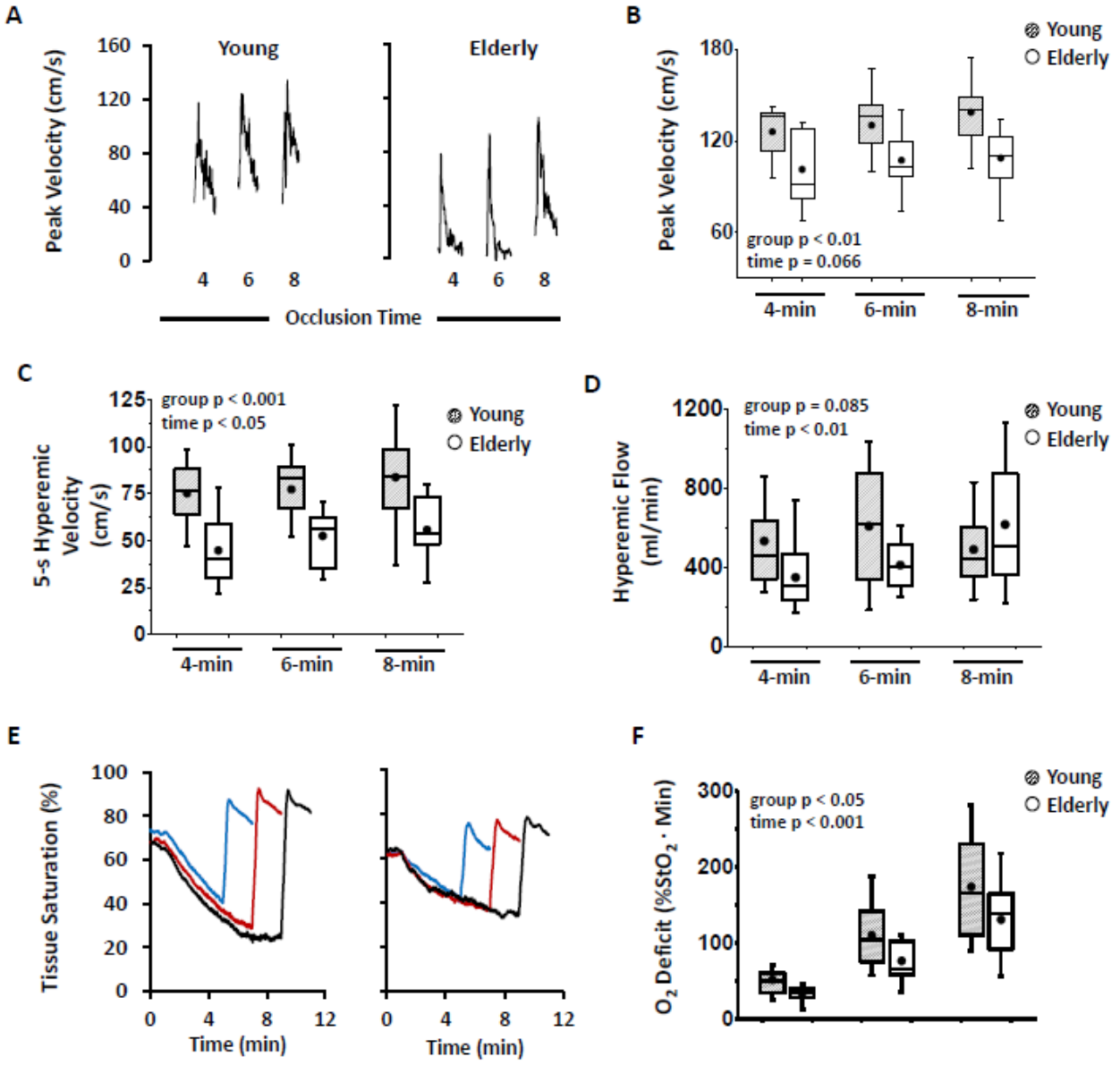

Figure 2. Influence of arterial cuff occlusion time on reactive hyperemia in young and elderly individuals. (**A**) Representative brachial artery velocities from a young (left) and elderly (right) subject, immediately following cuff deflation, after 4, 6 and 8 minutes of cuff occlusion. Group mean data for peak brachial artery velocity (**B**), average 5 second hyperemic velocity (**C**), and average hyperemic flow (**D**), following each cuff occlusion period in 12 young (6 male/6 female), and 11 elderly (6 male/5 female) subjects. The young group is represented by the hatched boxes, the elderly group is represented by open boxes. (**E**) Representative tissue saturation profile, measured by near-infrared spectroscopy, during the 4-, 6- and 8-minute vascular occlusion tests from the same young (left) and elderly (right) individuals illustrated in panel A. (**F**) Group mean data showing the average change in tissue desaturation, expressed as the area enclosed within the desaturation curve, across each of the occlusion periods in the 2 same young and elderly subjects described above. The young group is represented by the hatched boxes circles, the elderly group represented by open boxes. Data were analyzed using a mixed factorial MANOVA**.**

Table 3. Intra-individual Correlations Between Oxygen Deficit and Measures of Reactive Hyperemia

Subject No.	Age	Sex	O_2 Deficit			Peak Velocity (cm/sec)				5-sec Avg. Velocity (cm/sec)				5-sec Avg. Flow (ml/min)			
			4 min	6 min	8 min	4 min	6 min	8 min	Correlation	4 min	6 min	8 min	Correlation	4 min	6 min	8 min	Correlation
1	28	M	65	142	240	118	131	146	1.000	64	86	78	0.592	581	855	779	0.650
2	24	M	70	157	240	137	143	150	0.999	87	100	97	0.758	693	827	731	0.291
3	27	F	56	89	159	139	143	175	0.978	89	81	107	0.824	375	321	369	0.097
4	22	M	45	92	151	101	167	169	0.842	55	101	122	0.961	414	762	968	0.977
5	24	F	24	58	93	115	99	148	0.670	69	52	87	0.542	273	222	323	0.510
6	22	M	56	131	218	111	105	120	0.660	64	57	63	-0.139	534	478	548	0.234
7	76	M	36	105	161	92	103	110	0.998	21	29	28	0.807	305	402	441	0.985
8	76	M	46	101	165	85	94	107	0.998	27	31	48	0.958	320	326	524	0.899
9	80	M	41	111	218	114	120	121	0.898	67	70	73	0.976	527	558	761	0.960
10	66	F	28	65	92	118	120	134	0.883	59	62	76	0.909	468	518	600	0.974
11	74	F	44	96	142	73	98	93	0.766	30	56	52	0.790	173	306	351	0.969
12	69	F	34	65	112	82	97	96	0.756	40	54	51	0.650	233	279	330	0.996
13	25	M	104	188	282	142	134	147	0.391	76	77	100	0.892	858	901	1134	0.940
14	23	F	52	116	173	96	74	102	0.185	47	32	37	-0.663	274	183	215	-0.663
15	23	F	31	72	112	137	156	128	-0.312	77	90	69	-0.384	305	356	353	0.842
16	28	M	48	143	221	137	138	136	-0.593	99	86	96	-0.278	1163	933	1127	-0.196
17	22	F	32	58	90	136	139	112	-0.841	93	88	66	-0.954	504	1038	378	-0.245
18	19	F	37	78	110	143	133	133	-0.864	82	77	81	-0.180	420	421	470	0.840
19	77	M	36	58	138	92	140	106	-0.015	36	65	54	0.347	231	490	408	0.405
20	78	F	30	42	75	68	73	68	-0.288	30	35	31	-0.029	205	251	236	0.436
21	61	M	19	60	103	132	103	123	-0.295	78	59	80	0.099	743	612	831	0.413
22	82	F	12	35	56	128	117	123	-0.461	50	58	59	0.911	286	356	400	0.996
23	72	M	40	102	175	128	114	113	-0.856	54	56	61	0.980	348	422	507	1.000
Young Mean ± SE			52 ± 6	110 ± 12	174 ± 19	126 ± 5	130 ± 7	139 ± 6		75 ± 5	77 ± 6	84 ± 7		533 ± 76	608 ± 89	616 ± 94	
Elderly Mean ± SE			33 ± 3	76 ± 8	131 ± 15	101 ± 7	107 ± 5	109 ± 6		45 ± 5	52 ± 4	56 ± 5		349 ± 51	411 ± 36	490 ± 55	
All Mean ± SE			43 ± 4	94 ± 8	153 ± 13	114 ± 5	119 ± 5	124 ± 5		61 ± 5	65 ± 4	70 ±1 5		445 ± 50	514 ± 53	556 ± 56	

References

Addor, G., Delachaux, A., Dischl, B., Hayoz, D., Liaudet, L., Waeber, B., & Feihl, F. (2008). A comparative study of reactive hyperemia in human forearm skin and muscle. *Physiol Res, 57*(5), 685-692.

Anderson, T. J., Charbonneau, F., Title, L. M., Buithieu, J., Rose, M. S., Conradson, H., . . . Lonn, E. M. (2011). Microvascular function predicts cardiovascular events in primary prevention: long-term results from the Firefighters and Their Endothelium (FATE) study. *Circulation, 123*(2), 163-169. doi:10.1161/CIRCULATIONAHA.110.953653

Banitt, P. F., Smits, P., Williams, S. B., Ganz, P., & Creager, M. A. (1996). Activation of ATP-sensitive potassium channels contributes to reactive hyperemia in humans. *Am J Physiol, 271*(4 Pt 2), H1594-1598. doi:10.1152/ajpheart.1996.271.4.H1594

Bank, A. J., Sih, R., Mullen, K., Osayamwen, M., & Lee, P. C. (2000). Vascular ATP-dependent potassium channels, nitric oxide, and human forearm reactive hyperemia. *Cardiovasc Drugs Ther, 14*(1), 23-29.

Bonetti, P. O., Pumper, G. M., Higano, S. T., Holmes, D. R., Jr., Kuvin, J. T., & Lerman, A. (2004). Noninvasive identification of patients with early coronary atherosclerosis by assessment of digital reactive hyperemia. *J Am Coll Cardiol, 44*(11), 2137-2141. doi:10.1016/j.jacc.2004.08.062

Carlsson, I., Sollevi, A., & Wennmalm, A. (1987). The role of myogenic relaxation, adenosine and prostaglandins in human forearm reactive hyperaemia. *J Physiol, 389*, 147-161.

Crecelius, A. R., Richards, J. C., Luckasen, G. J., Larson, D. G., & Dinenno, F. A. (2013). Reactive hyperemia occurs via activation of inwardly rectifying potassium channels and Na+/K+-ATPase in humans. *Circ Res, 113*(8), 1023-1032. doi:10.1161/CIRCRESAHA.113.301675

Dakak, N., Husain, S., Mulcahy, D., Andrews, N. P., Panza, J. A., Waclawiw, M., . . . Quyyumi, A. A. (1998). Contribution of nitric oxide to reactive hyperemia: impact of endothelial dysfunction. *Hypertension, 32*(1), 9-15.

de Berrazueta, J. R., Guerra-Ruiz, A., Garcia-Unzueta, M. T., Toca, G. M., Laso, R. S., de Adana, M. S., . . . Llorca, J. (2010). Endothelial dysfunction, measured by reactive hyperaemia using strain-gauge plethysmography, is an independent predictor of adverse outcome in heart failure. *Eur J Heart Fail, 12*(5), 477-483. doi:10.1093/eurjhf/hfq036

Gale, C. R., Martyn, C. N., Cooper, C., & Sayer, A. A. (2007). Grip strength, body composition, and mortality. *International Journal of Epidemiology, 36*(1), 228-235. doi:10.1093/ije/dyl224

Herr, M. D., Hogeman, C. S., Koch, D. W., Krishnan, A., Momen, A., & Leuenberger, U. A. (2010). A real-time device for converting Doppler ultrasound audio signals into fluid flow velocity. *American Journal of Physiology-Heart and Circulatory Physiology, 298*(5), H1626-H1632. doi:10.1152/ajpheart.00713.2009

Huang, A. L., Silver, A. E., Shvenke, E., Schopfer, D. W., Jahangir, E., Titas, M. A., . . . Vita, J. A. (2007). Predictive value of reactive hyperemia for cardiovascular events in patients with peripheral arterial disease undergoing vascular surgery. *Arterioscler Thromb Vasc Biol, 27*(10), 2113-2119. doi:10.1161/ATVBAHA.107.147322

Ishibashi, Y., Takahashi, N., Shimada, T., Sugamori, T., Sakane, T., Umeno, T., . . . Murakami, Y. (2006). Short duration of reactive hyperemia in the forearm of subjects with multiple cardiovascular risk factors. *Circ J, 70*(1), 115-123.

Johnson, M. L., Robinson, M. M., & Nair, K. S. (2013). Skeletal muscle aging and the mitochondrion. *Trends Endocrinol Metab, 24*(5), 247-256. doi:10.1016/j.tem.2012.12.003

Kilbom, A., & Wennmalm, A. (1976). Endogenous prostaglandins as local regulators of blood flow in man: effect of indomethacin on reactive and functional hyperaemia. *J Physiol, 257*(1), 109-121.

Kragelj, R., Jarm, T., & Miklavcic, D. (2000). Reproducibility of parameters of postocclusive reactive hyperemia measured by near infrared spectroscopy and transcutaneous oximetry. *Ann Biomed Eng, 28*(2), 168-173.

Leeson, P., Thorne, S., Donald, A., Mullen, M., Clarkson, P., & Deanfield, J. (1997). Non-invasive measurement of endothelial function: effect on brachial artery dilatation of graded endothelial dependent and independent stimuli. *Heart, 78*(1), 22-27. doi:10.1136/hrt.78.1.22

London, G. M., Pannier, B., Agharazii, M., Guerin, A. P., Verbeke, F. H., & Marchais, S. J. (2004). Forearm reactive hyperemia and mortality in end-stage renal disease. *Kidney Int, 65*(2), 700-704. doi:10.1111/j.1523-1755.2004.00434.x

Matsuzawa, Y., Kwon, T. G., Lennon, R. J., Lerman, L. O., & Lerman, A. (2015). Prognostic Value of Flow-Mediated Vasodilation in Brachial Artery and Fingertip Artery for Cardiovascular Events: A Systematic Review and Meta-Analysis. *J Am Heart Assoc, 4*(11). doi:10.1161/jaha.115.002270

Mayeur, C., Campard, S., Richard, C., & Teboul, J. L. (2011). Comparison of four different vascular occlusion tests for assessing reactive hyperemia using near-infrared spectroscopy. *Critical Care Medicine, 39*(4), 695-701. doi:10.1097/CCM.0b013e318206d256

McLay, K. M., Fontana, F. Y., Nederveen, J. P., Guida, F. F., Paterson, D. H., Pogliaghi, S., & Murias, J. M. (2016). Vascular responsiveness determined by near-infrared spectroscopy measures of oxygen saturation. *Experimental Physiology, 101*(1), 34-40. doi:10.1113/EP085406

McLay, K. M., Nederveen, J. P., Pogliaghi, S., Paterson, D. H., & Murias, J. M. (2016). Repeatability of vascular responsiveness measures derived from near-infrared spectroscopy. *Physiol Rep, 4*(9). doi:10.14814/phy2.12772

Meijer, P., Wouters, C. W., van den Broek, P. H., Scheffer, G. J., Riksen, N. P., Smits, P., & Rongen, G. A. (2008). Dipyridamole enhances ischaemia-induced reactive hyperaemia by increased adenosine receptor stimulation. *Br J Pharmacol, 153*(6), 1169-1176. doi:10.1038/bjp.2008.10

Metter, E. J., Talbot, L. A., Schrager, M., & Conwit, R. (2002). Skeletal muscle strength as a predictor of all-cause mortality in healthy men. *Journals of Gerontology Series a-Biological Sciences and Medical Sciences, 57*(10), B359-B365. doi:DOI 10.1093/gerona/57.10.B359

Nugent, A. G., McGurk, C., McAuley, D., Maguire, S., Silke, B., & Johnston, G. D. (1999). Forearm reactive hyperaemia is not mediated by nitric oxide in healthy volunteers. *Br J Clin Pharmacol, 48*(3), 457-459.

Paine, N. J., Hinderliter, A. L., Blumenthal, J. A., Adams, K. F., Jr., Sueta, C. A., Chang, P. P., . . . Sherwood, A. (2016). Reactive hyperemia is associated with adverse clinical outcomes in heart failure. *Am Heart J, 178*, 108-114. doi:10.1016/j.ahj.2016.05.008

Rosenberry, R., Munson, M., Chung, S., Samuel, T. J., Patik, J., Tucker, W. J., . . . Nelson, M. D. (2018). Age-related microvascular dysfunction: novel insight from near-infrared spectroscopy. *Exp Physiol, 103*(2), 190-200. doi:10.1113/EP086639

Sparks, H. V., Jr., & Belloni, F. L. (1978). The peripheral circulation: local regulation. *Annu Rev Physiol, 40*, 67-92. doi:10.1146/annurev.ph.40.030178.000435

Tagawa, T., Imaizumi, T., Endo, T., Shiramoto, M., Harasawa, Y., & Takeshita, A. (1994). Role of nitric oxide in reactive hyperemia in human forearm vessels. *Circulation, 90*(5), 2285-2290.

Wolin, M. S., Rodenburg, J. M., Messina, E. J., & Kaley, G. (1990). Similarities in the pharmacological modulation of reactive hyperemia and vasodilation to hydrogen peroxide in rat skeletal muscle arterioles: effects of probes for endothelium-derived mediators. *Journal of Pharmacology and Experimental Therapeutics, 253*(2), 508-512.

Wu, Y., Wang, W., Liu, T., & Zhang, D. (2017). Association of Grip Strength With Risk of All-Cause Mortality, Cardiovascular Diseases, and Cancer in Community-Dwelling Populations: A Meta-analysis of Prospective Cohort Studies. *Journal of the American Medical Directors Association, 18*(6), 551 e517-551 e535. doi:10.1016/j.jamda.2017.03.011

CHAPTER 5

LIMB IMMOBILIZATION DOES NOT DECOUPLE SKELETAL MUSCLE OXIDATIVE FUNCTION FROM REACTIVE HYPEREMIA

Methods

Subjects

Healthy young men were recruited from the Dallas-Fort Worth Community. Exclusion criteria included females (to avoid hormonal variation between limb immobilization visits), or male subjects who were < 18 years old or > 35 years old, had a history of cardiovascular disease, known diabetes, arthritis, peripheral artery disease, hypertension, orthopedic or physical limitations that would prevent full participation, currently use tobacco, or have a body mass index > 35 kg/m^2. All participants signed written informed consent and the study was approved by the University of Texas at Arlington Institutional Review Board.

Experimental Protocol

All subjects were instructed to arrive to the laboratory having fasted for a minimum of 4 hours, and having abstained from caffeine, alcohol, and strenuous exercise for 24 hours prior to each visit. All experiments were performed in a quiet, temperature controlled laboratory maintained at 24 ± 1°C, humidity 41 ± 3%.

Upon arrival to the laboratory, subjects' seated blood pressure and heart rate were measured using an automated blood pressure cuff (Connex Spot Monitor, model 71WX-B, Welch Allyn, Skaneateles Falls, NY). Height and weight were then measured using a dual-function scale and stadiometer (Professional 500KL, Health-O-Meter, McCook, IL). Subjects were then asked to lie supine on a bed with their non-dominant limb resting on a bedside table in an extended and comfortably adducted position. Blood pressure was monitored continuously in the dominant arm via beat-to-beat finger blood pressure (Finometer PRO, Finapres Medical Systems, Arnhem, The Netherlands) and intermittently using the previously mentioned automated blood pressure cuff. Heart rate was measured by three-lead electrocardiography using the CM_5 configuration (MLA 0313 lead wires, ADInstruments, Colorado Springs, CO). Beat-to-beat blood pressure and electrocardiogram signals were then captured by a physiological

data acquisition system (ADInstruments PowerLab 16/35). An occlusive cuff was placed on the upper arm and connected to a rapid inflation device (SC5, Hokanson, Bellevue, WA). Tissue saturation (StO_2) was measured continuously in the flexor digitorum profundus using near-infrared spectroscopy (MetaOx and OxiplexTS, ISS, Champaign, IL). The probe was placed over the belly of the flexor digitorum profundus and secured using an elastic strap. A soft foam wrap was also placed around the forearm and NIRS probe to prevent interference by ambient light.

Handgrip Strength

Hand grip strength was measured using a Jamar hand grip dynamometer with the handle set in Position 2 as recommended by Trampisch et al (Trampisch, Franke, Jedamzik, Hinrichs, & Platen, 2012). All subjects were seated in the same chair, with the elbow flexed at approximately 90° and with the wrist in a neutral or slightly flexed position (Roberts et al., 2011; Trampisch et al., 2012). Subjects were instructed to squeeze and given standardized verbal encouragement by the same technician in order to obtain maximal effort. The highest of three attempts was recorded as the maximal hand grip strength.

Forearm Measurements

Forearm volume was assessed using a water displacement method using a custom-built vessel similar to those used by Chromy et al (Chromy, Zalud, Dobsak, Suskevic, & Mrkvicova, 2015). The vessel was filled until the water level began to exit the drainage spout. Once water had ceased to drain from the spout, subjects were instructed to slowly lower their hand into the water up to the crease of the wrist. Water displaced by the hand was captured in a plastic receptacle and a scientific scale (Amput Electronics, Model 457) was tared. The subject was then instructed to lower their arm into the water up to the crease of the elbow. Water displaced by the forearm was once again captured and weighed. This process was repeated a minimum of two times and the mass of water averaged to yield cubic centimeters of forearm volume.

Forearm circumference was measured in three locations: ≈2cm distal to the crease of the elbow, at the widest region of the forearm midway between the elbow and the wrist, and at the crease of the wrist. Measurements were performed twice at each location and averaged. Adipose tissue thickness was measured at each of these locations. All measurements were performed by the same technician to reduce intra-observer variability.

Reactive Hyperemia

Brachial artery velocity and diameter were measured using duplex ultrasound (Vivid-i, GE Healthcare, Little Chalfont, UK). Images of the brachial artery were obtained using a 12 MHz linear array probe at the medial aspect of the upper arm distal to the occlusive cuff. The video signal from the ultrasound device was recorded using a screen-capturing software (Vascular Imager, Medical Imaging Applications LLC., Coralville, Iowa). Using edge detection software (FMD Studio, Quipu, Florence, Italy), offline analysis of these video files was performed to assess brachial artery diameter at rest and within the first 15 seconds following deflation of the occlusive cuff. The audio signal from the ultrasound was transmitted to the data acquisition system via a Doppler audio translator (Herr et al., 2010).

After establishing a stable, resting baseline the occlusive cuff was inflated on the upper arm for 5-minutes at a pressure of 220 mmHg. At the 5-minute mark the cuff was rapidly deflated; post-occlusive reactive hyperemia and recovery were measured for the following 3 minutes. Tissue saturation was measured continuously by NIRS throughout this period.

Reactive hyperemia analysis

Reactive hyperemia was first assessed as the peak velocity, or the highest brachial artery velocity observed within the first 15 seconds following cuff deflation. A 5-second average of the brachial artery velocity was also calculated during this 15-second period. Using this average velocity and the diameters

obtained through the edge detection software, hyperemic flow was then calculated using the following equation:

$$Flow = \pi r^2 \times 5\, sec\, avg\ \ velocity \times 60$$

Using the NIRS-derived StO_2 we calculated the ischemic stimulus achieved during arterial cuff occlusion— the area bounded on the Y-axis by the average baseline tissue saturation and the tissue saturation tracing, and bounded on the X-axis by the time of cuff occlusion— using the same approach as previously described (Rosenberry et al., 2019).

Skeletal Muscle Oxidative Function

Skeletal muscle oxidative function was assessed using a NIRS-based protocol that has been validated against PCR recovery, measured by magnetic resonance spectroscopy (Ryan, Brophy, Lin, Hickner, & Neufer, 2014; Ryan, Erickson, et al., 2014; Ryan, Southern, Reynolds, & McCully, 2013). Subjects remained supine and instrumented as described above, with the exception of brachial artery ultrasound. After establishing a stable, resting baseline, subjects were instructed to isometrically squeeze the hand grip dynamometer (Smedley Hand Grip Dynamometer, Stoelting Co. Wood Dale, Il) at 50% of their maximal voluntary contraction until the difference between oxyhemoglobin/myoglobin (HbO_2) and deoxyhemoglobin/myoglobin (HHb), referred to as Hb_{diff}, reached ≈50% of the difference between their resting baseline and the minimum value observed during the final seconds of the arterial cuff occlusion. Following cessation of the isometric exercise, a series of eighteen cuff occlusions was performed. The timing for this series was performed as follows: 5s on/5s off for occlusions #1-5; 7s on/7s off for occlusions #7-10; 10s on/15s off for occlusions #11-14; and 10s on/20s off for occlusions #15-18 (Figure 1A). After the occlusion series was complete, subjects remained at rest until they returned to a stable baseline state.

Mitochondrial oxidative function analysis

Skeletal muscle VO_2 was assessed by calculating the rate of change of Hb_{diff} during each of the 18 cuff occlusions. Each slope was then plotted against the post-hand grip exercise time to produce a curve, which was then fit with the following monoexponential curve using commercially available software (OriginPro, OriginLab, Corp., Northampton, MA) as previously described (Rosenberry, Chung, & Nelson, 2018; Ryan, Brophy, et al., 2014; Ryan, Erickson, et al., 2014; Ryan et al., 2013):

$$y = END - \Delta \times e^{-kt}$$

"y" is the relative mVO2 during cuff inflation, "End" was defined as the mVO2 measured immediately following exercise; delta "Δ" is the change in mVO2 from rest to the end of exercise; "k" is the fitting rate constant; "t" is time. The initial rate of oxygen consumption was defined as the first slope measured after cessation of exercise. The recovery time constant (τVO_2) is representative of mitochondrial oxidative function, with faster times representing greater function.

Limb Immobilization

Following completion of all study measures, subjects were then provided with a commercially available forearm brace (Supplemental Figure 1). This rigid brace was fixed in place using hook-and-loop straps, and when worn properly prevents flexion and extension about the wrist joint, as well as finger flexion and extension. Subjects were instructed to wear the brace firmly strapped to the forearm at all times, except for when bathing. Subjects were instructed to continue wearing the brace until it was removed just prior to the commencement of study measures at Visit 2 (≈ 30 days).

Statistical Analysis

Data are expressed as mean ± standard deviation unless otherwise specified. Data were assessed for statistical difference using a Student's paired-sample *t*-test. G*Power was used to calculate Cohen's d_Z

and achieved statistical power. Based upon previous data (refs), we expected limb immobilization to recapitulate the difference in reactive hyperemia previously observed between young and elderly participants (≈ 20 ± 20 cm/s). This level of change produced a large effect size (Cohen's d_Z = 1.06). Based upon these historical data, and a statistical power of 0.85 we anticipate needing 11 subjects to complete this study. To account for subject attrition, our a priori sample size was estimated to be 15.

Results

Fifteen young, healthy men volunteered for the study. Three subjects were excluded from the study due to poor data quality; 2 related to NIRS and 1 related to brachial artery velocity. The remaining twelve subjects (age 19 ± 1 yrs; height 172 ± 6 cm; weight 64 ± 12 kg; BMI 22 ± 3 kg/m^2) completed both laboratory visits, separated by 28 ± 2 days of limb immobilization. No adverse events were reported, and all subjects claimed to tolerate the limb immobilization well.

Effect of limb immobilization on forearm morphology and function

Despite subjects adhering to the immobilization protocol, we observed no differences in handgrip strength, adipose tissue thickness, forearm volume, or forearm circumference (Table 1).

Skeletal Muscle Oxidative Function

To assess the efficacy of limb immobilization as a means of inducing impairments in skeletal muscle oxidative function, we evaluated the recovery time constant of skeletal muscle VO_2 (τVO_2) following a brief period of handgrip exercise. Contrary to previous findings, limb immobilization had no measurable effect on τVO_2 (Figure 1), suggesting that skeletal muscle oxidative function was not impaired by forearm immobilization.

Reactive Hyperemia

Baseline brachial artery velocity did not change with limb immobilization (pre: 9.4 ± 3.2 cm/sec vs. post 12.1 ± 6.8 cm/sec; P = 0.23), nor did baseline tissue saturation change (Pre: 73.1 ± 3.4 % vs. post: 75.2 ± 5.3 %; P = 0.27). Consistent with the lack of change in τVO_2, the slope of tissue desaturation during arterial cuff occlusion— an index of resting skeletal muscle metabolic rate— did not change with limb immobilization (Figure 2, P = 0.80). As a result, for the same fixed period of arterial occlusion before and after limb immobilization, the ischemic stimulus did not differ (Figure 3, P = 0.44).

Reactive hyperemia was also unchanged, as evidenced by the lack of differences observed in peak brachial artery velocity (Figure 3, P = 0.13), 5-second average hyperemic velocity (Figure 3) and 5-second average hyperemic flow (P = 0.81, P = 0.20 respectively) (Figure 3). Of note, when measured during reactive hyperemia (i.e. ≤ 15 seconds after the cuff was released), pre- and post-immobilization, there were no differences in brachial artery diameter (pre: 0.318 ± 0.01 cm vs. post: 0.319 ± 0.06 cm), nor heart rate (pre: 67 ± 8 bpm vs. post: 73 ± 9 bpm), nor mean arterial pressure (pre: 82 ± 2 mmHg vs. post: 83 ± 5).

Discussion

The aim of the present study was to further define the relationship between the degree of tissue desaturation and the magnitude of reactive hyperemia in young healthy males. We hypothesized that by transiently reducing skeletal muscle oxidative function with limb immobilization, the ischemic stimulus during a fixed period of arterial occlusion would also be reduced, and in turn would lead to an attenuated hyperemic response. In contrast to this hypothesis, limb immobilization failed to reduced forearm strength, volume or oxidative function, and in turn did not change reactive hyperemia.

The rationale of this study was based on a relatively large body of evidence showing isolated reductions in either skeletal muscle oxidative function or reactive hyperemia following a period of limb immobilization. For example, 21 days of experimental arm casting has been repeatedly shown to reduce

skeletal muscle oxidative function (Homma et al., 2009; Kitahara et al., 2003; Matsumura et al., 2008; Motobe et al., 2004). Limb immobilization also appears to impair reactive hyperemia. For example, Silber and Sinoway studied individuals following clinical cast removal, showing a marked improvement in reactive hyperemia following return to normal daily activity for ≈ 29 days (Silber & Sinoway, 1990). Likewise, using experimental limb immobilization with an arm sling, Birk et al found that only 8 days of disuse was sufficient to reduce reactive hyperemia (Birk, Dawson, Timothy Cable, Green, & Thijssen, 2013), with similar results reported following 14 days of bed rest (Shoemaker et al., 1998).

In contrast to these prior reports, we failed to reduce oxidative function or reactive hyperemia with ≈ 28 days of limb immobilization.

There are many plausible explanations for why no significant effect was achieved. First, because we used removable wrist braces and not fixed plaster casts, it is possible that adherence to the immobilization protocol was not sufficient to produce physiological effects. Indeed, for the purpose of sanitation and subject comfort, participants were allowed to remove the brace during daily hygiene activities. This may have allowed sufficient activity to preserve handgrip strength and muscle function. For example, Homma et al found that ≈ 50 seconds of rhythmic handgrip exercise, performed twice weekly at 30% of maximal handgrip strength, was sufficient to prevent declines in PCr recovery time (Homma et al., 2009). Additionally, all subjects were enrolled in and actively attending college courses at the time of this study, and thus routinely walked about the campus. It is possible that even this low level of whole-body physical activity was sufficient to maintain vascular function in the forearm (Birk et al., 2012; Thijssen et al., 2009).

It is also possible that subjects were already in a moderately deconditioned state prior to undergoing limb immobilization. This is evidenced by the relatively low maximal grip strength measured prior to immobilization in our participants (34 ± 6 kg), which was nearly 20% lower than the reported grip

strength of previous limb immobilization studies (Matsumura et al., 2008; Motobe et al., 2004). Remarkably, our average pre-immobilization grip strength matched the post-immobilization grip strength reported by Motobe et al., which started at 40.6 ± 2.1 kg and fell to 34.3 ± 2.3kg (Motobe et al., 2004). It is therefore possible that our subject had very little reserve for the muscle to decondition.

Finally, environmental conditions may have also played a significant role in our null findings. A recent study by Hafen et al. found that 10 minutes of daily heat therapy prevented impairments in skeletal muscle mitochondrial function after 10 days of immobilization (Hafen et al., 2019). This is relevant because our study was performed primarily in the month of September in North Texas, and during this time the daily high temperature was 35.4 ± 2.1°C on average. As stated, subjects routinely walk about the university campus and presumably spent time outdoors aside from the walking commute about the campus. It is possible that this physical activity, combined with the environmental heat exposure may have contributed to the maintenance of forearm muscle oxidative function.

On a positive note, while limb immobilization failed to produce the desired response, the data herein show a high degree of test-retest reproducibility; adding some confidence in our interpretation of these results. The close agreement between measures of τVO_2, tissue saturation, and brachial artery hemodynamics before and ≈ 28 days after limb immobilization lend confidence in our ability to detect group differences, had any been present.

In summary, the extent to which the ischemic stimulus determines the magnitude of the hyperemic response remains unclear, yet no less important. Future studies are needed to further characterize this relationship and determine the clinical utility of quantifying and adjusting for the ischemic stimulus in studies of reactive hyperemia. It may be that the resiliency and addictiveness of young, healthy males prevented any deleterious effects. Future studies are therefore needed in order to partition the independent contribution of the ischemic stimulus to reactive hyperemia.

Figures and Tables

Table 1. Forearm Morphology and Function

	Visit 1	*Visit 2*
Hand Grip Strength (kg)	34 ± 6	32 ± 5
Forearm Volume (cm^2)	832 ± 166	821 ± 183
Proximal Forearm Circumference (cm)	24 ± 2	23 ± 2
Mid Forearm Circumference (cm)	22 ± 2	22 ± 2
Distal Circumference (cm)	15 ± 1	15 ± 1
Proximal Adipose Tissue Thickness (mm)	5 ± 3	5 ± 3
Mid Adipose Tissue Thickness (mm)	5 ± 3	5 ± 3
Distal Adipose Tissue Thickness (mm)	4 ± 2	5 ± 2

Data expressed mean ± SD

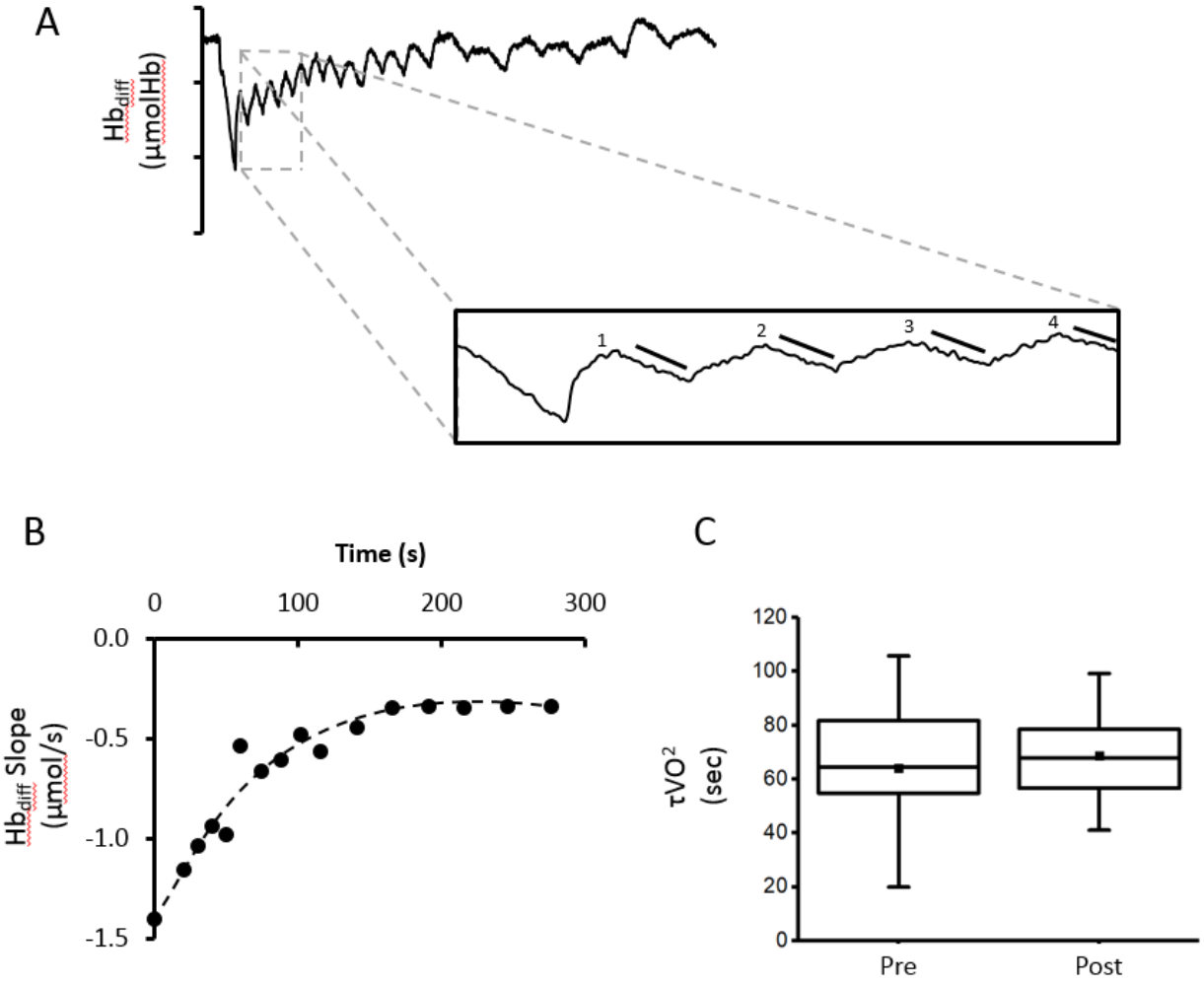

Figure 1. NIRS-derived measurements of skeletal muscle oxidative function
A) A representative tracing of Hb_{diff} from one individual. Immediately following the rapid decline in Hb_{diff} induced by isometric hand grip exercise, the cuff occlusion series is initiated. (Pop-out) Cuff occlusions 1-4 exhibiting distinct declines in Hb_{diff} (bold bars) used to calculate the slope. B) Slopes derived from *A* plotted against post-exercise time and fit to monoexponential curve to derive τVO_2. C) Group data from a subset of participants (n=7) showing no difference in τVO_2 between pre and post immobilization.

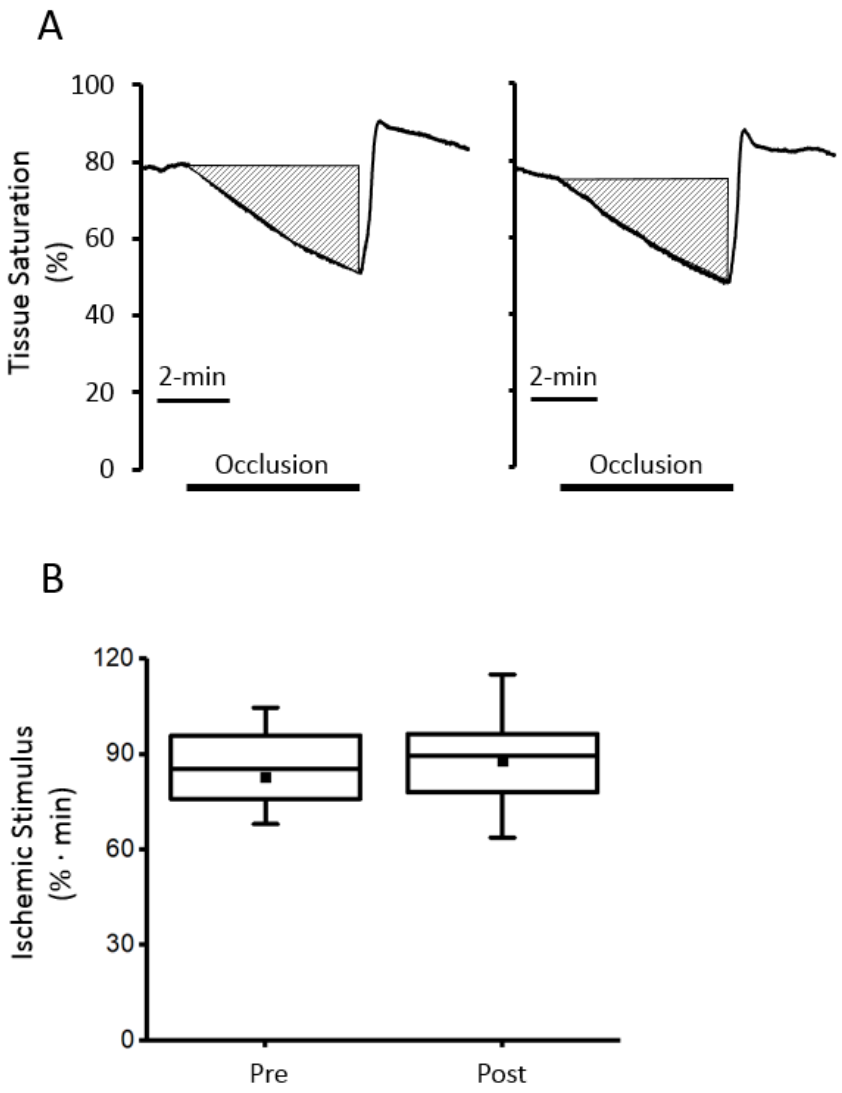

Figure 2. NIRS-derived measurements of tissue saturation during cuff occlusion
A) Representative tissue saturation tracings from one individual pre- and post-immobilization. Traces show 1 minute prior to cuff inflation and 5 minutes of occlusion, followed by 3 minutes of post-occlusion recovery. Shaded area was calculated to yield the ischemic stimulus. B) Group data (n=12) showing the ischemic stimulus during cuff occlusion was not different pre- and post-immobilization.

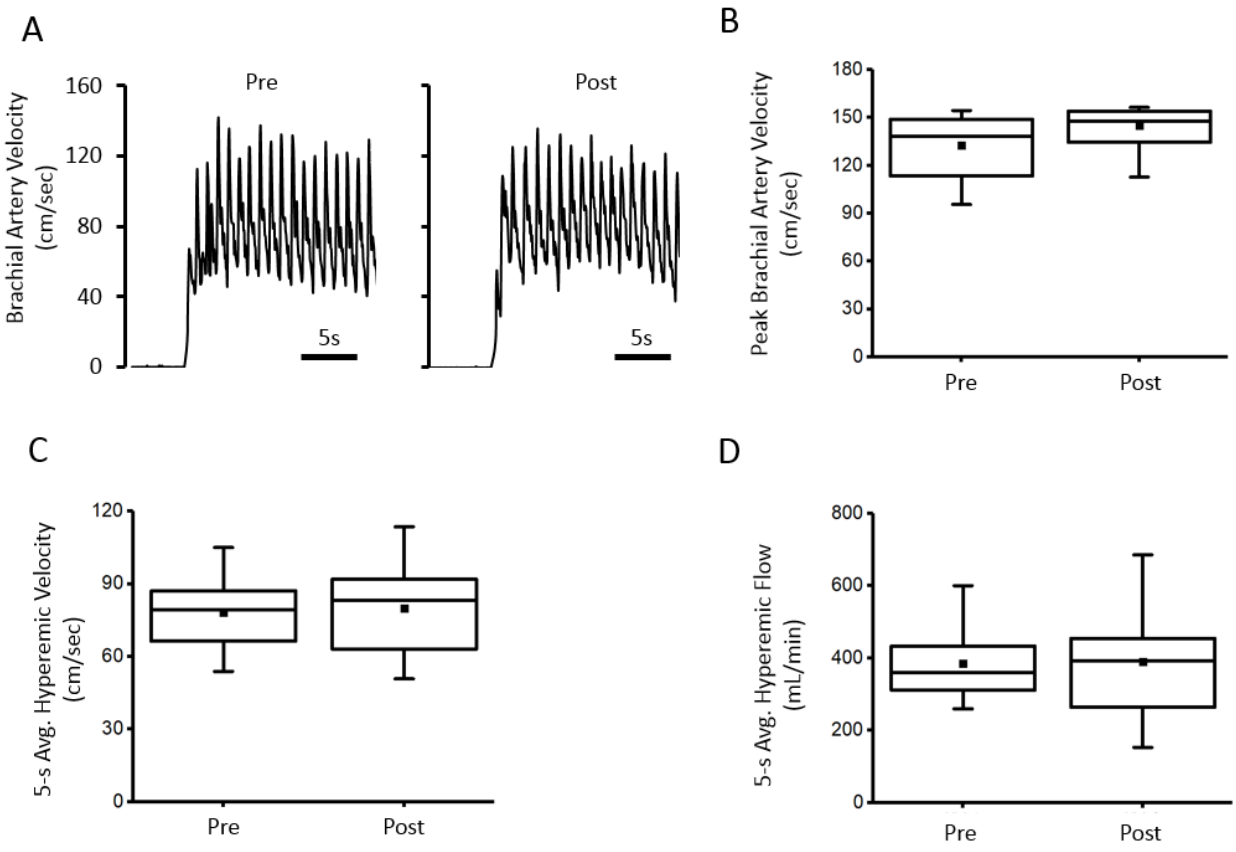

Figure 3. Brachial artery velocity during reactive hyperemia

A) Representative tissue brachial artery velocity tracings from one individual pre- (left) and post-immobilization (right). Traces show 5 seconds prior to cuff deflation and the first 15 seconds of reactive hyperemia. Group data (n=12) showing B) peak brachial artery velocity C) 5-s average hyperemic velocity and D) 5-s average hyperemic flow show no difference pre- and post-immobilization.

Supplemental Figure 1. Resting Wrist Orthosis
Wrist brace worn by subjects preventing flexion and extension about the wrist as well as finger flexion and extension.

References

Anderson, T. J., Charbonneau, F., Title, L. M., Buithieu, J., Rose, M. S., Conradson, H., . . . Lonn, E. M. (2011). Microvascular function predicts cardiovascular events in primary prevention: long-term results from the Firefighters and Their Endothelium (FATE) study. *Circulation, 123*(2), 163-169. doi:10.1161/CIRCULATIONAHA.110.953653

Birk, G. K., Dawson, E. A., Atkinson, C., Haynes, A., Cable, N. T., Thijssen, D. H., & Green, D. J. (2012). Brachial artery adaptation to lower limb exercise training: role of shear stress. *J Appl Physiol (1985), 112*(10), 1653-1658. doi:10.1152/japplphysiol.01489.2011

Birk, G. K., Dawson, E. A., Timothy Cable, N., Green, D. J., & Thijssen, D. H. (2013). Effect of unilateral forearm inactivity on endothelium-dependent vasodilator function in humans. *Eur J Appl Physiol, 113*(4), 933-940. doi:10.1007/s00421-012-2505-7

Chromy, A., Zalud, L., Dobsak, P., Suskevic, I., & Mrkvicova, V. (2015). Limb volume measurements: comparison of accuracy and decisive parameters of the most used present methods. *Springerplus, 4*, 707. doi:10.1186/s40064-015-1468-7

Hafen, P. S., Abbott, K., Bowden, J., Lopiano, R., Hancock, C. R., & Hyldahl, R. D. (2019). Daily heat treatment maintains mitochondrial function and attenuates atrophy in human skeletal muscle subjected to immobilization. *J Appl Physiol (1985), 127*(1), 47-57. doi:10.1152/japplphysiol.01098.2018

Herr, M. D., Hogeman, C. S., Koch, D. W., Krishnan, A., Momen, A., & Leuenberger, U. A. (2010). A real-time device for converting Doppler ultrasound audio signals into fluid flow velocity. *American Journal of Physiology-Heart and Circulatory Physiology, 298*(5), H1626-H1632. doi:10.1152/ajpheart.00713.2009

Homma, T., Hamaoka, T., Murase, N., Osada, T., Murakami, M., Kurosawa, Y., . . . Katsumura, T. (2009). Low-volume muscle endurance training prevents decrease in muscle oxidative and endurance function during 21-day forearm immobilization. *Acta Physiol (Oxf), 197*(4), 313-320. doi:10.1111/j.1748-1716.2009.02003.x

Huang, A. L., Silver, A. E., Shvenke, E., Schopfer, D. W., Jahangir, E., Titas, M. A., . . . Vita, J. A. (2007). Predictive value of reactive hyperemia for cardiovascular events in patients with peripheral arterial disease undergoing vascular surgery. *Arterioscler Thromb Vasc Biol, 27*(10), 2113-2119. doi:10.1161/ATVBAHA.107.147322

Kitahara, A., Hamaoka, T., Murase, N., Homma, T., Kurosawa, Y., Ueda, C., . . . Katsumura, T. (2003). Deterioration of muscle function after 21-day forearm immobilization. *Med Sci Sports Exerc, 35*(10), 1697-1702. doi:10.1249/01.MSS.0000089339.07610.5F

Matsumura, M., Ueda, C., Shiroishi, K., Esaki, K., Ohmori, F., Yamaguchi, K., . . . Hamaoka, T. (2008). Low-volume muscular endurance and strength training during 3-week forearm immobilization was effective in preventing functional deterioration. *Dyn Med, 7*, 1. doi:10.1186/1476-5918-7-1

Motobe, M., Murase, N., Osada, T., Homma, T., Ueda, C., Nagasawa, T., . . . Hamaoka, T. (2004). Noninvasive monitoring of deterioration in skeletal muscle function with forearm cast immobilization and the prevention of deterioration. *Dyn Med, 3*(1), 2. doi:10.1186/1476-5918-3-2

Ohmori, F., Hamaoka, T., Shiroishi, K., Osada, T., Murase, N., Kurosawa, Y., . . . Katsumura, T. (2010). Low-volume strength and endurance training prevent the decrease in exercise hyperemia induced by non-dominant forearm immobilization. *Eur J Appl Physiol, 110*(4), 845-851. doi:10.1007/s00421-010-1566-8

Pathare, N. C., Stevens, J. E., Walter, G. A., Shah, P., Jayaraman, A., Tillman, S. M., . . . Vandenborne, K. (2006). Deficit in human muscle strength with cast immobilization: contribution of inorganic phosphate. *Eur J Appl Physiol, 98*(1), 71-78. doi:10.1007/s00421-006-0244-3

Roberts, H. C., Denison, H. J., Martin, H. J., Patel, H. P., Syddall, H., Cooper, C., & Sayer, A. A. (2011). A review of the measurement of grip strength in clinical and epidemiological studies: towards a standardised approach. *Age Ageing, 40*(4), 423-429. doi:10.1093/ageing/afr051

Rosenberry, R., Chung, S., & Nelson, M. D. (2018). Skeletal Muscle Neurovascular Coupling, Oxidative Capacity, and Microvascular Function with 'One Stop Shop' Near-infrared Spectroscopy. *J Vis Exp*(132). doi:10.3791/57317

Rosenberry, R., Munson, M., Chung, S., Samuel, T. J., Patik, J., Tucker, W. J., . . . Nelson, M. D. (2018). Age-related microvascular dysfunction: novel insight from near-infrared spectroscopy. *Experimental Physiology, 103*(2), 190-200. doi:10.1113/EP086639

Rosenberry, R., Trojacek, D., Chung, S., Cipher, D. J., & Nelson, M. D. (2019). Inter-individual differences in the ischemic stimulus and other technical considerations when assessing reactive hyperemia. *Am J Physiol Regul Integr Comp Physiol*. doi:10.1152/ajpregu.00157.2019

Ryan, T. E., Brophy, P., Lin, C. T., Hickner, R. C., & Neufer, P. D. (2014). Assessment of in vivo skeletal muscle mitochondrial respiratory capacity in humans by near-infrared spectroscopy: a comparison with in situ measurements. *J Physiol, 592*(15), 3231-3241. doi:10.1113/jphysiol.2014.274456

Ryan, T. E., Erickson, M. L., Verma, A., Chavez, J., Rivner, M. H., & McCully, K. K. (2014). Skeletal muscle oxidative capacity in amyotrophic lateral sclerosis. *Muscle Nerve, 50*(5), 767-774. doi:10.1002/mus.24223

Ryan, T. E., Southern, W. M., Reynolds, M. A., & McCully, K. K. (2013). A cross-validation of near-infrared spectroscopy measurements of skeletal muscle oxidative capacity with phosphorus magnetic resonance spectroscopy. *J Appl Physiol (1985), 115*(12), 1757-1766. doi:10.1152/japplphysiol.00835.2013

Shoemaker, J. K., Hogeman, C. S., Silber, D. H., Gray, K., Herr, M., & Sinoway, L. I. (1998). Head-down-tilt bed rest alters forearm vasodilator and vasoconstrictor responses. *J Appl Physiol (1985), 84*(5), 1756-1762. doi:10.1152/jappl.1998.84.5.1756

Silber, D. H., & Sinoway, L. I. (1990). Reversible impairment of forearm vasodilation after forearm casting. *J Appl Physiol (1985), 68*(5), 1945-1949. doi:10.1152/jappl.1990.68.5.1945

Thijssen, D. H., Dawson, E. A., Black, M. A., Hopman, M. T., Cable, N. T., & Green, D. J. (2009). Brachial artery blood flow responses to different modalities of lower limb exercise. *Med Sci Sports Exerc, 41*(5), 1072-1079. doi:10.1249/MSS.0b013e3181923957

Trampisch, U. S., Franke, J., Jedamzik, N., Hinrichs, T., & Platen, P. (2012). Optimal Jamar dynamometer handle position to assess maximal isometric hand grip strength in epidemiological studies. *J Hand Surg Am, 37*(11), 2368-2373. doi:10.1016/j.jhsa.2012.08.014

CHAPTER 6

CONCLUSION

This body of work has yielded novel insights into both the technical process of measuring reactive hyperemia and the interpretation of reactive hyperemia as an index of peripheral microvascular function. Overall, there remains a general lack of consensus regarding the "best" laboratory technique to use when assessing reactive hyperemia (venous occlusion plethysmography, Doppler ultrasound, peripheral artery tonometry, NIRS), and which analytical endpoint best represents reactive hyperemia (e.g. velocity time integral, peak velocity, peak blood flow, total hyperemic blood flow etc.). This lack of consensus between investigations makes comparison and meta-analysis more challenging. To bring greater consistency to the literature, future investigations ought to incorporate comprehensive reporting of multiple endpoints, allowing readers to form a more holistic interpretation of the data. In addition, the complex and redundant signaling pathways underlying this phenomenon make it difficult to identify at risk populations and therapeutic targets.

In Chapters 3 and 4 we identified age-dependent impairments in reactive hyperemia using near-infrared spectroscopy and Doppler ultrasound of the brachial artery. More interestingly, however, was our characterization of the relationship between the degree of tissue ischemia and the magnitude of the hyperemic response. We found that after adjusting for the strength of the ischemic stimulus, age-dependent differences in reactive hyperemia were completely abrogated. Importantly, these findings do not suggest that aging is not a risk factor for microvascular dysfunction. Rather, they indicate that brachial artery reactive hyperemia may not reflect microvascular function as precisely as previous literature asserts. Furthermore, these results emphasize the relationship between skeletal muscle oxidative function and microvascular blood flow regulation, thus underscoring the importance of incorporating ischemic stimulus quantification during studies utilizing arterial cuff occlusion.

In Chapters 5 and Appendix A we attempted to manipulate the balance between reactive hyperemia and the ischemic stimulus. In our first experiment, we sought to acutely impair microvascular vasodilation while leaving skeletal muscle oxidative function intact by employing an ischemia reperfusion

model. Despite multiple studies demonstrating ischemia reperfusion's deleterious effects on flow mediated vasodilation, we were unable to alter any measures of reactive hyperemia or tissue oxygen consumption. In our second experiment, we sought to impair skeletal muscle oxidative function, thus minimizing the ischemic stimulus and proportionately blunting the hyperemic response. To impair skeletal muscle oxidative function, our subjects underwent ~30 days of limb immobilization. Despite excellent adherence, limb immobilization failed to reduce skeletal muscle metabolic rate, forearm anthropometrics, or grip strength. Not surprisingly, because we were not successful in altering skeletal muscle metabolic rate, the ischemic stimulus was also preserved across the limb immobilization period, as was reactive hyperemia.

While these "failed" experiments did not allow us to directly test our *a priori* hypotheses, they did help to advance my training in several important ways. Through these experiments, I became familiar with the literature surrounding ischemia-reperfusion injury and the metabolic/vascular effects of immobilization. I also acquired the technical training necessary to reproducibly measure flow-mediated dilation. Moreover, these studies have helped form the foundation of future investigations in our lab. For example, based on the present results, an obvious next step for the Applied Physiology and Advanced Imaging Laboratory is to turn towards mitochondrial uncoupling drugs (e.g. 2-4 dinitrophenol) to augment skeletal muscle metabolic rate and the degree of tissue ischemia during a fixed occlusion period. Indeed, these drugs function by uncoupling the electron transport chain, allowing protons to bypass ATP-synthase and cross the inner mitochondrial membrane more freely. This allows for a greater rate of oxygen consumption without affecting the true metabolic demands of the tissue, thus producing a greater hypoxic condition during a fixed period of occlusion. By measuring reactive hyperemia under native conditions and following augmentation of the ischemic stimulus via mitochondrial uncoupling, it should be possible to determine how changes in tissue ischemia affects reactive hyperemia. Most importantly, this approach avoids confounding influences that may arise with alternative approaches to increasing

skeletal muscle metabolic rate (i.e. exercise). For example, while performing handgrip either before or during the arterial cuff occlusion may speed skeletal muscle metabolism, it may also increase circulating myokines or other metabolic vasodilators, not present under the resting metabolic rate condition. Another major advantage of this approach over our limb immobilization approach is that it would be far less likely to cause additional confounding influences that may accompany extended periods of disuse, like capillary rarefaction.

The greatest challenge of the work contained within this dissertation is that the "clinical impact" remains unclear. Indeed, as the demand for individualized healthcare continues to grow, so does the demand for improved tools for the detection and diagnosis of pathologies. In order to assess the clinical impact of adjusting reactive hyperemia for the ischemic stimulus, long-term patient studies are needed. This would require leveraging large clinical trials with patient follow-up for major adverse cardiovascular events built into the trial design. Based on our interpretation of the data contained within this dissertation, we would expect that adjusting reactive hyperemia for the ischemic stimulus would lower the total number of individuals with "impaired reactive hyperemia". However, we would also expect that individuals identified as having impaired reactive hyperemia after adjusting for the ischemic stimulus, would have "true" microvascular dysfunction and would be a significantly higher risk of future events. If true, adjusting reactive hyperemia for the ischemic stimulus would provide clinicians and investigators with a relatively simple, non-invasive method for better stratifying patients; with better defined therapeutic targets.

APPENDIX A

ISCHEMIA REPERFUSION INJURY DOES NOT IMPAIR REACTIVE HYPEREMIA

Introduction

Recent work from our laboratory, (Chapters 3 and 4) (Rosenberry et al., 2018; Rosenberry, Trojacek, Chung, Cipher, & Nelson, 2019) has raised several fundamental questions regarding *reactive hyperemia* – the hyperemic response following a period of arterial cuff occlusion. In its most basic form, reactive hyperemia is regarded as an index of the microvascular responsiveness to a period of tissue ischemia. A fundamental assumption being that the level of tissue ischemia achieved during a fixed period of arterial occlusion is consistent across individuals. Our data challenges this assumption, showing marked inter-individual differences in skeletal muscle metabolism, with associated differences in the magnitude of tissue ischemia, following a fixed period of arterial cuff occlusion. We therefore reason that inter-individual differences in skeletal muscle metabolic rate need to be accounted for before microvascular responsiveness can be assessed.

To explore this question further, we sought a model which would allow us to perturb the balance between reactive hyperemia (i.e. microvascular function) and skeletal muscle metabolic rate. Here we aimed to reduce microvascular function using a well-established ischemia-reperfusion model, while maintaining skeletal muscle metabolic rate. To acutely impair vasodilatory function, we employed an ischemia-reperfusion model (i.e. 20 minutes of arterial cuff occlusion) in the non-dominant arm (Gute, Ishida, Yarimizu, & Korthuis, 1998; Loukogeorgakis et al., 2005; Loukogeorgakis et al., 2007; Seal & Gewertz, 2005). This model has reproducibly been shown to cause marked, transient, reductions in vascular function through cellular adhesion pathways, inflammatory infiltration, and increased reactive oxygen species (Collard & Gelman, 2001; Granger, 1999; Gute et al., 1998; Welbourn et al., 1991). Further evidence has shown that prolonged ischemia produces acute inflammation, lymphocyte extravasation, and cellular adhesion (Collard & Gelman, 2001; Granger, 1999; Prasad, Stone, Holmes, & Gersh, 2009; Welbourn et al., 1991; Zamboni et al., 1993). While in vivo measurements of these phenomena have, to our knowledge, not been performed in humans following a 20-minute occlusion period, this approach is

well-established for measuring the effects of ischemia-reperfusion on flow mediated dilation (Andreas et al., 2011; Kharbanda et al., 2002; Loukogeorgakis et al., 2005; Loukogeorgakis, Panagiotidou, Yellon, Deanfield, & MacAllister, 2006; Loukogeorgakis et al., 2007).

Methods

Young, healthy men were recruited for this investigations. All subjects participated in a single laboratory visit having fasted for a minimum of 6 hours, and having abstained from caffeine, alcohol, and vigorous exercise for 24 hours prior to the visit. All tests were performed in a temperature controlled laboratory at 24°C. Subjects were asked to lie supine on a bed with their non-dominant arm resting on a bedside table at heart level. Brachial artery velocity was measured using Doppler ultrasound (Vivid-i, GE Healthcare, Little Chalfont, UK), while tissue oxygen saturation was measured using near-infrared spectroscopy (OxiplexTS, ISS, Champaign, IL); as previously described in detail by our group {Rosenberry, 2019 #1633}. Heart rate and beat-to-beat blood pressure were measured continuously throughout the visit by electrocardiography, using the CM_5 configuration (MLA 0313 lead wires, ADInstruments, Colorado Springs, CO) and finger plethysmography (Finometer PRO, Finapres Medical Systems, Arnhem, The Netherlands) respectively.

Experimental Protocol

Reactive hyperemia was assessed using a dose-response protocol, consisting of 4- and 8-minute arterial cuff occlusions, performed in a random order to prevent an ordering effect. In this way, both the individual hyperemic responses to each period of cuff occlusion, as well as the slope of the hyperemic dose response, could be used to assess reactive hyperemia. After completing baseline reactive hyperemia measurements, which were each separated by a 20-minute “wash-out” period, an arterial cuff was then inflated over the upper arm for 20 minutes, followed by 20 minutes of reperfusion; a model previously shown to impair flow mediated dilation of the brachial artery (Andreas et al., 2011; Loukogeorgakis et al., 2005;

Loukogeorgakis et al., 2006; Loukogeorgakis et al., 2007). After this period had elapsed, we repeated the 4- and 8-minute occlusions in the same order as at baseline.

In order to test whether the repeat 4- and 8-minute cuff occlusions, prior to the 20 minute ischemia-reperfusion period, "preconditioned" the ischemic limb, a subset of individuals (n = 2) only a single 5-minute arterial occlusion before and after the ischemia-reperfusion protocol. All other aspects of the instrumentation and positioning were identical to those described above.

Reactive Hyperemia

Reactive hyperemia was defined as the peak brachial artery velocity measured within the first 15 seconds following deflation of the occlusive cuff placed on the upper arm. The ischemic stimulus was determined by calculating the area enclosed within the tissue saturation tracing during the ischemic period as described in Ch. 4.

Statistical Analysis

Data are reported as mean $\pm$ SD. Only descriptive statistics are reported.

Results

Data were collected in four young healthy men (age 26 ± 3, height 179.9 ± 1.9, weight 80.3 ± 8.7). As expected, ischemia-reperfusion had no discernible effect on skeletal muscle metabolic rate, as evidenced by similar rates of tissue saturation (4-min pre 0.14 ± 0.04 %/sec vs. 4-min post 0.15 ± 0.04 %/sec; 8-min pre 0.10 ± 0.03 %/sec vs. 8-min post 0.09 ± 0.02 %/sec). As a result, the ischemic stimulus achieved during the 4 minute (Pre: 68 ± 20 %·min vs. Post: 70 ± 18 %·min), and 8 minute arterial (Pre 233 ± 69 %·min vs. Post: 234 ± 62 %·min) cuff occlusions was well preserved. In contrast to our hypothesis, and multiple investigations showing deleterious effects of ischemia-reperfusion on flow mediated dilation, ischemia-reperfusion did not have any effect on reactive hyperemia. Peak brachial artery velocity in response to 4-minutes of arterial occlusion was not impaired by ischemia reperfusion (Pre 118±26 cm/s vs. Post 131±20

cm/s), nor was it in response to 8 minutes of arterial occlusion (Pre 115±30 cm/s vs. Post 131±22 cm/s). Moreover, we consistently observed increases in FMD following ischemia-reperfusion (4-min pre 10.66 ± 10.85% vs. post 12.53 ± 7.54%; 8-min pre 12.88 ± 4.3% vs. post 19.66 ± 7.6%). Of note, the large standard deviations in FMD are likely attributable to the relatively wide range in resting brachial artery diameter between individuals (3.51–5.05mm). As a result, some individuals possessed a much greater reserve for dilation (subject 04: 8-min pre ischemia-reperfusion, baseline 3.67mm to peak 4.35mm, FMD 18.50%) compared to others with larger resting diameters (subject 01: 8-min pre-ischemia reperfusion, baseline 4.38mm to peak 4.74mm, FMD 8.22%).

In light of these unexpected findings, and the potential that our experimental design, that included multiple arterial cuff occlusions prior to ischemia-reperfusion, was "preconditioning" the ischemic limb, we repeated the protocol in 2 additional subjects, using only a single 5-minute cuff occlusion protocol to assess reactive hyperemia. Consistent with the original protocol, ischemia-reperfusion did not affect peak velocity (Pre 136 ± 2 cm/s, Post 136 ± 14 cm/s), or the ischemic stimulus (Pre 98 ± 5 %·min, Post 137 ± 13 %·min), when only a single 5-minute cuff occlusion was used. In these two individuals, it would appear that there is an equal hyperemic response, despite a greater ischemic stimulus, following ischemia-reperfusion. However, the magnitude of reactive hyperemia observed in response to this ischemia stimulus is quite similar to some that we have previously reported (Rosenberry et al., 2019). Moreover, in that investigation, we also observed multiple young healthy males who exhibit maximal hyperemic responses, regardless of the degree of tissue ischemia. In a sample of only two individuals, and without performing a dose-response protocol, it is impossible to determine whether this represents a blunting of the hyperemic response following ischemia-reperfusion or whether these individuals are simply maximal responders for a broad range of ischemic stimuli. Consistent with our measurements of FMD after 4- and 8-minutes of cuff occlusion, we also observed increases in FMD following the 5-minute protocol (pre 6.74 ± 3.01% vs. post 9.05 ± 1.32).

Discussion

Although previous investigations have demonstrated that ischemia-reperfusion impairs flow mediated dilation, we found no evidence that ischemia-reperfusion impairs reactive hyperemia.

The most likely explanation for our negative results is key differences in both the cuff occlusion location, and the primary end-point being studied. All prior studies that have successfully used this experimental model to induce "vascular dysfunction", inflated the blood pressure cuff over the distal limb (forearm) and assessed brachial artery flow mediated dilation as the primary endpoint (Andreas et al., 2011; Kharbanda et al., 2002; Loukogeorgakis et al., 2005; Loukogeorgakis et al., 2006; Loukogeorgakis et al., 2007). We inflated the arterial cuff over the upper arm because: (a) upper arm occlusion has been shown to be more prognostically significant (Green, Jones, Thijssen, Cable, & Atkinson, 2011), and (b) space limitations prevent us from placing both the near-infrared spectroscopy probe, and the arterial cuff, over the forearm. Moreover, our primary end-point was peak brachial artery velocity. That peak velocity was unchanged suggests that ischemia-reperfusion may negatively affect nitric oxide bioavailability, and that reactive hyperemia is not controlled by nitric oxide (see Chapter 2 for details regarding specific mechanisms of action).

That we found similar results between the 4- and 8-minute cuff occlusion, dose-response protocol, and the single 5-minute cuff occlusion protocol, suggests that our negative results are unlikely the product of ischemia preconditioning. Indeed, Loukogeorgakis et al. found that two bouts of ischemic preconditioning in the forearm (5 minutes on, 5-minutes off) were not sufficient to protect the limb from ischemia-reperfusion-induced reductions in flow-mediated dilation (Loukogeorgakis et al., 2007). Although our sample size is extremely limited, based on the consistency of the negative results, we abandoned this approach as a model for impairing microvascular function, and turned our attention to the other side of the equation (skeletal muscle metabolic rate, Chapter 5).

References

Andreas, M., Schmid, A. I., Keilani, M., Doberer, D., Bartko, J., Crevenna, R., . . . Wolzt, M. (2011). Effect of ischemic preconditioning in skeletal muscle measured by functional magnetic resonance imaging and spectroscopy: a randomized crossover trial. *J Cardiovasc Magn Reson, 13*, 32. doi:10.1186/1532-429X-13-32

Collard, C. D., & Gelman, S. (2001). Pathophysiology, clinical manifestations, and prevention of ischemia-reperfusion injury. *Anesthesiology, 94*(6), 1133-1138.

Granger, D. N. (1999). Ischemia-reperfusion: mechanisms of microvascular dysfunction and the influence of risk factors for cardiovascular disease. *Microcirculation, 6*(3), 167-178.

Green, D. J., Jones, H., Thijssen, D., Cable, N. T., & Atkinson, G. (2011). Flow-mediated dilation and cardiovascular event prediction: does nitric oxide matter? *Hypertension, 57*(3), 363-369. doi:10.1161/HYPERTENSIONAHA.110.167015

Gute, D. C., Ishida, T., Yarimizu, K., & Korthuis, R. J. (1998). Inflammatory responses to ischemia and reperfusion in skeletal muscle. *Molecular and Cellular Biochemistry, 179*(1-2), 169-187. doi:Doi 10.1023/A:1006832207864

Kharbanda, R. K., Mortensen, U. M., White, P. A., Kristiansen, S. B., Schmidt, M. R., Hoschtitzky, J. A., . . . MacAllister, R. (2002). Transient limb ischemia induces remote ischemic preconditioning in vivo. *Circulation, 106*(23), 2881-2883.

Loukogeorgakis, S. P., Panagiotidou, A. T., Broadhead, M. W., Donald, A., Deanfield, J. E., & MacAllister, R. J. (2005). Remote ischemic preconditioning provides early and late protection against endothelial ischemia-reperfusion injury in humans: role of the autonomic nervous system. *J Am Coll Cardiol, 46*(3), 450-456. doi:10.1016/j.jacc.2005.04.044

Loukogeorgakis, S. P., Panagiotidou, A. T., Yellon, D. M., Deanfield, J. E., & MacAllister, R. J. (2006). Postconditioning protects against endothelial ischemia-reperfusion injury in the human forearm. *Circulation, 113*(7), 1015-1019. doi:10.1161/CIRCULATIONAHA.105.590398

Loukogeorgakis, S. P., Williams, R., Panagiotidou, A. T., Kolvekar, S. K., Donald, A., Cole, T. J., . . . MacAllister, R. J. (2007). Transient limb ischemia induces remote preconditioning and remote postconditioning in humans by a K(ATP) channel-dependent mechanism. *Circulation, 116*(12), 1386-1395. doi:10.1161/Circulationaha.106.653782

Prasad, A., Stone, G. W., Holmes, D. R., & Gersh, B. (2009). Reperfusion injury, microvascular dysfunction, and cardioprotection: the "dark side" of reperfusion. *Circulation, 120*(21), 2105-2112. doi:10.1161/CIRCULATIONAHA.108.814640

Rosenberry, R., Munson, M., Chung, S., Samuel, T. J., Patik, J., Tucker, W. J., . . . Nelson, M. D. (2018). Age-related microvascular dysfunction: novel insight from near-infrared spectroscopy. *Experimental Physiology, 103*(2), 190-200. doi:10.1113/EP086639

Rosenberry, R., Trojacek, D., Chung, S., Cipher, D. J., & Nelson, M. D. (2019). Inter-individual differences in the ischemic stimulus and other technical considerations when assessing reactive hyperemia. *Am J Physiol Regul Integr Comp Physiol*. doi:10.1152/ajpregu.00157.2019

Seal, J. B., & Gewertz, B. L. (2005). Vascular dysfunction in ischemia-reperfusion injury. *Annals of Vascular Surgery, 19*(4), 572-584. doi:10.1007/s10016-005-4616-7

Welbourn, C. R., Goldman, G., Paterson, I. S., Valeri, C. R., Shepro, D., & Hechtman, H. B. (1991). Pathophysiology of ischaemia reperfusion injury: central role of the neutrophil. *Br J Surg, 78*(6), 651-655.

Zamboni, W. A., Roth, A. C., Russell, R. C., Graham, B., Suchy, H., & Kucan, J. O. (1993). Morphologic analysis of the microcirculation during reperfusion of ischemic skeletal muscle and the effect of hyperbaric oxygen. *Plast Reconstr Surg, 91*(6), 1110-1123.

APPENDIX B

CONCURRENT MEASUREMENT OF SKELETAL MUSCLE BLOOD FLOW DURING EXERCISE WITH DIFFUSE CORRELATION SPECTROSCOPY AND DOPPLER ULTRASOUND*

Chandan-Ganesh Bangalore-Yogananda,[†] Ryan Rosenberry,[†] Sagar Soni, Hanli Liu, Michael D. Nelson, Fenghua Tian. Concurrent measurement of skeletal muscle blood flow during exercise with diffuse correlation spectroscopy and Doppler ultrasound, Biomed. Opt. Express9, 131-141 (2018)

1. Introduction

Skeletal muscle blood flow is a key determinant of aerobic capacity, which is an independent predictor of quality of life and cardiovascular disease morbidity and mortality (American College of Sports et al., 2009; Aspenes et al., 2011; Blair et al., 1995; Blair et al., 1989; Paterson, Govindasamy, Vidmar, Cunningham, & Koval, 2004; Venturelli, Schena, & Richardson, 2012). Monitoring skeletal muscle blood flow regulation is therefore essential to provide pathophysiological insight, clinical diagnosis, and evaluate treatment efficacy. Numerous non-invasive methods exist to quantify skeletal muscle blood flow, such as venous occlusion plethysmography. However, these techniques measure changes in bulk conduit flow and do not provide regional (microvascular) or temporal information. In contrast, arterial-spin-labeled magnetic resonance imaging (ASL-MRI) and positron emission tomography (PET) can measure skeletal muscle microvascular perfusion, but are expensive and technically challenging and therefore not available to all clinics or laboratories. Exposure to radiation, as with PET, also limits application to certain populations.

Near-infrared diffuse correlation spectroscopy (DCS) is an emerging technique for measurement of regional blood flow at the microvascular level. In addition to being completely non-invasive and portable, DCS has a relatively high temporal resolution and a relatively large penetration depth (Bi, Dong, Poh, & Lee, 2015). Moreover, DCS has been validated in a variety of organs and tissues, against several different standards, including laser Doppler (Shang, Chen, Toborek, & Yu, 2011), Xenon-CT (Kim et al., 2014), fluorescent microsphere flow measurements (Zhou et al., 2009), and ASL-MRI (Yu et al., 2007). Unfortunately, the vast majority of these validation experiments were performed on the brain, which is inherently less susceptible to motion artifact (especially during exercise). In fact, the only prior investigation to validate DCS in skeletal muscle was done using a cuff inflation and deflation protocol in which the muscle remains virtually motionless (Yu et al., 2007).

The purpose of the present study was therefore to validate DCS-derived skeletal muscle blood flow measurements against an established flow imaging modality (Doppler ultrasound) during rhythmic exercise. Indeed, Doppler ultrasound is currently the most commonly used flow imaging modality to assess skeletal muscle blood flow regulation and kinetics during exercise (Casey, Curry, & Joyner, 2008). Its high temporal resolution provides a perfect opportunity for flow synchronization between the two modalities, providing comprehensive and comparative evaluation of muscle blood flow kinetics to improve our understanding of DCS.

2. Materials and Methods

2.1 Subjects

Healthy subjects between 20–35 years of age were recruited from the local community of the University of Texas at Arlington (UTA). The experimental protocol was approved by the UTA Institutional Review Board (IRB). Written informed consent was obtained from each subject prior to the experiment.

2.2 Instruments

A single-wavelength DCS system was used to measure the relative changes in muscle blood flow. The system was built in-house and validated through phantom and human arm cuff occlusion experiments. It consists of a continuous-wave, long-coherence-length laser diode (785 nm & 100 mW, Crystalaser Inc., Reno, NV) as light source and a single-photon-counting avalanche photodiode (APD) as detector (SPCM-AQRH-14-FC, Pacer USA LLC., Palm Beach Gardens, FL). The output of the APD is connected to a computer with a 32-bit, 8-channel data acquisition card (PCI-6602, National Instruments Corp., Austin, TX). A LabVIEW (National Instruments Corp., Austin, TX) program was developed for photon counting. Similar to Dong et al. (Dong et al., 2012), a software autocorrelator calculates the autocorrelation function and absolute intensity (sum of photon counts) of diffused light, which reduced overall cost and complexity of the system as compared with a hardware autocorrelator. A 3D-printed probe was used to hold a multi-

mode fiber from the source laser and a single-mode fiber to the APD detector. In this study, the probe was affixed to the left forearm (the exercising side) over the belly of the flexor digitorum profundus – the main muscle used during handgrip exercise (Fig. 1). The source-to-detector distance was 1.5 cm. The data sampling rate was 1 Hz.

Brachial artery blood flow velocity and diameter were measured with a duplex ultrasound system (Vivid-i, GE Healthcare, Little Chalfont, United Kingdom) on the left upper arm (the exercising side). This system had a 12 MHz linear array probe with 60 degree of insonation. The ultrasound gate was optimized to ensure complete insonation of the entire vessel cross-section with constant intensity. The continuous Doppler audio signal was converted to real-time blood flow velocity waveforms using a validated Doppler audio converter (Herr et al., 2010) and recorded using a PowerLab data acquisition system (ADInstruments Inc., Boulder, CO). Brachial artery diameter was measured with B-mode ultrasound imaging, which was conducted once in each of the four experimental stages (to be described in section *2.3*).

Noninvasive arterial blood pressure was measured using a servo-controlled finger photoplethysmography (Human NIBP Controller, ADInstruments Inc., Boulder, CO) that was placed on the middle or index finger of the right hand (the non-exercising side) and supported on a bedside table positioned at heart level. In addition, an automated sphygmomanometer (Welch Allyn, Skaneateles Fall, NY) recorded resting blood pressure periodically, and was used to verify and calibrate the finger photoplethysmography measurements.

The analog outputs from Doppler ultrasound and arterial blood pressure module along with the amplified signal from a Smedley handgrip dynamometer (Stoelting, Wood Dale, IL), were connected to a high-performance, physiological data acquisition system (PowerLab 16/35, ADInstruments Inc., Boulder, CO) for simultaneous data recording. Since the DCS system does not have an analog output, a TTL gating signal

to the PowerLab was used to time align the DCS data (to be described in section *2.4.2*) with all the other physiological signals.

2.3 Experimental protocols

All experiments were performed in a dimly-lit, temperature controlled room. Upon arrival to the laboratory, body weight and height were measured using a standard stadiometer and weight scale, and body mass index (BMI) (Keys, Fidanza, Karvonen, Kimura, & Taylor, 1972) was derived. Subjects were then positioned supine on a bed and instrumented for finger photoplethysmography, ultrasound, and DCS. The handgrip dynamometer was positioned on the subject's left side, so that the arm could comfortably be extended and supported at heart level. Prior to any data collection, each subject was instructed to grip the handgrip dynamometer as hard as possible to establish individual maximal voluntary contraction (MVC). Subjects were then given a short break prior to data collection. After hemodynamic data stabilized, baseline data were recorded, followed by rhythmic handgrip exercise at 20% and then 50% of MVC respectively, and post-exercise recovery. Each stage lasted two minutes (Fig. 2). During the exercise period, the subject repeatedly griped the dynamometer for two seconds and then relaxed for two seconds, guided by a recorded voice prompt. To minimize muscle-fiber motion artifact during exercise, data were recorded only during the relaxation portion of the handgrip duty cycle (i.e., two DCS data points per cycle, which were then averaged to derive a single reading per cycle.), using the previously described gating algorithm (Gurley, Shang, & Yu, 2012).

2.4 Data analysis

2.4.1 Finger blood pressure and Doppler ultrasound

Arterial blood pressure and Doppler ultrasound data were analyzed offline by a single observer (RR) using the LabChart Pro software environment (ADInstruments Inc., Boulder, CO). For the real-time arterial blood pressure waveforms, a peak-detection algorithm was applied to identify the systolic and diastolic

components as the peak and valley of each arterial pulse. Then mean arterial pressure (MAP, mmHg) was calculated on a beat-to-beat basis.

Similarly, mean blood flow velocity (MBFV, cm/s) was calculated as the beat-to-beat average from the real-time Doppler ultrasound waveforms. Then brachial artery blood flow (ml/min) was estimated as: MBFV · πr^2 · 60; where r is the radius of brachial artery (cm) measured with B-mode ultrasound imaging. It is noted that the radius of brachial artery was measure once in each experimental stage (baseline, 20% and 50% MVC, and recovery). Hence brachial artery blood flow was also estimated as stage-wise average, not in real time.

2.4.2 DCS

The intensity autocorrelation function measured with the DCS system was analyzed to quantify the relative changes in muscle blood flow. Specially, the analytical solution of the correlation diffusion equation from a point source in a semi-infinite medium is given as:

$$G_1(r,\tau) = \frac{3\mu_s'}{4\pi}\left[\frac{e^{-K_D(\tau)r_1}}{r_1} - \frac{e^{-K_D(\tau)r_2}}{r_2}\right] \quad (1)$$

where $K_D(\tau) = \sqrt{3\mu_a\mu_s' + \mu_s'^2 k_0^2 \alpha\langle \Delta\, r^2(\tau)\rangle}$, μ_a is the absorption coefficient, μ_s' is the reduced scattering coefficient, α is the fraction of photon scattering events in the medium; $r_1 = \sqrt{r^2 + z_0^2}$, $r_2 = \sqrt{r^2 + (z_0 + 2z_b)^2}$, r is the source–detector separation, $z_0 = \frac{1}{\mu_s'}$ and $z_b = \frac{2(1+R_{eff})}{3(1-R_{eff})}$, where R_{eff} represents the effective reflection coefficient. $\langle \Delta\, r^2(\tau)\rangle$ represents the mean square displacement of the moving scatterers after a delay time τ. Based on the Brownian motion model, $\langle \Delta\, r^2(\tau)\rangle = 6D_B\,\tau$, where D_B is the effective diffusion coefficient of the scatterers.

To fit the analytical solution into the measured intensity autocorrelation function, the analytical solution needs to be normalized to get $g_2(\tau)$ function:

$$g_2(\tau) = 1 + \beta \frac{|G_1(\vec{r},\tau)|^2}{\langle I(\vec{r},t)\rangle^2} \quad (2)$$

where $I(\vec{r},t)$ is the detected diffusing light intensity at position *r* and time *t*, and β is a numerical factor related to the detector geometry, number of detected speckles and other experimental parameters.

By minimizing the difference between the analytical solution and measured data of $g_2(\tau)$, we can yield a blood flow index given as: BFI = αD_B. Then, relative muscle blood flow for the baseline, rMBF, can be calculated as:

$$\mathrm{rMBF} = \frac{\mathrm{BFI}(t)}{\mathrm{BFI}(t_0)} \times 100\% \quad (3)$$

The absorption coefficient (μ_a) and reduced scattering coefficient (μ_s') are required inputs in the fitting. In this study, each subject's μ_a and μ_s' values were measured prior to the experiment with a frequency-domain near-infrared tissue oximeter (OxiplexTS™, ISS, Inc.) and then kept constant.

Further, the absolute light intensity measured with the DCS system over time, I(*t*), was also analyzed to derive the changes in optical density, ΔOD, which is given as:

$$\Delta\mathrm{OD} = log_{10}\left[\frac{\mathrm{I}(t)}{\mathrm{I}(t_0)}\right] \quad (4)$$

The wavelength used in this study was 785 nm, which was very close to the isosbestic point of oxygenated hemoglobin (HbO_2) and deoxygenated hemoglobin (Hb). Therefore ΔOD primarily reflects absorption changes of total hemoglobin (HbT = HbO_2 + Hb).

3. Results

Fourteen subjects volunteered to participate. Five were not included in data analysis due to poor quality of Doppler ultrasound data (*n* = 4) or DCS data (*n* = 1). The results are reported on the remaining nine subjects (all males; age = 27.4 ± 2.9 years; BMI = 27.2 ± 3.8).

Figure 3 shows raw data of handgrip force, arterial blood pressure and brachial artery blood flow velocity from one representative subject. The subject was able to maintain relatively constant gripping force during both 20%-MVC and 50%-MVC exercise. Blood pressure increased gradually in these two stages. Brachial artery blood flow velocity increased moderately during 20%-MVC handgrip and exhibited large increase during 50%-MVC handgrip. As expected, reversal blood flow was observed during each contraction period, increasing with increased grip force.

3.1 Changes in arterial blood pressure

Fig. 4 shows changes in mean arterial pressure at the group level. Significant changes (corrected $p < 0.001$, paired *t*-test) were seen in each stage, i.e., an increase from baseline to 20%-MVC exercise then to 50%-MVC exercise, followed by a decrease during post-exercise recovery.

3.2 Changes in blood flow

Brachial artery diameter measured with B-mode ultrasound did not change from baseline (mean ± SE = 0.35 ± 0.01 cm) to 20%-MVC exercise (0.36 ± 0.01 cm), but increased significantly ($p < 0.001$, paired *t*-test) during 50%-MVC exercise (0.38 ± 0.01 cm). This increase persisted into recovery stage (0.39 ± 0.01 cm). Figs. 5(a) to 5(c) show changes in brachial artery blood flow velocity measured with Doppler ultrasound, local muscle blood flow and optical density measured with DCS at the group level (mean ± SE, $n = 9$). As illustrated, brachial artery blood flow velocity and local muscle blood flow had steady changes from baseline to 20%-MVC exercise and then to 50%-MVC exercise. In contrast, changes in optical density, which primarily reflect absorption of total hemoglobin, were slow and did not reach a plateau in any stage.

The main difference between Doppler ultrasound and DCS-derived readings was in the recovery from exercise. Fig. 5(d) shows a close comparison among the normalized decay curves of brachial artery blood flow velocity, local muscle blood flow and optical density in the recovery stage: brachial artery blood flow velocity measured with Doppler ultrasound had a gradual decay throughout the recovery stage that was

well fitted with an exponential process (time constant τ = 130 seconds) (Ryan, Southern, Reynolds, & McCully, 2013). However, local muscle blood flow measured with DCS exhibited a biphasic feature: a sharp decay in the first phase (τ_1 = 29 seconds) followed by a much slower decay in the second phase (τ_2 = 607 seconds). The much slower decay in the second phase was very close to the gradual decay in optical density (τ = 553 seconds).

3.3 Correlations of DCS-derived muscle blood flow with arterial blood pressure and Doppler ultrasound

To better understand how global cardiovascular factors affected local muscle blood flow during exercise, and to evaluate the relationship between Doppler-derived and DCS-derived flow measures, linear correlation analyses were conducted. Because these changes were relatively stable during baseline, 20%-MVC and 50%-MVC exercise (not including recovery), 2-minute averaged data of each stage were used. Further, brachial artery blood flow velocity was integrated with brachial artery diameter (measured once in each stage with B-mode ultrasound imaging) to estimate the real brachial artery blood flow. As shown in Fig. 6, the brachial artery blood flow measured with Doppler ultrasound showed excellent correlation with DCS-derived muscle blood flow, as did mean arterial pressure.

4. Discussion

To our knowledge, this is the first study to validate DCS-derived measurements of skeletal muscle blood flow during exercise. To accomplish our goal, we compared DCS with Doppler ultrasound, which is an established flow imaging modality commonly used to assess skeletal muscle blood flow during exercise. The major findings were two-fold: First, we demonstrate close agreement between DCS and Doppler ultrasound, both in terms of the magnitude of change and the temporal relationship. Second, we found that DCS was more reliable than traditional Doppler ultrasound, highlighting the clinical application of this new technology.

DCS is a relatively novel form of near-infrared technology to examine relative blood flow changes within deep tissues, especially for skeletal muscle (Table 1). While DCS has previously been validated against

several different standards, as reviewed in the beginning of this paper, its validation in skeletal muscle during rhythmic exercise has not – to our knowledge – previously been performed. To address this limitation, we performed simultaneous recordings of skeletal muscle blood flow at rest and during rhythmic handgrip exercise using DCS and Doppler ultrasound. We chose Doppler ultrasound because it is by far the most widely used technique to assess skeletal muscle blood flow during exercise, providing strong external validity (Casey et al., 2008). We show excellent agreement between these two modalities, supporting DCS is a valid measure of skeletal muscle blood flow.

Like other investigators before us (Gurley et al., 2012; Munk, Symons, Shang, Cheng, & Yu, 2012), our initial DCS experiments revealed significant motion artifact during muscle contraction (*data not shown*). To overcome this issue, some investigators have co-registered their dynamometer recordings and DCS measurements for offline correction of the blood flow data (Munk et al., 2012). In contrast, we, and others (Gurley et al., 2012), developed an online gating algorithm to synchronize data acquisition with the relaxation phase of each handgrip cycle. With this advancement, we were able to capture local muscle blood flow data in good quality at two distinct exercise intensities (20% and 50% MVC) in all subjects except one. In contrast, we were forced to exclude four of the original 14 subjects in this study due to data quality concerns with Doppler ultrasound, which is susceptible to motion artifact (particularly during higher intensity exercise). The DCS data quality was preserved in each of these cases, which highlights an important advantage of DCS over Doppler ultrasound. Indeed, the measurement of exercise skeletal muscle blood flow by Doppler ultrasound requires advanced training and practice for proficient and reliable data acquisition. DCS requires very little technical training, and is almost entirely operator independent.

While we observed good agreement between DCS and Doppler ultrasound during the plateau portion of each exercise intensity, we consistently observed transient differences in both the on-kinetics and off-kinetics for skeletal muscle blood flow between the two modalities. For example, during the recovery

stage, note the gradual and consistent decay in Doppler ultrasound readings compared with the bi-phasic decay in DCS-derived muscle blood flow (Fig. 5d). These transient differences reflect key technical differences between the two modalities: while Doppler ultrasound measures the velocity of blood flow in a major artery based on the Doppler effect, DCS blood flow measurement is more complex. A recent study based on Monte Carlo simulations (Boas et al., 2016) showed that the DCS-derived blood flow index provides a direct measure of tissue blood flow, but is also sensitive to changes in hematocrit and average vessel diameter. For the DCS-derived muscle blood flow shown in Fig. 5d, we interpret the first phase (τ_1 = 29 seconds) as the blood flow changes in local microcirculation; whereas the second phase (τ_2 = 607 seconds) reflects the heightened rate of oxygen delivery needed to support the increase in skeletal muscle oxygen demand post-exercise; which slow to return to baseline. Indeed, the second phase has a very similar time constant to the gradual decay in optical density (τ = 553 seconds) that reflects absorption of total hemoglobin.

In conclusion, this study demonstrates an overall agreement and transient difference between DCS and Doppler ultrasound in measuring exercise skeletal muscle blood flow. Because skeletal muscle blood flow is a key determinant of aerobic capacity, which is an independent predictor of quality of life and cardiovascular disease morbidity and mortality, the finding from this study are highly relevant to the study of muscle physiology and pathology.

Figures and Tables

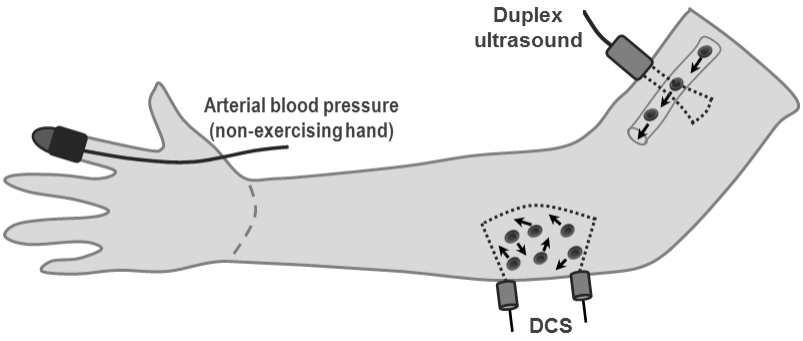

Figure 1. Schematic of experimental setup. Blood pressure was measured using a servo-controlled finger photoplethysmography on the middle or index finger of the right hand (the non-exercising side). Brachial artery blood flow velocity and diameter were measured on the right upper arm with a duplex ultrasound system. The DCS probe was affixed to the left forearm over the belly of the flexor digitorum profundus – the main muscle involved in handgrip exercise.

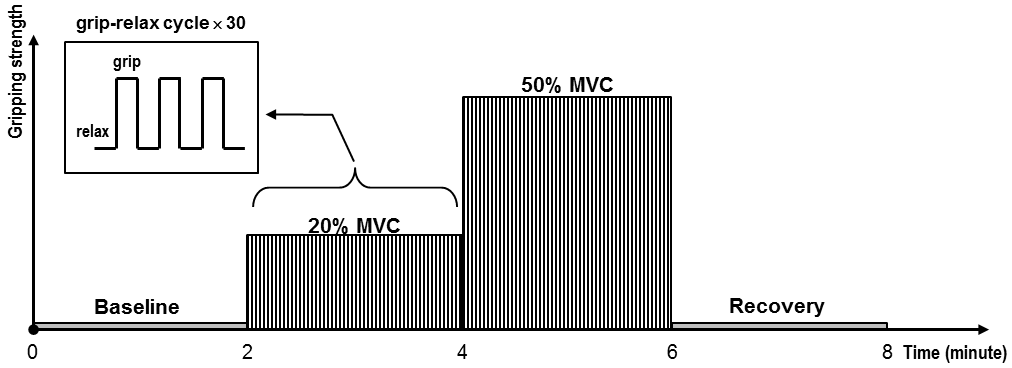

Figure 2. Paradigm of the handgrip exercise experiment. The experiment consisted of four stages: baseline, rhythmic handgrip exercise at 20% and then 50% of maximal voluntary contraction (MVC), and post-exercise recovery. Each stage lasted two minutes. During the exercise period, the subject repeatedly griped the dynamometer for two seconds and then released for two seconds.

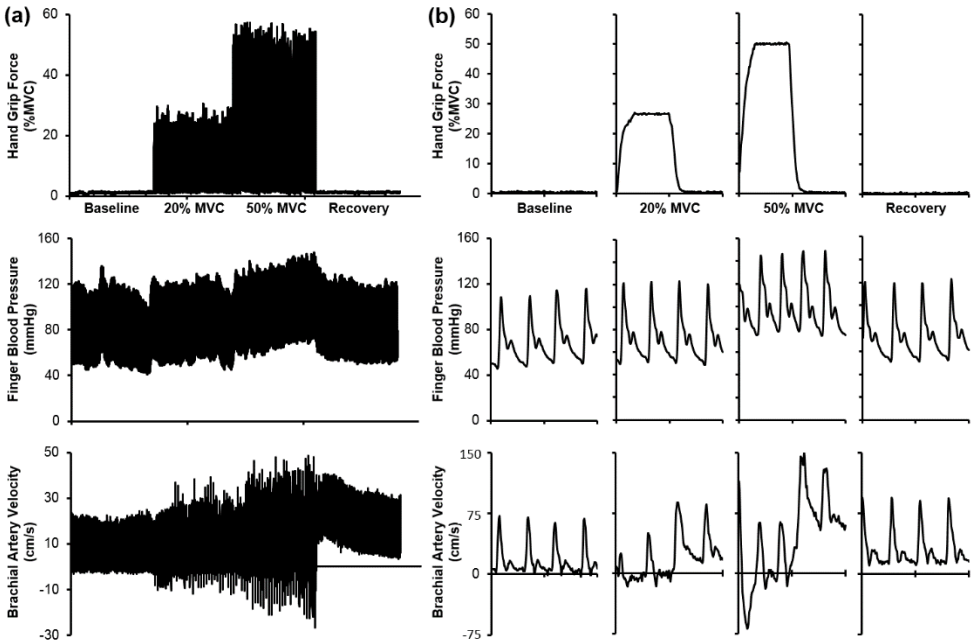

Figure 3. Raw data of handgrip force (top), arterial blood pressure (middle) and brachial artery blood flow velocity (bottom) from one subject: (a) Real-time data throughout baseline, handgrip exercise at 20% and then 50% of maximal voluntary contraction (MVC), and post-exercise recovery. (b) Enlarged 4-second data segments in each stage: baseline, 20%-MVC and 50%-MVC exercise, and recovery.

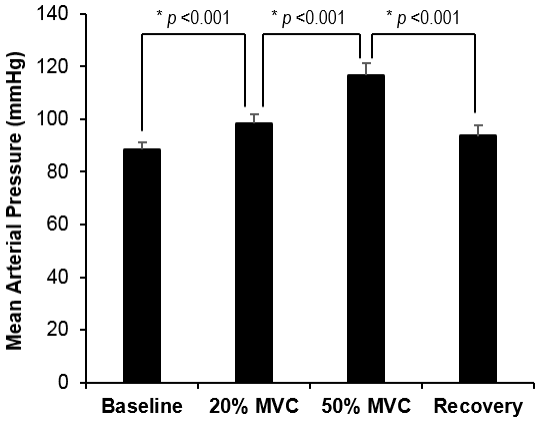

Figure 4. Changes in mean arterial pressure (mean ± SE, *n* = 9) through the four experimental stages: baseline, handgrip exercise at 20% and then 50% of maximal voluntary contraction (MVC), and post-exercise recovery. Difference between every two successive states was examined with paired *t*-test, and the resultant *p*-value was corrected with the Bonferroni method for multiple comparisons.

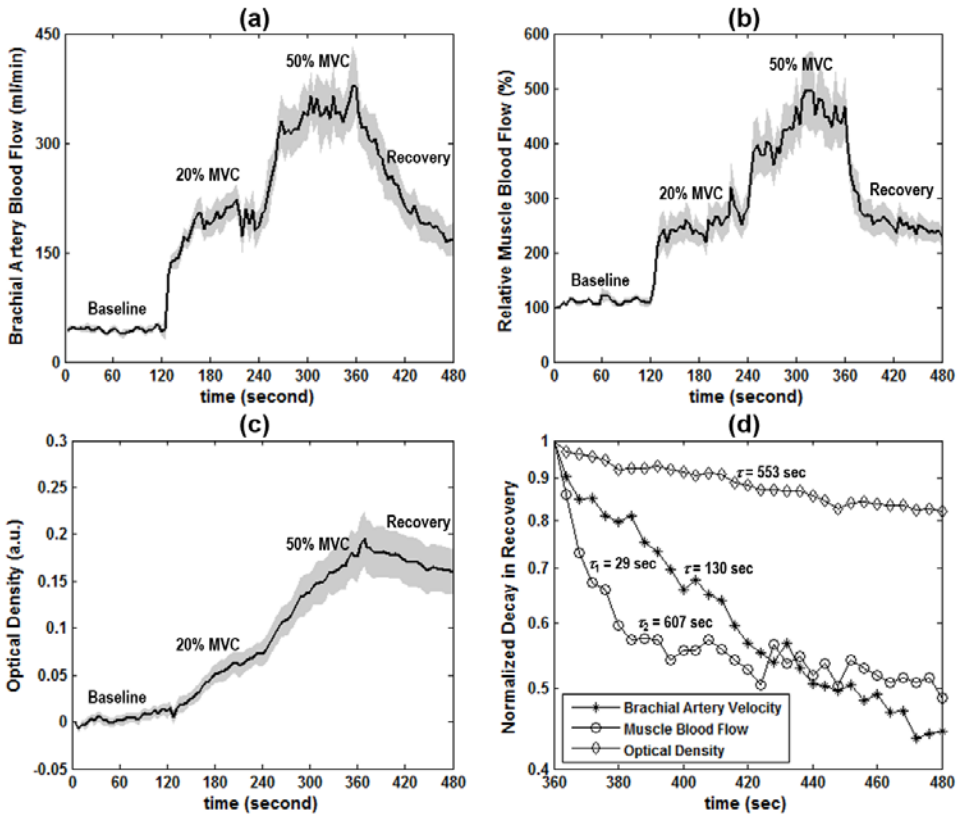

Figure 5. Doppler ultrasound and DCS results at the group level: (a) to (c) Brachial artery blood flow velocity measured with Doppler ultrasound, regional muscle blood flow and optical density measured with DCS (mean ± SE, *n* = 9). (d) Normalized decay of brachial artery blood flow velocity, regional muscle blood flow and optical density in recovery stage.

Table 1. Summary of DCS studies on skeletal muscle blood flow

Reference	Sample size and study population	Muscle Studied and Protocol	Main Findings
Yu et al., 2005	10 healthy, 1 patient with PAD	Gastrocnemius; 30 plantar flexion exercises (toe up-down) within one minute	In healthy subjects, plantar flexion increased relative blood flow 4.7 fold; 2.5-fold increase in the PAD patient.
Henry et al., 2015	10 healthy	Gastrocnemius; 0.5Hz, 30% MVC	~2.2 fold increase in relative blood flow
Gurley et al., 2012	9 healthy	Forearm flexor muscle; handgrip exercise 25% MVC	~5 fold increase in absolute blood flow
Shang et al., 2012	14 women with fibromyalgia; 23 matched healthy controls	Vastus lateralus; 6 set of 12 isometric contractions of knee extensor exercise increasing from 20 to 70% MVC. Blood flow measured immediately post fatiguing exercise	~200% increase in relative blood flow in patients and controls.
Present Data	9 healthy men	Flexor digitorum profundus; 20% and 50% MVC handgrip exercise	250% and 450% increase in relative blood flow with 20% and 50% HG, respectively

Table 1. Previous studies utilizing diffuse correlation spectroscopy to measure blood flow in skeletal muscle.

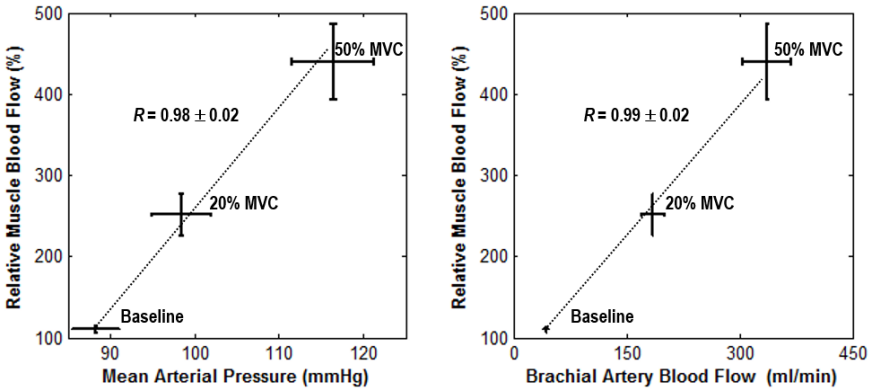

Figure 6. Correlations of DCS-derived muscle blood flow with (a) mean arterial blood pressure and (d) brachial artery blood flow during baseline, 20%-MVC and then 50%-MVC exercise.

References

American College of Sports, M., Chodzko-Zajko, W. J., Proctor, D. N., Fiatarone Singh, M. A., Minson, C. T., Nigg, C. R., . . . Skinner, J. S. (2009). American College of Sports Medicine position stand. Exercise and physical activity for older adults. *Med Sci Sports Exerc, 41*(7), 1510-1530. doi:10.1249/MSS.0b013e3181a0c95c

Aspenes, S. T., Nilsen, T. I., Skaug, E. A., Bertheussen, G. F., Ellingsen, O., Vatten, L., & Wisloff, U. (2011). Peak oxygen uptake and cardiovascular risk factors in 4631 healthy women and men. *Med Sci Sports Exerc, 43*(8), 1465-1473. doi:10.1249/MSS.0b013e31820ca81c

Bi, R., Dong, J., Poh, C. L., & Lee, K. (2015). Optical methods for blood perfusion measurement--theoretical comparison among four different modalities. *J Opt Soc Am A Opt Image Sci Vis, 32*(5), 860-866. doi:10.1364/JOSAA.32.000860

Blair, S. N., Kohl, H. W., 3rd, Barlow, C. E., Paffenbarger, R. S., Jr., Gibbons, L. W., & Macera, C. A. (1995). Changes in physical fitness and all-cause mortality. A prospective study of healthy and unhealthy men. *JAMA, 273*(14), 1093-1098.

Blair, S. N., Kohl, H. W., 3rd, Paffenbarger, R. S., Jr., Clark, D. G., Cooper, K. H., & Gibbons, L. W. (1989). Physical fitness and all-cause mortality. A prospective study of healthy men and women. *JAMA, 262*(17), 2395-2401. doi:10.1001/jama.262.17.2395

Boas, D. A., Sakadzic, S., Selb, J., Farzam, P., Franceschini, M. A., & Carp, S. A. (2016). Establishing the diffuse correlation spectroscopy signal relationship with blood flow. *Neurophotonics, 3*(3), 031412. doi:10.1117/1.NPh.3.3.031412

Casey, D. P., Curry, T. B., & Joyner, M. J. (2008). Measuring muscle blood flow: a key link between systemic and regional metabolism. *Curr Opin Clin Nutr Metab Care, 11*(5), 580-586. doi:10.1097/MCO.0b013e32830b5b34

Dong, J., Bi, R., Ho, J. H., Thong, P. S., Soo, K. C., & Lee, K. (2012). Diffuse correlation spectroscopy with a fast Fourier transform-based software autocorrelator. *J Biomed Opt, 17*(9), 97004-97001. doi:10.1117/1.JBO.17.9.097004

Gurley, K., Shang, Y., & Yu, G. (2012). Noninvasive optical quantification of absolute blood flow, blood oxygenation, and oxygen consumption rate in exercising skeletal muscle. *J Biomed Opt, 17*(7), 075010. doi:10.1117/1.JBO.17.7.075010

Henry, B., Zhao, M., Shang, Y., Uhl, T., Thomas, D. T., Xenos, E. S., . . . Yu, G. (2015). Hybrid diffuse optical techniques for continuous hemodynamic measurement in gastrocnemius during plantar flexion exercise. *J Biomed Opt, 20*(12), 125006. doi:10.1117/1.JBO.20.12.125006

Herr, M. D., Hogeman, C. S., Koch, D. W., Krishnan, A., Momen, A., & Leuenberger, U. A. (2010). A real-time device for converting Doppler ultrasound audio signals into fluid flow velocity. *Am J Physiol Heart Circ Physiol, 298*(5), H1626-1632. doi:10.1152/ajpheart.00713.2009

Keys, A., Fidanza, F., Karvonen, M. J., Kimura, N., & Taylor, H. L. (1972). Indices of relative weight and obesity. *J Chronic Dis, 25*(6), 329-343. doi:10.1016/0021-9681(72)90027-6

Kim, M. N., Edlow, B. L., Durduran, T., Frangos, S., Mesquita, R. C., Levine, J. M., . . . Detre, J. A. (2014). Continuous optical monitoring of cerebral hemodynamics during head-of-bed manipulation in brain-injured adults. *Neurocrit Care, 20*(3), 443-453. doi:10.1007/s12028-013-9849-7

Munk, N., Symons, B., Shang, Y., Cheng, R., & Yu, G. (2012). Noninvasively measuring the hemodynamic effects of massage on skeletal muscle: a novel hybrid near-infrared diffuse optical instrument. *J Bodyw Mov Ther, 16*(1), 22-28. doi:10.1016/j.jbmt.2011.01.018

Paterson, D. H., Govindasamy, D., Vidmar, M., Cunningham, D. A., & Koval, J. J. (2004). Longitudinal study of determinants of dependence in an elderly population. *J Am Geriatr Soc, 52*(10), 1632-1638. doi:10.1111/j.1532-5415.2004.52454.x

Ryan, T. E., Southern, W. M., Reynolds, M. A., & McCully, K. K. (2013). A cross-validation of near-infrared spectroscopy measurements of skeletal muscle oxidative capacity with phosphorus magnetic resonance spectroscopy. *J Appl Physiol (1985), 115*(12), 1757-1766. doi:10.1152/japplphysiol.00835.2013

Shang, Y., Chen, L., Toborek, M., & Yu, G. (2011). Diffuse optical monitoring of repeated cerebral ischemia in mice. *Opt Express, 19*(21), 20301-20315. doi:10.1364/OE.19.020301

Shang, Y., Gurley, K., Symons, B., Long, D., Srikuea, R., Crofford, L. J., . . . Yu, G. (2012). Noninvasive optical characterization of muscle blood flow, oxygenation, and metabolism in women with fibromyalgia. *Arthritis Res Ther, 14*(6), R236. doi:10.1186/ar4079

Venturelli, M., Schena, F., & Richardson, R. S. (2012). The role of exercise capacity in the health and longevity of centenarians. *Maturitas, 73*(2), 115-120. doi:10.1016/j.maturitas.2012.07.009

Yu, G., Durduran, T., Lech, G., Zhou, C., Chance, B., Mohler, E. R., 3rd, & Yodh, A. G. (2005). Time-dependent blood flow and oxygenation in human skeletal muscles measured with noninvasive near-infrared diffuse optical spectroscopies. *J Biomed Opt, 10*(2), 024027. doi:10.1117/1.1884603

Yu, G., Floyd, T. F., Durduran, T., Zhou, C., Wang, J., Detre, J. A., & Yodh, A. G. (2007). Validation of diffuse correlation spectroscopy for muscle blood flow with concurrent arterial spin labeled perfusion MRI. *Opt Express, 15*(3), 1064-1075. doi:10.1364/oe.15.001064

Zhou, C., Eucker, S. A., Durduran, T., Yu, G., Ralston, J., Friess, S. H., . . . Yodh, A. G. (2009). Diffuse optical monitoring of hemodynamic changes in piglet brain with closed head injury. *J Biomed Opt, 14*(3), 034015. doi:10.1117/1.3146814

APPENDIX C

DETERMINANTS OF SKELETAL MUSCLE OXYGEN CONSUMPTION ASSESSED BY NEAR-INFRARED DIFFUSE CORRELATION SPECTROSCOPY DURING INCREMENTAL HANDGRIP EXERCISE*

Ryan Rosenberry, Wesley J. Tucker, Mark J. Haykowsky, Darian Trojacek, Houda H. Chamseddine, Carrie A. Arena-Marshall, Ye Zhu, Jing Wang, J. Mikhail Kellawan, Fenghua Tian, Michael D. Nelson. (2019).

Determinants of skeletal muscle oxygen consumption assessed by near-infrared diffuse correlation spectroscopy during incremental handgrip exercise. *J Appl Physiol*.

Introduction

Prior research, using invasive hemodynamic measures, have assessed the determinants of muscle oxygen consumption (mVO_2) during large (cycling) and small (single leg knee-extension) muscle mass exercise, in healthy individuals and clinical populations (Esposito, Mathieu-Costello, Shabetai, Wagner, & Richardson, 2010; Hogan, Roca, West, & Wagner, 1989; Richardson, Noyszewski, Kendrick, Leigh, & Wagner, 1995; Roca et al., 1989). Near-infrared diffuse correlation spectroscopy (DCS) is an emerging, non-invasive, technique for the simultaneous assessment of O_2 delivery and utilization at the microvascular level (Baker et al., 2017; Carp, Farzam, Redes, Hueber, & Franceschini, 2017; Hammer et al., 2018; Henry et al., 2015); with recent application in exercising skeletal muscle (Bangalore-Yogananda et al., 2018; Hammer et al., 2018; Tucker et al., 2019). Our group has reported that DCS-derived skeletal muscle blood flow index (i.e. muscle perfusion) and conventional measures of convective O_2 delivery (measured by Doppler ultrasound) are highly related in terms of the magnitude and rate of change during exercise (Bangalore-Yogananda et al., 2018; Tucker et al., 2019). Moreover, we have shown good agreement between DCS-derived measures of mVO_2 compared to conventional measurements made at the macrovascular level (Tucker et al., 2019)—at least during a single workload exercise challenge.

Despite the above-mentioned similarities between DCS and conventional approaches however; we and others, have also observed several key differences, which highlight the added utility of this technology. For example, when perfusion pressure was experimentally reduced (by raising the exercising limb above the heart), steady-state Doppler-derived bulk conduit blood flow decreased significantly, whereas DCS-derived steady-state microvascular perfusion was maintained across conditions; which we interpreted as evidence of microvascular autoregulation (Tucker et al., 2019). A similar observation was also made by Hammer *et al*. (Hammer et al., 2018), who found DCS-derived microvascular perfusion to be uncoupled from convective oxygen delivery during heavy incremental exercise.

Given that our prior observation was limited to a single, moderate-intensity exercise workload (Tucker et al., 2019), and because Hammer et al. (Hammer et al., 2018) did not directly measure skeletal mVO_2, we hypothesized that changes in skeletal muscle O_2 delivery (related to macro- vs. microvascular uncoupling, or otherwise) would be compensated for by greater oxygen extraction, and that DCS would closely track changes measured directly from the venous effluent. To test this hypothesis, we compared direct macrovascular (Doppler-derived flow and oxygen extraction) and indirect microvascular (DCS-derived blood flow index and tissue saturation) measures, across a wide range of exercise intensities, using an incremental handgrip exercise test. The data highlight key limitations associated with relying solely on the arterial-venous O_2 difference to reflect changes in O_2 extraction, and highlight why DCS-derived tissue measures, provide important, complementary, insight into the determinants of muscle oxygen consumption.

Methods

Ethical approval and subjects

The study was approved by the Institutional Review Board for research involving Human Subjects at the University of Texas at Arlington. All subjects provided signed consent after receiving a verbal and written description of the experimental protocol and potential risks.

Ten healthy, recreationally active, young (18-35 years old) men, all of whom volunteered for our previous study (Tucker et al., 2019), participated in the present investigation. Aside from the participant characteristics, none of the data reported previously are included herein. Moreover, unlike the single workload data presented previously, the data herein evaluate the determinants of muscle O_2 consumption across a range of exercise intensities (i.e. incremental exercise test). Exclusion criteria included: body mass index (BMI) <18.5 or >35 kg/m^2, handgrip maximal voluntary contraction (MVC) <40 kg or >65 kg (to limit subject heterogeneity), female sex (to avoid large inter-individual differences in the

relative exercise intensities across the incremental exercise test), history of cardiovascular, pulmonary, or metabolic disease, anemia, current medication or tobacco use, orthopedic limitations, poor venous access, and poor acoustic window for brachial artery imaging by ultrasound.

Experimental Design

Screening and familiarization

All subjects participated in a separate familiarization visit, and underwent dual-energy X-ray absorptiometry to quantify fat/lean mass.

Experimental testing visit

Experimental testing visits were performed on a separate day, after the initial screening/familiarization visit. All studies were performed in a quiet, temperature- (~22°C) and ambient-light controlled room. Subjects were studied in a fasted state, having abstained from alcohol and vigorous exercise for >24 h and caffeine for >12 h. Upon arrival at the laboratory, subjects were positioned supine on a bed and asked to rest quietly while a retrograde IV catheter was inserted into a deep vein in the forearm of the exercising (non-dominant) arm. Subjects were then instrumented for measurement of continuous blood pressure, heart rate, arterial O_2 saturation, brachial blood flow (described in detail below). A Smedly handgrip dynamometer was positioned next to the subject's exercising arm, so that the arm could comfortably be extended and supported. Once fully instrumented, subjects performed an incremental rhythmic handgrip exercise test, using a 50% contraction duty cycle (2-s contraction, 2-s relaxation) at a rate of 15 contractions per min. The first workload started at 10 kg and progressed 3 kg every 3 minutes thereafter. Simultaneous measurements of oxygen delivery and utilization by both approaches (conventional and DCS-derived) were performed throughout. Exercise was guided by a monitor that displayed the handgrip force output to give the subject visual feedback on force production, and a recorded voice prompt to guide contraction/relaxation. The exercise test was terminated

volitionally by the subject, or by the investigator when brachial artery image quality was compromised, or the subject was unable to achieve the prescribed force target despite verbal encouragement to do so.

Instrumentation and Measurements

Anthropometrics

Dual-Energy X-ray Absorptiometry (DXA) was used to determine whole-body body fat percent, fat mass, and fat-free mass (DXA, Lunar Prodigy, GE Healthcare, Little Chalfont, UK). A DXA-certified radiology technician also constructed a region-of-interest from the left arm antecubital fossa through the fingertips on the left hand to quantify forearm lean mass. Height and weight were measured with a dual-function stadiometer and weighing scale (Professional 500KL, Health-O-Meter, McCook, IL, USA). Forearm adipose tissue thickness was measured with skinfold calipers (Slim Guide®, Creative Health Systems, Plymouth, MI, USA) on the left arm at the location of the *flexor digitorum profundus*.

Central hemodynamic responses

Beat-by-beat arterial blood pressure was measured from a small finger cuff placed around the middle finger of the subject's non-exercising hand using photoplethysmography (Finometer PRO, Finapres Medical Systems, Arnhem, The Netherlands) that was calibrated to an automated brachial artery blood pressure cuff (Connex Spot Monitor, Model 71WX-B, Welch Allyn, Skaneateles Falls, NY, USA). MAP was calculated as the mean pressure across a continuous average of arterial waveforms. Heart rate was measured via three-lead electrocardiography (ECG) using standard CM_5 placement of ECG electrodes (MLA 0313; ADInstruments, Colorado Springs, CO, USA). Arterial oxygen saturation (Sa_{O_2}) was noninvasively obtained by placing a pulse oximeter (ML 320; ADInstruments, Colorado Springs, CO, USA) over the index finger of the subject's non-exercising hand. The analog outputs for arterial blood pressure, heart rate, and Sa_{O_2} modules were connected to a high-performance, physiological data acquisition

system (PowerLab 16/35, ADInstruments Inc., Colorado Springs, CO, USA) for simultaneous data recording.

Forearm blood flow

Brachial artery blood flow velocity and diameter were measured with a duplex ultrasound system (Vivid-i, GE Healthcare, Little Chalfont, United Kingdom) on the upper left portion of the exercising arm (proximal to the antecubital fossa). This ultrasound system had a 12-MHz linear array probe with 60 degrees of insonation. The ultrasound gate was optimized to ensure complete insonation of the entire vessel cross-section with constant intensity. The continuous Doppler audio signal was converted to real-time blood flow velocity waveforms using a validated Doppler audio converter (Herr et al., 2010) and recorded using a PowerLab data acquisition system (ADInstruments Inc., Colorado Springs, CO, USA). Brachial artery diameter was measured with B-mode ultrasound imaging, with measurements made during the resting baseline and during the final 30 seconds of each 3-minute exercise stage. The analog outputs from the Doppler ultrasound module along with the amplified signal from the handgrip dynamometer were connected to the data acquisition system detailed above for simultaneous data recording.

Forearm deep venous blood sampling

An 18-gauge IV catheter was inserted retrograde to venous blood flow into a deep forearm vein. Confirmation that the selected vein drained from the active muscle group of interest (*flexor digitorum profundus*) was obtained using ultrasound and/or a portable vein illuminator imaging device (VeinViewer® Flex, Christie Medical Holdings Inc., Memphis, TN, USA) prior to insertion of the catheter. The catheter was placed in this manner to improve the likelihood of sampling venous effluent draining from the exercising muscle, while also decreasing the potential contribution from non-exercising muscle and/or the skin. Blood samples were taken during the resting baseline and during the final 30 s of each 3-min exercise stage of the incremental handgrip exercise test to measure venous oxygen content (Cv_{O_2}). A 3-

ml discard was drawn prior to the 2-ml blood sample. A 2-ml saline flush followed each sample to prevent the catheter from clotting.

Near-infrared diffuse correlation spectroscopy

Detailed methodology of our in-house DCS system has previously been published (Bangalore-Yogananda et al., 2018; Tucker et al., 2019). Briefly, the system consists of two continuous-wave, long-coherence-length laser diodes (785 nm & 852 nm, Crystalaser Inc., Reno, NV) that are alternatively switched (MEMS 2x2 Blocking Switch, Dicon Fiberoptics Inc., Richmond, CA), and a single-photon-counting avalanche photodiode (APD) as the photon detector (SPCM-AQRH-14-FC, Pacer USA LLC., Palm Beach Gardens, FL). The output of the APD is connected to a computer with a 32-bit, 8-channel data acquisition card (PCI-6602, National Instruments Corp., Austin, TX). A LabVIEW (National Instruments Corp., Austin, TX) program was developed for photon counting. A software autocorrelator calculates the autocorrelation function and absolute intensity (sum of photon counts) of diffused light (Dong et al., 2012). A 3D-printed probe was used to hold a multi-mode fiber (125 μm in core diameter) from the optical switch and a single-mode fiber (5 μm in core diameter) to the APD detector. The probe was affixed to the forearm of the exercise arm, directly over the belly of the *flexor digitorum profundus*, using Velcro strips. The source-to-detector distance was 2.5 cm. The data sampling rate was 0.25 Hz.

DCS determines a blood flow index (BFI) based on the autocorrelation function of light reflectance, measured at each of the two near-infrared wavelengths (785 nm and 852 nm), and averaged. Then, relative muscle blood flow from the initial baseline at t_0, rMBF, was calculated:

$$\mathrm{rMBF} = \frac{\mathrm{BFI}(t)}{\mathrm{BFI}(t_0)} \times 100\% \quad (1)$$

Based on conventional NIRS methods, the absolute intensity of light reflectance was also used to determine the hemoglobin concentrations. First, the absolute light intensity measured at each wavelength over time, I(t), was converted to the changes in optical density, ΔOD:

$$\Delta OD = \log_{10}[I(t_0)/(t)] \quad (2)$$

Then two ΔOD outputs measured respectively at 785 nm and 852 nm were used to quantify the relative changes in oxygenated hemoglobin/myoglobin (HbO_2) and deoxygenated hemoglobin/myoglobin (Hb) concentrations, $\Delta HbO_2(t)$ and $\Delta Hb(t)$, based on the modified Beer-Lambert Law (Cope et al., 1988). Finally, the change in total hemoglobin concentration was derived as:

$$\Delta HbT(t) = \Delta HbO_2(t) + \Delta Hb(t) \quad (3)$$

Since conventional NIRS only quantifies the relative changes in hemoglobin concentrations from an initial baseline, the hemoglobin baseline values [$HbO_2(t_0)$, $Hb(t_0)$ and $HbT(t_0)$], were measured prior to the experiment with a frequency-domain near-infrared tissue oximeter (OxiplexTS, ISS Inc., Champaign, IL), and then the real-time absolute hemoglobin concentrations were derived as:

$$HbO_2(t) = HbO_2(t_0) + \Delta HbO_2(t)$$

$$Hb(t) = Hb(t_0) + \Delta Hb(t)$$

$$HbT(t) = HbT(t_0) + \Delta HbT(t) \quad (4)$$

Further, the real-time tissue O_2 saturation was derived as:

$$StO_2(t) = \frac{HbO2(t)}{HbO2(t)+Hb(t)} \times 100\% \quad (5)$$

By combining the $\Delta[HbO_2]$ and $\Delta[Hb]$ changes from NIRS, and the rMBF change from DCS, the relative change of skeletal muscle metabolic rate of oxygen, MRO_2, was then calculated as (Boas et al., 2003):

$$\mathrm{MRO_2} = \mathrm{rMBF}\left[1 + \frac{\Delta \mathrm{Hb(t)}}{\mathrm{Hb(t0)}}\right]\left[1 + \frac{\Delta \mathrm{HbT(t)}}{\mathrm{HbT(t0)}}\right]^{-1} \quad (6)$$

Data Analysis

Doppler ultrasound, arterial blood pressure, heart rate, and DCS-derived variables were measured throughout rest, exercise, and post-exercise recovery. To minimize muscle-fiber motion artifact during exercise, DCS data were recorded only during the relaxation phase of the handgrip duty cycle, as previously described (Bangalore-Yogananda et al., 2018; Gurley, Shang, & Yu, 2012). Accordingly, brachial artery blood flow measurements were also only made during the relaxation phase of the handgrip duty cycle, to match DCS. Venous blood sampling was limited to a single resting baseline, and a single sample taken during the final 30 seconds of each incremental workload. With the exception of data presented continuously in figures, resting baseline values represent a 1-min average of the final minute of a 2-min baseline and exercise values represent the final 30 sec of each 3-min exercise stage.

Venous blood constituents

An I-STAT analyzer (I-STAT 1, Abbott Point of Care, Princeton, NJ, USA) was used to analyze the whole blood sample for hemoglobin and forearm venous O_2 saturation (SvO_2) using CG8+ test cartridges (Abbott Point of Care, Princeton, NJ, USA). All blood samples were analyzed in duplicate, and averaged.

Calculated physiological variables

Doppler ultrasound, arterial blood pressure, heart rate, and Sa_{O_2} data were analyzed offline by a single observer (R.R.) using the LabChart Pro software environment (ADInstruments Inc., Colorado Springs, CO, USA). For real-time arterial blood pressure waveforms, a peak-detection algorithm was applied to identify the systolic and diastolic components as the peak and valley of each arterial wave. Then mean arterial pressure (MAP, mmHg) was calculated on a beat-to-beat basis. Similarly, mean blood flow velocity (MBV, cm/s) was calculated as the beat-to-beat average from the real-time Doppler ultrasound waveforms.

Forearm brachial artery blood flow (FBF) was calculated as [MBV × π(brachial artery diameter/2)^2] × 60, where brachial artery diameter (cm) was measured with B-mode ultrasound imaging. FBF was indexed to lean forearm mass and reported as ml/min per 100g lean forearm tissue. Forearm vascular conductance was calculated as FBF/MAP × 100 mmHg. Arterial oxygen concentration (C_aO_2) was calculated as [(Sa_{O_2} × Hb × 1.36) + 0.003 × Pa_{O_2}]. Pa_{O_2} is the partial pressure of O_2 in arterial blood and was assumed to be 100 mmHg (Bentley et al., 2014). Venous blood samples were used to calculate C_vO_2 using formula [(SvO_2 × Hb × 1.36) + 0.003 × PvO_2]. Skeletal muscle oxygen uptake (mVO_2) was calculated using the Fick equation: FBF × (C_aO_2 − C_vO_2). Arterial and venous O_2 transport were calculated as FBF multiplied by C_aO_2 and C_vO_2, respectively (Epstein, Beiser, Stampfer, Robinson, & Braunwald, 1967).

NIRS and DCS. All raw DCS and NIRS data were analyzed in MATLAB (Version R2016A, MathWorks Inc., Natick, MA, USA) and exported to Microsoft Excel (Microsoft Corporation, Redmond, WA, USA) for subsequent analyses.

Statistics

All statistical analyses were performed with SPSS Software (SPSS 24.0, IBM Corp., Armonk, NY, USA) and Prism version 8 (GraphPad Software, La Jolla, CA, USA). For all statistical tests, significance was accepted at $p < 0.05$. All data are presented as mean ± SE, unless otherwise noted.

To examine exercise intensity dependent changes in physiological variables, we used a one-way repeated measure analysis of variance (ANOVA). As described above, baseline was defined as the 1-minute average prior to exercise, whereas the the final 30 sec average of each exercise workload was used for comparative purposes. For all repeated measures ANOVA testing, if the sphericity assumption was violated (Greenhouse-Geisser $\varepsilon < 0.75$), degrees of freedom (df values) were adjusted using the

Greenhouse-Geisser correction. When significant overall effects were observed, a Bonferroni correction post-hoc analysis was performed to determine where significant differences existed.

To examine the overall relationship between Doppler-derived brachial artery blood flow and DCS-derived blood flow index, we modelled the kinetic responses illustrated in Figure 1A and Figure 1D, using an exponential growth model with the time constant representing the amount of time required to change 63% of the amplitude or range of the response. In addition, to assess the intra-individual relationship between Doppler-derived brachial artery blood flow and DCS-derived blood flow index across exercise intensity, we performed intra-individual linear regression analysis. Similarlly, inter-individual relationships between Doppler-dervied blood flow and DCS-derived blood flow index, deoxyhemaglobin/myoglobin and DCS-derived blood lfow index, and DCS-derived relative muscle oxygen consumption and conventionally measured mVO2, Pearson correlations were performed.

Results

Ten subjects volunteered to participate in the study; however, two of these subjects were excluded from the final analysis due to technical difficulties with our DCS device. Subject characteristics for the eight subjects included are presented in **Table 1**.

All subjects completed the 19 kg workload; however, only three subjects progressed beyond this workload, with one subject reaching 25 kg and two subjects reaching 22 kg. For comparative purposes, we chose to report data only on the workloads completed by all subjects.

Conventional Determinants of mVO_2

Brachial artery blood flow increased 2-fold from rest to 10 kg of rhythmic handgrip exercise ($P < 0.01$), followed by a linear increase with each subsequent workload (**Figure 1A)**. Likewise, the arterial-venous O_2 difference also increased nearly 2-fold with the onset of exercise (from rest to 10 kg; $P < 0.001$);

however, in contrast to brachial artery blood flow, remained unchanged thereafter (**Figure 1B).** Of note, the change in the arterial-venous O_2 difference was entirely driven by a decrease in venous O_2 saturation (which changed from 65.3 ± 2.5% at rest to 39.9 ± 3.0% with 10 kg rhythmic handgrip), as we observed no major differences in hemoglobin or arterial saturation. Accordingly, mVO_2 increased 4-fold with the onset of exercise ($P < 0.001$), with subsequent linear increases seemingly driven entirely by brachial artery blood flow (**Figure 1A)**.

DCS-Derived Determinants of mVO_2

Similar to Doppler-derived brachial artery blood flow, DCS-derived blood flow index shared a steep rise with the onset of exercise, followed by a linear increase thereafter (**Figure 1D**). Likewise, similar to the directly measured venous O_2 saturation, DCS-derived tissue saturation significantly decreased with the onset of exercise; however, in contrast to the directly measured venous O_2 saturation, tissue saturation continued to decline with each subsequent workload (**Figure 1E**). These changes in tissue O_2 saturation were driven almost entirely by deoxyhemoglobin/myoglobin (a surrogate measure of O_2 extraction), which increased rapidly during the onset of exercise, followed by a progressive linear increase thereafter (**Figure 2B)**. Oxyhemoglobin/myoglobin remained unchanged throughout exercise (**Figure 2A)**; as a result, total hemoglobin/myoglobin increased throughout the exercise challenge (**Figure 2C**, $P < 0.01$). Once integrated, relative mVO_2 shared a similar increase across the incremental challenge, as conventionally measured mVO_2 (**Figure 1E)**.

Fick Principle and Fick's Law of Diffusion

To help interpret the apparent discrepancy between the determinants of mVO_2 when assessed by the conventional approach, versus DCS-derived MRO_2, we plotted the mean convective and diffusive components of O_2 transport between two distinct phases in the incremental exercise test: (1) rest to 10 kg of force (**Figure 3A**), and (2) 10 kg to 19 kg of force (**Figure 3B)**. The Fick principle curve depicts mVO_2

as a function of convective O_2 delivery (curved line) vs. venous PO_2. Fick's law of diffusion depicts VO_2 as a function of venous PO_2 with the slope (straight line) representative of muscle O_2 diffusive conductance (Houstis et al., 2018; Poole, Richardson, Haykowsky, Hirai, & Musch, 2018a). The intersection of these lines determines the VO_2 achieved. As illustrated, the transition from rest to 10 kg of rhythmic handgrip exercise was achieved by a greater increase in diffusive O_2 conductance (10-fold increase) compared to convective O_2 delivery (4-fold increase) that resulted in increased O_2 extraction. The increase in mVO_2 from 10 kg to 19kg was achieved by a 1.8-fold increase in both convective O_2 delivery and diffusive O_2 conductance that resulted in minimal change in the arterial-venous O_2 difference. These models are supported by expressing the proportionate changes in both arterial and venous O_2 transport across each exercise workload, and calculating their respective difference (i.e. oxygen utilization, **Figure 3C**). Indeed, the greatest increase in O_2 utilization occurs during the transition from rest to 10 kg of rhythmic handgrip. During this transition, because diffusive O_2 conductance increases to a greater extent than convective O_2 delivery, an appreciable increase in oxygen extraction (i.e. arterial-venous O_2 difference) is observed. However, after this first 10 kg workload, when diffusive and convective O_2 conductance are matched, no further changes in O_2 extraction (i.e. arterial-venous O_2 difference) are observed. This is supported at the microvascular level using DCS. Indeed, during the transition from 10kg to 19kg, absolute oxygen extraction increases with each transition (defined by the rise in deoxyhemoglobin/myoglobin, **Figure 2B**), but does so at a similar rate as oxygen delivery (i.e. DCS-derived BFI, **Figure 1D**); thus preserving the arterial-venous oxygen difference.

Relationships between conventional and DCS-derived determinants of muscle oxygen consumption

As mentioned, brachial artery blood flow and DCS-derived blood flow index shared a similar response, increasing sharply with the onset of exercise, followed by a linear increase thereafter (**Figure 1A and 1D**). To assess the agreement between these two variables, we performed nonlinear regression modeling. Consistent with our prior reports (Bangalore-Yogananda et al., 2018; Tucker et al., 2019), Doppler-derived

brachial blood flow and DCS-derived blood flow index were very closely related, sharing very similar time constants (264 vs. 270 s, respectively), along with large overlap between their respective 95% confidence intervals (216-324 vs. 192-414 s, Doppler vs. DCS, respectively). In addition to evaluating the goodness of fit, we also evaluated the within-subject agreement between the two approaches. As illustrated in **Figure 4A**, we observed excellent within-subject agreement between Doppler-derived brachial blood flow and DCS-derived blood flow index (correlation coefficients ranging from 0.79 to 0.99, median = 0.97). We also observed good between-subject agreement between Doppler-derived brachial blood flow and DCS-derived blood flow index (r^2=0.57) (**Figure 4A**).

Similar to the comparisons made between Doppler-derived and DCS-derived blood flow, we also assessed relationships between DCS-derived blood flow index and deoxyhemoglobin/myoglobin (a measure of tissue O_2 extraction (DeLorey, Kowalchuk, & Paterson, 2003; Ferreira, Koga, & Barstow, 2007); **Figure 4B**). The tight relationship observed supports the conventionally-derived data described immediately above. Together, the data show that when diffusive O_2 conductance is greater than convective O_2 delivery (i.e. rest to 10 kg) the change in mVO_2 is driven largely by O_2 extraction (i.e. increased deoxyhemoglobin/myoglobin); whereas, when diffusive and convective O_2 conductance are similar (i.e. 10 kg through 19 kg) the change in mVO_2 is driven by seemingly proportional changes in oxygen delivery (DCS-derived blood flow index) and oxygen extraction.

Consistent with the close linear relationships already mentioned, we also observed good agreement between conventionally-derived mVO_2 and DCS-derived MRO_2. Indeed, within-subject correlation coefficients ranged from 0.54 and 0.98, with a between-subject agreement of 0.68 (Figure 4C).

Discussion

Diffuse correlation spectroscopy is emerging as a non-invasive optical imaging technique for quantifying skeletal muscle oxygen delivery and utilization at the microvascular level. By comparing DCS

with conventional measures of convective O_2 delivery and utilization, we show that the two approaches are far more similar than they are different. The data also highlight a common misconception of the Fick principle (Padilla, Musch, & Poole, 2005; Poole & Musch, 2008), namely that increases in skeletal mVO_2 are almost entirely dependent on convective O_2 delivery, and show instead an equal contribution from diffusive O_2 conductance. Taken together, these data highlight the potential role DCS can play, both clinically and as a research tool, for extending our pathophysiologic understanding of exercise (in)tolerance across the spectrum of health and disease non-invasively.

The observed plateau in venous O_2 saturation, and the arterial-venous O_2 difference, is in line with several recent reports involving handgrip exercise (Berg, Nyberg, Windedal, & Wang, 2018; Nyberg, Berg, Helgerud, & Wang, 2017, 2018). Yet, this observed plateau is in direct contrast with the DCS-derived tissue saturation measurement, which showed a linear decline throughout the incremental exercise challenge. Each technique therefore provided—at least at first glance— seemingly different interpretations of the determinants of mVO_2. That the arterial-venous O_2 difference was unchanged during exercise performed at workloads greater than 10 kg, suggested that the increase in mVO_2 was entirely driven by proportional increases in convective O_2 delivery. However, after more detailed analysis incorporating Fick's law of diffusion, one can appreciate that the increase in mVO_2 is also driven by an increase in muscle O_2 diffusive conductance (**Figures 3A and 3B**). While the exact mechanism driving these changes is beyond the scope of the present investigation, the initial increase in diffusive O_2 conductance is likely attributable to a rapid decrease in intramuscular pO_2 at the onset of exercise; which has been shown to reach its nadir even at submaximal workloads (Mole et al., 1999; Richardson et al., 1995; Richardson, Noyszewski, Leigh, & Wagner, 1998). Increases in the diffusive O_2 conductance are also likely to be attributable to longitudinal capillary recruitment and increased capillary hematocrit (Poole, Copp, Ferguson, & Musch, 2013; Poole, Copp, Hirai, & Musch, 2011). Given the observed increase in NIRS-

derived total hemoglobin in our participants, it is interesting to speculate that capillary hematocrit concentration likely played an important role (Barstow, 2019a).

Importantly, if diffusive O_2 conductance was not matched with the marked linear increase in O_2 delivery observed, the arterial-venous O_2 difference would have declined during the transitions from 10 kg to 19 kg (i.e. an effective shunt). Alternatively, had diffuse O_2 conductance increased beyond the rate of O_2 delivery (as was the case during the transition from rest to 10 kg), arterial-venous O_2 difference would have continued to increase throughout exercise. That the arterial-venous O_2 difference did not increase with each subsequent workload suggests that muscle O_2 extraction was matched with muscle O_2 delivery. Indeed, the close linear relationship between DCS-derived blood flow index and NIRS-derived deoxyhemoglobin/myoglobin (an indirect measure of muscle O_2 extraction (DeLorey et al., 2003; Ferreira et al., 2007)) supports this interpretation. Because the arterial-venous O_2 difference is simply a fractional representation of oxygen extraction, it does not provide insight into the absolute amount of oxygen being extracted. To determine this, one needs to account for absolute oxygen delivery (as illustrated in Figure 3C). As such, when both convective oxygen delivery and diffusive oxygen conductance increase proportionately (as was the case in our study between 10 to 19 kg), the arterial-venous oxygen difference remains constant. Accordingly, both approaches (conventional vs. DCS) seem to provide complementary insight into the determinants of oxygen utilization.

That we observed a close relationship, and excellent within-subject agreement, between DCS-derived muscle blood flow index and Doppler-derived forearm blood flow is entirely consistent with a growing number of publications (Bangalore-Yogananda et al., 2018; Tucker et al., 2019). While these data support DCS-derived blood flow index as a viable approach for measuring microvascular skeletal muscle O_2 delivery, we recognize that others have not found the same tight relationship. For example, Hammer *et al*. (2018) found a clear dissociation between DCS-derived skeletal muscle perfusion and Doppler-derived forearm blood flow during incremental handgrip exercise. However, in the present investigation,

the highest workload achieved by all of the subjects was 19 kg, which was ~40% of their maximal voluntary contraction. In contrast, Hammer *et al*. (2018) consistently achieved intensities above 50% of maximal voluntary contraction. In addition, in the present investigation, data were collected continuously at 0.25 Hz, throughout rhythmic handgrip exercise. In contrast, Hammer *et al*. (2018) employed a unique post-exercise data collection approach, which may have contributed to the differences between these two studies. Caution is therefore warranted when interpreting the tight relationship, between Doppler-derived blood flow and DCS-derived blood flow index presented herein, as differences may exist between conduit artery and microcirculatory blood flow kinetics, and may differ depending on muscle mass and exercise intensity. It is also interesting to note that differences observed in the magnitude of change between DCS-derived blood flow index (~2.5-3 fold change at 19 kg) compared to Doppler-derived brachial artery blood flow (~7-10 fold change at 19 kg). We interpret this difference to reflect the indiscriminant nature of conduit blood vessels, which supply blood to the entire limb, compared to the muscle-specific increases reflected by DCS.

Experimental Considerations

This study is not without limitation. We cannot completely rule out the contribution of oxy- and deoxymyoglobin to the changes in the NIRS signal observed throughout exercise. Indeed, NIRS is incapable of differentiating between hemoglobin and myoglobin, and myoglobin has indeed previously been shown to deoxygenate during heavy intensity rhythmic exercise (Richardson et al., 1993). However, because oxymyoglobin decreases rapidly during the onset of exercise, before reaching a steady plateau (despite greater intensity exercise) (Richardson et al., 1993), we contend that the NIRS changes reported herein were likely driven by deoxy- and oxyhemoglobin; however, since we cannot be sure, we have reported our NIRS measurements as a grouped variable (i.e. Hb + Mb).

Additionally, we only report data for the workloads for which we had a complete dataset. In the majority of cases, the primary reason for terminating the test was poor Doppler data quality secondary to excessive upper arm movement (alternative muscle recruitment). It is possible that we have omitted important micro- versus macrovascular differences in oxygen delivery, as previously highlighted by Hammer *et al*. (2018).

Despite making efforts to optimize our venous sampling—selecting a deep vein draining from the most active region of the forearm during exercise, and inserting the catheter in a retrograde fashion—we cannot rule out that a portion of the venous sample originated from muscles other than the *flexor digitorum profundus*. Consequently, the venous blood samples may partly reflect forearm muscle oxygen consumption from non-exercising tissue. This is in contrast to the DCS-derived measures, which reflects a volume-weighted measure of perfusion and extraction. Consideration is also warranted when considering the sample time between our DCS measures and the venous sampling. As stated, DCS data were only taken during the 2-second relaxation period, while venous sampling was not limited to a specific phase of the handgrip duty cycle. Indeed, the rhythmic nature of handgrip exercise inevitably imposes a pulsatile pattern on both the blood flow and oxygen extraction characteristics, which cannot be accounted for by the approach used herein. Despite this potential consideration however, the strong relationships between DCS-derived blood flow index and NIRS-derived demoxyhemoglobin/myoglobin illustrated in Figure 4B, and its close approximation of the arterial-venous O_2 difference measure by conventional approaches, suggest that this confounding factor likely had a minimal impact.

Previous work by McDonough et al (McDonough, Behnke, Padilla, Musch, & Poole, 2005) showed that in order to meet exercise-dependent increases in O_2 demand, fast-twitch muscle fibers rely more heavily on increases in fractional O_2 extraction while slow-twitch fibers exhibit greater proportional increases in convective O_2 delivery. It is important to consider these findings when comparing the forearm

model used herein with future DCS-based investigations targeting lower limb muscles, as the proportional differences in fiber type may influence the results and subsequent interpretation.

NIRS measures changes in tissue oxygenation in small arterioles, capillaries and venules within a specific region of interest. Therefore, the relative contributions of each of these compartments to the optical signal during handgrip exercise is unclear. However, it has been shown that the majority (~84%) of the skeletal muscle microvascular volume is comprised of capillaries, with the remainder split between the arterioles and venules (Barstow, 2019b; Poole, Wagner, & Wilson, 1995). As such, changes in BFI and/or oxygenated and deoxygenated hemoglobin/myoglobin likely represent changes predominantly in the microcirculation (Lutjemeier, Ferreira, Poole, Townsend, & Barstow, 2008). Moreover, DCS reflects only a small fraction of the limb being interrogated (in this case, forearm), and thus may not be representative of changes across the entire limb. In contrast, brachial artery flow measurements and venous sampling yields a much more global view.

We plotted the mean convective and diffusive components of O_2 transport between two distinct phases of our incremental exercise test to help explain apparent differences between the conventional and DCS approaches; particularly as it relates to tissue vs. venous oxygen saturation. While this approach helped our overall interpretation of the data, it requires that mitochondrial PO_2 be negligible. Because we cannot be sure of that this was the case, caution is warranted when interpreting these results.

Finally, in addition to our relatively small sample size, we only included male subjects, with a relatively narrow range in grip strength. Both exclusion criteria were designed to limit inter-individual variability with respect to the relative exercise intensity performed throughout the incremental test. Future investigations are indeed warranted to assess potential sex differences, as well as explore unique individual differences across a broader population.

Clinical Implications

Exercise intolerance is a hallmark feature in many diseases, and is associated with decreased quality of life and functional performance. Understanding the mechanisms contributing to exercise intolerance is therefore therapeutically important (Houstis et al., 2018; Poole et al., 2018a). Indeed, prior work has shown that exercise intolerance may by be due to convective or diffusive O_2 transport limitations or both (Esposito et al., 2010; Hirai, Musch, & Poole, 2015; Poole, Richardson, Haykowsky, Hirai, & Musch, 2018b; Roca et al., 1992). Importantly, these works also bring attention to how pharmacological treatment or exercise prescription may or may not be effective in addressing the pathophysiologic basis for the limited ability to exercise.

Exercise intolerance can be objectively measured by O_2 consumption, either at the whole-body level or at the level of an individual muscle. The latter case is both technically challenging, and requires multiple venous measurements from an indwelling catheter. Moreover, as evidenced by the present data, it may not provide a readily apparent understanding of the determinants of mVO_2. DCS offers a non-invasive alternative, with the added benefit of evaluating the microvascular environment in question. This approach could assist clinicians in identifying patients who are more convectively or diffusively limited, which will better inform their treatment plan. Application of this technology could therefore have a major impact in the era of precision medicine, and help to drive therapeutic discovery.

In conclusion, the data herein provide novel insight into the potential utility of DCS for simultaneous, non-invasive evaluation of the microvascular determinants of mVO_2. Moreover, DCS appears to provide a more holistic representation of the determinants of mVO_2, particularly with regards to O_2 extraction, highlighting its added value over traditional approaches measured at the macrovascular level.

Figures and Tables

Table 1. Subject Characteristics.

Variable	Mean ± SD
Age (years)	27 ± 4
Height (cm)	181.0 ± 6.3
Weight (kg)	88.6 ± 16.4
BMI (kg/m^2)	26.9 ± 4.3
Total body fat (%)	23.2 ± 9.4
Left forearm total mass (g)	1689 ± 195
Left forearm lean mass (g)	1551 ± 185
Left forearm adipose tissue thickness (mm)	5 ± 1
Maximal voluntary contraction (MVC) (kg)	53 ± 8

n = 8.

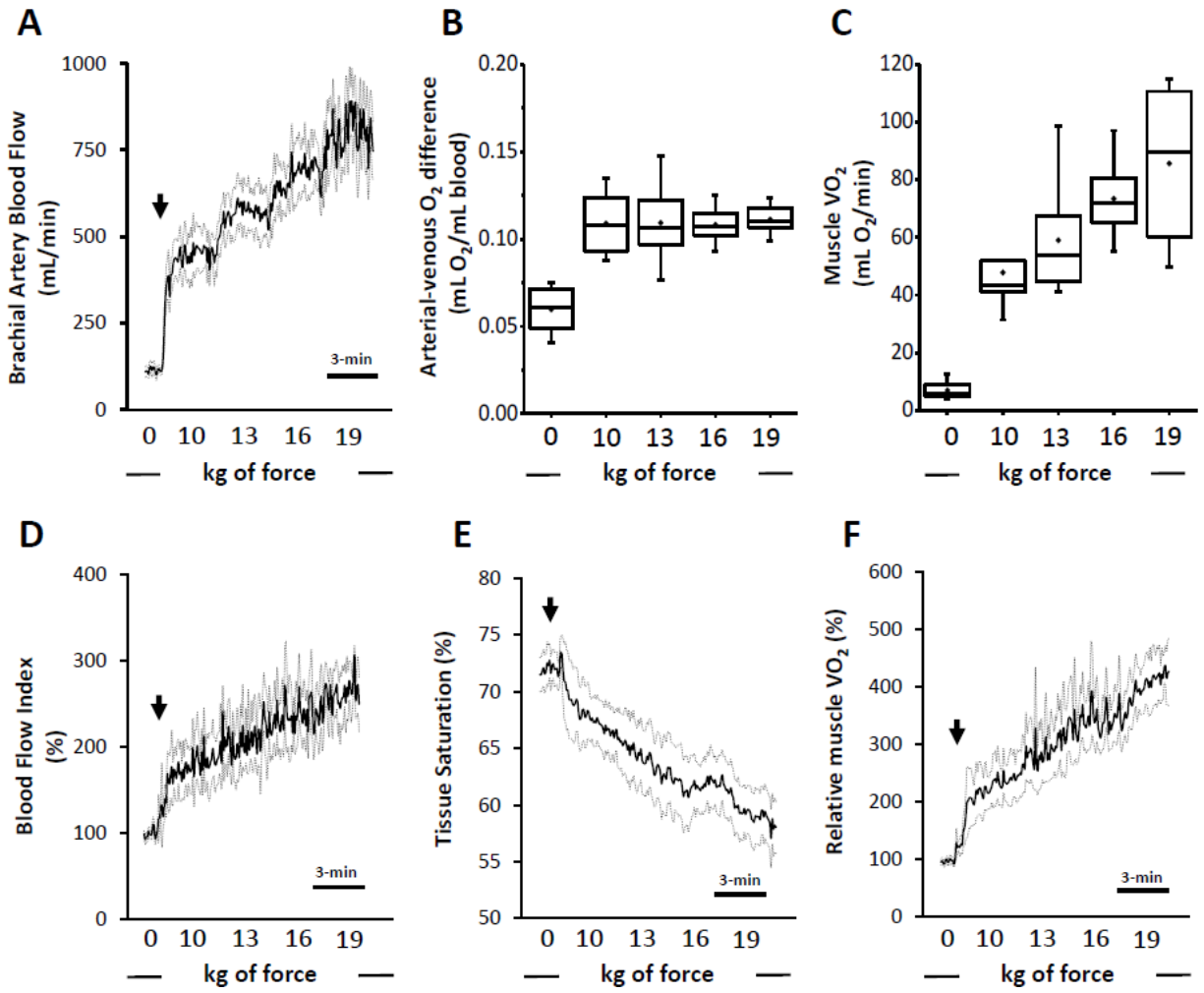

Figure 1. Top three panels illustrate conventional measures of muscle oxygen consumption: (A) Doppler-derived brachial artery blood flow; (B) arterial-venous oxygen difference; and (C) skeletal muscle oxygen consumption (mVO2). Bottom three panels illustrate DCS-derived determinants of relative muscle oxygen consumption: (D) DCS-derived blood flow index; (E) near-infrared spectroscopy derived skeletal muscle tissue saturation; and (F) relative muscle oxygen consumption (MRO2). Rhythmic handgrip began with a fixed workload of 10 kg, and progressed by 3 kg every 3 minutes thereafter. Data are reported as mean + SE. n = 8.

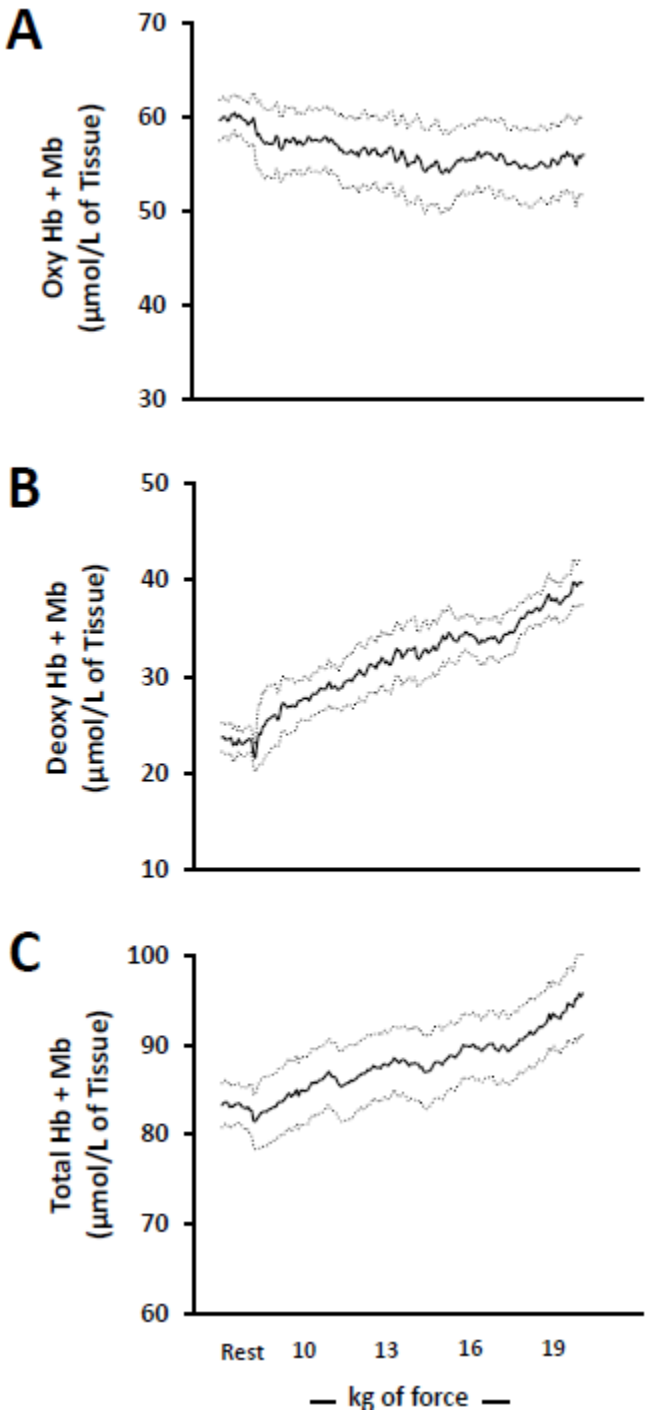

Figure 2. Near-infrared derived oxygenated (Panel A), deoxygenated (Panel B), and total (Panel C) hemoglobin/myoglobin at rest and throughout the incremental handgrip exercise protocol. Rhythmic handgrip began with a fixed workload of 10 kg, and progressed by 3 kg every 3 minutes thereafter. Data are reported as mean ± SE. n = 8. Oxygenated hemoglobin/myoglobin remained unchanged from rest throughout exercise; whereas, deoxygenated and total hemoglobin/myoglobin increased with graded exercise ($P < 0.01$ for both).

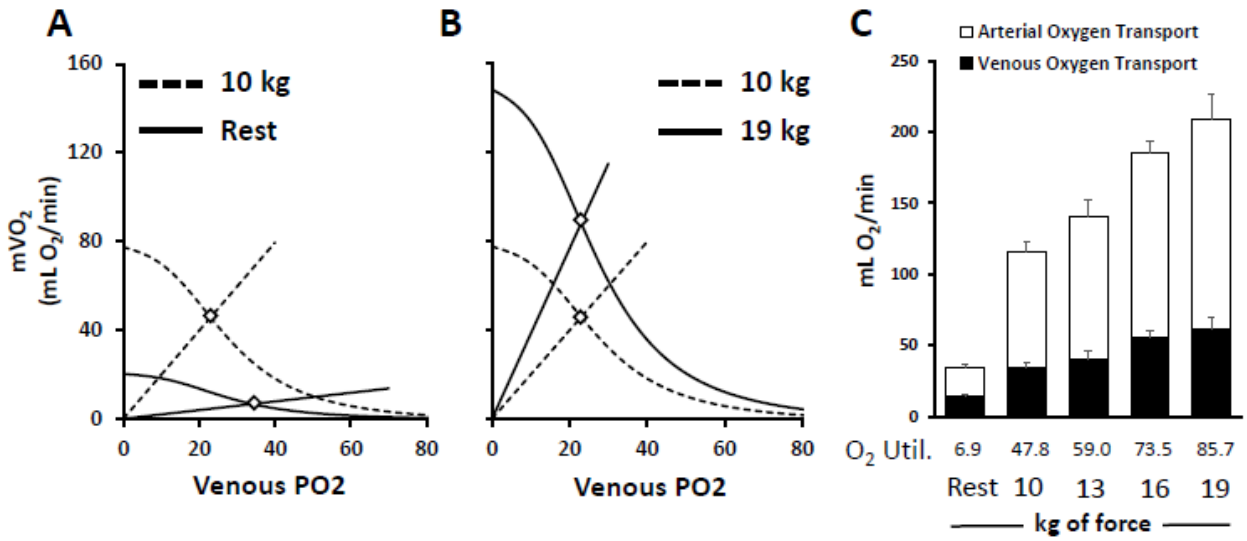

Figure 3. The Fick principle curve depicts muscle oxygen consumption (mVO2) as a function of convective O2 delivery (curved line) vs. venous partial pressure of oxygen (PO2). Fick's law of diffusion depicts mVO2 as a function of venous PO2 with the slope (straight line) representative of muscle O2 diffusive conductance. The intersection of these lines determines the mVO2 achieved. Panel A illustrates the transition from rest to 10 kg of rhythmic handgrip exercise was achieved by a greater increase in diffusive oxygen conductance compared to convective oxygen delivery. Panel B illustrates that the increase in mVO2 from 10 kg to 19kg was achieved by an increase in both convective oxygen delivery and diffuse oxygen conductance that resulted in a minimal change in venous PO2. Panel C illustrates the arterial (white bars) and venous (black bars) oxygen transport at rest, and at the end of each respective exercise workload. Oxygen utilization (O2 Util.) was calculated as the differences between arterial and venous oxygen transport, expressed in mL O2 per minute. Data reported as mean + SE. n = 8.

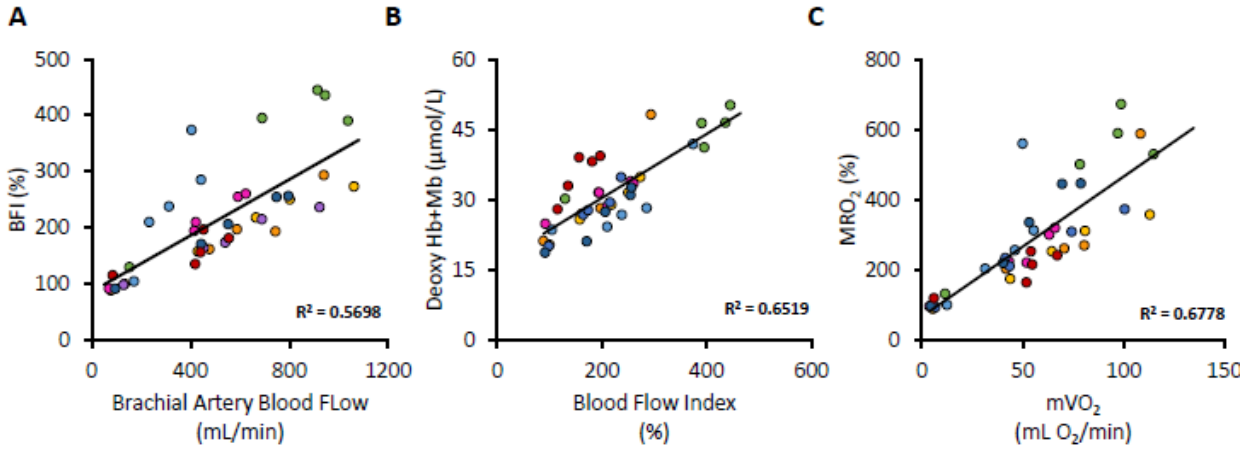

Figure 4. (A) Relationship between Doppler-derived brachial artery blood flow and DCS-derived blood flow index across the incremental exercise test. (B) Relationship between DCS-derived blood flow index and NIRS-derived deoxy Hb+Mb (an indicator fractional O2 extraction). (C) Relationship between conventional mVO2 and DCS-derived MRO2. Individuals are color-coded across each panel to highlight intra-individual relationships, which ranged between 0.62 and 0.99 for panel A, 0.76 and 0.98 for panel B, and 0.54 and 0.98 for panel C.

References

Baker, W. B., Li, Z., Schenkel, S. S., Chandra, M., Busch, D. R., Englund, E. K., . . . Mohler, E. R. (2017). Effects of exercise training on calf muscle oxygen extraction and blood flow in patients with peripheral artery disease. *Journal of Applied Physiology, 123*(6), 1599-1609. doi:10.1152/japplphysiol.00585.2017

Bangalore-Yogananda, C. G., Rosenberry, R., Soni, S., Liu, H., Nelson, M. D., & Tian, F. (2018). Concurrent measurement of skeletal muscle blood flow during exercise with diffuse correlation spectroscopy and Doppler ultrasound. *Biomed Opt Express, 9*(1), 131-141. doi:10.1364/boe.9.000131

Barstow, T. J. (2019a). Understanding near infrared spectroscopy and its application to skeletal muscle research. *J Appl Physiol (1985), 126*(5), 1360-1376. doi:10.1152/japplphysiol.00166.2018

Barstow, T. J. (2019b). Understanding near infrared spectroscopy and its application to skeletal muscle research. *J Appl Physiol, 126*(5), 1360-1376. doi:10.1152/japplphysiol.00166.2018

Bentley, R. F., Kellawan, J. M., Moynes, J. S., Poitras, V. J., Walsh, J. J., & Tschakovsky, M. E. (2014). Individual susceptibility to hypoperfusion and reductions in exercise performance when perfusion pressure is reduced: evidence for vasodilator phenotypes. *Journal of Applied Physiology, 117*(4), 392-405. doi:10.1152/japplphysiol.01155.2013

Berg, O. K., Nyberg, S. K., Windedal, T. M., & Wang, E. (2018). Maximal strength training-induced improvements in forearm work efficiency are associated with reduced blood flow. *American Journal of Physiology - Heart and Circulatory Physiology, 314*(4), H853-h862. doi:10.1152/ajpheart.00435.2017

Boas, D. A., Strangman, G., Culver, J. P., Hoge, R. D., Jasdzewski, G., Poldrack, R. A., . . . Mandeville, J. B. (2003). Can the cerebral metabolic rate of oxygen be estimated with near-infrared spectroscopy? *Phys Med Biol, 48*(15), 2405-2418.

Carp, S. A., Farzam, P., Redes, N., Hueber, D. M., & Franceschini, M. A. (2017). Combined multi-distance frequency domain and diffuse correlation spectroscopy system with simultaneous data acquisition and real-time analysis. *Biomed Opt Express, 8*(9), 3993-4006. doi:10.1364/BOE.8.003993

Cope, M., Delpy, D. T., Reynolds, E. O., Wray, S., Wyatt, J., & van der Zee, P. (1988). Methods of quantitating cerebral near infrared spectroscopy data. *Adv Exp Med Biol, 222*, 183-189.

DeLorey, D. S., Kowalchuk, J. M., & Paterson, D. H. (2003). Relationship between pulmonary O2 uptake kinetics and muscle deoxygenation during moderate-intensity exercise. *J Appl Physiol (1985), 95*(1), 113-120. doi:10.1152/japplphysiol.00956.2002

Dong, J., Bi, R., Ho, J. H., Thong, P. S., Soo, K. C., & Lee, K. (2012). Diffuse correlation spectroscopy with a fast Fourier transform-based software autocorrelator. *J Biomed Opt, 17*(9), 97004-97001. doi:10.1117/1.Jbo.17.9.097004

Epstein, S. E., Beiser, G. D., Stampfer, M., Robinson, B. F., & Braunwald, E. (1967). Characterization of the circulatory response to maximal upright exercise in normal subjects and patients with heart disease. *Circulation, 35*(6), 1049-1062.

Esposito, F., Mathieu-Costello, O., Shabetai, R., Wagner, P. D., & Richardson, R. S. (2010). Limited maximal exercise capacity in patients with chronic heart failure: partitioning the contributors. *J Am Coll Cardiol, 55*(18), 1945-1954. doi:10.1016/j.jacc.2009.11.086

Ferreira, L. F., Koga, S., & Barstow, T. J. (2007). Dynamics of noninvasively estimated microvascular O2 extraction during ramp exercise. *J Appl Physiol (1985), 103*(6), 1999-2004. doi:10.1152/japplphysiol.01414.2006

Gurley, K., Shang, Y., & Yu, G. (2012). Noninvasive optical quantification of absolute blood flow, blood oxygenation, and oxygen consumption rate in exercising skeletal muscle. *J Biomed Opt, 17*(7), 075010. doi:10.1117/1.JBO.17.7.075010

Hammer, S. M., Alexander, A. M., Didier, K. D., Smith, J. R., Caldwell, J. T., Sutterfield, S. L., . . . Barstow, T. J. (2018). The noninvasive simultaneous measurement of tissue oxygenation and microvascular hemodynamics during incremental handgrip exercise. *Journal of Applied Physiology, 124*(3), 604-614. doi:10.1152/japplphysiol.00815.2017

Henry, B., Zhao, M. J., Shang, Y., Uhl, T., Thomas, D. T., Xenos, E. S., . . . Yu, G. Q. (2015). Hybrid diffuse optical techniques for continuous hemodynamic measurement in gastrocnemius during plantar flexion exercise. *Journal of Biomedical Optics, 20*(12). doi:Artn 125006

10.1117/1.Jbo.20.12.125006

Herr, M. D., Hogeman, C. S., Koch, D. W., Krishnan, A., Momen, A., & Leuenberger, U. A. (2010). A real-time device for converting Doppler ultrasound audio signals into fluid flow velocity. *Am J Physiol Heart Circ Physiol, 298*(5), H1626-1632. doi:10.1152/ajpheart.00713.2009

Hirai, D. M., Musch, T. I., & Poole, D. C. (2015). Exercise training in chronic heart failure: improving skeletal muscle O2 transport and utilization. *Am J Physiol Heart Circ Physiol, 309*(9), H1419-1439. doi:10.1152/ajpheart.00469.2015

Hogan, M. C., Roca, J., West, J. B., & Wagner, P. D. (1989). Dissociation of maximal O2 uptake from O2 delivery in canine gastrocnemius in situ. *J Appl Physiol (1985), 66*(3), 1219-1226. doi:10.1152/jappl.1989.66.3.1219

Houstis, N. E., Eisman, A. S., Pappagianopoulos, P. P., Wooster, L., Bailey, C. S., Wagner, P. D., & Lewis, G. D. (2018). Exercise Intolerance in Heart Failure With Preserved Ejection Fraction: Diagnosing and Ranking Its Causes Using Personalized O2 Pathway Analysis. *Circulation, 137*(2), 148-161. doi:10.1161/circulationaha.117.029058

Lutjemeier, B. J., Ferreira, L. F., Poole, D. C., Townsend, D., & Barstow, T. J. (2008). Muscle microvascular hemoglobin concentration and oxygenation within the contraction-relaxation cycle. *Respir Physiol Neurobiol, 160*(2), 131-138. doi:10.1016/j.resp.2007.09.005

McDonough, P., Behnke, B. J., Padilla, D. J., Musch, T. I., & Poole, D. C. (2005). Control of microvascular oxygen pressures in rat muscles comprised of different fibre types. *J Physiol, 563*(Pt 3), 903-913. doi:10.1113/jphysiol.2004.079533

Mole, P. A., Chung, Y., Tran, T. K., Sailasuta, N., Hurd, R., & Jue, T. (1999). Myoglobin desaturation with exercise intensity in human gastrocnemius muscle. *Am J Physiol, 277*(1), R173-180. doi:10.1152/ajpregu.1999.277.1.R173

Nyberg, S. K., Berg, O. K., Helgerud, J., & Wang, E. (2017). Blood flow regulation and oxygen uptake during high-intensity forearm exercise. *J Appl Physiol (1985), 122*(4), 907-917. doi:10.1152/japplphysiol.00983.2016

Nyberg, S. K., Berg, O. K., Helgerud, J., & Wang, E. (2018). Reliability of forearm oxygen uptake during handgrip exercise: assessment by ultrasonography and venous blood gas. *Physiol Rep, 6*(10), e13696. doi:10.14814/phy2.13696

Padilla, D. J., Musch, T. I., & Poole, D. C. (2005). Abusing the fick principle. *Med Sci Sports Exerc, 37*(4), 702.

Poole, D. C., Copp, S. W., Ferguson, S. K., & Musch, T. I. (2013). Skeletal muscle capillary function: contemporary observations and novel hypotheses. *Experimental Physiology, 98*(12), 1645-1658. doi:10.1113/expphysiol.2013.073874

Poole, D. C., Copp, S. W., Hirai, D. M., & Musch, T. I. (2011). Dynamics of muscle microcirculatory and blood-myocyte O(2) flux during contractions. *Acta Physiol (Oxf), 202*(3), 293-310. doi:10.1111/j.1748-1716.2010.02246.x

Poole, D. C., & Musch, T. I. (2008). Solving the Fick principle using whole body measurements does not discriminate "central" and "peripheral" adaptations to training. *European Journal of Applied Physiology, 103*(1), 117-119. doi:10.1007/s00421-007-0668-4

Poole, D. C., Richardson, R. S., Haykowsky, M. J., Hirai, D. M., & Musch, T. I. (2018a). Exercise limitations in heart failure with reduced and preserved ejection fraction. *J Appl Physiol, 124*(1), 208-224. doi:10.1152/japplphysiol.00747.2017

Poole, D. C., Richardson, R. S., Haykowsky, M. J., Hirai, D. M., & Musch, T. I. (2018b). Exercise limitations in heart failure with reduced and preserved ejection fraction. *J Appl Physiol (1985), 124*(1), 208-224. doi:10.1152/japplphysiol.00747.2017

Poole, D. C., Wagner, P. D., & Wilson, D. F. (1995). Diaphragm microvascular plasma PO2 measured in vivo. *J Appl Physiol, 79*(6), 2050-2057. doi:10.1152/jappl.1995.79.6.2050

Richardson, R. S., Noyszewski, E. A., Kendrick, K. F., Leigh, J. S., & Wagner, P. D. (1995). Myoglobin O2 desaturation during exercise. Evidence of limited O2 transport. *J Clin Invest, 96*(4), 1916-1926. doi:10.1172/JCI118237

Richardson, R. S., Noyszewski, E. A., Leigh, J. S., & Wagner, P. D. (1998). Lactate efflux from exercising human skeletal muscle: role of intracellular PO2. *J Appl Physiol (1985), 85*(2), 627-634. doi:10.1152/jappl.1998.85.2.627

Richardson, R. S., Poole, D. C., Knight, D. R., Kurdak, S. S., Hogan, M. C., Grassi, B., . . . Wagner, P. D. (1993). High muscle blood flow in man: is maximal O2 extraction compromised? *J Appl Physiol 75*(4), 1911-1916. doi:10.1152/jappl.1993.75.4.1911

Roca, J., Agusti, A. G., Alonso, A., Poole, D. C., Viegas, C., Barbera, J. A., . . . Wagner, P. D. (1992). Effects of training on muscle O2 transport at VO2max. *J Appl Physiol (1985), 73*(3), 1067-1076. doi:10.1152/jappl.1992.73.3.1067

Roca, J., Hogan, M. C., Story, D., Bebout, D. E., Haab, P., Gonzalez, R., . . . Wagner, P. D. (1989). Evidence for tissue diffusion limitation of VO2max in normal humans. *J Appl Physiol (1985), 67*(1), 291-299. doi:10.1152/jappl.1989.67.1.291

Tucker, W. J., Rosenberry, R., Trojacek, D., Chamseddine, H. H., Arena-Marshall, C. A., Zhu, Y., . . . Nelson, M. D. (2019). Studies into the determinants of skeletal muscle oxygen consumption: Novel insight from near-infrared diffuse correlation spectroscopy. *Journal of Physiology-London*.

APPENDIX D

SKELETAL MUSCLE NEUROVASCULAR COUPLING, OXIDATIVE CAPACITY, AND MICROVASCULAR FUNCTION WITH 'ONE STOP SHOP' NEAR-INFRARED SPECTROSCOPY*

Ryan Rosenberry, Susie Chung, Michael D. Nelson. Skeletal Muscle Neurovascular Coupling, Oxidative Capacity, and Microvascular Function with 'One Stop Shop' Near-infrared Spectroscopy. *J. Vis. Exp.* (132), e57317, doi:10.3791/57317 (2018).

Introduction

The hyperemic response to a brief period of tissue ischemia has emerged as a key non-invasive measure of (micro)vascular function. During occlusion of a conduit artery, downstream arterioles dilate in an effort to offset the ischemic insult. Upon release of the occlusion, the decreased vascular resistance results in hyperemia, the magnitude of which is dictated by one's ability to dilate the downstream microvasculature. While reactive hyperemia is a strong independent predictor of cardiovascular events (Huang et al., 2007; Suryapranata et al., 1994) and therefore a clinically significant endpoint, its functional significance to exercise tolerance and quality of life is less clear.

Indeed, dynamic exercise represents a major cardiovascular stress that demands a highly coordinated neurovascular response in order to match oxygen delivery to metabolic demand. For example, skeletal muscle blood flow can increase nearly 100-fold during isolated muscle contractions(Richardson et al., 1993), which would overwhelm the pumping capacity of the heart if such a hemodynamic response were extrapolated to whole-body exercise. Accordingly, to avoid severe hypotension, sympathetic (i.e. vasoconstrictor) nervous activity increases to redistribute cardiac output away from inactive and visceral tissues and towards active skeletal muscle(Clifford & Hellsten, 2004). Sympathetic outflow is also directed to the exercising skeletal muscle(Hansen, Thomas, Jacobsen, & Victor, 1994); however, local metabolic signaling attenuates the vasoconstrictor response in order to ensure adequate tissue oxygen delivery(Fadel, Keller, Watanabe, Raven, & Thomas, 2004; Hansen, Thomas, Harris, Parsons, & Victor, 1996; Nelson et al., 2014; Nelson et al., 2015; Rosenmeier, Fritzlar, Dinenno, & Joyner, 2003; Thomas & Victor, 1998). Collectively, this process is termed functional sympatholysis(Remensnyder, Mitchell, & Sarnoff, 1962), and is imperative to the normal regulation of skeletal muscle blood flow during exercise. Since skeletal muscle blood flow is a key determinant of aerobic capacity — an independent predictor of quality of life and cardiovascular disease morbidity and

mortality(Kodama et al., 2009) — understanding the control of skeletal muscle blood flow and tissue oxygen delivery during exercise is of great clinical significance.

Oxygen delivery is only half of the Fick equation, however, with oxygen utilization satisfying the other half of the equation. Among the major determinates of oxygen utilization, mitochondrial oxidative phosphorylation plays an essential role in supplying adequate energy for cellular processes both at rest and during exercise. Indeed, impairments in muscle oxidative capacity can limit functional capacity and quality of life(Cabalzar et al., 2017; Tyni-Lenné, Gordon, Jansson, Bermann, & Sylvén, 1997; Westerblad, Place, & Yamada, 2010). Various measures are commonly used to provide an index of muscle oxidative capacity, including invasive muscle biopsies and expensive and time-consuming magnetic resonance spectroscopy (MRS) techniques.

Here, we propose a novel, non-invasive approach, using near-infrared spectroscopy (NIRS), to assess each of these three major clinical endpoints (reactive hyperemia, sympatholysis and muscle oxidative capacity) in a single clinic or laboratory visit. The major advantages of this approach are three-fold: first, this technique is easily portable, relatively low cost, and easy to perform. Current Doppler ultrasound approaches for measuring reactive hyperemia are highly operator-dependent — requiring extensive skill and training — and requires sophisticated, high-cost, data acquisition hardware and post-processing software. Moreover, this could conceivably be introduced into the clinic and/or large clinical trials for bedside monitoring or testing therapeutic efficacy. Second, by virtue of the methodology, this technique focuses specifically on the skeletal muscle microvasculature, increasing the overall specificity of the technique. Alternative approaches using Doppler ultrasound focus entirely on upstream conduit vessels and infer changes downstream, which can dampen the signal. Third, this technique is completely non-invasive. Skeletal muscle oxidative capacity is traditionally assessed with invasive and painful muscle biopsies, and functional sympatholysis may be assessed with intra-arterial injection of sympathomimetics and sympatholytics. This approach avoids these requirements all together.

Protocol

This protocol follows the guidelines of the institutional review board at the University of Texas at Arlington and conforms to the standards set by the latest version of the Declaration of Helsinki. Accordingly, written informed consent was (and should be) obtained prior to commencement of research procedures.

1. Instrumentation

The following instrumentation description is based on the near-infrared (NIR) spectrometer and data acquisition system used in our lab (see *Table of Materials*). Thus, the instructions include steps that are necessary for the optimal function of these devices. These steps include the calibration of the NIR probe using the accompanying software and calibration phantom, and the application of a dark cloth to exclude ambient light. In the event that different data collection hardware and/or software are used, investigators should consult their own specific user manuals for calibration and ambient light considerations.

Figure 1 illustrates the experimental set-up and instrumentation described immediately below.

1.1. Instruct the subject to lie supine with their legs inside a lower body negative pressure (LBNP) chamber (**Figure 1A**), so that their belt line is approximately even with the opening to the LBNP box. For instructions on how to build a LBNP chamber, see *References* (Esch, Scott, & Warburton, 2007).

1.2. Place three electrocardiogram electrodes on the subject: two in an inferior, mid-clavicular location and one on the subject's left side medial to the iliac crest. This configuration provides the best results due to limited access to the lower limbs, instrumentation of the upper limbs, and arm movement during hand grip exercise.

1.3. Place a non-invasive blood pressure monitor module on the subject's dominant wrist. Place the finger blood pressure cuffs on each finger and connect them to the module (**Figure 1B**). Ensure the finger blood pressure cuffs are properly calibrated according to the user's manual accompanying your device.

1.4. Instruct the subject to grasp a hand grip dynamometer (HGD) with their non-dominant arm in a slightly abducted position. The arm should be comfortably positioned on a bedside table. The distance and angle of the HGD should be adjusted to allow for optimal grip strength with minimal arm movement (**Figure 1C**).

1.5. Secure the HGD to a bedside table.

1.6. Measure the maximum voluntary contraction (MVC) of the participant. Tell the participant that, when prompted, they must squeeze the HGD as hard as possible while only utilizing the muscles in the hand and forearm. Instruct the subject that they must refrain from recruiting their upper arm, chest, shoulder, or abdominal muscles when performing the maximum grip.

1.7. Repeat Step 1.6 three times, separated by at least 60 s. Record the maximum force achieved (best of 3). This maximum force will be used to calculate the exercise intensity for skeletal muscle oxidative capacity and neurovascular coupling (below).

1.8. Place a rapid-inflation cuff around the upper arm of the exercising hand. Connect the airline from the rapid inflation controller to the cuff.

1.9. Identify the flexor digitorum profundus. Use a skin marker to demarcate the borders of the palpable muscle.

1.10. Ensure that the NIR spectrometer is properly calibrated according to the user's manual included with your device. Clean the skin over which the NIR probe will be positioned with an alcohol prep wipe.

1.11. Place the NIR probe over the center of the belly of the muscle (flexor digitorum profundus) and affix it securely to the forearm.

1.12. Wrap the probe and forearm with dark cloth, minimizing interference from ambient light (**Figure 1C**, **Figure 1D**).

1.13. When ready to perform the functional sympatholysis portion of the study, seal the subject into the LBNP chamber.

2. Skeletal muscle oxidative capacity

A representative data tracing illustrating the experimental procedure for measuring skeletal muscle oxidative capacity is depicted in **Figure 2**. This experimental approach has previously been validated against *in vivo* phosphorus MRS(Ryan, Southern, Reynolds, & McCully, 2013) and *in situ* muscle respirometry(Ryan, Brophy, Lin, Hickner, & Neufer, 2014), and is gaining wide spread acceptance(Adami & Rossiter, 2017).

2.1. Instrument the subject as indicated above (*Instrumentation*).

2.2. Instruct the subject to lie still for 2 min while monitoring deoxyhemoglobin (HHb) and oxyhemoglobin (HbO_2) via the NIR probe.

This rest period allows the subject to recover from any movement artifact associated with the instrumentation process, and ensures stable baseline measurements. If after 2 min no significant fluctuations have occurred, the subject may be considered at a steady state, or resting baseline.

2.3. Prior to cuff occlusion, notify your subject that you will be inflating the cuff. Inflate the upper arm cuff at least 30 mmHg above systolic blood pressure for 5 min (i.e. suprasystolic). Instruct the subject to keep their arm as still and relaxed as possible both during cuff inflation and following cuff deflation. This 5 min brachial artery cuff occlusion protocol closely reflects the currently accepted clinical standard for vascular occlusion tests(Corretti et al., 2002; Green, Jones, Thijssen, Cable, & Atkinson, 2011; Ryan, Erickson, Brizendine, Young, & McCully, 2012; Southern, Ryan, Reynolds, & McCully, 2014; Thijssen et al., 2011).

2.4. Record the initial/baseline value (prior to cuff occlusion) and the nadir value of tissue saturation (StO_2) during the cuff occlusion and determine the midpoint between these two values.

$$\mathrm{St_{O2}}\ (\%) = \frac{\mathrm{Hb_{O2}}}{\mathrm{Hb_{O2}} + \mathrm{HHb}} \times 100$$

2.5. Allow the subject to recover from the cuff occlusion and return to the resting baseline values. Once the subject has maintained a resting baseline for at least 1 full min, continue to the next step.

2.6. Instruct subject to squeeze and maintain an isometric hand grip at 50% of their MVC. Encourage the subject to maintain their isometric contraction until the tissue desaturates by 50%. Upon achieving this value, tell the subject to relax their hand and inform them that no more exercise or movement is needed.

2.7. Within 3-5 s following exercise cessation, administer the following rapid cuff occlusion series (one series = 1 inflation + 1 deflation), as previously established (Ryan, Southern, Reynolds, et al., 2013):

Series #1-6: 5 s on/5 s off

Series #7-10: 7 s on/10 s off

Series #11-14: 10 s on/15 s off

Series #15-18: 10 s on/20 s off

2.8. After completing the 18th inflation/deflation series, instruct the subject to rest, allowing tissue saturation to return to initial baseline values. After these values have remained consistent for at least 2 min, repeat steps 2.4 and 2.5.

2.9. <u>Calculating Skeletal Muscle Oxidative Capacity</u>

2.9.1. Calculate the slope of change in the StO_2 for each of the individual 18 cuff occlusions, forming the monoexponential recovery points illustrated in Figure 2C.

2.9.2. Fit the calculated data from 2.7 to the following monoexponential curve(Ryan, Brophy, et al., 2014; Ryan, Erickson, et al., 2014; Ryan, Southern, Reynolds, et al., 2013):

$$y = End - \Delta \times e^{-kt}$$

Note: 'y' is the relative muscle oxygen consumption rate ($m\dot{V}O_2$) during cuff inflation, 'End' represents the $m\dot{V}O_2$ immediately following the cessation of exercise; delta ('Δ') signifies the change in $m\dot{V}O_2$ from rest to the end of exercise; '*k*' is the fitting rate constant; 't' is time. Tau is calculated as 1/k.

3. Reactive Hyperemia

A representative data tracing illustrating the experimental procedure for measuring reactive hyperemia is depicted in **Figure 3**.

3.1. With the subject lying supine and instrumented as described above (*Instrumentation*), instruct the subject to lie as still as possible.

3.2. Once the subject has achieved a consistent resting state, continue to record at least 1 min of baseline data and then rapidly inflate a blood pressure cuff on the upper arm to a suprasystolic pressure (30 mmHg above systolic blood pressure).

3.3. At the 5 min mark, rapidly deflate the cuff while recording the hyperemic response.

3.4. Continue recording for at least 3 min to capture the subject's recovery.

3.5. <u>Calculating Reactive Hyperemia</u>

3.5.1. The NIRS parameters calculated are depicted in **Figure 3**.

3.5.2. Baseline StO_2 is calculated as the average StO_2 over 1 full min prior to the onset of arterial cuff occlusion.

3.5.3. Resting skeletal muscle metabolic rate is indicated by the desaturation rate (i.e. average slope) during cuff occlusion (defined as Slope 1)*(Mayeur, Campard, Richard, & Teboul, 2011)*(McLay, Fontana, et al., 2016).

3.5.4. Reactive hyperemia is calculated in the following ways:

a) the average upslope following cuff release (i.e. reperfusion rate, defined as slope 2), calculated from the moment of cuff release through the linearly increasing phase of the rebound trace;

b) the highest StO_2 value reached after cuff release (denoted as StO_{2max});

c) the reactive hyperemia area under the curve (AUC); calculated from the time of cuff release to 1-, 2- and 3-min post cuff-occlusion (AUC 1-min, AUC 2-min, and AUC 3-min, respectively); and

d) the hyperemic reserve, calculated as the change in StO_2 above baseline and reported as a percent (%) change. This value is calculated as the highest saturation achieved during the post-occlusive rebound minus the average saturation calculated in step 3.5 (see above). Note: Large differences in baseline data will greatly affect the interpretation of the hyperemic reserve.

4. Functional Sympatholysis

A representative data tracing illustrating the experimental procedure for measuring functional sympatholysis is depicted in **Figure 4**.

4.1. Instrument the subject as indicated above (*Instrumentation*).

4.2. Ensure an airtight seal in the LBNP chamber.

4.3. With the subject lying still and at rest, collect 3 min of baseline data.

4.4. At the 3 min mark, turn on the vacuum. Adjust the vacuum so that the pressure inside the LBNP chamber is between -20 and -30 mmHg. Allow the vacuum to run for 2 min while monitoring the subject's response.

4.5. At the 5 min mark, turn off the vacuum and allow the subject to rest for 3 min.

4.6. At the 8 min mark, initiate the voice prompt guiding the subject through the rhythmic hand grip exercise (20% MVC).

4.7. Confirm that the subject is maintaining their squeeze throughout the entirety of each gripping phase and relaxing completely during between each repetition. Monitor their force output and confirm that they are achieving 20% MVC with each grip. Continue exercise until the 11 min mark.

4.8. At the 11 min mark, turn on the vacuum encouraging the subject to continue their rhythmic exercise. Allow the vacuum to run from 11-13 min, then turn it off.

4.9. Have the subject continue performing rhythmic hand grip exercise at 20% of their MVC for an additional 2 min. Upon exercise cessation, have the subject rest quietly and lie still.

4.10. Calculating Functional Sympatholysis

4.10.1. Normalize the change in oxyhemoglobin with LBNP to the total labile signal (TLS), determined during 5 min cuff occlusion:

$$\Delta \mathrm{Hb}_{\mathrm{O2\ (rest)}}(\%\ \mathrm{TLS}) = \frac{\Delta \mathrm{Hb}_{\mathrm{O2\ (baseline)}} - \Delta \mathrm{Hb}_{\mathrm{O2\ (rest+LBNP)}}}{\Delta \mathrm{Hb}_{\mathrm{O2\ (baseline)}} - \Delta \mathrm{Hb}_{\mathrm{O2\ (nadir)}}} \times 100$$

$$\Delta \mathrm{Hb}_{\mathrm{O2\ (exercise)}}(\%\ \mathrm{TLS}) = \frac{\Delta \mathrm{Hb}_{\mathrm{O2\ (exercise)}} - \Delta \mathrm{Hb}_{\mathrm{O2\ (exercise+LBNP)}}}{\Delta \mathrm{Hb}_{\mathrm{O2\ (baseline)}} - \Delta \mathrm{Hb}_{\mathrm{O2\ (nadir)}}} \times 100$$

4.8.2 Calculate each event as the final 20 min average of each event.

4.8.3 Calculate the exercise-induced attenuation of the oxyhemoglobin reduction:

$$\frac{\Delta \mathrm{Hb}_{\mathrm{O2\ (rest)}} - \Delta \mathrm{Hb}_{\mathrm{O2\ (exercise)}}}{\Delta \mathrm{Hb}_{\mathrm{O2\ (rest)}}} \times 100$$

Representative Results

Skeletal muscle oxidative capacity

Figure 2 illustrates a representative participant response during a NIRS-derived skeletal muscle oxidative capacity assessment. **(A)** Panel A shows the tissue saturation profile during a 5 min arterial cuff occlusion protocol, handgrip exercise, and intermittent arterial occlusion during recovery from exercise. **(B)** Panel B illustrates the expected tissue desaturation/re-saturation profile during the intermittent arterial occlusions during the recovery period. The rate of desaturation is directly proportional to the rate of muscle oxygen consumption, and is plotted in **(C)** for each of the intermittent cuff occlusion periods. The calculated muscle oxygen consumption recovery data is then fit to a monoexponential curve and the recovery time constant derived. Using the same approach, a growing number of studies have evaluated skeletal muscle oxidative capacity in both health and disease, across a variety of muscle groups (**Table 1**).

Reactive Hyperemia

Figure 3 illustrates the NIRS-derived reactive hyperemia profile during a representative vascular occlusion test. This same approach has been used across a wide range of study populations and muscle groups with good success (**Table 2**). The data indicate that NIRS-derived reactive hyperemia not only provides valuable insight into vascular reactivity, but that the test is easily adaptable and clinically meaningful.

Functional Sympatholysis

Table 3 summarizes the existing literature using the exact same neurovascular coupling approach described herein to measure functional sympatholysis, showing both mechanistic and clinically relevant outcomes. In healthy control subjects, when LBNP is superimposed on mild handgrip, the reflex decrease

in muscle oxygenation is attenuated by ~50% (**Figure 4**). Failure to attenuate sympathetic (vasoconstrictor) nerve activity during exercise, as with cardiovascular or neurological disease (**Table 3**), disrupts the balance between oxygen delivery and utilization, and causes functional muscle ischemia.

Discussion

The methods described herein enable non-invasive, clinical evaluation of reactive hyperemia, neurovascular coupling, and skeletal muscle oxidative capacity in a single clinic or laboratory visit.

Critical Considerations

Although NIRS is relatively robust and easy to use, collection of these data require careful placement of the optodes directly over the muscle belly, secured tightly in place to avoid movement artifact, and covered with a black vinyl sheet in a dimly lit room to avoid interference of the near infrared from external light. In addition, obtaining good quality data relies heavily on clear communication between the tester and the subject, and the testing team. We, and others, have found that when performed with appropriate care and attention, NIRS is highly reproducible within a single study visit, and across multiple visits(McLay, Nederveen, Pogliaghi, Paterson, & Murias, 2016; Nelson et al., 2014; Nelson et al., 2015; Southern et al., 2014). Moreover, the physiological outcome variables reported herein (i.e. skeletal muscle oxidative capacity, reactive hyperemia, and neurovascular coupling) are sensitive to experimental/clinical intervention, both within and between study visits(Ryan, Southern, Brizendine, & McCully, 2013),(Southern et al., 2015),(Nelson et al., 2014),(Nelson et al., 2015).

There is currently limited consensus on the appropriate reporting of the NIRS outcome variables. For example, when measuring skeletal muscle oxidative capacity, investigators have fit the recovery kinetics of HbO_2(Ryan, Brizendine, & McCully, 2013), HHb(Ryan, Brophy, et al., 2014), Hb_{diff}(Ryan, Southern, Brizendine, et al., 2013) and tissue O_2 saturation (present study and others(Adami, Cao, Porszasz, Casaburi, & Rossiter, 2017)). Likewise, a similar spread in the outcome variables have also been

reported for NIRS-based reactive hyperemia.(Bopp, Townsend, Warren, & Barstow, 2014; Kragelj, Jarm, Erjavec, Presern-Strukelj, & Miklavcic, 2001; Lacroix et al., 2012; Willingham, Southern, & McCully, 2016) Some of this discrepancy may relate to the type of NIRS device used. For example, frequency-domain devices (as used here) provide absolute quantification of HbO_2 and HHb, and thus may not be affected by acute changes in total Hb content (negating the need to correct the data). In contrast however, continuous-wave devices are greatly affected by acute changes in total hemoglobin, requiring data correction(Ryan et al., 2012).

Modifications and troubleshooting

One important and currently unavoidable limitation of NIRS is its limited penetration depth (~2 cm). Therefore, limb adiposity can significantly reduce — and even completely eliminate — the NIRS signal and should be considered when screening potential subjects. To control for this, investigators are encouraged to measure forearm skinfold thickness, and exclude participants with significant peripheral adiposity.

Any factor that can modulate vascular responsiveness, neurovascular coupling, and/or skeletal muscle oxidative capacity (i.e. medication, genetic mutations, etc) will indeed affect the primary end-point measurements described herein. Investigators are therefore encouraged to take these factors into account when adapting this protocol and planning future experimentation.

For functional sympatholysis determination, investigators may wish to include a second resting LBNP challenge to ensure the signal is still present and that the differences observed during exercise-LBNP were not simply due to a loss of signal or measurement error. It is recommended to allow 3-5 min to allow the oxyhemoglobin signal to full recovery to baseline values before repeating the resting LBNP challenge.

Future applications or directions after mastering this technique

NIR spectroscopy uses laser light to assess the concentration of oxygenated and deoxygenated hemoglobin in tissue. During measurement of reactive hyperemia and functional sympatholysis, relative changes in these parameters are believed to represent changes in microvascular flow. Diffuse correlation spectroscopy (DCS) is an emerging near-infrared imaging approach which, in addition to evaluating the concentration of oxy- and deoxyhemoglobin, can also quantify microvascular perfusion(Gurley, Shang, & Yu, 2012). Given the obvious similarities between these two imaging approaches, incorporation of DCS into the proposed techniques would be virtually seamless and may provide additional insight into the quantification of microvascular function and perfusion.

Once this technique is mastered, application to clinical populations, such as those with heart failure, will provide important mechanistic insight into exercise intolerance and cardiovascular dysfunction.

Figures and Tables

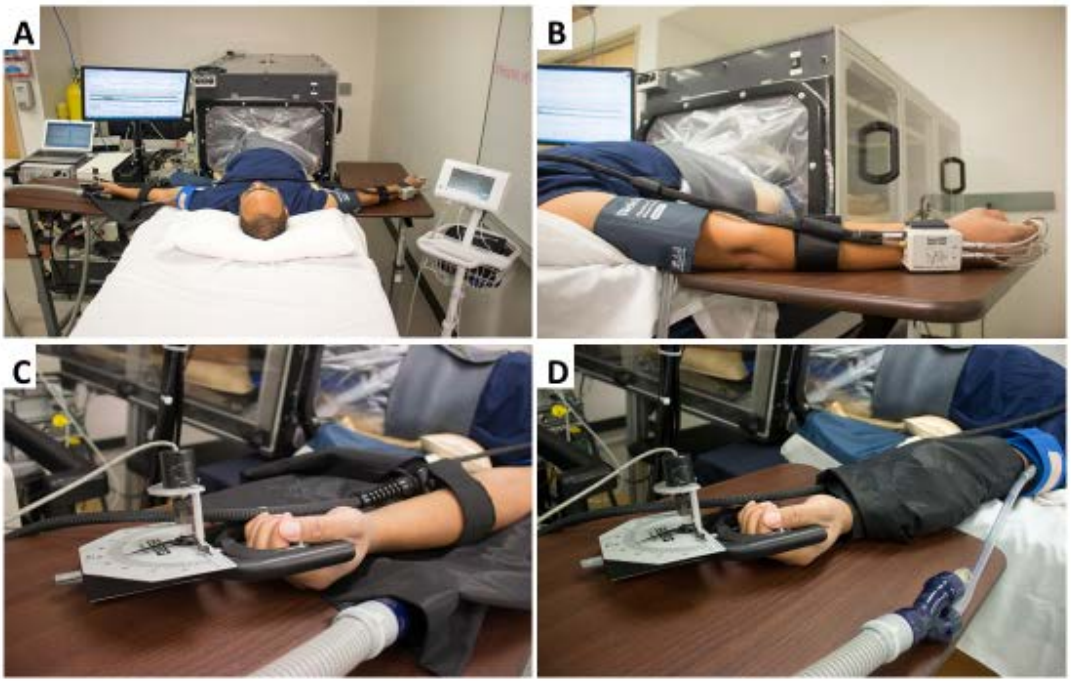

Figure 1. **Experimental set-up and instrumentation**. **(A)** Representative experimental set-up, with a typical subject lying supine on a bed with their legs inside the LBNP chamber and fully instrumented. **(B)** Dominant arm instrumented with a non-invasive beat-to-beat blood pressure device for beat-to-beat arterial blood pressure measurement, and a brachial artery blood pressure cuff for calibration and verification of the beat-to-beat system. **(C)** Instrumentation of the non-dominant arm. The hand is comfortably gripping a handgrip dynamometer (connected to data acquisition system), the forearm muscle is instrumented with the near-infrared spectroscopy probe. **(D)** Once instrumented, the NIRS optodes are covered with a black vinyl cloth (to eliminate interference from ambient light). In addition, a rapid cuff inflation system is placed over the brachial artery.

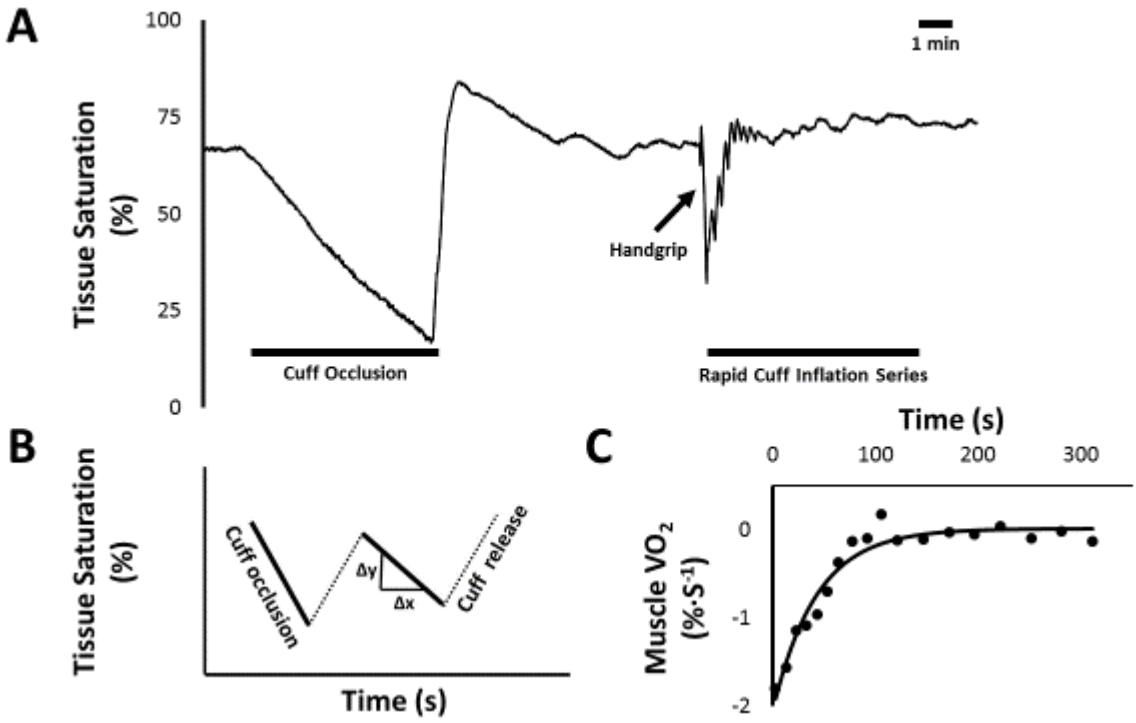

Figure 2. Skeletal muscle oxidative capacity protocol. (A) Raw data tracing from a representative subject measured via NIRS, showing tissue saturation (StO_2) over time. After establishing a stable baseline, the brachial artery of the non-dominant arm is occluded for five min in order to establish the subject's desaturation reserve (difference between baseline StO_2 and the nadir). After recovery from the occlusion, the subject is instructed to perform a 50% isometric handgrip, followed by 18 rapid cuff inflation series to assess muscle oxygen consumption recovery kinetics. **(B)** Data analysis is then performed offline by calculating the average slope of each cuff occlusion series following exercise; illustrated here using hypothetical cuff occlusion series data. **(C)** In order to calculate the recovery time constant of muscle oxygenation, the slope of each of the 18 rapid cuff occlusions (i.e. post-exercise muscle oxygen consumption, $m\dot{V}O_2$) from Panel A is plotted against time and fit to a monoexponential curve.

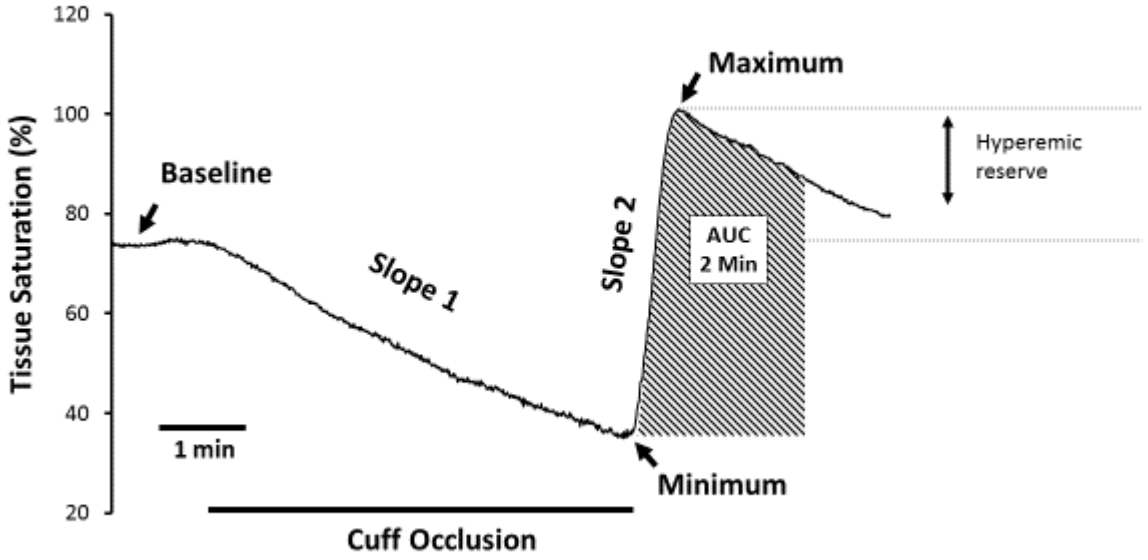

Figure 3. Reactive hyperemia experimental protocol. With the subject lying supine, record at least 1 min of baseline data, followed by 5 min of total arterial cuff occlusion, and at least 3 min of recovery following cuff release. Note the obvious overlap between the skeletal muscle oxidative capacity protocol (**Figure 2**) and this protocol. 'Baseline' defines the period of time prior to arterial cuff occlusion. 'Slope 1' defines the desaturation rate during cuff occlusion, and is regarded as a measure of resting skeletal muscle metabolic rate. The lowest StO_2 value obtained during ischemia is defined as 'StO_2 minimum', and is regarded as a measure of the ischemic stimulus to vasodilate. The tissue saturation reperfusion rate is denoted as 'Slope 2', and is an index of reactive hyperemia; as are StO_2 maximum, and the reactive hyperemia 'area under the curve' (AUC). To gain insight into the hyperemic reserve, the StO_2 maximum is expressed as a percent change from baseline.

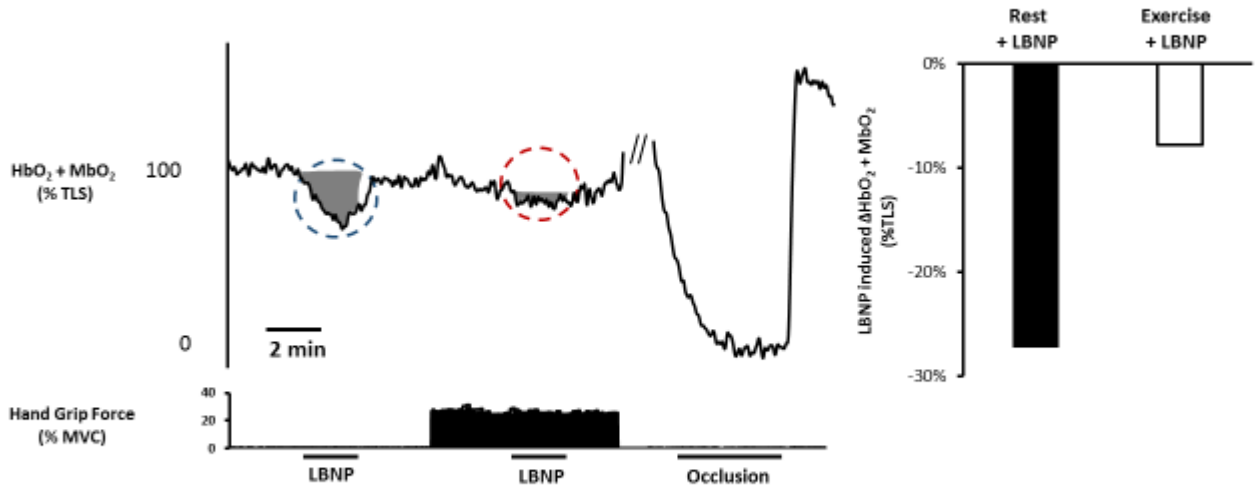

Figure 4. Functional sympatholysis experimental protocol. Left panel: Raw data tracing from a representative subject. With the subject lying supine in the LBNP chamber, allow 3 min of steady-state baseline data collection. Turn on LBNP to -20 mmHg for 2 min. Oxyhemoglobin/myoglobin should decrease in response to the reflex sympathetic vasoconstriction (blue circle, shaded area). Allow 2 min for the recovery. Ask the subject to perform rhythmic handgrip exercise at 20% MVC (measured prior to data collection). After 3 min of rhythmic exercise, repeat -20 mmHg LBNP for 2 min while the subject continues to exercise, followed by 2 min of exercise without LBNP. The reduction in oxyhemoglobin/myoglobin should be significantly attenuated (red circle, shaded area). If not already performed, inflate a blood pressure cuff over the brachial artery of the exercising arm for 5 min to establish the subject's range of desaturation. Right Panel: LBNP-induced change in oxyhemoglobin/myoglobin at rest and during handgrip exercise calculated from the data on the left. Note: the shaded areas in the figure are only meant to highlight the changes in oxyhemoglobin/myoglobin, see protocol for details on how to analyze the outcome variables used to calculate sympatholysis.

Reference/Data Set	Study Population	Sample size (n)	Age of participants (years ± SD)	Tau (τ) (seconds)	Muscle group	NIRS Variable reported	Device
Brizendine et al. (2013)	Endurance Athletes	8	25 ± 3	19	Vastus lateralis	Hb_{diff}/total blood volume	Continuous wave (Oxymon MK III)
Ryan et al. (2014)	Young, healthy	21	26 ± 2	55	Vastus lateralis	HHb	Continuous wave (Oxymon MK III)
Southern et al. (2015)	Elderly	23	61 ± 5	63	Wrist flexor	Hb_{diff}	Continuous wave (Oxymon MK III)
Southern et al. (2015)	Elderly + Heart Failure	16	65 ± 7	77	Wrist flexor	Hb_{diff}	Continuous wave (Oxymon MK III)
Adami et al. (2017)	Smokers with normal spirometry	23	63 ± 7	80	Medial forearm	Tissue saturation index (TSI)	Continuous wave (Portamon)
Adami et al. (2017)	COPD Gold 2-4	16	64 ± 9	100	Medial forearm	Tissue saturation index (TSI)	Continuous wave (Portamon)
Erickson et. Al (2013)	Spinal cord injury	9	43 ± 11	143	Vastus lateralis	HbO_2	Continuous wave (Oxymon MK III)

Table 1: Summary of previously published reports across the health continuum using near-infrared spectroscopy to measure skeletal muscle oxidative capacity.

Reference	Study Population	Muscle Group	Reported Outcomes	Outcome Value
Lacroix, *J Biomed Opt*, 2012	Healthy Males	Forearm	Peak Oxyhemoglobin	28.05 ± 3.15 µM
			Peak Total Hemoglobin	10.56 ± 1.80 µM
			Increase Rate to Peak HbO_2	0.75 ± 0.22 µM/s
			Increase Rate to Peak Total Hb	0.52 ± 0.16 µM/s
Kragelj, *Ann Biomed Eng*, 2001	Peripheral Vascular Disease	Forearm	Oxygen Consumption	0.68 ± 0.04 ml/min
			Time to Peak	153 ± 16 s
			Maximal Absolute Change in HbO_2	2.93 ± 0.22 µM/100ml
Suffoletto, *Resuscitation*, 2012	Post-Cardiac Arrest ICU Admittants	Thenar Eminence	Desaturation Rate	-5.6 ± 2 %/min
			Resaturation Rate	0.9 ± 0.6 %/sec
Dimopoulos, *Respir Care*, 2013	Pulmonary Artery Hypertension	Thenar Eminence	Baseline Saturation with 21% O_2	65.8 ± 14.9 %
			O2 Consumption Rate with 21% O_2	35.3 ± 9.1 %/min
			Reperfusion Rate with 21% O_2	535 ± 179 %/min
Doerschug, *Am J Physiol Heart Circ Physiol*, 2007	Organ Failure & Sepsis	Forearm	Baseline Saturation	84%
			Reoxygenation Rate	3.6 %/s
Mayeur, *Crit Care Med*, 2011	Septic Shock	Thenar Eminence	Baseline Saturation	80 ± 1.0 %
			Desaturation Slope	-9.8 ± 3.7 %/min
			Recovery Slope	2.3 ± 1.4 %/sec
McLay, *Exp Physiol*, 2016	Healthy Males	Tibialis Anterior	Baseline Saturation	71.3 ± 2.9 %
			Minimum Saturation	44.8 ± 8.6 %
			Desaturation Slope	-0.1 ± 0.03 %/s
			Recovery Slope	1.63 ± 0.5 %/s
			Peak Saturation	82.6 ± 2.3 %
McLay, Physiol Rep, 2016	Healthy Males	Tibialis Anterior	Baseline Saturation	71.1 ± 2.4 %
			Minimum Saturation	46.2 ± 7.5 %
			Peak Saturation	82.1 ± 1.4 %
			Recovery Slope	1.32 ± 0.38 %/s

Table 2: Summary of previously published reports across the health continuum using near-infrared spectroscopy to measure reactive hyperemia.

Reference	Study Population	% Attenuation
Nelson MD, J. Physiol, 2015	Healthy	-57
	Becker Muscular Dystrophy	-13
Vongpatanasin, J. Physiol, 2011	Healthy	-93
	Hypertension	-14
Fadel, J. Physiol, 2004	Pre-Menopause	-84
	Post-Menopause	-19
Sander, PNAS, 2000	Healthy	-74
	Duchenne Muscular Dystrophy	.+7
Nelson MD, Neurology, 2014	Healthy	-54
	Duchenne Muscular Dystrophy	-7
Price, Hypertension, 2013	Hypertension Pre-Treatment	-52
	Hypertension Post-Nebivolol Treatment	-97
Hansen, J. Clin. Invest., 1996	Healthy Exercise at 20% MVC	-92
	Healthy Exercise at 30% MVC	-125

Table 3: Summary of previously published reports across the health continuum using near-infrared spectroscopy, in combination with lower body negative pressure and handgrip exercise, to assess functional sympatholysis.

REFERENCES

Adami, A., Cao, R., Porszasz, J., Casaburi, R., & Rossiter, H. B. (2017). Reproducibility of NIRS assessment of muscle oxidative capacity in smokers with and without COPD. *Respiratory Physiology & Neurobiology, 235*, 18-26. doi:10.1016/j.resp.2016.09.008

Adami, A., & Rossiter, H. B. (2017). Principles, Insights and Potential Pitfalls of the Non-Invasive Determination of Muscle Oxidative Capacity by Near-Infrared Spectroscopy. *J Appl Physiol (1985)*, jap 00445 02017. doi:10.1152/japplphysiol.00445.2017

Bopp, C. M., Townsend, D. K., Warren, S., & Barstow, T. J. (2014). Relationship between brachial artery blood flow and total [hemoglobin+myoglobin] during post-occlusive reactive hyperemia. *Microvasc Res, 91*, 37-43. doi:10.1016/j.mvr.2013.10.004

Cabalzar, A. L., Oliveira, D. J. F., Reboredo, M. d. M., Lucca, F. A., Chebli, J. M. F., & Malaguti, C. (2017). Muscle function and quality of life in the Crohn s disease. *Fisioterapia em Movimento, 30*, 337-345.

Clifford, P. S., & Hellsten, Y. (2004). Vasodilatory mechanisms in contracting skeletal muscle. *J Appl Physiol (1985), 97*(1), 393-403. doi:10.1152/japplphysiol.00179.2004

Corretti, M. C., Anderson, T. J., Benjamin, E. J., Celermajer, D., Charbonneau, F., Creager, M. A., . . . Vogel, R. (2002). Guidelines for the ultrasound assessment of endothelial-dependent flow-mediated vasodilation of the brachial artery - A report of the International Brachial Artery Reactivity Task Force. *Journal of the American College of Cardiology, 39*(2), 257-265. doi:Doi 10.1016/S0735-1097(01)01746-6

Esch, B. T., Scott, J. M., & Warburton, D. E. (2007). Construction of a lower body negative pressure chamber. *Adv Physiol Educ, 31*(1), 76-81. doi:10.1152/advan.00009.2006

Fadel, P. J., Keller, D. M., Watanabe, H., Raven, P. B., & Thomas, G. D. (2004). Noninvasive assessment of sympathetic vasoconstriction in human and rodent skeletal muscle using near-infrared spectroscopy and Doppler ultrasound. *J Appl Physiol (1985), 96*(4), 1323-1330. doi:10.1152/japplphysiol.01041.2003

Green, D. J., Jones, H., Thijssen, D., Cable, N. T., & Atkinson, G. (2011). Flow-mediated dilation and cardiovascular event prediction: does nitric oxide matter? *Hypertension, 57*(3), 363-369. doi:10.1161/HYPERTENSIONAHA.110.167015

Gurley, K., Shang, Y., & Yu, G. (2012). Noninvasive optical quantification of absolute blood flow, blood oxygenation, and oxygen consumption rate in exercising skeletal muscle. *J Biomed Opt, 17*(7), 075010. doi:10.1117/1.jbo.17.7.075010

Hansen, J., Thomas, G. D., Harris, S. A., Parsons, W. J., & Victor, R. G. (1996). Differential sympathetic neural control of oxygenation in resting and exercising human skeletal muscle. *J Clin Invest, 98*(2), 584-596. doi:10.1172/JCI118826

Hansen, J., Thomas, G. D., Jacobsen, T. N., & Victor, R. G. (1994). Muscle metaboreflex triggers parallel sympathetic activation in exercising and resting human skeletal muscle. *Am J Physiol, 266*(6 Pt 2), H2508-2514.

Huang, A. L., Silver, A. E., Shvenke, E., Schopfer, D. W., Jahangir, E., Titas, M. A., . . . Vita, J. A. (2007). Predictive value of reactive hyperemia for cardiovascular events in patients with peripheral arterial disease undergoing vascular surgery. *Arterioscler Thromb Vasc Biol, 27*(10), 2113-2119. doi:10.1161/ATVBAHA.107.147322

Kodama, S., Saito, K., Tanaka, S., Maki, M., Yachi, Y., Asumi, M., . . . Sone, H. (2009). Cardiorespiratory Fitness as a Quantitative Predictor of All-Cause Mortality and Cardiovascular Events in Healthy Men and Women A Meta-analysis. *Jama-Journal of the American Medical Association, 301*(19), 2024-2035.

Kragelj, R., Jarm, T., Erjavec, T., Presern-Strukelj, M., & Miklavcic, D. (2001). Parameters of postocclusive reactive hyperemia measured by near infrared spectroscopy in patients with peripheral vascular disease and in healthy volunteers. *Annals of Biomedical Engineering, 29*(4), 311-320. doi:Doi 10.1114/1.1359451

Lacroix, S., Gayda, M., Gremeaux, V., Juneau, M., Tardif, J. C., & Nigam, A. (2012). Reproducibility of near-infrared spectroscopy parameters measured during brachial artery occlusion and reactive hyperemia in healthy men. *J Biomed Opt, 17*(7), 077010. doi:10.1117/1.JBO.17.7.077010

Mayeur, C., Campard, S., Richard, C., & Teboul, J. L. (2011). Comparison of four different vascular occlusion tests for assessing reactive hyperemia using near-infrared spectroscopy. *Critical Care Medicine, 39*(4), 695-701. doi:10.1097/CCM.0b013e318206d256

McLay, K. M., Fontana, F. Y., Nederveen, J. P., Guida, F. F., Paterson, D. H., Pogliaghi, S., & Murias, J. M. (2016). Vascular responsiveness determined by near-infrared spectroscopy measures of oxygen saturation. *Experimental Physiology, 101*(1), 34-40. doi:10.1113/EP085406

McLay, K. M., Nederveen, J. P., Pogliaghi, S., Paterson, D. H., & Murias, J. M. (2016). Repeatability of vascular responsiveness measures derived from near-infrared spectroscopy. *Physiol Rep, 4*(9). doi:10.14814/phy2.12772

Nelson, M. D., Rader, F., Tang, X., Tavyev, J., Nelson, S. F., Miceli, M. C., . . . Victor, R. G. (2014). PDE5 inhibition alleviates functional muscle ischemia in boys with Duchenne muscular dystrophy. *Neurology, 82*(23), 2085-2091. doi:10.1212/WNL.0000000000000498

Nelson, M. D., Rosenberry, R., Barresi, R., Tsimerinov, E. I., Rader, F., Tang, X., . . . Victor, R. G. (2015). Sodium nitrate alleviates functional muscle ischaemia in patients with Becker muscular dystrophy. *J Physiol, 593*(23), 5183-5200. doi:10.1113/JP271252

Remensnyder, J. P., Mitchell, J. H., & Sarnoff, S. J. (1962). Functional sympatholysis during muscular activity. Observations on influence of carotid sinus on oxygen uptake. *Circ Res, 11*, 370-380.

Richardson, R. S., Poole, D. C., Knight, D. R., Kurdak, S. S., Hogan, M. C., Grassi, B., . . . Wagner, P. D. (1993). High Muscle Blood-Flow in Man - Is Maximal O2 Extraction Compromised. *Journal of Applied Physiology, 75*(4), 1911-1916.

Rosenmeier, J. B., Fritzlar, S. J., Dinenno, F. A., & Joyner, M. J. (2003). Exogenous NO administration and alpha-adrenergic vasoconstriction in human limbs. *J Appl Physiol (1985), 95*(6), 2370-2374. doi:10.1152/japplphysiol.00634.2003

Ryan, T. E., Brizendine, J. T., & McCully, K. K. (2013). A comparison of exercise type and intensity on the noninvasive assessment of skeletal muscle mitochondrial function using near-infrared spectroscopy. *Journal of Applied Physiology, 114*(2), 230-237. doi:10.1152/japplphysiol.01043.2012

Ryan, T. E., Brophy, P., Lin, C. T., Hickner, R. C., & Neufer, P. D. (2014). Assessment of in vivo skeletal muscle mitochondrial respiratory capacity in humans by near-infrared spectroscopy: a comparison with in situ measurements. *J Physiol, 592*(15), 3231-3241. doi:10.1113/jphysiol.2014.274456

Ryan, T. E., Erickson, M. L., Brizendine, J. T., Young, H. J., & McCully, K. K. (2012). Noninvasive evaluation of skeletal muscle mitochondrial capacity with near-infrared spectroscopy: correcting for blood volume changes. *J Appl Physiol (1985), 113*(2), 175-183. doi:10.1152/japplphysiol.00319.2012

Ryan, T. E., Erickson, M. L., Verma, A., Chavez, J., Rivner, M. H., & McCully, K. K. (2014). Skeletal muscle oxidative capacity in amyotrophic lateral sclerosis. *Muscle Nerve, 50*(5), 767-774. doi:10.1002/mus.24223

Ryan, T. E., Southern, W. M., Brizendine, J. T., & McCully, K. K. (2013). Activity-induced changes in skeletal muscle metabolism measured with optical spectroscopy. *Med Sci Sports Exerc, 45*(12), 2346-2352. doi:10.1249/MSS.0b013e31829a726a

Ryan, T. E., Southern, W. M., Reynolds, M. A., & McCully, K. K. (2013). A cross-validation of near-infrared spectroscopy measurements of skeletal muscle oxidative capacity with phosphorus magnetic resonance spectroscopy. *J Appl Physiol (1985), 115*(12), 1757-1766. doi:10.1152/japplphysiol.00835.2013

Southern, W. M., Ryan, T. E., Kepple, K., Murrow, J. R., Nilsson, K. R., & McCully, K. K. (2015). Reduced skeletal muscle oxidative capacity and impaired training adaptations in heart failure. *Physiol Rep, 3*(4). doi:10.14814/phy2.12353

Southern, W. M., Ryan, T. E., Reynolds, M. A., & McCully, K. (2014). Reproducibility of near-infrared spectroscopy measurements of oxidative function and postexercise recovery kinetics in the medial gastrocnemius muscle. *Appl Physiol Nutr Metab, 39*(5), 521-529. doi:10.1139/apnm-2013-0347

Suryapranata, H., Zijlstra, F., MacLeod, D. C., van den Brand, M., de Feyter, P. J., & Serruys, P. W. (1994). Predictive value of reactive hyperemic response on reperfusion on recovery of regional myocardial function after coronary angioplasty in acute myocardial infarction. *Circulation, 89*(3), 1109-1117.

Thijssen, D. H., Black, M. A., Pyke, K. E., Padilla, J., Atkinson, G., Harris, R. A., . . . Green, D. J. (2011). Assessment of flow-mediated dilation in humans: a methodological and physiological guideline. *Am J Physiol Heart Circ Physiol, 300*(1), H2-12. doi:10.1152/ajpheart.00471.2010

Thomas, G. D., & Victor, R. G. (1998). Nitric oxide mediates contraction-induced attenuation of sympathetic vasoconstriction in rat skeletal muscle. *J Physiol, 506 (Pt 3)*, 817-826.

Tyni-Lenné, R., Gordon, A., Jansson, E., Bermann, G., & Sylvén, C. (1997). Skeletal muscle endurance training improves peripheral oxidative capacity, exercise tolerance, and health-related quality of life in women with chronic congestive heart failure secondary to either ischemic cardiomyopathy or idiopathic dilated cardiomyopathy. *The American Journal of Cardiology, 80*(8), 1025-1029. doi:https://doi.org/10.1016/S0002-9149(97)00597-3

Westerblad, H., Place, N., & Yamada, T. (2010). Mechanisms of Skeletal Muscle Weakness. In D. E. Rassier (Ed.), *Muscle Biophysics: From Molecules to Cells* (pp. 279-296). New York, NY: Springer New York.

Willingham, T. B., Southern, W. M., & McCully, K. K. (2016). Measuring reactive hyperemia in the lower limb using near-infrared spectroscopy. *J Biomed Opt, 21*(9), 091302. doi:10.1117/1.JBO.21.9.091302